

Assessment of current and future water security in the Barossa and Eden Valleys

Seth Westra, Ruby Leigh, Matthew Knowling, Eva Beh, Anjana Devanand, Mark Thyer,
Michael Leonard, Holger Maier, Bree Bennett, Aaron Zecchin, Sam Culley, David McInerney



DOCUMENT STATUS RECORD

Project Title: Assessment of current and future water security in the Barossa and Eden Valleys

Client: South Australian Department of Environment and Water

File Name: CRAFT_BarossaWaterSecurity_FINAL.docx

Issue No.	Date of Issue	Description	Signatures	
			Authors	Approved
1	21/12/2021	Preliminary Draft	RL, AD, SW	SW
2	06/04/2022	Final Report	RL, AD, SW	SW

Disclaimer:

1. The Water Research Centre has taken all reasonable steps to ensure that the information contained within this report is accurate at the time of production. In some cases, we may have relied upon the information supplied by the client.
2. This report has been prepared in accordance with good professional practice. No other warranty expressed or implied is made as to the professional advice given in this report.
3. The Water Research Centre maintains no responsibility for the misrepresentation of results due to incorrect usage of the information contained within this report.
4. This report should remain together and be read as a whole.
5. This report has been prepared solely for the benefit of the client listed above. No liability is accepted by the Water Research Centre with respect to the use of this report by third parties without prior written approval.

Contact Details:

Water Research Centre
University of Adelaide

Physical:
Engineering North Building
North Terrace Campus
University of Adelaide, Adelaide.

Postal:
Professor Seth Westra
Water Research Centre
School of Civil, Environmental and Mining Engineering
University of Adelaide, Adelaide, 5005

Telephone: (08) 8313 5451

Executive Summary

The South Australian Department of Environment and Water (DEW) is developing a water security strategy for the Barossa and Eden Valleys. To support the development of the strategy, this report describes the outcomes of a climate ‘stress test’ of water resources in the region both now and over the next 30 years to the year 2050, with consideration of:

- Current and projected future availability of native water resources (surface water and groundwater) under current and changing climate conditions;
- Current and projected future demand for water, with a particular focus on irrigation demands from the viticultural industry; and
- Implications of a set of possible adaptation pathways identified as part of the Barossa and Eden Valley water security strategy.

Building on significant prior investigations into surface water, groundwater and imported water resources in the region, as well as understanding of demand patterns (including but not limited to vineyard irrigation), an integrated systems modelling framework has been developed to support this research. The modelling framework enables exploration of system dynamics and interactions under current and future climates, and allows the investigation of both current system performance and the performance of alternative adaptive pathways. Where possible, a ‘multiple lines of evidence’ approach was adopted, including but not limited to representation of climate futures and irrigation demands, to enable stress testing both of the Barossa and Eden Valley systems themselves, as well as our collective understanding of those systems.

The findings of the research are as follows.

- Relative to a climatological baseline of 1976-2005, three climate modelling lines of evidence (Climate Change in Australia, Climate Ready-SA and NARClIM) mostly indicate a drier and hotter future climate, but with a very large range of plausible future projections including a minority of projections indicating increases in precipitation. The annual average precipitation over the most recent decade (2011-2020) was 10% lower and potential evapotranspiration was 4% higher than the climatological baseline, and these conditions are broadly consistent with median projections for climate change in 2050. This indicates that the ‘lived experience’ over the recent decade provides a good indicator of ‘typical’ future climate conditions, whilst recognising the high levels of variability and that future decades may be substantially wetter or drier than the recent decade.
- Native surface water resources represent a small and diminishing resource from an irrigation supply perspective over the last decade, and this has been offset partially by increasing utilisation of groundwater resources. The sensitivity of recharge to climatic changes, and the importance of preserving groundwater levels from both ecological and water security perspectives, suggests that recent groundwater extractions may not be sustainable if continued over the longer term. This is likely to be the case particularly for the more severe climate change projections, but may also apply for more moderate projections. Combined with the surface water findings, these results imply that imported water—which is already a dominant source of water for the Barossa Valley—will continue to play a critical role in supporting water security for most future climate scenarios, particularly if accompanied by an objective of preservation or improvement of aquatic ecosystem health.
- There is evidence that water supplies in the recent decade did not meet irrigation water demand for both the Barossa and Eden Valley delineations. The magnitude of future water demands over multi-decadal time horizons is highly uncertain, and will depend on factors such as (1) system performance requirements (including but not limited to desired system reliability); (2) future irrigation requirements (including irrigation strategies on established vineyards as well as possible expansion of vineyard area); (3) other water requirements (e.g. town water and/or industrial needs); (4)

objectives related to environmental flow restoration; and (5) assumptions regarding future climate. For most combinations of these factors, it is clear that likely demands for water exceed current supplies for most future climate scenarios; however scale of any augmented water requirements depends significantly on a range of modelling assumptions.

- Four potential adaptation pathways have been identified, each with different assumptions regarding imported water sources, farm dam strategy, groundwater extractions and the use of balancing storages, amongst other changes. Overall, water reliability improves with increases in imported water, with all adaptive pathways achieving greater than 90% reliability for mid-range climate projections. As expected, the magnitude of the imported water volumes dominate the reliability estimates (in the sense that more imported water leads to enhanced reliability), but the presence of balancing stores may also make an important contribution. Several pathways converting farm dams to balancing stores, and this strategy was shown to produce some benefits in terms of key environmental flow metrics.
- The relatively low utilisation of native water sources (both surface water and groundwater) in the recent decade and under most climate change scenarios suggests a potential opportunity for reducing reliance on these sources and achieving stream restoration benefits in the event that additional imported water becomes available. However, the scale of climate change impacts on environmental flows suggest that, in order to achieve stream restoration objectives under a range of climate change projections, the farm dam strategy would need to be accompanied by other strategies (e.g. linked to groundwater system management and/or more active environmental flow management) that collectively are able to restore flows to the stream.

Finally, it is noted that the study was designed to provide an integrative system-wide perspective to inform strategic planning and policy development. The results presented herein should not be used for detailed sizing of imported water sources and/or balancing stores. Moreover, whereas the pathway results suggest that maximum water security benefits are achieved for the largest imported water capacities, net benefits have not been considered with respect to financial costs and other factors, and the largest capacities may not deliver the greatest net benefits to the community when these additional factors are taken into account. Similarly from an environmental point of view, key areas of uncertainty include representation of surface water / groundwater interaction (including the spatial heterogeneity of these interactions), and the role of on-farm sustainability practices. Further investigation may be warranted to develop an integrated environmental flow restoration initiative. It is therefore hoped that rather than represent the conclusion of a process, this report represents a step along the way of an on-going journey of improved system understanding and adaptive management.

Contents

Executive Summary	iii
Contents	v
List of Figures.....	ix
List of Tables.....	xvii
1 Introduction and Background	1
1.1 Study Objectives and Report Outline	1
1.2 Study Area(s).....	2
1.3 Historical and current land use in the Barossa and Eden Valley regions.....	4
1.4 Historical development of the Barossa’s water infrastructure.....	6
1.4.1 Farm dams.....	6
1.4.2 Imported water pipeline systems.....	7
1.4.3 Groundwater resources and associated infrastructure	8
1.4.4 Soil moisture resources and associated infrastructure	10
1.5 Previous water resource investigations and models.....	10
1.5.1 Summary of historical investigations.....	10
1.5.2 eWater Source	11
1.5.3 MODFLOW.....	13
2 Conceptual representation of the Barossa Water Resources System	14
2.1 System Purpose: Defining Performance Metrics	14
2.2 System Representation.....	16
3 Historical and Current Water Stores and Fluxes.....	20
3.1 Water into the system: Rainfall (P)	20
3.2 Water into the system: External water sources.....	23
3.2.1 Barossa Infrastructure Limited (BIL) (U_{BIL}).....	23
3.2.2 SA Water Off-peak (U_{SA}).....	24
3.2.3 Bunyip Pipeline (U_{BY}).....	25
3.2.4 Summary of External Water Sources	26
3.3 Water out of the system: Streamflow (Q)	26
3.3.1 Total Streamflow	27
3.3.2 Baseflow.....	30
3.4 Water out of the system: Evaporative Demand and Actual Evapotranspiration.....	32
3.4.1 Potential Evapotranspiration	32
3.4.2 Groundwater Evapotranspiration.....	33
3.5 Water through the system: Lateral groundwater inflow/outflow	34
3.6 Within system flux: Water use from native sources	34

3.6.1	Surface water	35
3.6.2	Groundwater	37
3.7	Within system flux: Groundwater Recharge.....	39
3.8	Storage: Farm dams.....	40
3.9	Storage: Groundwater storage	41
3.10	Summary of Historical Water Consumption	43
3.10.1	Barossa PWRA	43
3.10.2	Barossa Valley.....	44
3.10.3	Eden Valley.....	44
3.11	Demand estimation	45
3.11.1	Regression-based demand estimation.....	45
3.11.2	Process-based demand estimation.....	46
3.11.3	Results.....	47
4	Future climate stressors	51
4.1	Sources of Climate Information	51
4.1.1	Climate Change in Australia (CCIA).....	51
4.1.2	Climate Ready SA (CR-SA)	51
4.1.3	NARcliM	52
4.2	Changes in Rainfall	53
4.2.1	Annual and seasonal rainfall	53
4.2.2	Number of wet days	56
4.2.3	Daily extremes (99 th percentile wet day rainfall)	57
4.2.4	Rainfall seasonality	58
4.3	Changes in Potential Evapotranspiration	59
4.4	Changes in Temperature.....	61
4.4.1	Annual and Seasonal Changes to Daily Maximum Temperature	61
4.4.2	Annual Number of Days Over 35°C.....	64
4.5	Selection of Scenarios for Stress Testing	65
4.5.1	Range of Projections	65
4.5.2	Scenarios for Stress Testing.....	65
5	Representing system connections under change	67
5.1	System Dynamics Modelling	67
5.2	Annual average streamflow and climate	69
5.3	Baseflow.....	73
5.3.1	Baseflow from Source (Lyne-Hollick Filter)	73
5.3.2	Baseflow from MODFLOW	76
5.4	Storage in farm dams and climate	77

5.5	Water use from surface water	81
5.6	Rainfall and groundwater recharge.....	85
5.7	Groundwater Evaporation	86
5.8	Groundwater Storage	88
5.9	Irrigation demand.....	90
5.9.1	Regression Model	90
5.9.2	FAO-56 DCC Model	92
6	Current System Dynamics	95
6.1	Water Security Metrics	95
6.1.1	Barossa PWRA	95
6.1.2	Barossa Valley.....	102
6.1.3	Eden Valley	104
6.2	Ecological Metrics.....	108
6.2.1	Flowing days.....	108
6.2.2	Days over threshold flow	109
6.2.3	Medium flow days	111
6.2.4	Summary of ecological metrics	112
6.3	Summary of Current System Dynamics	112
7	Alternative System Configurations	114
7.1	Description of potential adaptive pathways.....	114
7.1.1	Business as usual	115
7.1.2	Pathway 1: Infrastructure investment supports existing industry and behaviours	115
7.1.3	Pathway 2: Sustainable economic growth - clean and green production	115
7.1.4	Pathway 3: Healthy waterways and soils.....	116
7.1.5	Pathway 4: Maximum water availability and expansion	116
7.2	Pathway 1: Enhanced infrastructure investment.....	116
7.2.1	Water Security Metrics	116
7.2.2	Environmental Flow Metrics	120
7.3	Pathway 2: Sustainable economic growth.....	120
7.3.1	Water Security Metrics	121
7.3.2	Environmental Flow Metrics	123
7.4	Pathway 3: Healthy waterways through investment.....	128
7.4.1	Water Security Metrics	128
7.4.2	Environmental Flow Metrics	132
7.5	Pathway 4: Maximum water availability and production outcomes	136
7.5.1	Water Security Metrics	136
7.5.2	Environmental Flow Metrics	138

7.6	Pathway summary	138
7.7	The importance of yield assumptions	140
8	Conclusions.....	141
8.1	Summary of Results.....	141
8.1.1	Recent system dynamics	141
8.1.2	Projected climate changes	142
8.1.3	Current system performance and the role of adaptive pathways	143
8.2	Assumptions and Limitations.....	144
8.2.1	Future water security.....	147
8.2.2	Ecological outcomes	148
8.2.3	Future Research.....	149
9	Acknowledgements.....	150
	Appendix A: Key areas and area/depth/volume conversions used in this report.....	151
	Appendix B: Primary Hydrological Data Sources	153
	Appendix C: System connections under change for the Barossa Valley region	156
	Appendix D: System connections under change for the Eden Valley region	169
	Appendix E: Stella diagnostics	180
	Weighted Plots	180
	Quantile plots	184
	References.....	187

List of Figures

Figure 1. The Climate Resilience Assessment Framework (adapted from Bennett et al, 2018).	1
Figure 2. The Barossa Geographical Indicator (GI) Zone (the hatched region), Barossa Valley and Eden Valley wine regions (red boundaries), location of the vineyards (green) and the prescribed water resources area (PWRA) (black boundary). Catchment boundaries (light blue) are delineated by Government of South Australia.	3
Figure 3. Planted vineyard area for the combined Barossa and Eden Valley regions obtained from Vine Health Australia Production Reports (Source: https://vinehealth.com.au/news/sa-winegrape-crush-survey/ , accessed 20 September 2021).....	4
Figure 4. Trend of area of white, shiraz, cabernet sauvignon and other red varieties as a percentage of total planted area in the Barossa Valley (top) and Eden Valley (bottom), obtained from Vine Health Australia Production Reports (Source: https://vinehealth.com.au/news/sa-winegrape-crush-survey/ , accessed 24 November 2021).....	5
Figure 5. Average grape yield per hectare for the combined Barossa and Eden Valley regions obtained from Vine Health Australia Production Reports (Source: https://vinehealth.com.au/news/sa-winegrape-crush-survey/ , accessed 20 September 2021), calculated as total crush divided by planted vineyard area.	6
Figure 6. The layout of SA Water and BIL pipeline network and the approximate location of Seppeltsfield vineyards that receive water from the Bunyip pipeline	8
Figure 7. Aquifer extent map with location of abstraction wells	9
Figure 8. Definition of ‘system model’ used in CRAFT (Bennett et al, 2018)	14
Figure 9. Schematic system model of water fluxes and storage of various components, focusing on the Barossa PWRA. Open boxes represent variables, arrows represent relationships, the green shaded box represents the climate inputs, and orange shaded boxes represent the system performance metrics. The primary models used to represent relationships are denoted by yellow shaded text.....	18
Figure 10. System model schematic using stock-and-flow diagram representation.....	19
Figure 11. Location of the SILO rainfall stations, streamflow gauges and spatial pattern of rainfall.....	21
Figure 12. Climatological (1900 to 2020) mean (bars) and standard deviation (line) of monthly rainfall in the Barossa PWRA.	22
Figure 13. The annual total rainfall in the Eden Valley, Barossa Valley and Barossa PWRA estimated as the arithmetic mean rainfall from the all the gauges in respective regions.....	22
Figure 14. Historical water use from external source BIL in GL/year for each water-use year (1 July to 30 June) and the BIL capacity.....	24
Figure 15 Historical water use from external source ‘SA Water Off-peak’ in ML/year for each water-use year (1 July to 30 June).	25
Figure 16. Historical annual total streamflow at Yaldara (in GL/year) for each water-use year (1 July to 30 June).....	28
Figure 17. Observed versus simulated streamflow at Yaldara from 1980/81 to 2019/20.	28
Figure 18. Historical (1980 to 2020) and Recent (2010 to 2020) daily flow duration curve for the outflow gauge station A5050502 (Data Source: SA Water Connect and streamflow from Source Model)	29
Figure 19. Daily downstream flow volumes at Yaldara for dry, wet and average rainfall years, from modelled (Source) time series	29
Figure 20. Annual (water year) aggregate baseflow (ML) at Yaldara from the Lyne-Hollick baseflow filter and MODFLOW. The filter alpha values represented are for $\alpha=0.95$, 0.975, 0.98 and 0.99.	31
Figure 21. Comparison of different alpha values on Lyne-Hollick filter for the 2015/16 water year.....	31
Figure 22. Climatological (1900 to 2020) mean (bars) and standard deviation (line) of monthly PET (mm) in the Barossa PWRA	33
Figure 23. The annual total mean PET (mm) in the Barossa PWRA from the gauge 23373.	33

Figure 24. Annual (water year) aggregate groundwater ET (ML) across Barossa PWRA. Corresponding groundwater recharge rates (Section 3.7 given for reference).....	34
Figure 25. Historical licensed irrigation water use from surface water sources for each water-use year (1 July to 30 June) for the Barossa PWRA.....	36
Figure 26. Change in licensed surface water use and allocation over the recent decade (2010/11 to 2019/20) for the Barossa and Eden Valley regions.....	37
Figure 27. Recent licensed groundwater use data for the Barossa PWRA for each water-use year (1 July to 30 June).....	38
Figure 28. Historical metered use and allocation of groundwater for the Barossa and Eden Valley delineations	39
Figure 29. Historical (1980/81-2019/20) annual average, annual maximum and farm dam storage capacity for each water-use year (1 July to 30 June) in GL, as modelled in Source.	41
Figure 30. Total Farm Dam Storage in GL (modelled daily) for a representative wet, dry and average year..	41
Figure 31. A selection of representative groundwater hydrographs identified by Li and Cranswick (2017) to capture overall Barossa PWRA groundwater trends (from Li and Cranswick (2016)). ‘AHD’ refers to the Australian Height Datum (approximately equal to mean sea level). Subplot titles are the observation well identifiers.	42
Figure 32. Time series estimates of total groundwater storage in the Barossa PWRA based on calibrated groundwater model of Li and Cranswick (2016).	43
Figure 33. Observed water use in the Barossa PWRA from 2008/09-2019/20.....	44
Figure 34. Observed water use in the Barossa Valley from 2010/11-2019/20	44
Figure 35. Observed water use in the Eden Valley from 2010/11-2019/20	45
Figure 36. Comparison of recent water use from different sources (coloured bars) and estimated demand from regression model (black line) and FAO56-DCC model (orange line) shown as depths (mm; right vertical axis) and volumes (GL; left vertical axis) in the Barossa PWRA.....	48
Figure 37. Comparison of regression on observed water use of the regression-based (blue) and process-based (red) model results	48
Figure 38. Comparison of recent water use from different sources (coloured bars) and estimated demand from regression model (black line) and FAO56-DCC model (orange line)) shown as depths (mm; right vertical axis) and volumes (GL; left vertical axis) in the Barossa Valley.....	49
Figure 39. Comparison of recent water use from different sources (coloured bars) and estimated demand from regression model (black line) and FAO56-DCC model (orange line)) shown as depths (mm; right vertical axis) and volumes (GL; left vertical axis) in the Eden Valley	50
Figure 40. Annual changes in rainfall relative to a 1976-2005 climatological baseline. Each box-and-whisker plot represents the variability from 4,500 separate time series. The median value is represented by the horizontal black line, the boxes are bounded by the upper and lower quartiles. The upper whisker represents the values from the upper quartile to no further than 1.5*IQR (Inter Quartile Range). The lower whisker likewise extends to the value at most 1.5*IQR . The dots above and below the whiskers represent outlying points.	54
Figure 41. Percentage change in annual number of wet days (wet day threshold = 1mm) for RCP4.5 and RCP8.5 emission scenarios, relative to a 1976-2005 climatological baseline. See caption for Figure 40 for further details.....	56
Figure 42 – Percentage change in annual 99th percentile wet day amount rainfall for RCP4.5 and RCP8.5 emission scenarios, relative to a 1976-2005 climatological baseline. See caption for Figure 40 for further details.....	57
Figure 43. Percentage change in seasonality for RCP4.5 and RCP8.5 emission scenarios, relative to a 1976-2005 climatological baseline. See caption for Figure 40 for further details.	58
Figure 44. Percentage change in annual average PET for RCP4.5 and RCP8.5 emission scenarios, relative to a 1976-2005 climatological baseline. See caption for Figure 40 for further details.	59

Figure 45. Percentage change in annual average maximum temperature for RCP4.5 and RCP8.5 emission scenarios, relative to a 1976-2005 climatological baseline. See caption for Figure 40 for further details.....61

Figure 46. Percentage change in annual number of days above 35 degrees Celsius (as a percentage relative to the baseline) for RCP4.5 and RCP8.5 emission scenarios, relative to a 1976-2005 climatological baseline. See caption for Figure 40 for further details.64

Figure 47. Scatter plots of streamflow outputs from Source as a result of the climate stress test. The axes are average annual rainfall and PET (mm), and the colour of the points represents the average annual streamflow in ML/year.68

Figure 48. The performance space, both relative (upper panels) and absolute (lower panels) change, of streamflow at Outlet Node 2 (Barossa Valley Gorge Source outflow) from simple scaling, both from Source (left) and Stella (right) results. Climate projections are overlaid onto the plotting space - the faint grey dots represent the 9000 replicates from CR-SA, the small black circles represent the mean of each of the 15 SA-CR GCMs (15 models for 3 time slices and 2 emissions scenarios, 90 points), the small black triangles represent the mean of each of the 6 NARClIM GCMs (36 points), and the coloured circles (SA-CR) and triangles (NARClIM) represent the mean of all the data for each future time slice and climate emission scenario (6 each). The yellow circle with cross through it represents the average P and PET for the most recent decade (2011-2020) relative to the 1976-2005 baseline.70

Figure 49. Residuals of the mean absolute streamflow values between Source and Stella.....71

Figure 50: The performance space (absolute change only) replicated for a decrease in the strength of the seasonal cycle (i.e. relatively wetter summers and drier winters; left panel), the historical seasonal cycle (middle panel) and an increase in the strength of the seasonal cycle (additional drying in summer and wetting in winter; right panel).72

Figure 51. The performance space, both relative (upper panels) and absolute (lower panels) change, of baseflow from filtering streamflow at Outlet Node 2 (Barossa Valley Gorge Source outflow) from simple scaling, both from Source (left) and Stella (right) results.74

Figure 52. Residuals of the mean absolute Lyne-Hollick baseflow values between Source and Stella.....74

Figure 53: The performance space (absolute change only) replicated for a decrease in the strength of the seasonal cycle (i.e. relatively wetter summers and drier winters; left panel), the historical seasonal cycle (middle panel) and an increase in the strength of the seasonal cycle (additional drying in summer and wetting in winter; right panel).75

Figure 54. The performance space, both relative (upper panels) and absolute (lower panels) change, of baseflow at Yaldara from simple scaling, both from MODFLOW (left) and Stella (right) results.....76

Figure 55. Residuals of the mean absolute baseflow values between MODFLOW and Stella.....77

Figure 56. The performance space, both relative (upper panels) and absolute (lower panels) change, of maximum farm dam storage from simple scaling, both from Source (left) and Stella (right) results.....78

Figure 57. Residuals of the mean absolute maximum farm dam storage values between Source and Stella 79

Figure 58. The performance space (absolute change only) replicated for a decrease in the strength of the seasonal cycle (i.e. relatively wetter summers and drier winters; left panel), the historical seasonal cycle (middle panel) and an increase in the strength of the seasonal cycle (additional drying in summer and wetting in winter; right panel).80

Figure 59. The performance space, both relative (upper panels) and absolute (lower panels) change, of surface water extraction from simple scaling, both from Source (left) and Stella (right) results.82

Figure 60. Residuals of the mean absolute surface water extraction values between Source and Stella82

Figure 61. The performance space (absolute change only) replicated for a decrease in the strength of the seasonal cycle (i.e. relatively wetter summers and drier winters; left panel), the historical seasonal cycle (middle panel) and an increase in the strength of the seasonal cycle (additional drying in summer and wetting in winter; right panel).84

Figure 62. The performance space, both relative (upper panels) and absolute (lower panels) change, of groundwater recharge from simple scaling, both from MODFLOW (left) and Stella (right) results.85

Figure 63. Residuals of the mean absolute recharge values between MODFLOW and Stella.....86

Figure 64. The performance space, both relative (upper panels) and absolute (lower panels) change, of groundwater evaporation from simple scaling, both from MODFLOW (left) and Stella (right) results.	87
Figure 65. Residuals of the mean absolute groundwater evaporation values between MODFLOW and Stella	88
Figure 66. The performance space, both relative (upper panels) and absolute (lower panels) change, of groundwater storage from simple scaling, both from MODFLOW (left) and Stella (right) results.	89
Figure 67. Residuals of the mean absolute storage values between MODFLOW and Stella	90
Figure 68. The performance space, both absolute (GL, bottom; mm, middle) and relative change (top), of regression-based demand from simple scaling, from Stella results.	92
Figure 69. Performance space of relative (top) and absolute irrigation demand (mm middle; GL bottom). The performance space of absolute irrigation demand from the regression model is shown for comparative purposes.	94
Figure 70. Mean Annual Demand Residuals (GL) between SARDI model and SARDI regression implemented in Stella	94
Figure 71. Unmet demand from regression-based model in Stella for the Barossa PWRA. Left to right: Average unmet demand [GL], percentage of years with unmet demand and average unmet demand in years with unmet demand [GL].	97
Figure 72. Ratio of supply on demand that corresponds to 90% reliability using the regression-based model in Stella for the Barossa PWRA. The white threshold line indicates the climate scenarios where supply is equal to demand.	98
Figure 73. Unmet demand from process-based model in Stella for the Barossa PWRA. Left to right: Average unmet demand [GL], percentage of years with unmet demand and average unmet demand in years with unmet demand [GL].	99
Figure 74. Ratio of supply on demand that corresponds to a 90% reliability using the process-based model in Stella for the Barossa PWRA. The white threshold line indicates the climate scenarios where supply is equal to demand.	100
Figure 75. Time series of Stella supply and demand for the baseline case (PET=1, P=1) and a moderate climate change scenario (P=0.9, PET=1.05) for the Barossa PWRA.	101
Figure 76. Unmet demand from process-based model in Stella for the Barossa Valley. Left to right: Average unmet demand [GL], percentage of years with unmet demand and average unmet demand in years with unmet demand [GL].	102
Figure 77. Ratio of supply on demand that corresponds to 90% reliability using the process-based model in Stella for the Barossa Valley. The white threshold line indicates the climate scenarios where supply is equal to demand.	103
Figure 78. Time series of Stella supply and demand for the baseline case (PET=1, P=1) and a moderate climate change scenario (P=0.9, PET=1.05) for the Barossa Valley.	104
Figure 79. Unmet demand from process-based model in Stella for the Eden Valley. Left to right: Average unmet demand [GL], percentage of years with unmet demand and average unmet demand in years with unmet demand [GL].	105
Figure 80. Ratio of supply on demand that corresponds to 90% reliability using the process-based model in Stella for the Eden Valley. The white threshold line indicates the climate scenarios where supply is equal to demand.	106
Figure 81. Time series of Stella supply and demand for the baseline case (PET=1, P=1) and a moderate climate change scenario (P=0.9, PET=1.05) for the Eden Valley.	107
Figure 82. Barossa PWRA Project Zones	108
Figure 83. The performance space of the absolute change in the number of flowing days for the Barossa Valley Gorge Zone from simple scaling from Source results.	109
Figure 84. The performance space of the absolute change in the number of flowing days for the Upper Flaxman Valley Zone from simple scaling from eWater Source results.	109

Figure 85. The performance space of the absolute change in the number of days over threshold flow for the Barossa Valley Gorge Zone from simple scaling from Source results.....	110
Figure 86. The performance space of the absolute change in the number of days over threshold flow for the Upper Flaxman Valley Zone from simple scaling from Source results.....	110
Figure 87. The performance space of the absolute change in the number of days over the 50 th percentile daily flow for the Barossa Valley Gorge Zone from simple scaling from Source results.....	111
Figure 88. The performance space of the absolute change in the number of days over the 50 th percentile daily flow for the Upper Flaxman Valley Zone from simple scaling from Source results.	112
Figure 89. Left column - Unmet demand from process-based model in Stella for the Barossa Valley (Pathway 1). Top to bottom: Average unmet demand [GL], percentage of years with unmet demand, and average unmet demand in years with unmet demand [GL]. Right column – Difference between water security metrics in the left panel (Pathway 1) and the corresponding metrics for the current system (business as usual). ..	117
Figure 90. Left plot – Ratio of supply on demand that corresponds to 90% reliability using the process-based model in Stella for the Barossa Valley (Pathway 1). The white threshold line indicates the climate scenarios where supply is equal to demand. Right plot – the difference in the fraction of supply on demand between the current system (business as usual) and Pathway 1.	118
Figure 91. Left column - Unmet demand from process-based model in Stella for the Eden Valley (Pathway 1). Top to bottom: Average unmet demand [GL], percentage of years with unmet demand, and average unmet demand in years with unmet demand [GL]. Right column – Difference between water security metrics in the left panel (Pathway 1) and the corresponding metrics for the current system (business as usual).	119
Figure 92. Left plot – Ratio of supply on demand that corresponds to 90% reliability using the process-based model in Stella for the Eden Valley (Pathway 1). The white threshold line indicates the climate scenarios where supply is equal to demand. Right plot – the difference in the fraction of supply on demand between the current system (business as usual) and Pathway 1.	120
Figure 93. Left column - Unmet demand from process-based model in Stella for the Barossa Valley (Pathway 2). Top to bottom: Average unmet demand [GL], percentage of years with unmet demand, and average unmet demand in years with unmet demand [GL]. Right column – Difference between water security metrics in the left panel (Pathway 2) and the corresponding metrics for the current system (business as usual). ..	122
Figure 94. Left plot – Ratio of supply on demand that corresponds to 90% reliability using the process-based model in Stella for the Barossa Valley (Pathway 2). The white threshold line indicates the climate scenarios where supply is equal to demand. Right plot – the difference in the fraction of supply on demand between the current system (business as usual) and Pathway 2.	123
Figure 95 Left plot – Ratio of supply on demand that corresponds to 90% reliability using the process-based model in Stella for the Eden Valley (Pathway 2). The white threshold line indicates the climate scenarios where supply is equal to demand. Right plot – the difference in the fraction of supply on demand between the current system (business as usual) and Pathway 2.	123
Figure 96. The performance spaces of environmental flow metrics for the Barossa Valley Gorge Zone from simple scaling from Source results (Pathway 2 – removal of high impact dams). Left column – Top to bottom: number of flow days; number of days above threshold flow; and the number of days over the 50 th percentile flow (for the current system configuration this is 9.13 ML/day). Right column – Difference between environmental flow metrics in the left panel (Pathway 2) and the corresponding metrics for the current system (business as usual).	125
Figure 97. The performance spaces of environmental flow metrics for the Upper Flaxman Valley Zone from simple scaling from Source results (Pathway 2 – removal of high impact dams). Left column – Top to bottom: number of flow days; number of days above threshold flow; and the number of days over the 50 th percentile flow (for the current system configuration this is 0.828ML/day). Right column – Difference between environmental flow metrics in the left panel (Pathway 2) and the corresponding metrics for the current system (business as usual).	127
Figure 98. Unmet demand from process-based model in Stella for the Barossa Valley (Pathway 3). Top to bottom: Average unmet demand [GL], percentage of years with unmet demand, and average unmet demand	

in years with unmet demand [GL]. Right column – Difference between water security metrics in the left panel (Pathway 3) and the corresponding metrics for the current system (business as usual).....129

Figure 99. Left plot – Ratio of supply on demand that corresponds to 90% reliability using the process-based model in Stella for the Barossa Valley (Pathway 3). The white threshold line indicates the climate scenarios where supply is equal to demand. Right plot – the difference in the fraction of supply on demand between the current system (business as usual) and Pathway 3.130

Figure 100. Left column - Unmet demand from process-based model in Stella for the Eden Valley (Pathway 3). Top to bottom: Average unmet demand [GL], percentage of years with unmet demand, and average unmet demand in years with unmet demand [GL]. Right column – Difference between water security metrics in the left panel (Pathway 3) and the corresponding metrics for the current system (business as usual). ..131

Figure 101. Left plot – Ratio of supply on demand that corresponds to 90% reliability using the process-based model in Stella for the Eden Valley (Pathway 3). The white threshold line indicates the climate scenarios where supply is equal to demand. Right plot – the difference in the fraction of supply on demand between the current system (business as usual) and Pathway 3.132

Figure 102. The performance spaces of environmental flow metrics for the Barossa Valley Gorge Zone from simple scaling from Source results (Pathway 3 – removal of high and medium impact dams). Left column – Top to bottom: number of flow days; number of days above threshold flow; and the number of days over the 50th percentile flow (for the current system configuration this is 9.13 ML/day). Right column – Difference between environmental flow metrics in the left panel (Pathway 3) and the corresponding metrics for the current system (business as usual).133

Figure 103. The performance spaces of environmental flow metrics for the Upper Flaxman Valley Zone from simple scaling from Source results (Pathway 3 – removal of high and medium impact dams). Left column – Top to bottom: number of flow days; number of days above threshold flow; and the number of days over the 50th percentile flow (for the current system configuration this is 0.828ML/day). Right column – Difference between environmental flow metrics in the left panel (Pathway 3) and the corresponding metrics for the current system (business as usual).135

Figure 104. Left plot – Ratio of supply on demand that corresponds to 90% reliability using the process-based model in Stella for the Barossa Valley (Pathway 4, no increase in planted area). The white threshold line indicates the climate scenarios where supply is equal to demand. Right plot – the difference in the fraction of supply on demand between the current system (business as usual) and Pathway 4.136

Figure 105. Left plot - Ratio of supply on demand that corresponds to 90% reliability using the process-based model in Stella for the Barossa Valley (Pathway 4, 1.35 times increase in planted area – 158.6 km²). The white threshold line indicates the climate scenarios where supply is equal to demand. Right plot – the difference in the fraction of supply on demand between the current system (business as usual) and Pathway 4.136

Figure 106. Left plot - Ratio of supply on demand that corresponds to 90% reliability using the process-based model in Stella for the Barossa Valley (Pathway 4, no increase in area, 2 tonne yield increase). The white threshold line indicates the climate scenarios where supply is equal to demand. Right plot – the difference in the fraction of supply on demand between the current system (business as usual) and Pathway 4.137

Figure 107. Left plot - Ratio of supply on demand that corresponds to 90% reliability using the process-based model in Stella for the Eden Valley (Pathway 4, no increase in planted area). The white threshold line indicates the climate scenarios where supply is equal to demand. Right plot – the difference in the fraction of supply on demand between the current system (business as usual) and Pathway 4.137

Figure 108. Left plot - Ratio of supply on demand that corresponds to 90% reliability using the process-based model in Stella for the Eden Valley (Pathway 4, 2.05 times increase in planted area – 47.6 km²). The white threshold line indicates the climate scenarios where supply is equal to demand. Right plot – the difference in the fraction of supply on demand between the current system (business as usual) and Pathway 4.138

Figure 109. Left plot - Ratio of supply on demand that corresponds to 90% reliability using the process-based model in Stella for the Eden Valley (Pathway 4, no increase in area, 2 tonne yield increase). The white threshold line indicates the climate scenarios where supply is equal to demand. Right plot – the difference in the fraction of supply on demand between the current system (business as usual) and Pathway 4.138

Figure 110. The performance space, both absolute and relative change, of Streamflow at Outlet Node 2 (Barossa Valley Gorge Source outflow) from simple scaling, both from Source (left) and Stella (right) results.	157
Figure 111. Residuals of the mean absolute streamflow values between Source and Stella	158
Figure 112. The performance space, both absolute and relative change, of Baseflow from filtering Streamflow at Outlet Node 2 (Barossa Valley Gorge Source outflow) from simple scaling, both from Source (left) and Stella (right) results.	159
Figure 113. Residuals of the mean absolute baseflow values between Source and Stella	160
Figure 114. The performance space, both absolute and relative change, of average maximum farm storage from simple scaling, both from Source (left) and Stella (right) results.....	161
Figure 115. Residuals of the mean absolute maximum farm dam values between Source and Stella	162
Figure 116. The performance space, both absolute and relative change, of average surface water extraction from simple scaling, both from Source (left) and Stella (right) results.....	163
Figure 117. Residuals of the mean absolute surface water extraction values between Source and Stella...	164
Figure 118. The performance space, both absolute (GL, bottom; mm, middle) and relative change (top), of regression-based demand from simple scaling, from Stella results.....	166
Figure 119. Performance space of absolute irrigation demand (mm top; GL bottom). The performance space of absolute irrigation demand from the regression model is shown for comparative purposes.	167
Figure 120. Mean Annual Demand Residuals (GL) between SARDI model and SARDI regression implemented in Stella.....	168
Figure 121. The performance space, both absolute and relative change, of average streamflow aggregated from five outflows from the Eden Valley from simple scaling, both from Source (left) and Stella (right) results.	170
Figure 122. The performance space, both absolute and relative change, of average maximum farm storage from simple scaling, both from Source (left) and Stella (right) results.....	172
Figure 123. The performance space, both absolute and relative change, of average surface water extraction from simple scaling, both from Source (left) and Stella (right) results.....	174
Figure 124. The performance space, both absolute (GL, bottom; mm, middle) and relative change (top), of regression-based demand from simple scaling, from Stella results.....	177
Figure 125. Performance space of absolute irrigation demand (mm top; GL bottom). The performance space of absolute irrigation demand from the regression model is shown for comparative purposes.	178
Figure 126. Mean Annual Demand Residuals (GL) between SARDI model and SARDI regression implemented in Stella.....	179
Figure 127. Scatter plots of annual average streamflow for a single PET perturbation (PET=1) and all rainfall perturbations tested (P=0.75-1.1). The scatter represents all of the raw points (from Source), coloured by rainfall perturbation, and the red points are the average of each of these perturbations. The left plot shows a univariate non-linear regression fitted to full scatter of raw data points; the right plots shows a univariate non-linear regression fitted to full scatter, with averages also included and weighted 100, while the other points are weighted 1.	180
Figure 128. Scatter plots of annual average baseflow for a single PET perturbation (PET=1) and all rainfall perturbations tested (P=0.75-1.1). The scatter represents all of the raw points (from Source and Lyne-Hollick filter), coloured by rainfall perturbation, and the red points are the average of each of these perturbations. The left plot shows a univariate non-linear regression fitted to full scatter of raw data points; the right plots shows a univariate non-linear regression fitted to full scatter, with averages also included and weighted 100, while the other points are weighted 1.	180
Figure 129. Scatter plots of annual average baseflow for a single PET perturbation (PET=1) and all rainfall perturbations tested (P=0.75-1.1). The scatter represents all of the raw points (from MODFLOW), coloured by rainfall perturbation, and the red points are the average of each of these perturbations. The left plot shows a univariate non-linear regression fitted to full scatter of raw data points; the right plots shows a univariate	

non-linear regression fitted to full scatter, with averages also included and weighted 100, while the other points are weighted 1.	181
Figure 130. Scatter plots of maximum farm dam storage for a single PET perturbation (PET=1) and all rainfall perturbations tested (P=0.75-1.1). The scatter represents all of the raw points (from Source), coloured by rainfall perturbation, and the red points are the average of each of these perturbations. The left plot shows a univariate non-linear regression fitted to full scatter of raw data points; the right plots shows a univariate non-linear regression fitted to full scatter, with averages also included and weighted 100, while the other points are weighted 1.	181
Figure 131. Scatter plots of annual average farm dam extraction for a single PET perturbation (PET=1) and all rainfall perturbations tested (P=0.75-1.1). The scatter represents all of the raw points (from Source), coloured by rainfall perturbation, and the red points are the average of each of these perturbations. The left plot shows a univariate non-linear regression fitted to full scatter of raw data points; the right plots shows a univariate non-linear regression fitted to full scatter, with averages also included and weighted 100, while the other points are weighted 1.	182
Figure 132. Scatter plots of annual average watercourse extraction for a single PET perturbation (PET=1) and all rainfall perturbations tested (P=0.75-1.1). The scatter represents all of the raw points (from Source), coloured by rainfall perturbation, and the red points are the average of each of these perturbations. The left plot shows a univariate logarithmic regression fitted to full scatter of raw data points; the right plots shows a univariate non-linear regression fitted to full scatter, with averages also included and weighted 100, while the other points are weighted 1.	182
Figure 133. Scatter plots of annual average recharge for a single PET perturbation (PET=1) and all rainfall perturbations tested (P=0.75-1.1). The scatter represents all of the raw points (from MODFLOW), coloured by rainfall perturbation, and the red points are the average of each of these perturbations. The left plot shows a univariate linear regression fitted to full scatter of raw data points; the right plots shows a univariate non-linear regression fitted to full scatter, with averages also included and weighted 100, while the other points are weighted 1.	183
Figure 134. Scatter plots of annual average groundwater ET for a single rainfall perturbation (P=1) and all PET perturbations tested (PET=1-1.1). The scatter represents all of the raw points (from MODFLOW), coloured by PET perturbation, and the red points are the average of each of these perturbations. The left plot shows a univariate linear regression fitted to full scatter of raw data points; the right plots shows a univariate non-linear regression fitted to full scatter, with averages also included and weighted 1000, while the other points are weighted 1.	183
Figure 135. Quantile plots of demand from SARDI model results and SARDI model results implemented in Stella as a regression with normal error term for equivalent recent decade perturbation, P=0.9 and PET =1.05 for the Barossa PWRA. From left to right: Normal Q-Q plot of SARDI results; Normal Q-Q plot of Stella results; Q-Q plot of Stella and SARDI results.	184
Figure 136. Quantile plots of demand from SARDI model results and SARDI model results implemented in Stella as a regression with normal error term for equivalent recent decade perturbation, P=0.9 and PET =1.05 for the Eden Valley. From left to right: Normal Q-Q plot of SARDI results; Normal Q-Q plot of Stella results; Q-Q plot of Stella and SARDI results.	185
Figure 137. Quantile plots of demand from SARDI model results and SARDI model results implemented in Stella as a regression with normal error term for equivalent recent decade perturbation, P=0.9 and PET =1.05 for the Barossa Valley. From left to right: Normal Q-Q plot of SARDI results; Normal Q-Q plot of Stella results; Q-Q plot of Stella and SARDI results.	186

List of Tables

Table 1. Number of farm dams and their capacity across the three study delineations.....	7
Table 2. Historical expansion of BIL capacity (Source: BIL annual reports)	8
Table 3. Number of licensed extraction wells in the three study areas	9
Table 4. Summary of water security and ecological system performance metrics to be explored in this report	15
Table 5. Historical imported water to the Barossa region from the Bunyip pipeline.....	25
Table 6. Historical water use from external sources in the Barossa GI zone (Source: DEW excel document named 'Barossa_water_use_2018-19')	26
Table 7. Volumes of licensed surface water allocation and use from different sources of information for the Barossa PWRA. The assumed unlicensed stock and domestic use is not shown in the table.	36
Table 8. Average surface water allocation and use for the recent decade (2010/11 to 2019/20) for the Barossa and Eden Valley	37
Table 9. Summary of model parameters used for the Barossa and Eden Valleys.....	47
Table 10. Percentage change of seasonal and annual precipitation averaged across all three stations in the Barossa. The median value, upper and lower quartile (25 to 75 th percentile) and 2.5 and 97.5 th percentile values are quoted.	55
Table 11 – Percentage change in the annual number of wet days (wet day threshold = 1mm)	56
Table 12 – Percentage change in Annual 99th percentile wet day amount rainfall	57
Table 13. Percentage change in seasonality from SA Climate Ready data	58
Table 14. Percentage change in annual and seasonal PET.....	59
Table 15. Relative change (°C) in annual and seasonal maximum temperature.....	62
Table 16. Percentage change in annual in number of days above 35 degrees Celsius from SA Climate Ready data	64
Table 17. Change in attribute estimated by various climate change lines of evidence, together with chosen bounds and perturbation increments used for climate stress tests	65
Table 18. Climate scenarios for further investigation, as a fractional change relative to the climatological baseline (1976-2005)	66
Table 19. Regression form of component model results to be implemented into the Barossa PWRA Stella model. All output units are in ML, as are input units (except P and E, which are in mm) and R ² values are presented in the right-most column. Variable abbreviations are as introduced in the system diagram in Figure 9.	69
Table 20. Summary of water security and environmental flow metrics for four time periods: the baseline (1976-2005), the past decade (2011-2021), a 2050 mid-range climate projection (baseline perturbed by P=0.94 and PET=1.035), and a 2050 climate change stress test (baseline perturbed by P=0.8 and PET=1.075). Data for the driest year and average over time period are represented.	113
Table 21: Summary of system pathways and changes to system configuration required to meet each pathway.	114
Table 22. Summary of pathway results for Barossa Valley	139
Table 23: Summary of pathway results for Eden Valley	139
Table 24: Key assumptions made in this report, and their limitations.....	145
Table 25. Relevant areas in the region and a conversion between depth and volume	151
Table 26. Rainfall stations in the key project delineations	153
Table 27. Summary of neighbouring rainfall stations.....	154
Table 28. Stations in the key project delineations from which FAO56 PET is estimated	154
Table 29. Regression form of component model results to be implemented into the Barossa Valley Stella model. All output units are in ML, as are input units (except P and E, which are in mm) and R ² values are presented in the right-most column.....	156

Table 30. Regression form of component model results to be implemented into the Eden Valley Stella model. All output units are in ML, as are input units (except P and E, which are in mm) and R² values are presented in the right-most column.169

1 Introduction and Background

1.1 Study Objectives and Report Outline

The South Australian Department of Environment and Water (DEW) is developing a water security strategy for the Barossa and Eden Valleys. As a part of the development of this strategy, the University of Adelaide has been asked to partner with DEW to evaluate the water security across the region both now and over the next 30 years to the year 2050, with consideration of:

- Current and projected future availability of native water resources (surface water and groundwater) under current and changing climate conditions;
- Current and projected future demand for water, with a particular focus on irrigation demands from the viticultural sector; and
- Implications of a set of possible adaptation pathways identified as part of a new Barossa Water Security Strategy

Given the significant climate uncertainty over the nominated 30 year future horizon, this study will apply the 'Climate Resilience Assessment Framework and Tools' (CRAFT; Bennett et al, 2018) to formally stress-test the Barossa water supply and demand system under a range of climate scenarios, considering both the 'baseline' system configuration and a range of identified adaptation pathways. The framework component of CRAFT comprises five distinct steps as illustrated in Figure 1, and involves stress-testing each system configuration under a range of future climate scenarios in a manner that supports adaptive decision making. Whilst the steps are described sequentially in Bennett et al (2018), in practice there is significant iteration associated with each step as insights are generated and as new information comes to light.

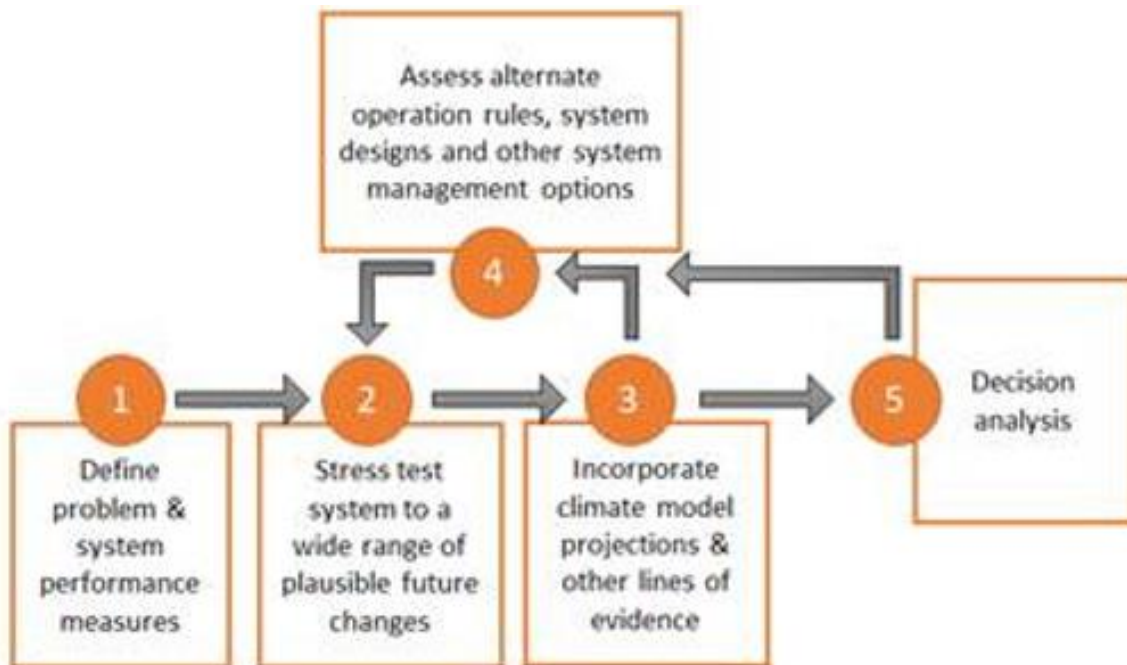


Figure 1. The Climate Resilience Assessment Framework (adapted from Bennett et al, 2018).

The work in this report represents the first application of CRAFT to a problem context of the scale and complexity of the Barossa and Eden Valley water resource system. As an applied research project undertaken by the University of Adelaide on behalf of DEW, the work seeks to simultaneously support DEW's immediate needs in the context of Barossa water security planning, while also developing the framework and tools to be generalized to other contexts. As such, this project has three primary objectives:

Objective 1. Apply CRAFT to the Barossa and Eden Valley water resources system in order to support the development of a regional water resources strategy

Objective 2. Articulate the value-add of applying CRAFT to water security assessments for mid-complexity water resource systems such as the Barossa and Eden Valleys

Objective 3. Identify and, where possible, implement improvements to CRAFT to enhance applicability and generalizability of both the framework and tools for future applications

This report describes the application of CRAFT to the Barossa and Eden Valley context (Objective 1), with Objectives 2 and 3 covered in an accompanying report. The remainder of Section 1 of this report provides further context to the study area, and summarises various historical investigations and modelling activities that have significantly informed the present work. Section 2 then provides the outcome of Step 1 of the framework part of CRAFT (henceforth referred to as ‘the framework’; see Figure 1), and thus describes the approach to system representation, including the description of system performance measures used for the remainder of the analysis. The water resources system comprises a complex set of processes representing both supply (including surface water, groundwater and external water sources) and demand (predominantly from irrigated viticulture), and a summary of historical and current water stores and fluxes associated with each part of the water balance is then presented in Section 3.

Future climate scenarios are required both for Step 2 of the framework (particularly with a view to delineating the bounds of ‘plausible future changes’) and for Step 3 (incorporation of alternative lines of evidence), and the primary lines of evidence used to inform the climate change analysis are documented in Section 4. The outcomes of the system ‘stress test’ (Step 2 of the framework) are then documented in two phases. The first phase represents the outcomes of the stress tests separately for each of the key components of the system, and this is documented in Section 5. The stress test is then conducted on the integrated system model (using a modelling framework that combines each of the key system components), and this is summarised in Section 6. Though a separate process associated with the water strategy work, four possible adaptive pathways were identified, and each of these pathways have been subjected to the same stress testing process as the current system configuration. This represents Step 4 of the framework, and the outcomes of these stress tests are documented in Section 6.2. This section also provides a comparison between the different adaptive pathways, with a view to supporting subsequent decision making processes as articulated in Step 5 of the framework.

1.2 Study Area(s)

The area of study comprises the Barossa and Eden Valleys, with various alternative delineations shown in Figure 2. The largest delineation is the Barossa Geographic Indicator zone, and the term ‘Barossa Valley’ is often used informally to refer to vineyard regions located within this zone. However, official regional definitions are typically different from the informal usages of this term. GI zones are official descriptions of Australian wine zones prepared by Wine Australia to protect the integrity of the regional labels. A specific regional label can be used to brand wines only if they are prepared using a minimum 85% of the fruit from the GI zone.

The Barossa GI zone contains two very distinct wine regions: the Barossa Valley and Eden Valley. These wine region divisions are based on attributes of the region, including elevation, climate, and the dominant winegrape varieties that are cultivated in the region. The location of the vineyards in the Barossa GI [as of December 2020, received from DEW] are overlaid on the regional delineations of the wine regions in Figure 2, and highlight differences in vineyard density across the two wine regions. Furthermore, the Barossa and Eden Valley wine regions are also different in terms of the availability of external water from alternative sources. In particular, most of the vineyards in the Barossa Valley wine region are connected to the largest supplier of external irrigation from the Murray River, the Barossa Infrastructure Limited (BIL), whereas the vineyards in the Eden Valley wine region are not and thus have much more limited water supply options.

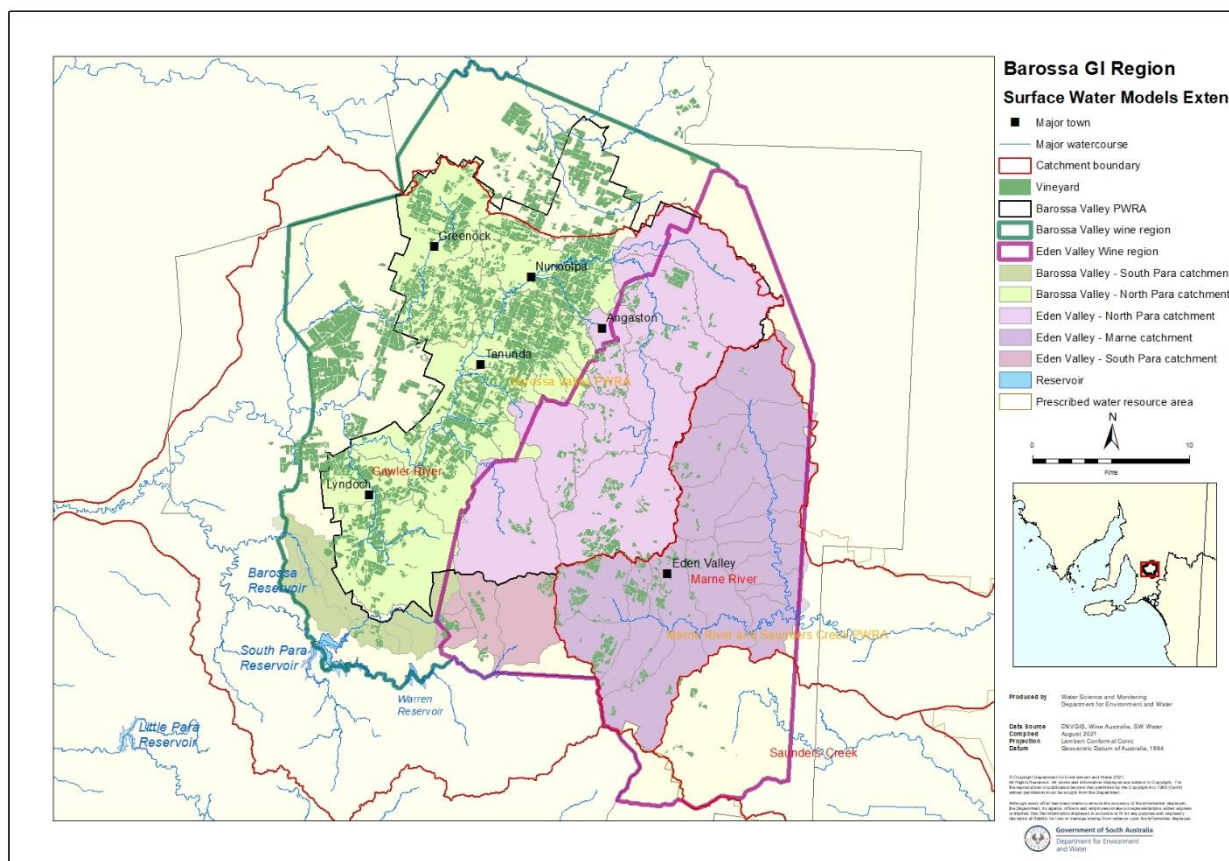


Figure 2. The Barossa Geographical Indicator (GI) Zone (the hatched region), Barossa Valley and Eden Valley wine regions (red boundaries), location of the vineyards (green) and the prescribed water resources area (PWRA) (black boundary). Catchment boundaries (light blue) are delineated by Government of South Australia.

An alternative regional delineation that is important for modelling the surface water and groundwater resources in the region is the Barossa Prescribed Water Resources Area (PWRA). Prescribed water resource areas are used by DEW to support water allocation planning. Importantly, the Barossa PWRA also defines or partially defines the spatial extent of several of the numerical models that are used to represent key processes described in this report. The spatial boundaries of the Barossa PWRA are different from the wine region definitions due to differences in the intent of their usage. In particular, whilst the Barossa GI and wine regions are defined to protect the regional labels, the Barossa PWRA is delineated roughly based on natural catchment boundaries used for water resources modelling and water allocation planning. The Barossa PWRA contains areas from both the Barossa and Eden valley wine regions, but does not completely include either of them.

In addition to the Barossa PWRA, the Marne River and Saunders Creek PWRA is located to the southeast of the Barossa PWRA and encompasses the portion of the Eden Valley that drains to the Murray River. This region has not been subject to significant investigation in this report, but may be relevant depending on the geographic scope of possible augmented water options.

To address the different drivers and contexts of each delineation, this report provides the results from analyzing three separate delineations: the Barossa and Eden Valley wine regions, and the Barossa PWRA. Where there is significant overlap between the analyses for each delineation, this report will focus on the Barossa PWRA with additional insights from the other regions included in an appendix. However, primary insights from all three delineations are provided in the body of this report.

1.3 Historical and current land use in the Barossa and Eden Valley regions

The Barossa Geographic Indicator (GI) zone is most widely recognised as one of Australia’s premier wine making regions, and also has a vibrant tourism industry. The current population is approximately 25,000 (based on Barossa Council data; 2020 figures), having increased by 20% from 2005 (<https://profile.id.com.au/barossa/highlights-2016>, accessed 27 Sep 2021). This is equivalent to an annual population growth rate of 1.2%, which is slightly below Australia’s average annual population growth rate of ~1.5% over this period (e.g. <https://data.worldbank.org/indicator/SP.POP.GROW?locations=AU>). Key townships include Nuriootpa, Tanunda, Angaston, Williamstown and Lyndoch. Given the importance of viticulture in this region, a brief overview of the development of the industry is provided.

Although the region has been associated with viticulture since 1850, the scale and role of vineyards in the region has changed significantly over time. Most recently, the Barossa and Eden valley regions witnessed significant increases in vineyard area during the early to mid-2000s (Figure 3) as part of what has been referred to as the ‘fifth boom cycle’ of the Australian wine industry that started from approximately the mid-1980’s and continued until approximately 2008 (Anderson, 2015). As can be seen in Figure 3, total planted area subsequently stabilized with only very minor growth in planted area from 2008 until present.

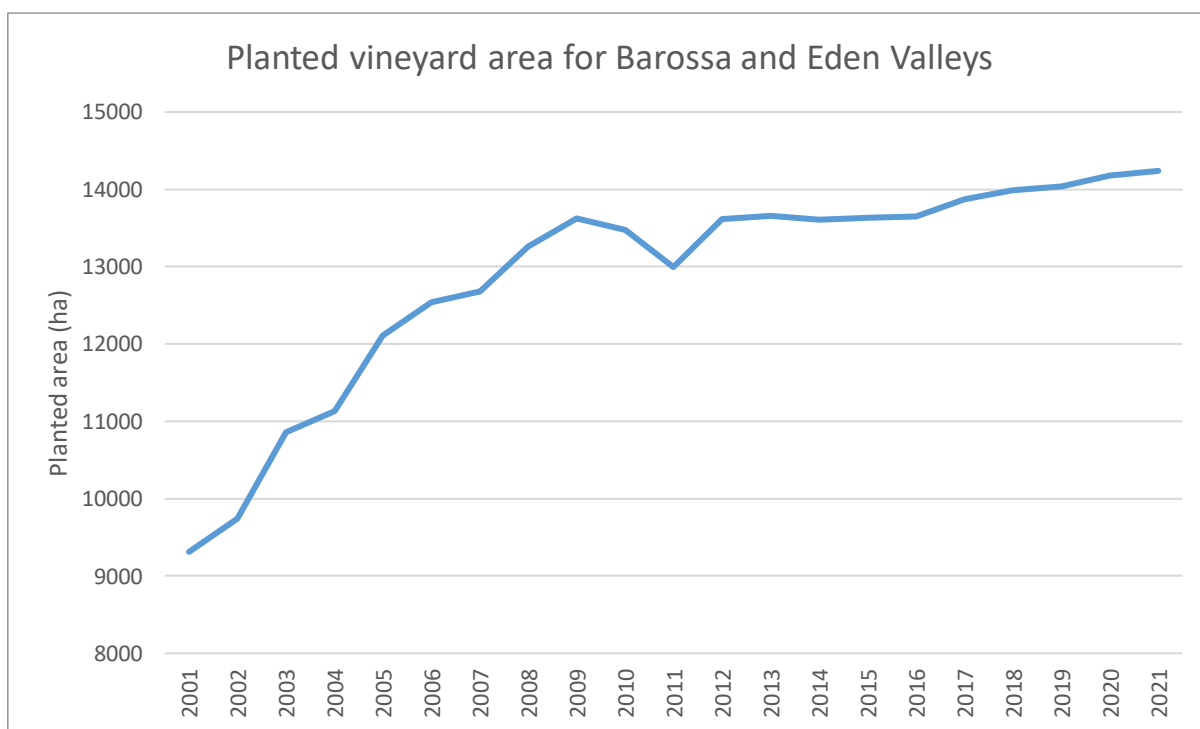


Figure 3. Planted vineyard area for the combined Barossa and Eden Valley regions obtained from Vine Health Australia Production Reports (Source: <https://vinehealth.com.au/news/sa-winegrape-crush-survey/>, accessed 20 September 2021)

Figure 4 shows the trend in percentage of planted area of different winegrape varieties in the Barossa and Eden Valleys. Whilst shiraz consistently has been the single most common winegrape variety in the Barossa Valley over the period since 2001, there have been significant changes in the relative composition of different varieties over the last two decades. For example, red varieties expanded from 68.5% to 87.3% of the total crush over the period from 2001 to 2021 across Barossa and Eden Valleys, with shiraz in particular increasing rapidly from 37.9% to 59.5% across the two valleys over this period. This increase was offset by a more than halving of white winegrape varieties. For the Barossa Valley in particular, white varieties decreased from 31.5% to 7.8% of the total planted area from 2001 to 2021. In contrast, the split between white and red varieties in Eden Valley has remained more steady over this period, with white varieties consistently comprising approximately 40-45% of the overall Eden Valley planted area.

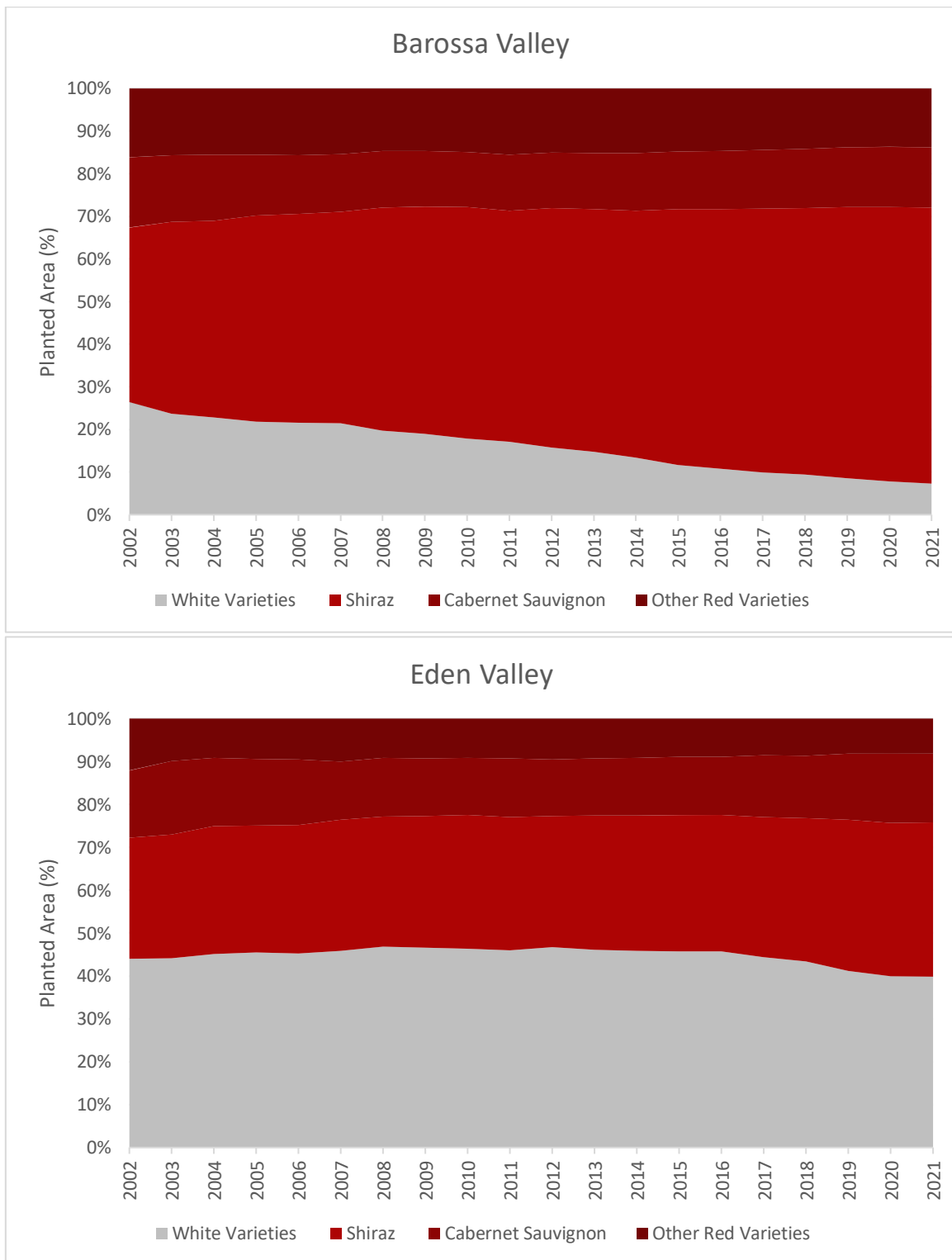


Figure 4. Trend of area of white, shiraz, cabernet sauvignon and other red varieties as a percentage of total planted area in the Barossa Valley (top) and Eden Valley (bottom), obtained from Vine Health Australia Production Reports (Source: <https://vinehealth.com.au/news/sa-winegrape-crush-survey/>, accessed 24 November 2021)

Figure 5 show the historical grape yields per hectare from the Barossa zone. The grape yields show significant year-to-year variations, ranging from 7 T/ha or more in the early period to a low of 2.3 T/ha for 2020; moreover, a visual inspection of this time series suggests what appears a trend of declining yields. The reasons behind the declines are not explored in the available reports reviewed in this research, but is generally thought to be due to changes in climate and associated increase in water scarcity, as well as a trend towards ‘premiumisation’ of wine production. The changes in vineyard area and variety over the period of

record also may have an influence on the average yield, though this has not been mentioned in the available reports.

These three factors—the planted area, the winegrape variety and the yield—represent important controls on overall water demand from the viticulture industry in the region, and depicting changes to these controls through time helps to illustrate the highly dynamic nature of the industry over a timespan of 20 years. This has important implications when developing plausible future water balance scenarios over multi-decadal timespans, with the horizon for the Barossa Water Security Strategy spanning up to 2050.

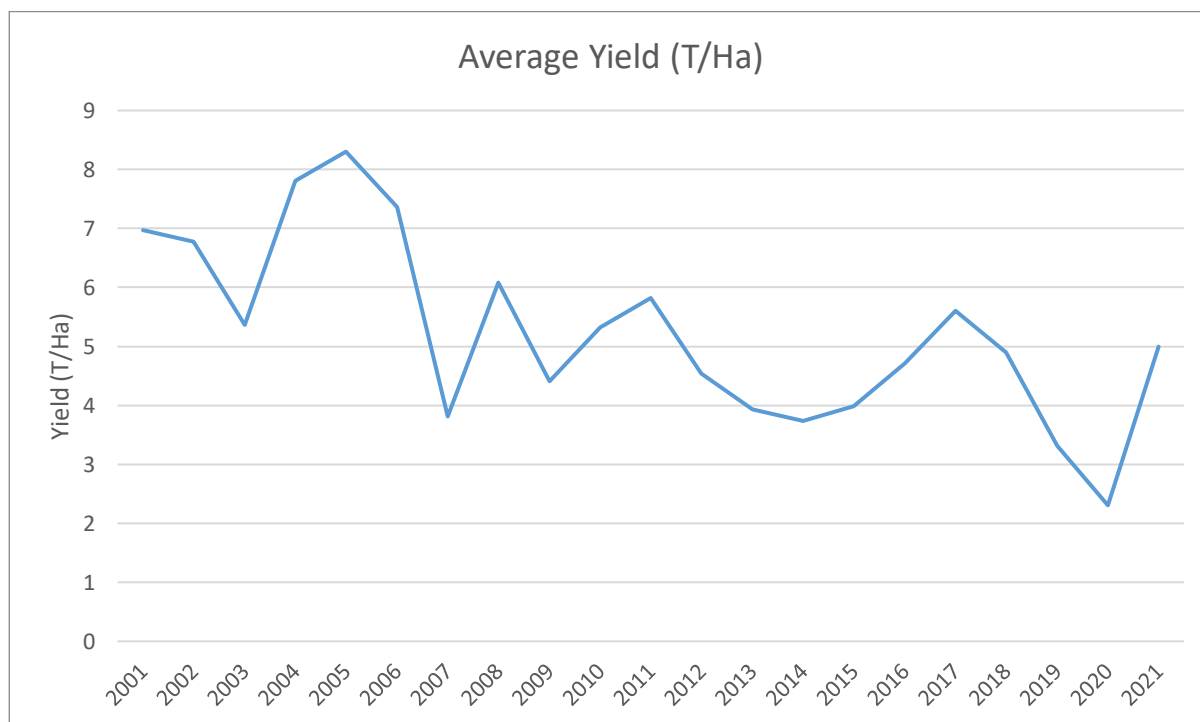


Figure 5. Average grape yield per hectare for the combined Barossa and Eden Valley regions obtained from Vine Health Australia Production Reports (Source: <https://vinehealth.com.au/news/sa-winegrape-crush-survey/>, accessed 20 September 2021), calculated as total crush divided by planted vineyard area.

1.4 Historical development of the Barossa’s water infrastructure

Water infrastructure in the Barossa GI zone has developed significantly over recent decades, with key developments aligning with corresponding developments in the region’s viticulture industry. A brief summary of available information on the historical development of infrastructure is provided here, with the phrase ‘water infrastructure’ defined broadly as comprising any distributed or centralized physical asset that enables access to native and/or imported water sources.

1.4.1 Farm dams

Farm dams are a major storage of surface water across the region. During the period from early 1970s to 1991 there was reported to have been a ten-fold increase in farm dam storage capacity in the Barossa Valley (Jones-Gill and Savadamuthu, 2014). Farm dam development has since slowed, particularly since prescription of water resources and the development of water allocation plans for the region (Jones-Gill and Savadamuthu, 2014).

Farm dams are used in the region to capture surface water for irrigation, stock, and domestic uses. The dams used for irrigation are licensed and water use is metered. The dams used to cater to stock and domestic water demands are not licensed, and the capacities of these non-licensed dams are estimated based on aerial surveys (Jones-Gill and Savadamuthu, 2014). Focusing first on the Barossa PWRA, it has been estimated that there are a total of 1780 farm dams in this region (Table 1; Montazeri and Savadamuthu, 2020), of which 255 are licensed dams with a total capacity of 5.94GL. The remainder (1525 dams) are non-licensed with an

estimated capacity of 2.76 GL (Table 1). Thus, the total estimated storage capacity of the farm dams in the PWRA is 8.70 GL, 68% of which is licensed for irrigation use (Montazeri and Savadamuthu, 2020).

Table 1. Number of farm dams and their capacity across the three study delineations.

Delineations		Dam count	Dam capacity (GL)
Barossa PWRA	Licensed	255	5.94
	Non-Licensed	1525	2.76
	TOTAL	1780	8.70
Barossa Valley	Licensed	173	2.91
	Non-Licensed	1173	2.97
	TOTAL	1346	5.89
Eden Valley	Licensed	206	5.36
	Non-Licensed	1678	3.09
	TOTAL	1884	8.45

For the Barossa Valley delineation there are a total of 1346 dams with a capacity of 5.89 GL, of which 173 dams with the capacity of 2.91 GL used for licensed purposes, and 1173 unlicensed dams with the capacity of 2.97 GL are non-licensed (Table 1). For the Eden Valley wine region, there are 1884 farm dams in the Eden Valley with a total storage capacity of 8.45 GL (Table 1). Of these, 206 dams are licenced, with a total capacity of 5.36 GL. The remainder of 1678 farm dams are non-licensed with an estimated capacity of 3.09 GL. Dam information was extracted from the Topography Waterbodies (<https://data.sa.gov.au/data/dataset/waterbodies-in-south-australia>) on 30/8/2021. Recognising that the Barossa PWRA sits wholly within the Barossa and Eden Valley delineations, it can be estimated that the overall Barossa GI zone has 3230 farm dams, comprising a total storage capacity of 14.34 GL, of which 8.27 GL (58%) is licensed.

Whilst rainfall represents a major input to farm dams, anecdotally some farm dams are also used to temporarily store water from imported sources such as from the Barossa Infrastructure Limited (BIL) scheme, to ensure security of supply during peak demands as might occur during heatwaves. At the time of writing, further information on the magnitude and dynamics of this water use pattern was not available, and this behaviour is not included in the Source surface water model (the Source model is discussed further in Section 1.5.2).

1.4.2 Imported water pipeline systems

The Barossa Valley wine region uses water from external sources for irrigation. These external sources of water are the River Murray and storm water harvested from urban areas in Gawler. The River Murray water is delivered through the Barossa Infrastructure limited (BIL) pipeline during the growing season, and the SA Water main pipeline during the off-peak (April to October) season (termed “SA water off-peak”). The BIL pipeline connection is available only in the Barossa Valley wine region and services 75% of the growers within that delineation (Source: Options consultation report). BIL has an annual capacity of 11 GL/year as of year 2020 (Source: BIL annual report). The water supplied by the BIL pipeline accounts for the largest irrigation water use in the Barossa Valley in the recent period. There has been progressive expansions of the BIL pipeline capacity since its inception in 2002 to cater to increasing demands for water, as shown in Table 2.

Table 2. Historical expansion of BIL capacity (Source: BIL annual reports)

From Year	BIL Capacity (GL/year)
2001/02 (inception)	7
2014/15	8
2015/16	9
2018/19	11

In addition to the BIL scheme, storm water from Gawler is delivered through the Bunyip pipeline that services the Seppeltsfield Vineyard in the western edge of the valley floor. Almost all of the water from the Bunyip pipeline (up to 2 GL) is delivered to Seppeltsfield after taking out 50ML to service the Hewett region (Barossa Wine and its Ecosystem, n. d.). The Bunyip scheme started operation in water year 2016 (Source: Bunyip Water Pty. Ltd, n. d.), and secures water from a mix of storm water runoff from urban areas in Gawler and recycled water from the Bolivar treatment plant.

Figure 6 shows the layout of BIL and SA Water pipelines in the region. The figure does not include the Bunyip pipeline, but the approximate location of Seppeltsfield vineyards that receives Bunyip water is marked for reference.

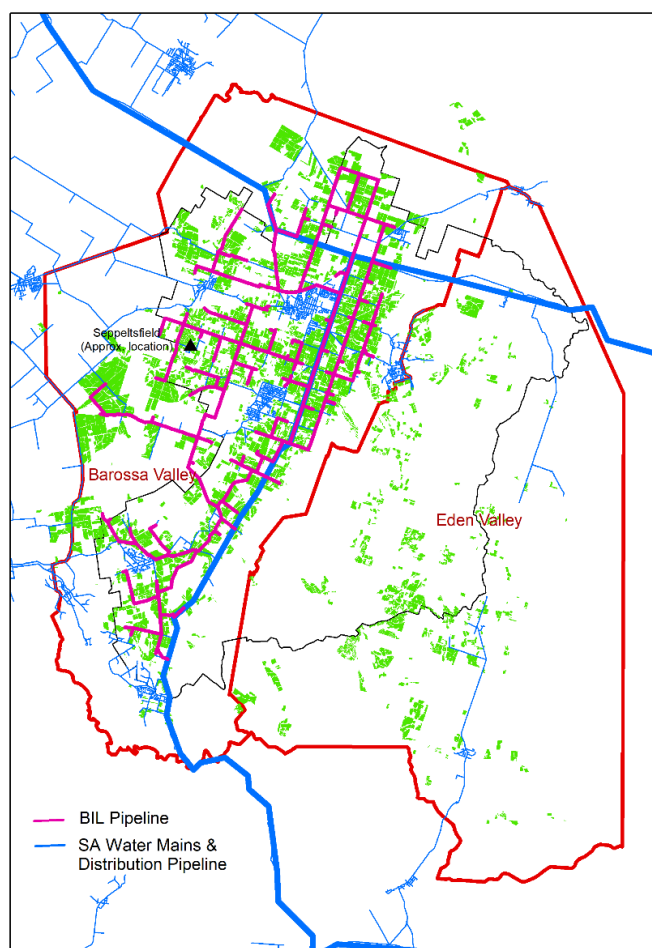


Figure 6. The layout of SA Water and BIL pipeline network and the approximate location of Seppeltsfield vineyards that receive water from the Bunyip pipeline

1.4.3 Groundwater resources and associated infrastructure

Groundwater systems in the form of aquifers (sediments that are capable of storing and transmitting significant volumes of water) represent an increasingly important source of water for the region, and are made accessible via abstraction wells and pumping systems. Anecdotally, some wine grape growers have also

invested in small-scale desalination to address water quality (particularly salinity) issues, although little is currently known about the penetration and/or likely future update of this technology. In the context of groundwater assets, ‘infrastructure’ thus refers to assets associated with accessing, extracting and treating the groundwater resources.

Groundwater occurs predominantly within an ‘upper’ unconfined/confined aquifer, a ‘lower’ confined sedimentary aquifer, and fractured rock aquifer(s). The sedimentary aquifers are largely restricted to the central Barossa Valley between Nuriootpa and Lyndoch, whereas the fractured rock aquifers extend across the entire Barossa PWRA and Eden Valley, as shown in Figure 7. The number of licensed wells for the three study areas are presented in Table 3. The reader is referred to Li and Cranswick (2015) for details regarding the hydrogeological setting of the Barossa PWRA.

Table 3. Number of licensed extraction wells in the three study areas

	Barossa PWRA	Barossa Valley	Eden Valley
Fractured	216	145	165
Lower	116	124	1
Upper	78	85	0
TOTAL	410	354	166

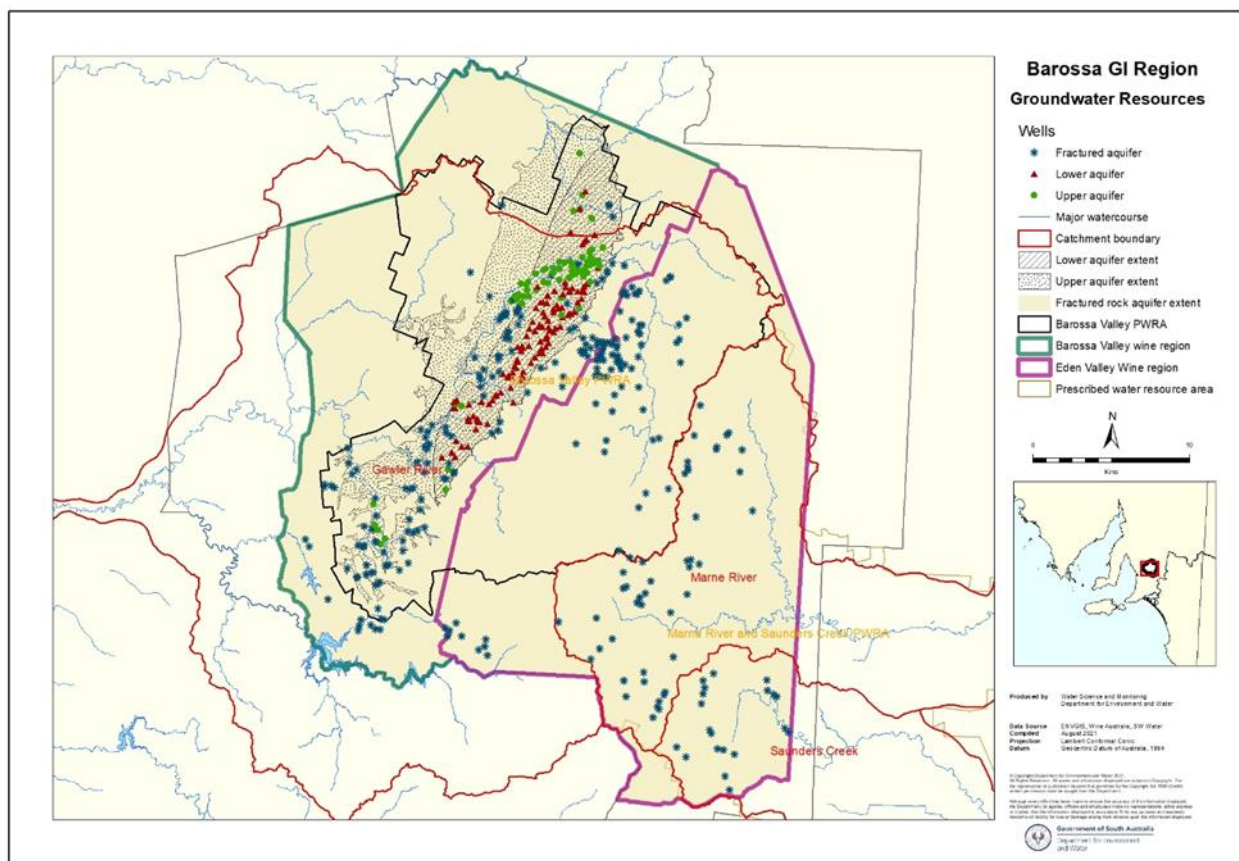


Figure 7. Aquifer extent map with location of abstraction wells

Groundwater is abstracted from all three of these main aquifers for irrigation (primarily for viticulture), stock and domestic water supply. The vast majority of groundwater use is for irrigation; only about 2% of estimated groundwater use is believed to be used for stock and domestic supply (Cranswick et al., 2016). The fact that abstraction wells were installed in and are still used to access groundwater from each aquifer reflects the suitably high transmissivity associated with the different aquifers (e.g., high well yields). The number of

abstraction wells in use is thought to be stable since the early 1990s following considerable expansion. The distribution of abstraction wells and the aquifer in which they are slotted is shown in Figure 7. The relative proportion of groundwater abstraction from different aquifers, as well as historical abstraction and allocation trends, is discussed in Section 3.6.

Groundwater from the upper sedimentary aquifer is not commonly used for irrigation due to its high salinity (900-12000 mg/L); a generally accepted salinity threshold limit for irrigation of vines is 1500 mg/L (Cranswick et al., 2016). Groundwater within the lower sedimentary and fractured rock aquifers, however, display significantly lower salinity (400-3000 and 450-3500 mg/L respectively), and is therefore abstracted for irrigation water supply. Groundwater salinities in the sedimentary aquifers are reflective of recharge mechanisms; for example, low salinity groundwater typically is present in proximity to losing rivers. Salinities in the fractured rock aquifers, however, are highly variable and more difficult to explain (Cranswick et al., 2015). The relatively saline water abstracted from the upper aquifer is sometimes mixed (i.e., 'shandied') with lower salinity water to provide an alternative irrigation water supply. Whilst groundwater salinity varies significantly spatially, changes in groundwater salinity trends have also been observed in some areas since the 1990s (Cranswick et al., 2015).

1.4.4 Soil moisture resources and associated infrastructure

Similar to groundwater, soil moisture in the upper unsaturated zone represents a 'natural infrastructure' for water storage that is often managed actively and deliberately through irrigation within agricultural contexts. Robinson and Sandercock (2014) reported on the available water holding capacity (AWHC) of soils in the greater Barossa region. AWHC is an indicator of how much water can be effectively available for crop growth. It is therefore an attribute of particular interest in the Barossa region and to the current study.

Notwithstanding the heterogeneity in soil type, water quality and topography, the majority of the Barossa PWRA displays high (>100 cm), moderate (70-100 cm) or moderately low (40-70 cm) AWHC, with highest AWHC values typically occurring in the Barossa Valley floor. While some of the areas with high AWHC already support vineyards within the Barossa PWRA, there is also the potential for vineyard expansion into areas with high AWHC that are not currently utilised for viticulture purposes. This has important implications on capacity to expand irrigated agriculture in the future (e.g., the potential for new plantings in the future, and the likely irrigation demands for these plantings depending on the AWHC in any newly planted areas). Soil moisture in these regions is managed through irrigation practice, for the purposes of reducing grapevine water stress to some degree (e.g., 'deficit irrigation') by supplementing rainfall. Irrigation is primarily achieved using surface drippers.

1.5 Previous water resource investigations and models

1.5.1 Summary of historical investigations

Historical water resource investigations have primarily focused on the Barossa PWRA delineation, to understand the rate of resource use in the Barossa PWRA and the impact of water use on the natural state of these resources. Over the past decade, these investigations have been performed using two primary models: an eWater Source surface water model and a MODFLOW groundwater model. A number of key references provide useful background to the models and datasets used in this report, and these are summarised briefly as follows:

- Jones-Gill and Savadamuthu (2014) established a hydrological model to incorporate rainfall-runoff relationships together with surface water use. This model was used to quantify the level of surface water use in the Barossa PWRA relative to resource capacity for seventeen project management zones, through modelling scenarios of different water management practices to assess their impact. A key finding is that the water use from farm dams and watercourses have reduced the average annual streamflow at Yaldara by around 23%.

- Montazeri and Savadamuthu (2020) provide an update of the surface water model to include additional farm dams, and recalibrated the model to include data up to 2016. A key finding was that the current level of development (farm dams and watercourse extractions) has potentially reduced the average annual streamflow in the Barossa PWRA by around 17% (>50% during dry years).
- Hancock et al. (2014) studied interactions between groundwater and surface water systems in the Barossa PWRA, and found that the groundwater and surface water systems can generally be classed as 'highly connected', with a combination of gaining and losing stream conditions depending on the season and location.
- Cranswick et al. (2015)¹ conducted a preliminary assessment of the capacity of groundwater resources in the Barossa PWRA to meet demands (both consumption and from ecosystem sustainability perspective). The desktop assessment involved synthesising previous reports, reviewing monitoring data and development of annual water balances for various aquifer delineations and groundwater management zones. Total resource capacity was estimated to be between 3.45 and 9.75 GL/y (median = 6.61 GL/y), and the preliminary extraction limit (PEL) was estimated to be between 1.25 and 4.28 GL/y (median = 3.31 GL/y). This exceeded the 10-year average groundwater use at the time (2.09 GL/y), but several high groundwater use years exceed the PEL.
- Li and Cranswick (2016) reported on the groundwater model development and application. The model builds upon Cranswick et al. (2015) to further support the estimation of groundwater resource capacity as well as appropriate ranges of extraction limits (using the model to better quantify the impacts of groundwater abstraction in space and time, including under different water use and climate scenarios). The model was deemed to be 'fit for purpose', in that it can 'successfully represent regional flow processes with medium to high confidence in 11 of 12 proposed groundwater management zones'. Scenario analyses reveal that groundwater levels and storages remain stable under climate change scenarios where recent 10-year average groundwater abstraction is considered. However, pumping at full allocation (7.8 GL/year) was found to cause dramatic reductions in groundwater storage, whereas pumping at five highest pumping years during the period 2006-2015 (3.5 GL/year) also caused declining storage trends, dampened in confined aquifers, with moderate reductions in baseflow in proximity of pumping.
- Cranswick et al. (2016) integrates the findings of Cranswick et al (2015) and Li and Cranswick (2016). The main objective is to determine 'sustainable extraction limits' (SELs), which will be used to inform the Water Allocation Plan. The report does so by describing the implications of Li and Cranswick's (2016) modelling results towards policy development. The report presented a series of resource condition limits (RCLs) that aim to ensure that resource conditions do not deteriorate beyond historical experience (as declining levels and increasing salinities have been observed). Based on this work, the aggregated Barossa PWRA was estimated to have a resource extraction limit (REL) range of 3.12 to 3.58 GL/y. The lower limit is above the recent 10-year average abstraction rate.

Further information pertaining to the key surface water and groundwater models used in the study area are described in the following sections.

1.5.2 eWater Source

Jones-Gill and Savadamuthu (2014) developed a model of the surface water resources of the Barossa PWRA in the eWater Source modelling platform. The model was calibrated using streamflow data from 01/06/2003 to 01/06/2013, and validated for the period 01/06/1999 to 30/05/2003. Montazeri and Savadamuthu (2020) updated the model to include additional farm dams and also extended the data used for calibration (using the period from 2003 to 2016). The development of the surface water model detailed in these reports is

¹ Report was not finalised officially. It remains in 'unpublished draft' form.

briefly summarized in this section. The reader is referred to the DEW surface water modelling reports (Jones-Gill and Savadamuthu, 2014; Montazeri and Savadamuthu 2020) for more detail.

The Barossa PWRA is divided into 365 minor sub-catchments for surface water modelling. The rainfall-runoff behaviour of these sub-catchments are modelled using the GR4J formulation in the eWater Source software. The division of these sub-catchments are based on multiple factors such as locations of farm dams/licensed water extractions, streamflow gauging stations, locations required for ecological flow assessments, environmental flows and/or scenario testing. Six functional units based on landuse and soil texture are represented in the rainfall-runoff models. The eWater Source model excludes Stockwell Creek, Victoria Creek, and small pockets of land along the boundary that are not hydrologically connected to the North Para and Greenock Creek Catchment areas.

The farm dams in the Barossa PWRA are modelled using the farm-dam plugin in eWater source. The volume of farm dams used for licensed extractions are available from the surface water licenses, and this information is used in the model. For unlicensed farm dams, the model uses information from an aerial survey undertaken in 2012. The surface area of these farm dams are available from the aerial survey, and an empirical estimate of the farm dam volume from the area is used for the modelling. The annual water demand from licensed farm dams is prescribed using the historical water use data from 2005 to 2013. Similarly, the historical water use from water course extractions are used to prescribe the demand of water users in the model. For unlicensed stock and domestic farm dams, an annual water demand of 30% of the dam volume is assumed and prescribed in the model, as historical water-use data is not available. The annual demand numbers are assigned a seasonal pattern following the monthly distribution of potential evapotranspiration. The actual water supplied in the model may be less than or equal to the prescribed demand based on the amount of water available during the simulation.

Montazeri and Savadamuthu (2020) calibrated the eWater source model to daily stream flow records from four gauging stations for the period 01/06/2003 to 31/12/2016. It is noted that the simulated annual and monthly correlations are better than the daily correlations. For annual streamflow at Yaldara, the calibrated model exhibits an R-squared value of 0.95 and Nash-Sutcliffe Efficiency of 0.90. At the daily scales, the simulated high flows are generally lower than the observed high flows. There are also some deficiencies in capturing flows during specific seasons (e.g. later autumn/early winter wetting events, late spring baseflow events). Overall the metrics of calibration and validation are reported to be satisfactory.

Similar to the Barossa PWRA, a new hydrological catchment model was developed for the Marne River catchment using eWater Source. Previous surface water assessments and modelling were undertaken in the Upper Marne River catchment with WaterCress by Savadamuthu (2002) which contributed to the development of the Marne Saunders WAP. The WaterCress model has been updated and refined and supports South Australia's requirements under the Murray Darling Basin Plan. The new Source model explicitly represents all runoff-capturing farm dams and licensed extractions and diversions and exhibits a similar level of functionality to the existing WaterCress model.

The catchment model was calibrated to observed daily streamflow data in the Marne Gorge for three periods:

- 1975–88: chosen to replicate the original calibration undertaken in WaterCress, which is also the calibration period used in developing the Marne Saunders WAP. The data used for this stage was solely from the older streamflow gauging station A4260529 (Savadamuthu 2002).
- 1975–2019: chosen to undertake calibration for the longest period of available streamflow covering both streamflow gauging station records. Poor quality data and flow days below 0.1 ML/d were filtered out in the calibration.
- 2010–19: chosen to calibrate to the recent post-Millennium drought conditions. The data used for this calibration stage was unfiltered and was solely from the newer streamflow gauging station (A4260605).

The model has been calibrated to observed streamflow data for the main streamflow gauging station in the Marne Gorge (A4260605). Daily flow duration curves are described as having a general good fit between modelled and observed data. As part of the model validation, each of the three model versions were run for the same period (1975–2019). Model validation has shown that the 1975–2019 calibrated model performed best in ‘average’ years across this period and modelled streamflow was closer to observed streamflow. This version of the model also performed well in dry years. However, modelled outputs show that this model version has a tendency to overestimate streamflow when compared to observed data for much of the flow range except in the high flow range. Each of the model versions may be more suitable for a different purpose. For example, the 1975–2019 best replicates ‘average’ conditions but the 2010–19 could be more appropriate for a WAP review or climate change analysis if the dry years are expected to continue in to the future. Nevertheless, the 1975–2019 model version is used in this study given that the ‘stress test’ work includes a range of scenarios comprising both increasing and decreasing rainfall volumes.

1.5.3 MODFLOW

The numerical groundwater flow model of Li and Cranswick (2016) was developed for the purposes of supporting the estimation of groundwater resource capacity as well as appropriate ranges of sustainable extraction limits (which are used to inform the WAP following subsequent analyses by Cranswick et al. (2016)). The model was designed to simulate regional-scale groundwater processes that are deemed to be relevant for groundwater resource management and policy development, including regional-scale aquifer responses to different climate and groundwater abstraction scenarios. The model was the first of its kind (e.g., capable of simulating stress impacts in space and time) for the Barossa PWRA.

The model integrates diverse and recently updated data and knowledge streams. In particular, the model was developed and calibrated on the basis of hydraulic, hydrochemical and salinity observation data, as well as baseflow and groundwater age estimates. It also integrated recently updated Barossa PWRA hydrogeological knowledge (e.g., independent time-averaged water balance estimates) reported by Cranswick et al. (2015), and recent work on surface water-groundwater interactions by Hancock et al. (2014).

2 Conceptual representation of the Barossa Water Resources System

Developing a quantitative representation of a given climate-sensitive system represents a core component of the CRAFT ‘stress testing’ framework, as it provides the basis for assessments of how changes in climatic forcings lead to changes in system states, fluxes, and outcomes (the latter referred to here as the system ‘performance’²). In this section the high-level conceptual approach to system representation is described, with more detailed description of each of the key water stores and fluxes described in Section 3.

As recommended in the CRAFT documentation (Bennett et al, 2018), a systems approach is adopted to describe the Barossa and Eden Valley water resource system(s). At its most basic, the delineation of the system used in CRAFT is illustrated in Figure 8, and shows that the climate-sensitive system represents a mapping between the climate forcings (or climate ‘inputs’) and measures of system performance. The term ‘system model’ refers to the numerical implementation of this mapping.

The CRAFT approach, as a specific implementation of ‘bottom-up’ climate impact assessment methods, uses measures of system performance as the starting point for determining system representation. As such, measures of performance used for the remainder of the analysis are now described.

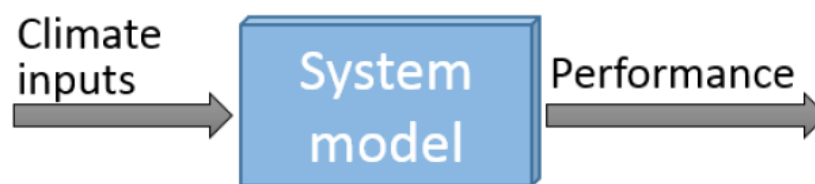


Figure 8. Definition of ‘system model’ used in CRAFT (Bennett et al, 2018)

2.1 System Purpose: Defining Performance Metrics

Defining system purpose is a core decision that influences all other aspects of system modelling, and is characterized by its normative content in that it ultimately depends on the values of key stakeholders, rather than being something that can be rationally determined by technical experts. The key elements of system purpose for the Barossa and Eden Valley water resource systems have been identified by DEW and supported through a series of stakeholder workshops, and comprise two key dimensions:

- Provision of water security to consumptive end-users (predominantly but not exclusively agricultural users); and
- Maintenance or enhancement of ecological outcomes.

² Within the systems literature, systems are typically defined by the ‘function’ or ‘purpose’, with ‘function’ usually used for natural (non-human) systems while ‘purpose’ is more commonly used for human systems. Another similar term that is more commonly used in the risk literature is ‘objectives’ (in the sense that ‘risk is the effect of uncertainty on objectives’). CRAFT has traditionally used system ‘performance’ as representing measures of the system’s purpose or objectives; however it is noted that in the context of this report these terms can be used largely interchangeably.

In translating these dimensions of purpose into quantitative performance metrics, it is noted that the scope of the modelling described in this report comprises simulation of changes to physical stores and fluxes of water throughout the water resources area³. This leads to the metrics described in Table 4, where:

- Metrics associated with water security are represented largely in terms of either volume of unmet demand, or percentage of years with unmet demand; and
- Metrics associated with ecological outcomes are based on ecologically significant parts of the flow duration curve (pers. comms. DEW, 20/09/2021).

Whilst these metrics necessarily only provide a limited snapshot of the functioning of the Barossa and Eden Valley water resource systems, this constraint needs to be balanced against the need for a sufficiently small set of metrics that can be analysed consistently and tracked over time and across different adaptive pathways to support decision making. Various additional system metrics, including intermediate calculations, are also documented in various places throughout this report; however the metrics described in Table 4 are the primary metrics used for comparison of the baseline system performance and adaptive pathways as described in Sections 6 and 6.2.

Table 4. Summary of water security and ecological system performance metrics to be explored in this report

Metric Type	System Performance Metric	Description
Water Security	Average unmet demand	The average volume deficit of the system to supply all required demand in any given year.
	Percentage of years with unmet demand	The percentage of years in which the system is unable to supply demand. This gives an indication of the expected frequency of failure.
	Average unmet demand in years with unmet demand	The average volume deficit of the system to supply all required demand, in each year where demand is not met. This gives an indication of how severe failure is when it occurs.
	Ratio of supply and demand for defined reliability	The total available water supply divided by the demand in a given year. All the ratios for a given perturbation scenario are ranked smallest to largest and the third smallest year is chosen for the perturbation combination. This corresponds to 90% reliability (3 rd worst year out of 30).
Ecological	Flow days	The number of flow days gives an indication of stream ecosystem health, as days with no flow can negatively impact dependent flora and fauna. Flow days are defined as any day with flow greater than 0.05ML.
	Medium flow days	The number of flow days larger than the 50 th percentile relative to the historical baseline
	Days over threshold flow	The number of days over the threshold flow rate, which is the flow rate required to produce a flow depth of 12cm. This is an important flow depth for several ecological functions.

³ Other elements that could be considered relevant are the impacts of water quality and/or prices on water use patterns, and ecological outcomes associated with different environmental flow metrics. Both these elements are outside the scope of this report.

Water security metrics are evaluated on a water balance basis for each delineation. In contrast, ecological metrics will be assessed for two separate zones: the Barossa Valley Gorge and Upper Flaxman Valley. These are important as they represent the end of system (Barossa Valley Gorge outflow is the outflow from the North Para River at Yaldara) and an important zone for representing ecosystem health, respectively.

2.2 System Representation

Having identified the system's 'key performance metrics', it is now possible to develop a modelling framework to capture key system dynamics that can influence the state of each performance metric. Within the scope and constraints of this study, the modelling framework should be:

- Capable of representing the impacts of climate change on key aspects of system dynamics, ultimately leading to the production of estimates of changes to system performance metrics;
- Capable of integrating a range of possible alternative system configurations (or 'adaptive pathways') that are designed to improve system performance for some or all future climate scenarios;
- Capable of integrating existing domain knowledge and modelling platforms where possible, including the eWater Source and MODFLOW models as well as any relevant irrigation demand models;
- Capable of rapidly integrating alternative process representations to enable testing of key assumptions (for example alternative representations of irrigation demand) and/or the outcome of expert elicitation processes for aspects where process models are unavailable;
- Easy to update with alternative adaptive pathways and/or updated understanding of key processes; and
- Accessible and easy to interpret, with a range of diagnostic and plotting functions to support visualization.

Based on these criteria, it was decided to use a systems dynamics modelling framework that was capable of reflecting stores and fluxes in a consistent manner, representing processes of both supply (including surface water, groundwater and imported water) and demand (particularly including irrigation demands, as well as stock and domestic water demands). Advantages of this approach are that it is possible to embed insights from the 'component' models (i.e. Source, MODFLOW, etc) as well as the insights from expert elicitation processes into the system dynamics model, while also having the capacity to rapidly implement changes to system configuration. Key disadvantages of the approach include:

- The need to lump models in space and time. In particular, the system dynamics model works at an annual timestep, and aggregates information in a lumped fashion across the three modelling domains (Barossa Valley, Eden Valley and Barossa PWRA).
- The requirement of an additional step of calibrating the system dynamics model on the component models (which in turn are calibrated based on observational data).

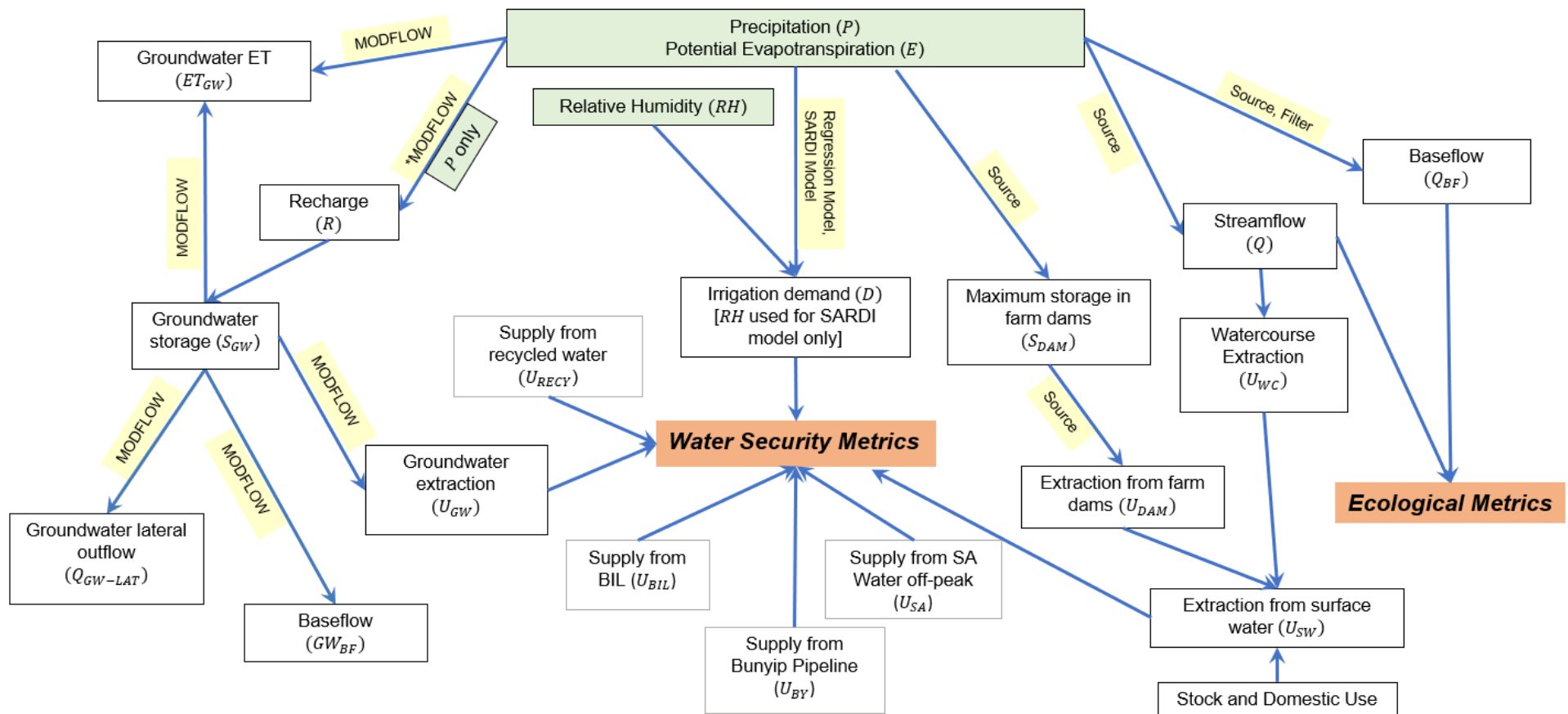
The primary alternative to the system dynamics approach was to couple each of the component models directly into a single integrated model; however this approach was not adopted because of the lack of model commensurability in terms of discretisation (e.g. Source is based on hydrological response units run at a daily scale, MODFLOW is a gridded model run at a six-monthly timestep, and the crop model is a column model run at a daily timestep), and in terms of processes (e.g. the 'losses' in Source do not represent the same processes as recharge in MODFLOW; evapotranspiration processes are represented very differently across the three primary component models; and so forth). Moreover, there is concern regarding the level of flexibility to quickly accommodate changes to representation (e.g. integrating the outcome of expert elicitation processes) and alternative adaptation pathways. As such, this approach was not pursued further here.

The overall conceptual representation of the system is summarized in Figure 9 and Figure 10. Figure 9 provides overall process description in the general form of an influence diagram, and describes how individual component models are used to represent relationships between key variables. The overall

structure is consistent with the schematic in Figure 8, with the green shaded box depicting the climate inputs, and the orange shaded box representing the key system performance metrics (Table 4). Each of the white open boxes represents a key intermediate variable, arrows denote relationships between those variables, and yellow shaded text represents the primary 'component' modelling sources that provide insight on those relationships. This figure shows the significant complexity of the Barossa water resources system, with multiple interactions between surface and groundwater (for example baseflow is an output of both the surface water and groundwater models), and between supply and demand.

An alternative representation of the same system is given in Figure 10, this time using a system dynamics representation. This representation depicts the approach taken to implementing the component models into Stella, which is the system dynamics model adopted for this study. There is significant commonality between the two representations, but the Stella platform has the additional advantage of highlighting a number of possible system 'interventions' such as increasing overall capacity of the imported water system or improving overall irrigation water use efficiency. These enable implementation of the various adaptive pathways as described in Section 6.2 of this report.

Having described overall model structure, we now turn to a description of the scientific basis of modelling each of the primary variables and connections associated with the system model. This is the focus of the next section.



*We note that the relationship between P and R is derived not directly from the MODFLOW model, but rather from an external relationship defined by Li and Cranswick (2016) required for input to the MODFLOW model.

Figure 9. Schematic system model of water fluxes and storage of various components, focusing on the Barossa PWRA. Open boxes represent variables, arrows represent relationships, the green shaded box represents the climate inputs, and orange shaded boxes represent the system performance metrics. The primary models used to represent relationships are denoted by yellow shaded text.

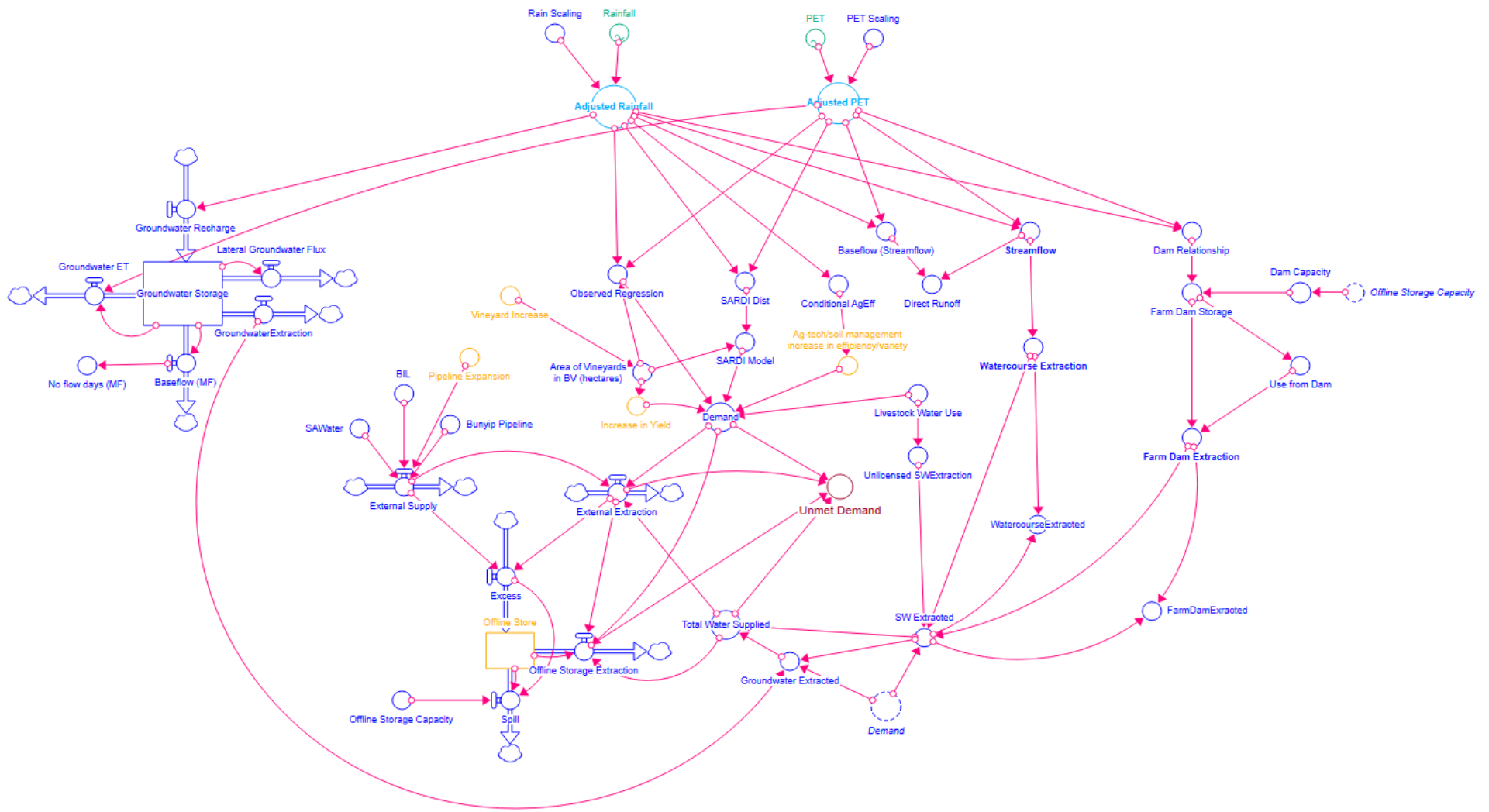


Figure 10. System model schematic using stock-and-flow diagram representation.

3 Historical and Current Water Stores and Fluxes

Using the depiction of the Barossa water resources system in Section 2.2 and particularly Figure 10, the following subsections describe best available knowledge on historical and current water stores and fluxes. The results are presented for all three delineations (Barossa PWRA, Barossa Valley and Eden Valley).

3.1 Water into the system: Rainfall (P)

Historical rainfall: key points

- Barossa PWRA had an average rainfall of 581 mm/year for the period from 1900 to 2020, with a significant spatial gradient ranging from 490 mm to 720 mm. The Barossa Valley annual average rainfall is slightly lower (552 mm/yr) whereas Eden Valley is slightly higher (599 mm/yr)
- This rainfall depth corresponds to an average rainfall volume of 51 GL/yr, 65 GL/yr and 14 GL/yr over the planted vineyard area for the Barossa PWRA, Barossa Valley and Eden Valley delineations, respectively.
- Barossa PWRA rainfall varied over the historical record from approximately 400 mm in a dry year to 800 mm in a wet year, with minor evidence of declining trend recently (low confidence). The average rainfall over the period from 2008-2020 was 538 mm.

Rainfall represents the primary flux of water into the region. Figure 11 shows the spatial pattern of mean annual total rainfall in the Barossa and Eden Valley from 1900 to 2016. There is a significant spatial gradient in rainfall across the regions with annual total rainfall amounts of ~720 mm in the upper reaches of the Jacob Creek sub-catchment to annual total rainfall amounts of ~490 mm in the Stockwell Creek area in the north. The spatial pattern of rainfall shown in the Figure 11 is based on SILO interpolated data grids which is a spatially interpolated dataset generated using all available point gauges (Jeffrey, 2001); as such, the spatial data shown in Figure 11 is likely to be derived from an interpolation of gauges both inside and outside the study areas.

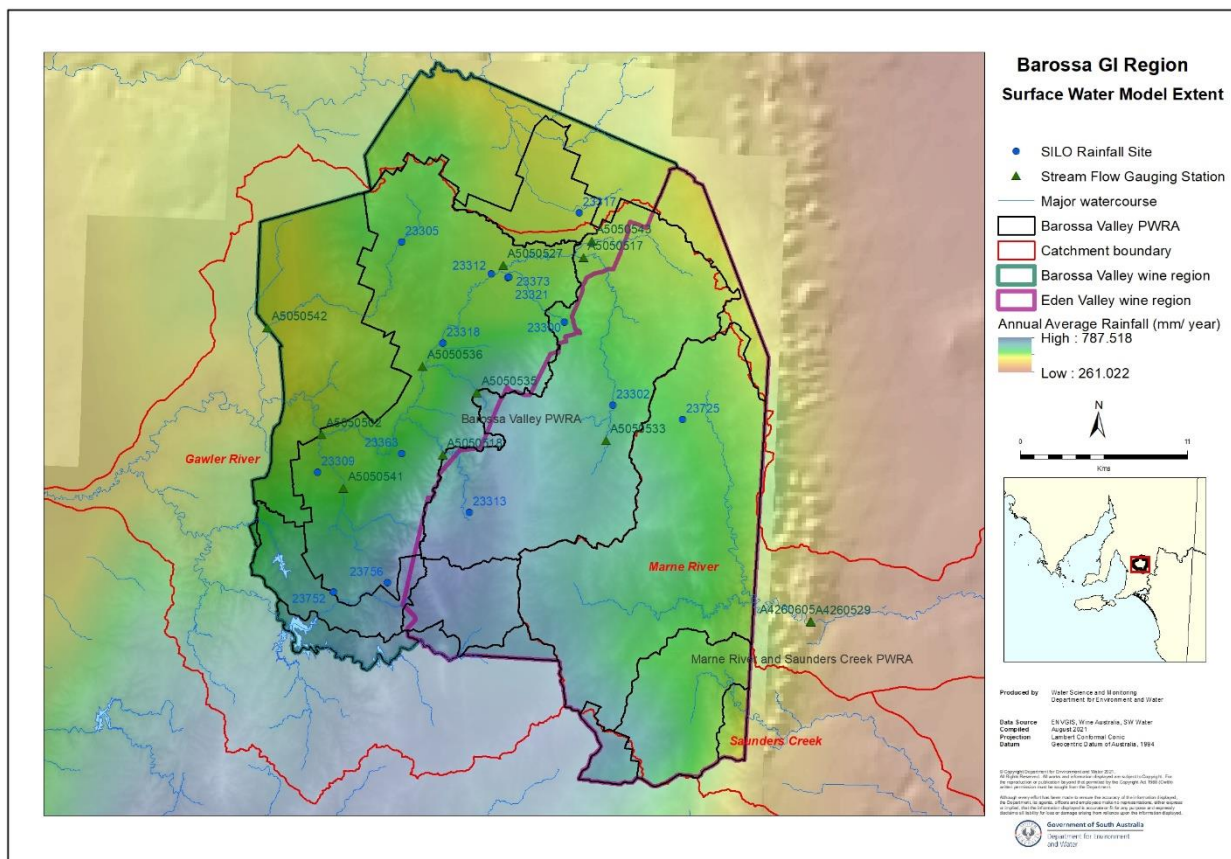


Figure 11. Location of the SILO rainfall stations, streamflow gauges and spatial pattern of rainfall

For modelling surface water and groundwater resources, 14 rain gauge stations in the region are used (Jones-Gill and Savadamuthu, 2014; Li and Cranswick, 2014; Construction and calibration of a hydrological model for the Marne River catchment: Technical report 2021). The locations of these gauging stations are shown in Figure 11. The SILO patched point dataset provides continuous recorded rainfall from 1889 to present. The station IDs, latitude-longitudes, and annual summary statistics of the stations are shown in Table 26 (Appendix B). All the data used in the study cover the full period of record with appropriate infilling as necessary.

Monthly climatological means for rainfall in the Barossa Pwra is provided in Figure 12, and shows a distinct seasonal cycle, with the greatest monthly rainfall occurring over the months from approximately May to September, and with the months from January to March having the lowest monthly rainfall. There is also significant year-to-year variability, with the temporal evaluation of annual total rainfall over the period from 1900 to 2020 shown in Figure 13. This shows an average of 581 mm/yr that is varying within a range from slightly less than 400 mm in a dry year to slightly above 800 mm in a wet year.

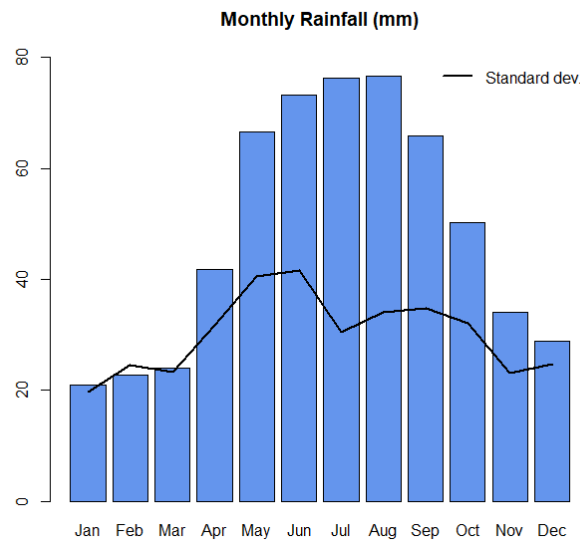


Figure 12. Climatological (1900 to 2020) mean (bars) and standard deviation (line) of monthly rainfall in the Barossa PWRA.

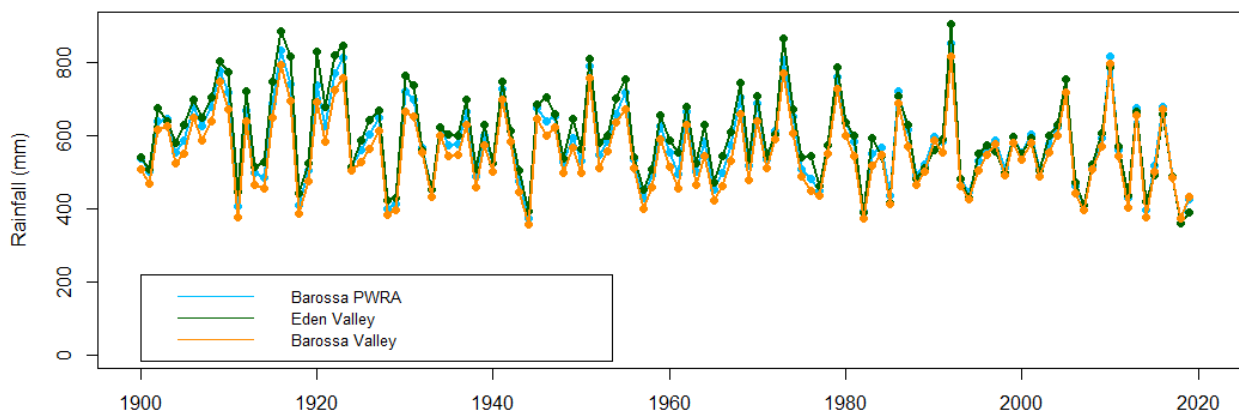


Figure 13. The annual total rainfall in the Eden Valley, Barossa Valley and Barossa PWRA estimated as the arithmetic mean rainfall from the all the gauges in respective regions.

The DEWNR/DEW surface water modelling reports (Jones-Gill and Savadamuthu, 2014; Montazeri and Savadamuthu, 2020) include an analysis of the monthly and annual patterns of the rainfall data from these gauges as well as a trend analysis of the historical data. The reports document the following signals:

- an upward trend indicating a wetter than average period occurs from approximately 1900 to the early 1920s;
- a relatively stable period, indicating average rainfall conditions from the early 1920s to 1960; and
- a decreasing trend indicating drier than average rainfall conditions from 1960 to 2015.

Montazeri and Savadamuthu (2020) notes a declining trend in rainfall post 1960 based on residual mass analysis; however, the statistical significance of the trend has not been reported. The presence of statistically significant trends has not been verified in this study.

Using the conversion factors in Table 25 (Appendix A) and making the simplification that the vineyards are homogeneously distributed throughout the region, the annual average rainfall over the vineyard areas of the Barossa PWRA is 52 GL/yr over the long-term record or 47 GL/yr over the period from 2008-2020, with a range from slightly below 40 GL in a dry year to close to 80 GL in a wet year. Similarly, the annual average rainfall for the Barossa Valley and Eden Valley delineations are 552 mm/yr and 559 mm/yr, respectively, leading to total rainfall over the planted vineyard area for each delineation of 65 GL/yr and 14 GL/yr.

3.2 Water into the system: External water sources

Historical external water: key points

- The BIL pipeline represents the most significant external source of water for growers within the Barossa Valley, with a current pipeline capacity of 11 GL. Assuming that 80% of vineyard area in the Barossa Valley uses BIL water (see Table 25), the scheme has the capacity to provide an average of approximately 120 mm/yr to each connected vineyard.
- SA off-peak water use over the period of 2008-2020 was 1.49 GL, translating to 0.9 GL for vineyards within the Barossa PWRA based on pro-rata estimates of vineyard area.
- Bunyip water provides up to an additional 2 GL, and primarily services the Seppeltsfield vineyard.

Water to support agricultural activity in the Barossa and Eden Valley regions historically has been sourced either directly from rainfall, or indirectly through a combination of native surface and groundwater resources; in contrast, external water sources traditionally have largely been a supplementary supply. Indeed, as described in Section 1.4, the region relied almost exclusively on rainfall-sourced water until the early-2000s. However, a combination of significant increases in planted area as described in Section 1.3, combined with decreasing rainfall patterns as described in the previous section, have led to a rapid drive over the last two decades to expand water supply infrastructure and bring in water from external sources. This infrastructure almost exclusively services the Barossa Valley region.

The primary external sources of water are the River Murray and storm water harvested from urban areas in Gawler. The River Murray water is delivered through the Barossa Infrastructure limited (BIL) pipeline during the growing season, and the SA Water main pipeline during the off-peak (April to October) season (termed “SA water off-peak”). Storm water from Gawler is delivered through the Bunyip pipeline that services the Seppeltsfield Vineyard in the western edge of the valley floor.

3.2.1 Barossa Infrastructure Limited (BIL) (U_{BIL})

The BIL pipeline connection is available only in the Barossa Valley wine region and services 75% of the growers in the region (Source: Regional Issues and Options Consultation Report). BIL has an annual capacity of 11 GL/year as of year 2020 (BIL annual report, 2020), with the historical expansion of the BIL scheme summarized in Section 1.4.2.

Figure 14 shows the total water use during the recent historical period from 2008/09 to 2019/20 (in GL/year) from the BIL pipeline. The data is also presented in Table 6 at the end of this section. The BIL pipeline capacity described in Table 2 is also plotted in the figure. The figure illustrates that the BIL pipeline has been operating near its capacity in recent years, except for year 2016-17 which was a higher rainfall year (more details in Section 5). The average 2008/09 to 2019/20 water use from the BIL pipeline is 7 GL/year.

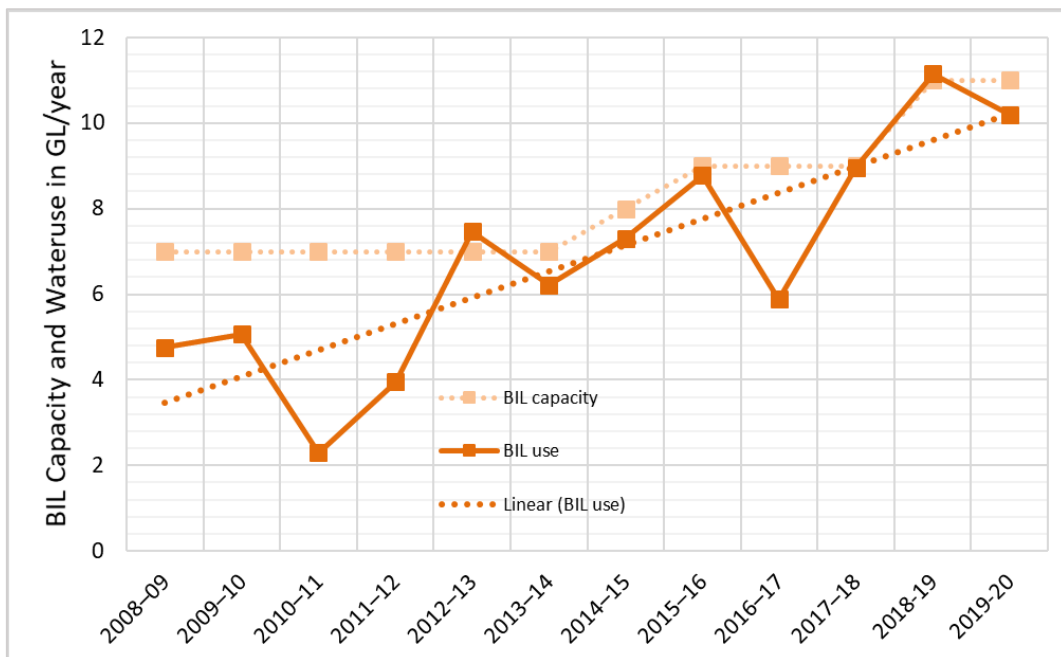


Figure 14. Historical water use from external source BIL in GL/year for each water-use year (1 July to 30 June) and the BIL capacity. To enable comparison with other key fluxes documented in this report, it is possible to use area estimates from Table 25 to convert total irrigated volume into an annual irrigation depth. Focusing on the Barossa Valley, and assuming that:

- 80% of the vineyard area within the Barossa Valley Wine Region are connected to the BIL scheme (this area estimate is slightly greater than the 75% of growers estimated to be connected to the BIL scheme described above, as we assume that larger growers are more likely to be connected to BIL), and
- water consumption is distributed evenly amongst the connected vineyards,

it is estimated the current BIL scheme is able to provide approximately 120 mm / year of irrigation water to those who have a BIL connection. Whilst this is significantly below the total annual rainfall even for a relatively dry year, it nevertheless represents a large proportion of the water balance, and is particularly large during the drier summer months when rainfall averages 20-30 mm per month (see Figure 12).

3.2.2 SA Water Off-peak (U_{SA})

The SA Water main pipeline and distribution network connects to both Barossa Valley and Eden Valley wine regions. The off-peak service transports water from the Murray for users who hold Murray water entitlements only during winter when the existing load on the SA Water pipe network is low. The amount of water available for supply through the off-peak scheme is lower than through BIL, and averages 1.49 GL/year over the 2008/09 to 2018/19 period (Source: DEW Excel document named 'Barossa_water_use_2018-19.xlsx').

Figure 15 shows the external water use during the recent historical period from 2008/09 to 2019/20 (in GL/year) from the SA Water off-peak scheme. The data is also presented in Table 6 at the end of this section.

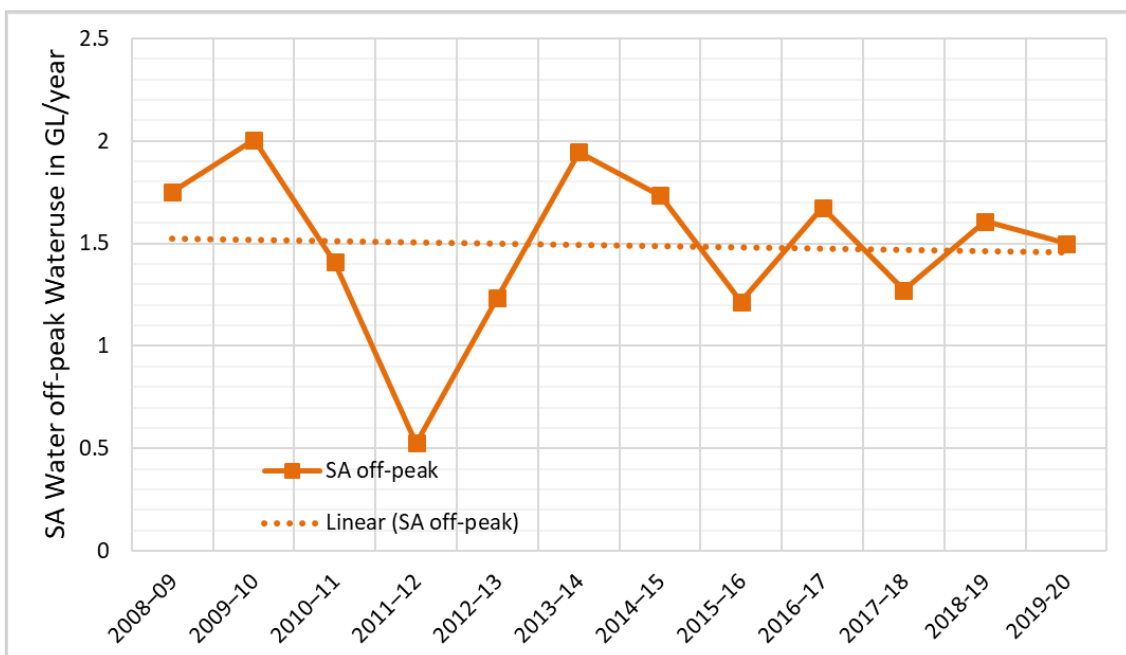


Figure 15 Historical water use from external source 'SA Water Off-peak' in ML/year for each water-use year (1 July to 30 June).

Based on current maximum contracted values (Personal comms, DEW, 19 October 2021), approximately 94% of the SA Water off-peak demand is from users in the Barossa Valley, with the other 6% being in the Eden Valley.

3.2.3 Bunyip Pipeline (U_{BY})

A third source of external water in the Barossa Valley is the Bunyip pipeline that services the Seppeltsfield Vineyard in the western edge of the valley floor. Practically all of the water from the Bunyip pipeline (up to 2GL) is delivered to Seppeltsfield, after taking out 50ML to service the Hewett region (Source: Barossa Wine and its Ecosystem report). Note that although this source cites 2GL capacity, Table 5 shows higher use in the 2019/20 water year. The Bunyip scheme started operation in water year 2016 (Bunyip Water Pty. Ltd, n. d.), and secures water from a mix of storm water runoff from urban areas in Gawler and recycled water from the Bolivar treatment plant. Imported water volumes for the four full years of operation were available (2017/18 to 2020/21 water years). Estimated imported water delivered to the Barossa region for vineyard use is summarised in Table 5 (2021, personal comms DEW, 30 November 2021).

Table 5. Historical imported water to the Barossa region from the Bunyip pipeline

Water-use Year	Bunyip water use (in GL/year)*
2017-18	1.5
2018-19	1.7
2019-20	2.3
2020-21	1.9

*50ML is removed from each imported water year total (for Hewett region) to obtain these values.

From analysis of GIS vineyard data and region map (<https://barossawine.com/wp-content/uploads/2017/12/Barossa-Wine-Region.pdf>), the Seppeltsfield vineyards are estimated to be fully within the Barossa Valley delineation, and 40% are within the Barossa PWRA.

3.2.4 Summary of External Water Sources

The data presented in Figure 14, Figure 15 and Table 5 are summarised in Table 6.

Table 6. Historical water use from external sources in the Barossa GI zone (Source: DEW excel document named 'Barossa_water_use_2018-19')

Water-use Year	BIL water use (in GL/year)	SA Water off-peak water use (in GL/year)	Bunyip water use (in GL/year)
2008–09	4.8	1.8	-
2009–10	5.1	2.0	-
2010–11	2.3	1.4	-
2011–12	4.0	0.5	-
2012–13	7.5	1.2	-
2013–14	6.2	1.9	-
2014–15	7.3	1.7	-
2015–16	8.8	1.2	-
2016–17	5.9	1.7	-
2017–18	9.0	1.3	1.5
2018-19	11.1	1.6	1.7
2019-20	10.2*	1.5^	2.3

*The number is based on the BIL 2020 annual report. A volume of 0.27 GL is deducted from the number from the BIL annual report to account for Nuriootpa Community Wastewater Management Scheme water (CWMS) locally recycled water, consistent with the analysis by DEW in the document 'Barossa_water_use_2018-19.xlsx' for the previous years.

^ Information for this year is not available. This is a representative value calculated as the mean of the previous five years.

3.3 Water out of the system: Streamflow (Q)

Historical streamflow: key points

- The primary streamflow gauge for the Barossa PWRA and Barossa Valley is at Yaldara (A5050502), representing 71% of the overall Barossa PWRA area. Annual average observed streamflow at this location was 11.7 GL/year over the period 1980/81-2019/20, with a much smaller streamflow of 7.66 GL/year over the recent decade (2010/11-2019/20)
- There is significant year-to-year variability, with annual total streamflow volume ranging from 0.48 GL (2018/19) to 30 GL (2016/17) at Yaldara in the last decade.
- Baseflow at Yaldara over the period 1990/91-2014/15 was estimated to be 1.0 GL/yr based on MODFLOW simulations, and 1.3 GL/yr based on application of the Lyne-Hollick filter, with the Lyne-Hollick filter approach showing significantly greater sensitivity to climate variability compared to MODFLOW.

3.3.1 Total Streamflow

The Barossa and Eden Valley delineations were not developed based on catchment boundaries, and thus there are a large number of catchments that are partially captured within each delineation. In contrast, the Barossa PWRA delineation follows catchment boundaries more closely. The various delineations were summarized in Figure 2.

The North Para River represents the largest single river in the region, and is the main water course in the Barossa PWRA. This river also represents a significant portion of the Barossa Valley delineation and the western portion of the Eden Valley delineation. As shown in Figure 2, the river flows from south to north in the eastern half of the Barossa PWRA, and then turns south west. The watercourse is typically characterised by ephemeral streams and seasonally disconnected permanent pools that are sustained by groundwater. Streamflow and salinity are mainly influenced by rainfall; lower winter rainfall results in reduced annual streamflow volumes (PWRA Technical Note 2019).

The four streamflow gauging locations in the Barossa PWRA are A5050533 (N Para/Mt McKenzie), A5050517 (North Para River at Penrice), A5050535 (Tanunda Ck/Bethany), A5050502 (N Para R/Yaldara). The data from these stations are used as the basis for comparison with modelled streamflow using the eWater Source model that has been developed to reflect surface water in the Barossa PWRA (see Section 1.5.2). The locations of these streamflow gauging stations are shown in Figure 11. All stations except A5050535 are located on the main North Para River watercourse. The principal long-term streamflow gauging station for the Barossa PWRA is located at Yaldara, at the outlet of the North Para catchment, and covers a catchment area of 376 km² out of the 528 km² total area of the Barossa PWRA.

The annual aggregate of streamflow at the Yaldara gauge is shown in Figure 16. The figure contains annual total streamflow in GL from the Source model together with recorded data downloaded from the Water Connect website (www.waterconnect.sa.gov.au) from 1947 to 2020. Years from the historical record missing more than 10% of days were removed from the analysis. Overall, this figure illustrates that Source represents the annual average and year-to-year variability of the historical streamflow reasonably well, although it appears to overestimate low flow years since the mid-1990s and underestimate flow during high flow years. This can also be observed in a scatter plot version of the results (Figure 17), whereby the model underestimates all of the high flows and overestimates all of the low flows. This is likely to have some implications subsequently in the climate stress test, in that Source may slightly underestimate the degree of variability associated with changes in climatic forcing. Annual average simulated streamflow at Yaldara was 11.1 GL/year over the period 1980/81-2019/20, and 8.86 GL/year over the recent decade (2010/11-2019/20). It can also be seen that there has been a long-term decline in streamflow at Yaldara, although the statistical significance of this trend relative to background variability has not been assessed in this work.

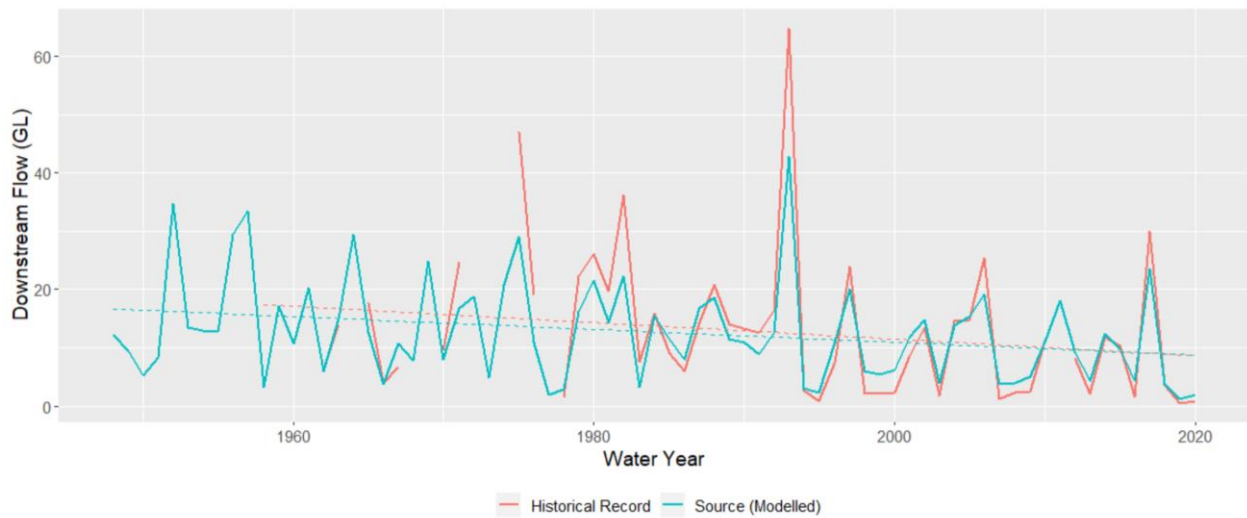


Figure 16. Historical annual total streamflow at Yaldara (in GL/year) for each water-use year (1 July to 30 June).

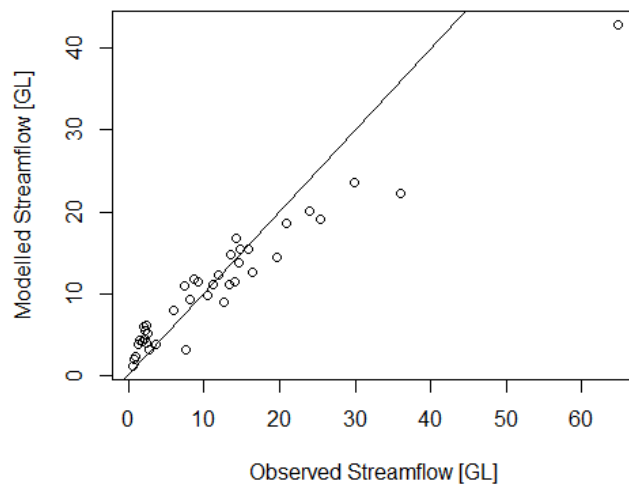


Figure 17. Observed versus simulated streamflow at Yaldara from 1980/81 to 2019/20.

The flow duration curve at Yaldara was created for both the modelled and recorded data sets (Figure 18), and shows that at the outflow location there is no flow at the gauge approximately 20% of the time. Analysis of the observed streamflow record at Yaldara shows that over the historical period from 1980 to 2020, 80% of the total flow comes from just 9.2% of the largest flow days. In recent years (2010 to 2020) this has decreased, with 80% of the total flow coming from 6.4% of the days.

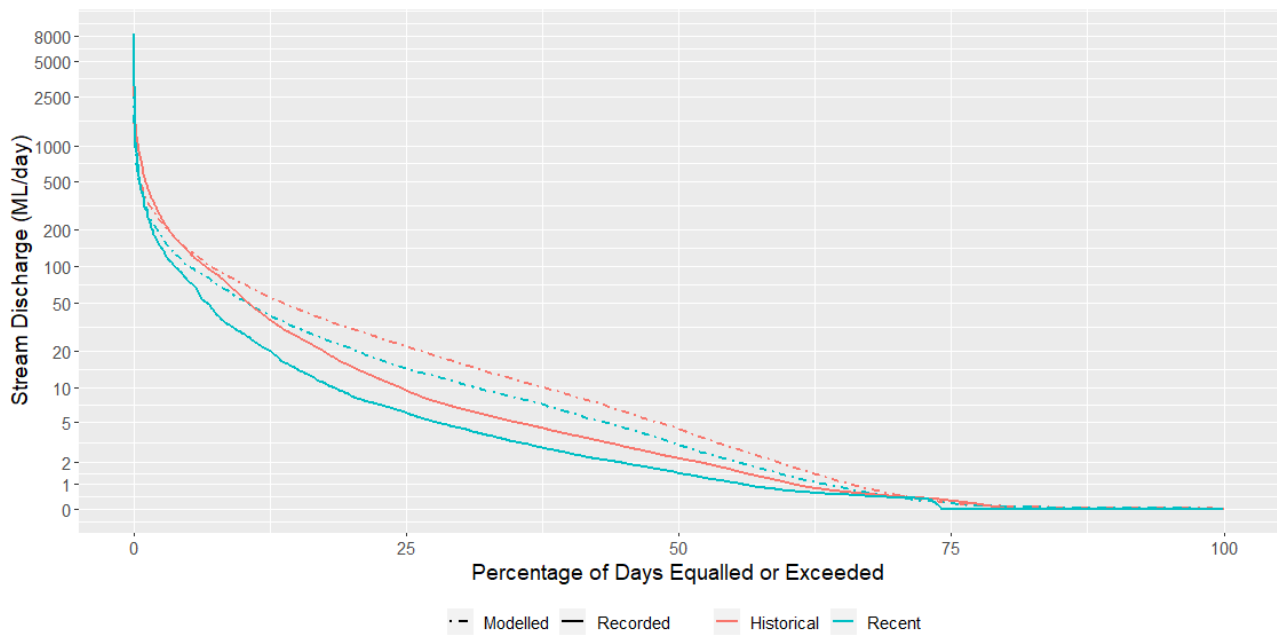


Figure 18. Historical (1980 to 2020) and Recent (2010 to 2020) daily flow duration curve for the outflow gauge station A5050502 (Data Source: SA Water Connect and streamflow from Source Model)

Figure 19 shows the daily modelled streamflow hydrographs from Source for water years representative of a dry (2009/10), wet (2010/11) and average (2019/20) year defined in terms of total annual flow. The three plots in Figure 19 emphasise the significant year-to-year variability in streamflow, both in total amount and seasonal variability.

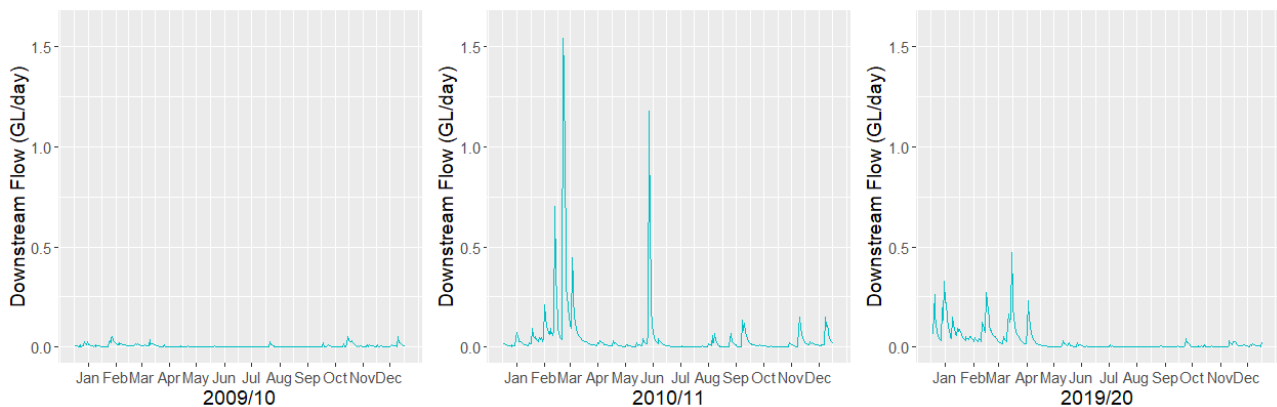


Figure 19. Daily downstream flow volumes at Yaldara for dry, wet and average rainfall years, from modelled (Source) time series

The other main watercourse in the Barossa PWRA is Greenock Creek. This creek was gauged (A5050542 - Greenock Creek at Lienert Rd) from 2002 to 2011, but is no longer gauged. This streamflow is, however, represented in the Source model and gives an annual aggregate streamflow of 0.27 GL/year (1980/81 to 2019/20) and 0.28 GL/year (2010/11-2019/20). In the recent decade, the maximum annual aggregate flow is 1.2 GL (2016/17) and the minimum was 0.041 GL/year (2018/19). In volume, streamflow in Greenock Creek is far less than at Yaldara, but follows similar year-to-year variability.

The second largest catchment in the region is the Marne River catchment, which is located in the eastern portion of Eden Valley (Figure 2). This catchment is ephemeral in nature and originates in the Mount Lofty Ranges near to Springton and flows eastwards. The main streamflow gauging station (A4260605) on the Marne River is located downstream of the Marne Gorge. It is situated 5 km west of Cambrai with an upstream catchment area of 240 km². The site has streamflow data available from 2001 and is currently telemetered. It replaces the former gauging station (A4260529) just downstream of the site. A4260529 still remains *in situ* and is used as a backup for A4260605 and has data available from 1972 to 2006.

The majority of the record at A4260605 is denoted as either of poor quality (theoretical rating) or the water level is below the recordable range. The majority of the high flows appear to be classified as good. There have been 18 gaugings undertaken between 2001 and 2017 and these align well to the rating curve. Further gaugings are required in the low (below 1.06 m stage) and high flow (above 1.35 m stage) range. The Marne River is ephemeral and hasn't recorded any flow since November 2017 but there does not appear to be a datum shift or any obvious anomaly in the flow record. The streamflow record for site A4260529 and A4260605 have been combined to create a longer period of record to support Source modelling of this catchment.

3.3.2 Baseflow

Given the significant historical emphasis of hydrological modelling in the Barossa PWRA, most of what is understood regarding baseflow across the Barossa and Eden Valley regions is associated with streamflow within this delineation, and this is the focus of the material presented here. Surface water and groundwater in the Barossa PWRA is generally characterized as 'highly connected', with losing (to groundwater) and gaining (from groundwater) stream conditions displaying strong dependence on the season and location (Hancock et al., 2014). Baseflow is of particular interest in the Barossa PWRA from an environmental and aquatic ecological asset standpoint (Cranswick et al., 2015). Groundwater is considered important in maintaining local surface water features (e.g., pools) in dry seasons.

Baseflow at Yaldara (among other gauges) over the period 1994/95-2013/14 was estimated by Cranswick et. al. (2015) using both the Lyne-Hollick Filter and EC Mass Balance approach. From this report the Lyne-Hollick filter produced an annual average baseflow of 2.2 GL/year and the EC Mass Balance approach gives 0.8 GL/year. The groundwater model of Li and Cranswick (2016) produced an annual average simulated baseflow at Yaldara of approximately 1 GL/year over the same period. Simulated baseflow rates from the groundwater model generally show good agreement with baseflow estimates based on field data and previous desktop analyses, although this is likely to be due to their incorporation in groundwater model calibration.

The analysis of Cranswick et. al. (2015) was repeated here for Yaldara gauge using both MODFLOW (1991-2015) and the Lyne-Hollick filter (1991-2020) with various values of the filter parameter ('alpha'). The aggregate annual values are shown in Figure 20 and with a daily timeseries plot for an individual flow year shown in Figure 21. From Figure 20 it can be seen that the mean baseflow estimates produced from MODFLOW lie within the range of the Lyne-Hollick filter curves produced by different alpha values.

Over the period from 1990/91-2014/15, the MODFLOW model produces an annual average baseflow of 1.0 GL/year, with relatively low levels of variability from year to year. The Lyne-Hollick filter applied on historical streamflow produces baseflow of 1.0, 1.3, 1.5 and 1.8 GL/year for α values of 0.99, 0.985, 0.98 and 0.975, respectively. In all cases, baseflow based on the Lyne-Hollick filter showed greater year-to-year variability, implying a greater degree of sensitivity to climate drivers compared to the MODFLOW results. Note that the average annual baseflow estimate by Cranswick et. al. (2015) of 2.2 GL/year was derived over a different time period and used an α value of 0.925. A value of $\alpha=0.99$ produces baseflow estimates that are closest to those from MODFLOW; however, as can be seen from the 2015/16 water year plot of daily baseflow (Figure 21), the filter with $\alpha=0.99$ shows an unrealistic pattern between October and November 2015. For this particular time the streamflow and baseflow have the same value. In contrast, visual inspection of the hydrograph suggests that baseflow using $\alpha=0.925$ and 0.95 follows the daily variation in streamflow more closely than might be expected based on typical baseflow dynamics. Therefore, the α value that seems to best reflect the expected daily pattern of baseflow as well as reflecting the annual volumes captured in the MODFLOW simulation is 0.985.

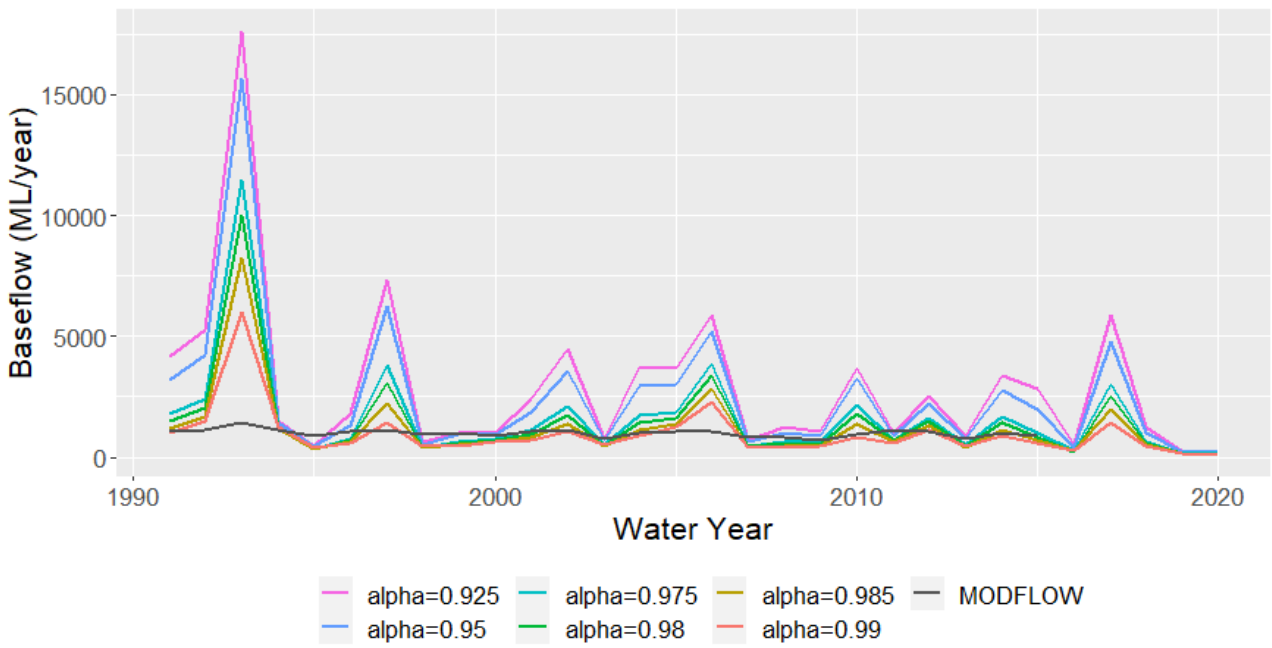


Figure 20. Annual (water year) aggregate baseflow (ML) at Yaldara from the Lyne-Hollick baseflow filter and MODFLOW. The filter alpha values represented are for $\alpha=0.95, 0.975, 0.98$ and 0.99 .

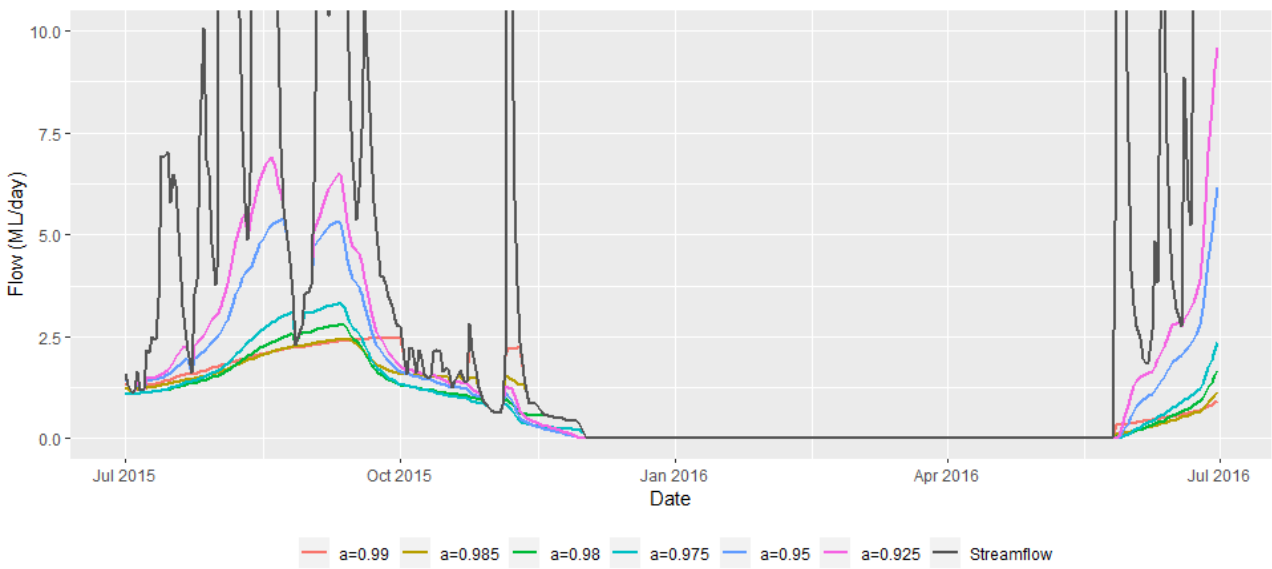


Figure 21. Comparison of different alpha values on Lyne-Hollick filter for the 2015/16 water year

3.4 Water out of the system: Evaporative Demand and Actual Evapotranspiration

Historical evapotranspiration: key points

- Annual average potential evapotranspiration in the Barossa PWRA is estimated to be 1237 mm/yr, with the recent decade being approximately 4% greater than the long-term average
- Evapotranspiration from shallow groundwater is estimated to be approximately 75% of the groundwater recharge over the last decade, and can be greater than 100% in dry years. This is important as the residual is the primary water available for both baseflow and consumptive water use.

Evapotranspiration represents the primary flux of water out of the system. In particular, assuming an annual average rainfall in the Barossa PWRA of 538mm, an annual average streamflow of 31 mm (based on the annual average streamflow at Yaldara of 11.7 GL/yr divided by a contributing area of 376 km²) and limited lateral flow of groundwater (Section 3.5), a water balance estimate would suggest that approximately 94% of rainfall in the region is ultimately evaporated or transpired from the region.

Despite its importance, evapotranspiration is difficult to measure directly, and to our knowledge no accurate measurement of actual evapotranspiration in the region (obtained, for example, from an eddy covariance flux tower) is available. As such, the key quantities are inferred either using estimates of potential evapotranspiration calculated from atmospheric variables, or as outputs from models. Both approaches are summarized briefly here. Both these quantities are used to inform aspects of the system dynamics model.

3.4.1 Potential Evapotranspiration

Potential evapotranspiration (PET) values for the Barossa PWRA are formulated using FAO56 (Penman-Monteith equation), from data recorded at gauge M023373, which can be seen on the map in Figure 11. The FAO-56 approach is based on measurements of temperature, relative humidity, wind speed and solar radiation, and is used to estimate evapotranspiration from a 'reference crop' (corresponding to a well-watered grass of uniform height that is actively growing and completely shading the ground). This is a conceptual quantity (in that it does not correspond to actual conditions of the Barossa), and is used as the basis for estimating evaporative demand in the Source model. As such, these PET estimates are to be used for indicative purposes only. More detailed evapotranspiration estimates specifically pertaining to viticulture crops are included in a crop model provided by SARDI, as summarized in Section 3.11.2.

Monthly climatological means for PET in the Barossa PWRA are provided in Figure 22, and shows a distinct seasonal cycle, with the greatest monthly PET occurring over the months from approximately November to February, and with the months from May to August having the lowest monthly PET.

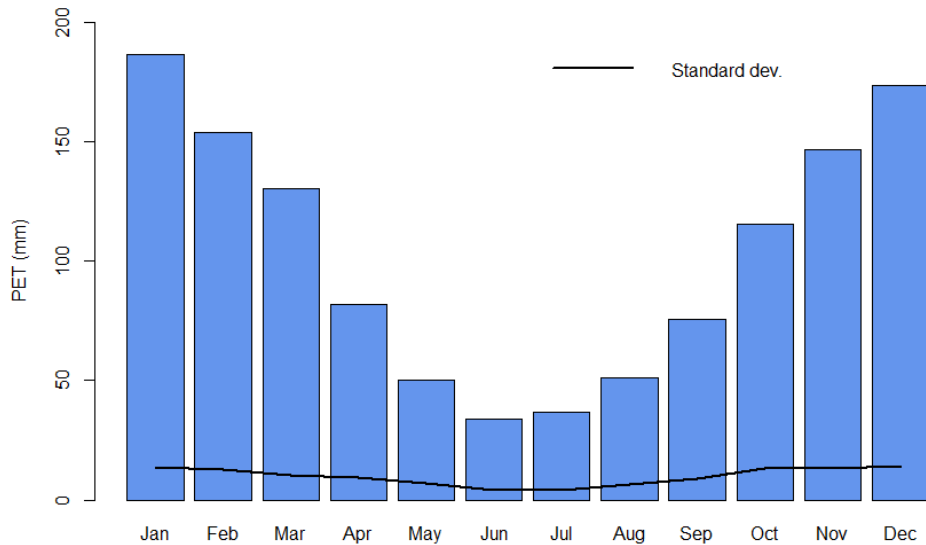


Figure 22. Climatological (1900 to 2020) mean (bars) and standard deviation (line) of monthly PET (mm) in the Barossa PWRA

There is also significant year-to-year variability, with the annual total mean PET over the period from 1900 to 2020 shown in Figure 23, with an average of 1237 mm/yr that is varying within a range from approximately 1090 (1992/93) mm to 1380 mm (2007/08). No trends are visible over the full record; however annual total mean PET appears have been increasing in recent decades, with an average of 1253 mm/yr (1980/81 to 2019/20) and 1276 mm/yr for the most recent decade (2010/11 to 2019/20). The cause of these trends in terms of the driving meteorological variables has not been investigated, and issues associated with the fidelity of the forcing data cannot be excluded. Nevertheless, given that there has been documented increases in atmospheric temperature in the region together with decreases in relative humidity, it is plausible that at least some of the recent increasing trend in PET is related to climate change.

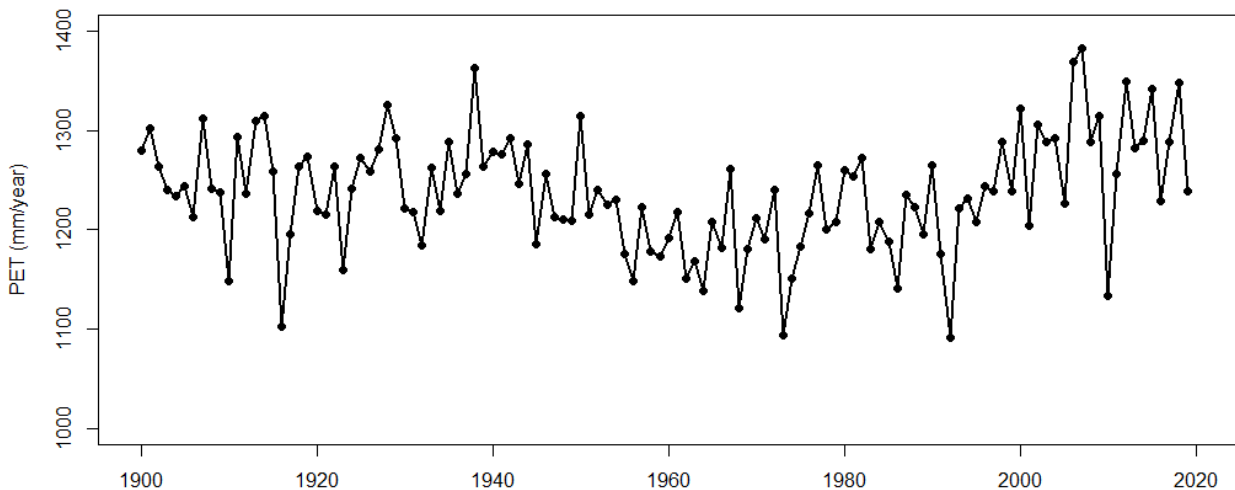


Figure 23. The annual total mean PET (mm) in the Barossa PWRA from the gauge 23373.

3.4.2 Groundwater Evapotranspiration

Evapotranspiration of shallow groundwater—distinct from that of surface water or water in the unsaturated zone—is thought to alone comprise a non-trivial part of the Barossa PWRA water balance. Regional-scale groundwater ET estimates across the Barossa PWRA are available only from groundwater modelling of Li and Cranswick (2016). A large proportion of groundwater recharge from rainfall discharges as groundwater ET (simulated annual groundwater ET rates are on average 75% of rainfall recharge, and varies between 58% of rainfall recharge in wet years such as 2009 and 104% of rainfall recharge in dry years such as 2012) (Figure

24). While simulated groundwater ET rates display significant annual variability (approximately 6 to 15 GL/year), relatively stable longer-term trends are apparent (mean of approximately 9 GL/year).

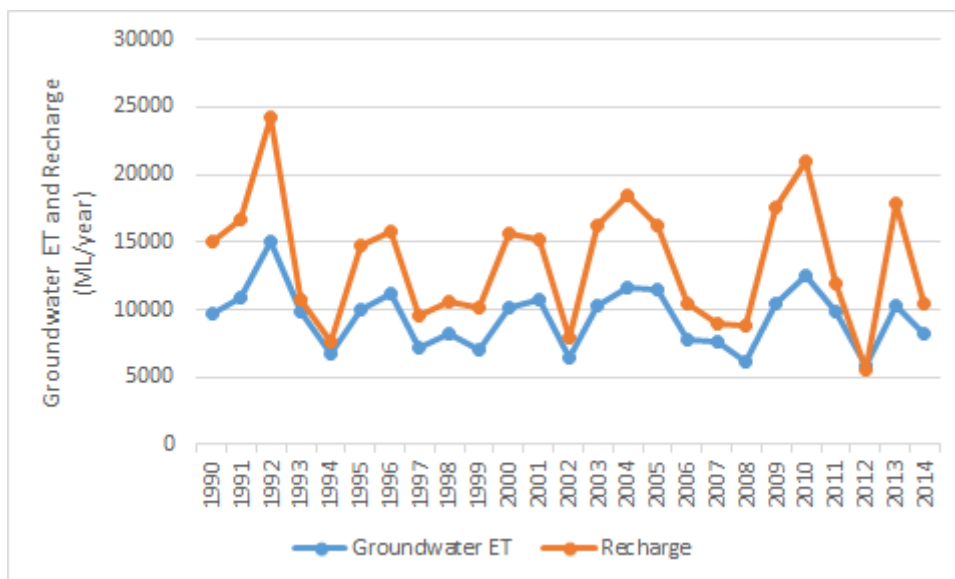


Figure 24. Annual (water year) aggregate groundwater ET (ML) across Barossa PWRA. Corresponding groundwater recharge rates (Section 3.7 given for reference).

3.5 Water through the system: Lateral groundwater inflow/outflow

Groundwater within both the lower sedimentary aquifer and fractured rock aquifers interacts with groundwater located outside of the Barossa PWRA, within fractured rock aquifers to the east (Barossa Ranges) and to the west. Aquifers to the east of the Barossa PWRA are thought to serve as a source of water, particularly to the lower aquifer in dry years when higher abstraction occurs. This is supported by groundwater salinity data (Li and Cranswick et al., 2016). Aquifers to the west exhibit less interaction with groundwater within Barossa PWRA.

While the magnitude of these interactions are not well known, it is currently understood that these interactions make up a small component of the overall Barossa PWRA water balance (net annual average rate of approximately 0.03 GL overall) (Li and Cranswick, 2016). Therefore, lateral water exchange through aquifers is not considered further from a water balance perspective in this report.

3.6 Within system flux: Water use from native sources

Historical water usage from native sources: key points

- Annual total licensed surface water extractions have more than halved over the last decade for the Barossa PWRA delineation to 0.9 GL/yr in the 2020 water year, and have also declined in recent years for both the Barossa and Eden Valleys to values of 0.46 GL and 0.7 GL, respectively, in 2020. Total usage has been consistently well below both farm dam capacity and licensed allocation.
- Farm dam consumption for stock and domestic usage is unlicensed, and although estimates are available for unlicensed consumption, little is known about trends over time.
- In contrast to surface water, groundwater extractions have increased over the recent decade in the three delineations, with 2020 extractions estimated to be 4 GL, 3 GL and 1.15 GL in the Barossa PWRA, Barossa Valley and Eden Valley, respectively. Extractions remain less than half the available allocations.

Water from native surface and groundwater resources in the Barossa PWRA, Barossa Valley and Eden Valley is used predominantly for irrigation, stock and domestic uses.

The amount of water used for irrigation in the three delineations from native sources is assessed based on licensed allocations. The water used per the license from both groundwater and surface water resources is metered. Data of the historical irrigation water allocation and water use in the Barossa PWRA are made available for this project by DEW for the six water years 2014-15 to 2019-20. In addition to the licensed extractions, some further unlicensed extractions are known to occur for stock and domestic uses. This same data was extracted for the Barossa and Eden Valley regions from Water Information and Licensing Management Application (WILMA) data for the Barossa PWRA, Marne & Saunders PWRA and Western Mount Lofty PWRA.

3.6.1 Surface water

Surface water is extracted from farm dams and water courses, with irrigation uses subject to license, whereas stock and domestic uses are unlicensed. Licenses specify the maximum amount of water that users can extract from surface water sources each year; the amount of water specified in the licenses is termed '*allocation*'. Users can extract licensed surface water from farm dams and watercourses in the region up to the licensed amount; the amount of water that the users extract are metered and the meter readings indicate the licensed water '*use*' during each year.

Information on surface water allocation and use in the Barossa PWRA has been obtained from three sources of information received from DEW:

- Surface water modelling report (Jones-Gill and Savadamuthu, 2014).
- Licensed allocation by license number and water use by meter id for the past six water-years from 2014-15 to 2019-20.
- Aggregate water-use during water-years 2004-05 to 2018-19.

Table 7 lists the volume of licensed surface water allocation and water use from the three sources of information provided by DEW specifically for the Barossa PWRA. This data shows surface water allocation for irrigation is in the order of 3.8 GL/yr (2005-13 data) or 4.0 GL/year (2014-15 data excluding 'rollover' and industrial uses); the corresponding average usage estimates range from 2.0 GL/yr (2005 to 2013) to 1.3 GL/yr (2014/15 to 2019/20). As mentioned previously, a constant value of 1.1 GL/year is assumed for stock and domestic use, which is not included as part of the licensed data described in Table 7 as this water use is not limited by license.

The metered water use data was used as the basis for assigning surface water demand in the eWater Source model (Jones-Gill and Savadamuthu, 2014). The 2005-2013 average water use data, along with additional assumed stock and domestic use, is used to assign 'water demand' in the model (Jones-Gill and Savadamuthu, 2014). The volume of water supplied during model simulations can be less than or equal to this assigned demand depending on the available water during specific years. Moreover, the assumed unlicensed stock and domestic water demand of 1.1 GL/year has been added to obtain the total historical water demand used as part of the Source modelling (Jones-Gill and Savadamuthu, 2014; Barossa water use data provide by DEW 19/10/2020).

Table 7. Volumes of licensed surface water allocation and use from different sources of information for the Barossa PWRA. The assumed unlicensed stock and domestic use is not shown in the table.

Source of Information	Description	Total Irrigation Water (in GL/year)
Report (Jones-Gill and Savadamuthu, 2014)	2005 to 2013 average water use	2.0
	2005 to 2013 average water allocation	3.8
License data received from DEW on 19/10/2020	2014-15 to 2019-20 average water use	1.3
	2014-15 to 2019-20 average water allocation	5.2 ¹
eWater Source Model	Water supplied each year in the historical simulation, average 2008-09 to 2019-20	1.8 ²

¹ The allocation is made up of 4 GL of irrigation, 0.8 GL of ‘rollover’ (previous year’s allocation) and 0.3 GL of industrial water use.

² This includes up to 1.1 GL/yr of assumed stock and domestic use.

There is inter-annual variability in the surface water use that is influenced by factors such as the amount of surface water available for use, together with irrigation requirements. Figure 25 shows the water use from surface water sources during the recent historical period from 2008/09 to 2019/20 (in GL/year). The figures are created using the annual water use numbers received from DEW (pers. comms. 19/10/2020). For the water year 2019-20 the numbers calculated from the license data are used. The total surface allocation volume for the last six water years available from the license data is also shown in the figure.

A best-fit linear regression to the surface water extractions shows a decrease of 0.08 GL/year. The higher surface water extraction of 2.1 GL/year in 2008-09 decreases to the lowest value of 0.8 GL/year in year 2019-20. The surface water usage in the last two years is less than half of the pre-2010 usage.

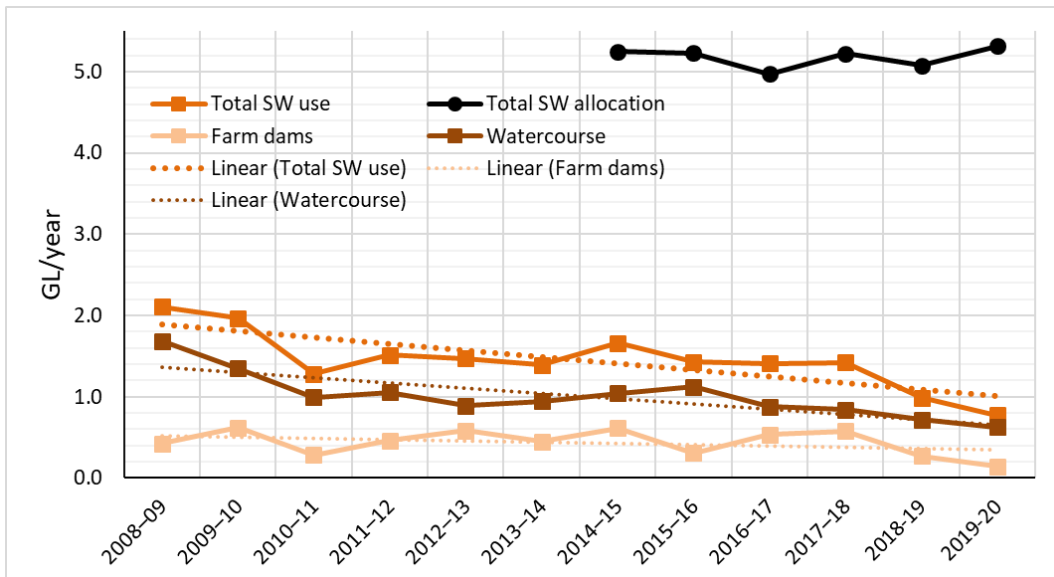


Figure 25. Historical licensed irrigation water use from surface water sources for each water-use year (1 July to 30 June) for the Barossa PWRA.

For the Barossa Valley and Eden Valley delineations, information of surface water allocation and use was extracted from WILMA. Average allocation and use over 2010/11 to 2019/20 period and is summarised Table 8.

Table 8. Average surface water allocation and use for the recent decade (2010/11 to 2019/20) for the Barossa and Eden Valley

Region	Surface Water (licensed) [GL]		Surface water (unlicensed) [GL]
	Allocation	Use	Estimated Use
Barossa Valley	2.5	0.68	0.89
Eden Valley	3.6	1.05	0.93

Figure 26 shows the change in licensed water allocation and use over the recent decade (2010/11 to 2019/20) for the Barossa and Eden Valleys. It can be seen that although surface water allocation is increasing in both regions, licensed surface water use is decreasing. Unlicensed surface water use is assumed to be constant over the period, and is assumed to be 30% of the unlicensed dam capacity in the respective regions (Water Allocation Plan Barossa Prescribed Water Resources Area, 2009).

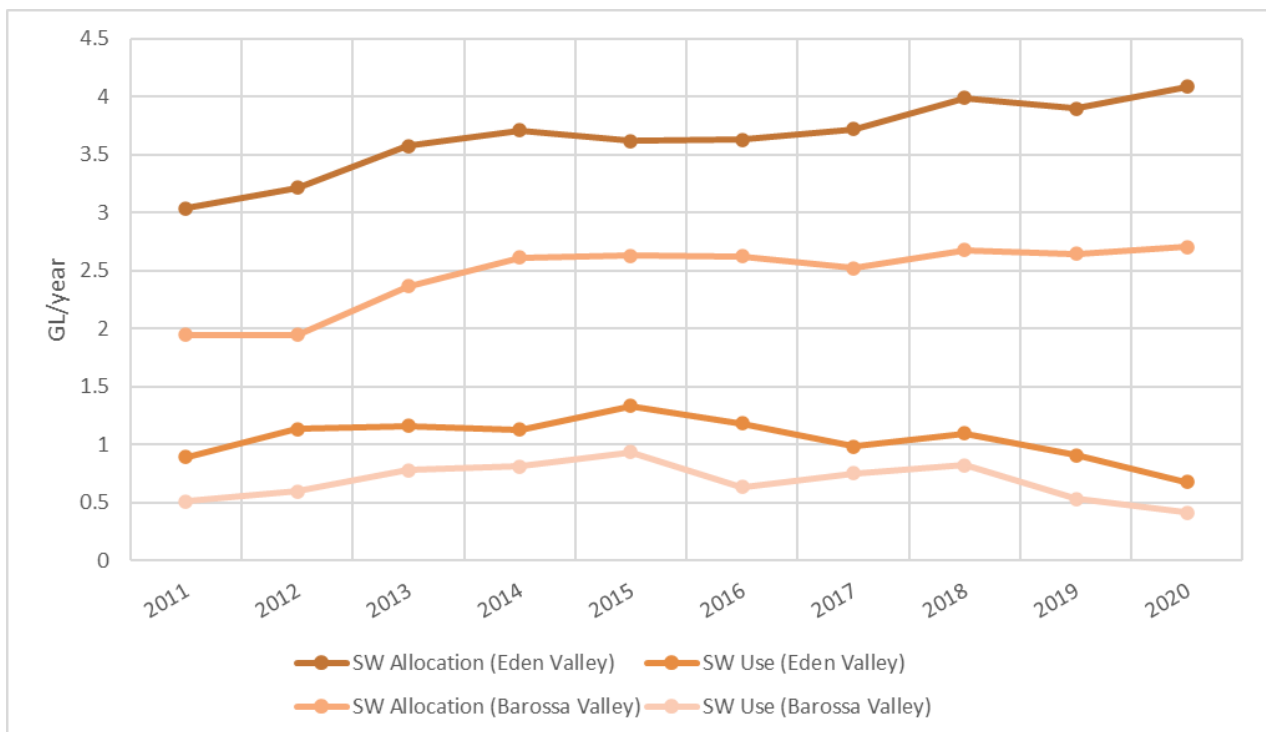


Figure 26. Change in licensed surface water use and allocation over the recent decade (2010/11 to 2019/20) for the Barossa and Eden Valley regions

3.6.2 Groundwater

The majority (typically 60%) of groundwater abstraction in the Barossa PWRA occurs from the fractured rock aquifers. Approximately equal amounts (typically 20%) of groundwater is abstracted from the upper and lower sedimentary aquifers. Groundwater is almost exclusively abstracted during summer to meet irrigation demand. For Eden Valley, the fractured aquifer extent covers the whole region.

Recent groundwater use for the Barossa PWRA (for the period 2010-11 to 2019-20) is shown in Figure 27. Groundwater usage varies considerably from year to year (from 1.3 to 4.4 GL over the period 2010 to 2019). This variability primarily reflects the availability, price and quality of other water sources. Importantly, total groundwater usage is not limited by allocation (Figure 27); the total annual allocation has always been above the total annual usage, with total annual allocation being relatively stable and above 6 GL over this period

(Cranswick et al., 2015) (Figure 27). Ground water use is also not limited by allocation in the Barossa Valley and Eden Valley delineations (Figure 28).

Figure 27 and Figure 28 also shows an increase in groundwater use in recent years for all three delineations. In the Barossa PWRA, the groundwater use has reached approximately 4 GL/year in the last couple of years. The slope of a linear regression line-of-best-fit is 0.25 GL/year. Groundwater use also shows a strong negative correlation with annual average rainfall over this period (e.g., a regression line slope of -4.5 ML abstraction per mm rainfall with an R^2 value of 0.65), highlighting that groundwater use occurs at least partially in response to rainfall deficits over the period of investigation.

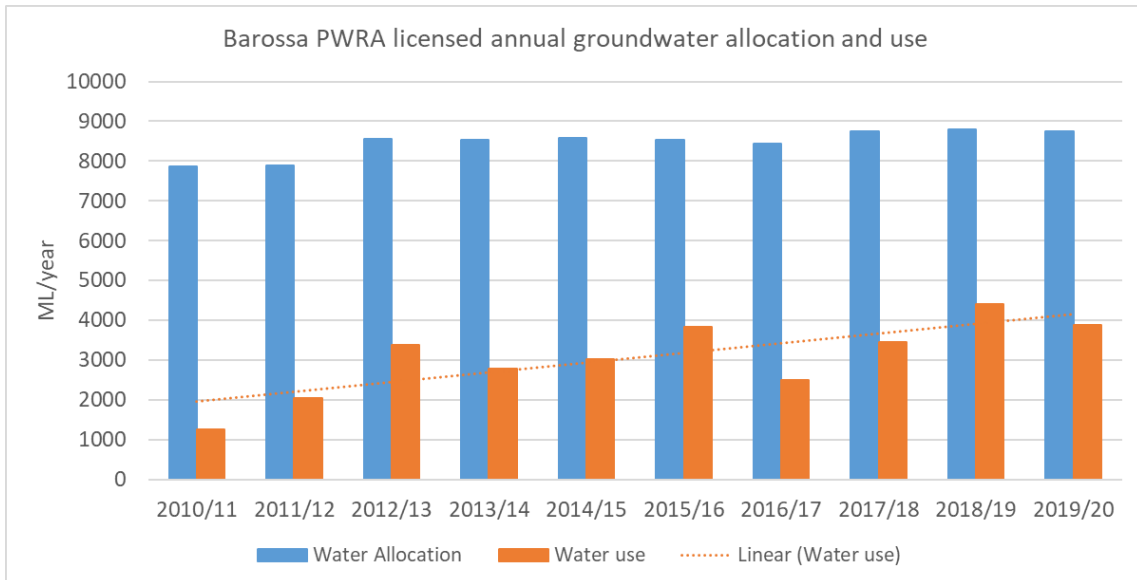


Figure 27. Recent licensed groundwater use data for the Barossa PWRA for each water-use year (1 July to 30 June).

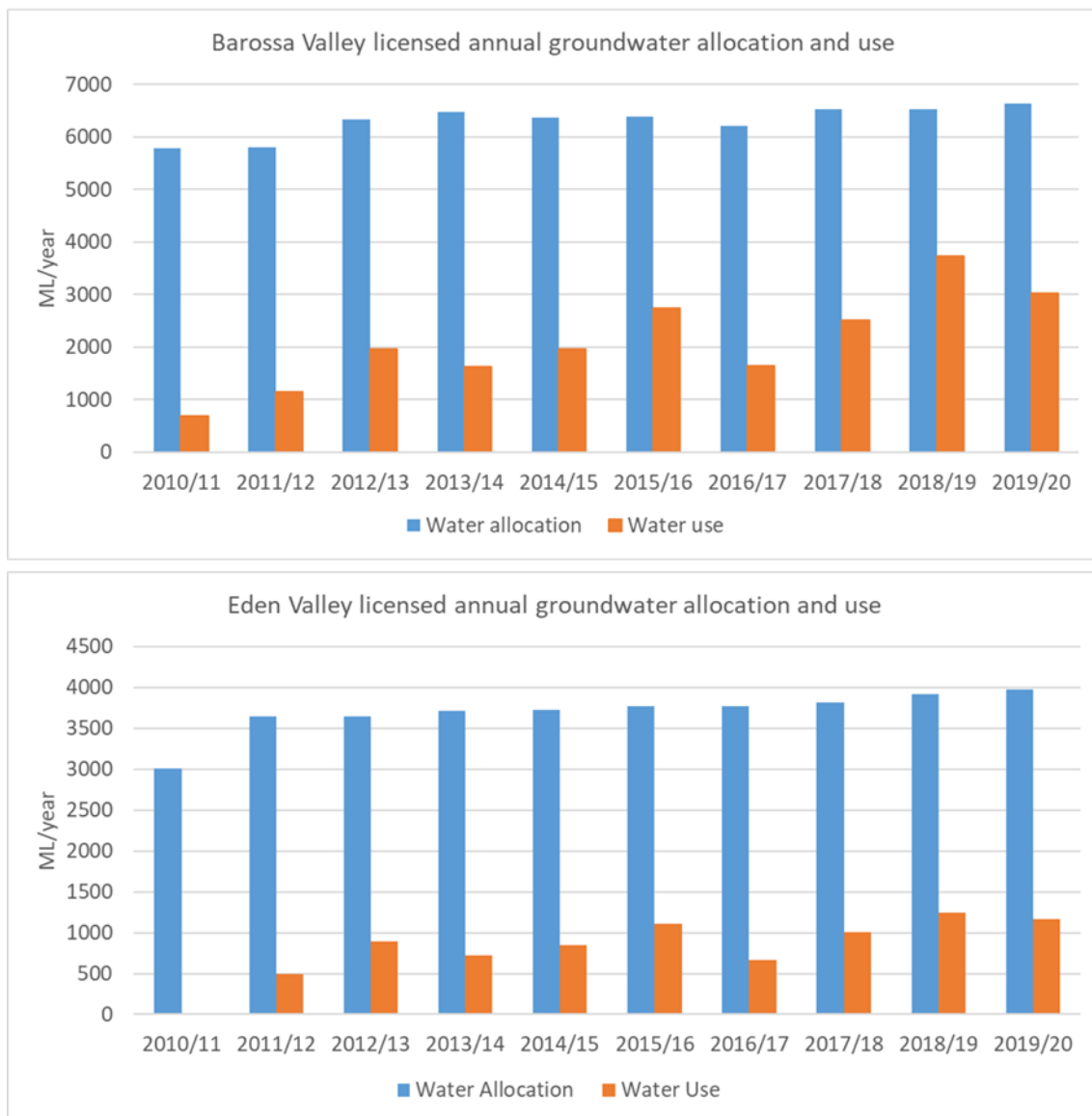


Figure 28. Historical metered use and allocation of groundwater for the Barossa and Eden Valley delineations

3.7 Within system flux: Groundwater Recharge

Historical groundwater recharge: key points

- Groundwater recharge is the primary flux of water into the aquifers, with lateral fluxes considered negligible. The estimated annual average recharge between 1990 and 2015 is 13 GL/yr, with significant year-to-year variability.

Groundwater recharge (also termed ‘rainfall recharge’) is critical to the sustainability of groundwater resources within the Barossa PWRA, both from a water quantity and water quality standpoint. As a result of the relatively low lateral influxes of water into the Barossa PWRA aquifers (Section 3.5), groundwater recharge is considered to be the primary source of fresh water into the aquifer system.

Recharge rates in the Barossa PWRA are highly variable both in space and time. Spatial recharge variability is driven by soil heterogeneity, rainfall ‘gradients’, topography, vegetation and various other factors. The spatial distribution of groundwater recharge (on a time-averaged basis) has been estimated by Cranswick et al.

(2015) using the widely-applied chloride mass balance method, yielding spatial recharge rates between 7.5 and 68 mm/year. These estimates were then updated by Li and Cranswick (2015) through groundwater model calibration on the basis of time-averaged hydraulic observation data.

Simulated annual groundwater recharge rates across the Barossa PWRA during the period 1990—2015 vary between approximately 6 and 24 GL, with a mean of 13 GL (Figure 24). The temporal variability in recharge, owing to rainfall variability, depth to water table changes, soil moisture etc., was estimated by Li and Cranswick (2016) using the departure-from-(long-term) mean annual rainfall as well as multipliers assigned to five annual rainfall ranges (<400, 400-500, 500-600, 600-700, >700 mm/year).

3.8 Storage: Farm dams

Historical farm dam storage: key points

- The estimated annual average and annual maximum farm dam storage volume in the Barossa PWRA is 3.18 GL and 4.45 GL, respectively, with evidence of declining trends. The storage level is consistently well below total farm dam capacity in this region.

Farm dams are used in the region to capture surface water for irrigation, stock, and domestic uses. As discussed previously, the dams used for irrigation are licensed and water use is metered. The dams used to cater to stock and domestic water demands are not licensed, and the capacities of these non-licensed dams are estimated based on aerial surveys (Jones-Gill and Savadamuthu, 2014) and incorporated into the eWater Source model. The total number and capacity of farm dams across the three delineations are summarized in Section 1.4.1, with the full region (comprising both the Barossa and Eden Valley delineations) having an estimated 3230 farm dams, comprising a total storage capacity of 14.34 GL, of which 8.27 GL (58%) is licensed.

To understand typical farm dam dynamics, we summarise several key elements of farm dam behaviour based on the eWater Source surface water model developed for the Barossa PWRA. The model contains a total of 399 farm ‘dams’ represented using the farm dam plugin in Source, with a total dam capacity modelled in the Source model of 8.25 GL—slightly lower than the total Barossa PWRA farm dam volume estimated by (Montazeri and Savadamuthu, 2020). The simulation is initialised with dams at 75% capacity. The data from the historical simulation for the period from the 1980/81 water year to the 2019/20 water year based on an estimate of present-day constant dam configuration and demands is used to explore farm dam dynamics, and thus provides an illustration of what would have occurred had the present-day settings been subject to the weather patterns over the period of record.

A time series of annual dam storage volume (both the maximum storage within each year, together with the mean storage) estimated by the eWater Source model is shown in Figure 29. The mean annual average farm storage from 1980/81 to 2019/20 is 3.18 GL and the mean annual maximum farm dam storage is 4.45GL. There is a clear decreasing trend in storage volume over this time, with the average storage in the dams being less than half the aggregated dam storage capacity. Based on the Source simulations, the 2019/2020 water year was the driest over the record.

Within-year dynamics are shown in Figure 30, which presents daily total farm dam storage in Source for water years representative of a wet (2010-11), dry (2019-20) and average (2009-10) year. As can be seen, typical farm dam volumes exhibit significant seasonality, which roughly corresponds to the seasonal cycle. Even for a relatively wet year, the maximum total farm volume is only about 60% of the total dam capacity.

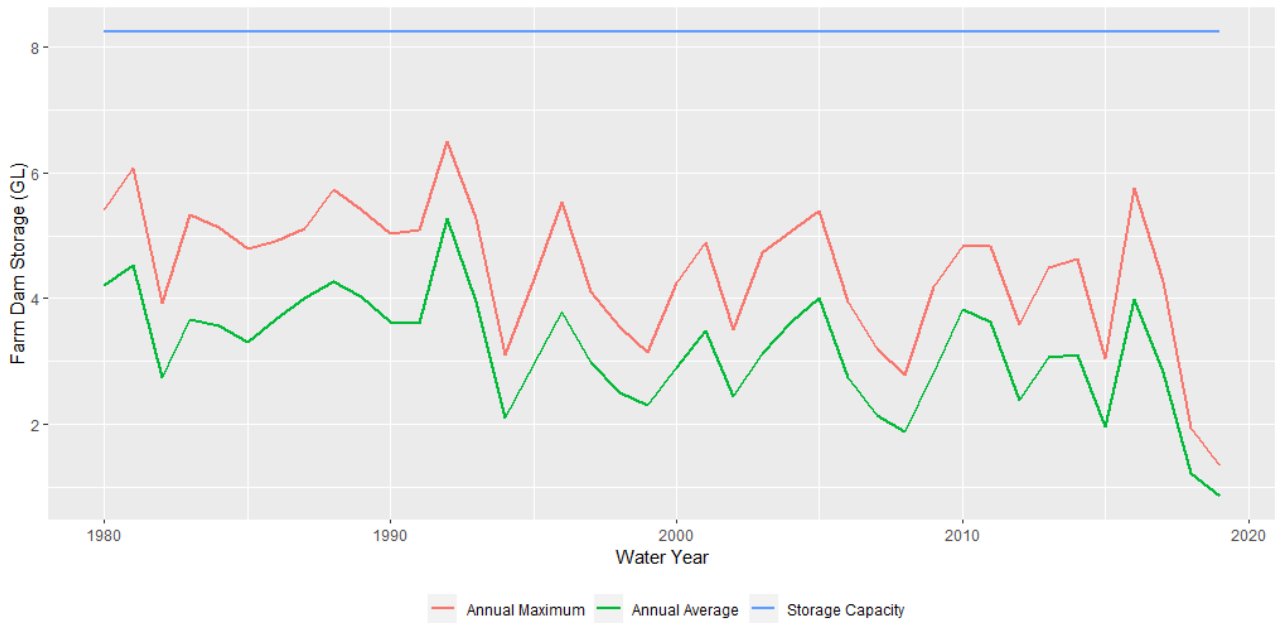


Figure 29. Historical (1980/81-2019/20) annual average, annual maximum and farm dam storage capacity for each water-use year (1 July to 30 June) in GL, as modelled in Source.

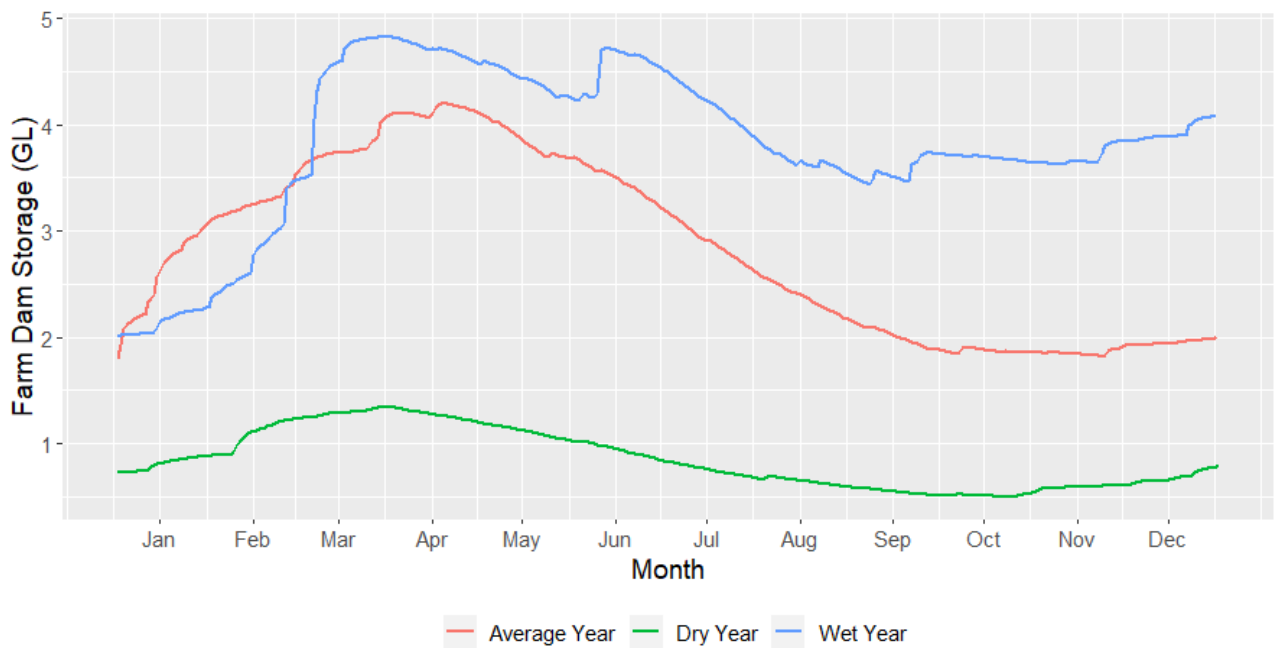


Figure 30. Total Farm Dam Storage in GL (modelled daily) for a representative wet, dry and average year

3.9 Storage: Groundwater storage

While groundwater REL recommendations have been put forward by Cranswick et al. (2015, 2016) (3.1 to 3.6 GL/year), estimates of total amount of groundwater storage volume have not yet been reported. To estimate the amount of groundwater storage, groundwater heads need to be analysed in combination with aquifer hydraulic properties.

Groundwater heads in the Barossa PWRA display pronounced seasonal variability (Figure 31). This variability can be attributed to both climate (e.g., rainfall recharge variability) and water use (e.g., groundwater abstraction during summer months for irrigation purposes). Larger seasonal variabilities (>5 m) are generally reflective of groundwater abstraction impacts. The influence of groundwater abstraction is apparent in all aquifers across much of the Barossa PWRA.

On a longer-term basis, groundwater heads generally display largely stable trends across much of the Barossa PWR, including prior to 1990 (Cranswick et al., 2015). Historical groundwater abstraction has not resulted in widespread inter-annual declining groundwater heads. Long-term declines, however, have been observed in several observation wells across all aquifers (five to 10 wells in total), and these declines are thought to reflect relatively localised groundwater abstraction impacts. It is also worth noting that there have been no significant changes in shallow groundwater level trends reported. This means that the impact of historical changes/increases in irrigation have not been observed in terms of groundwater levels.

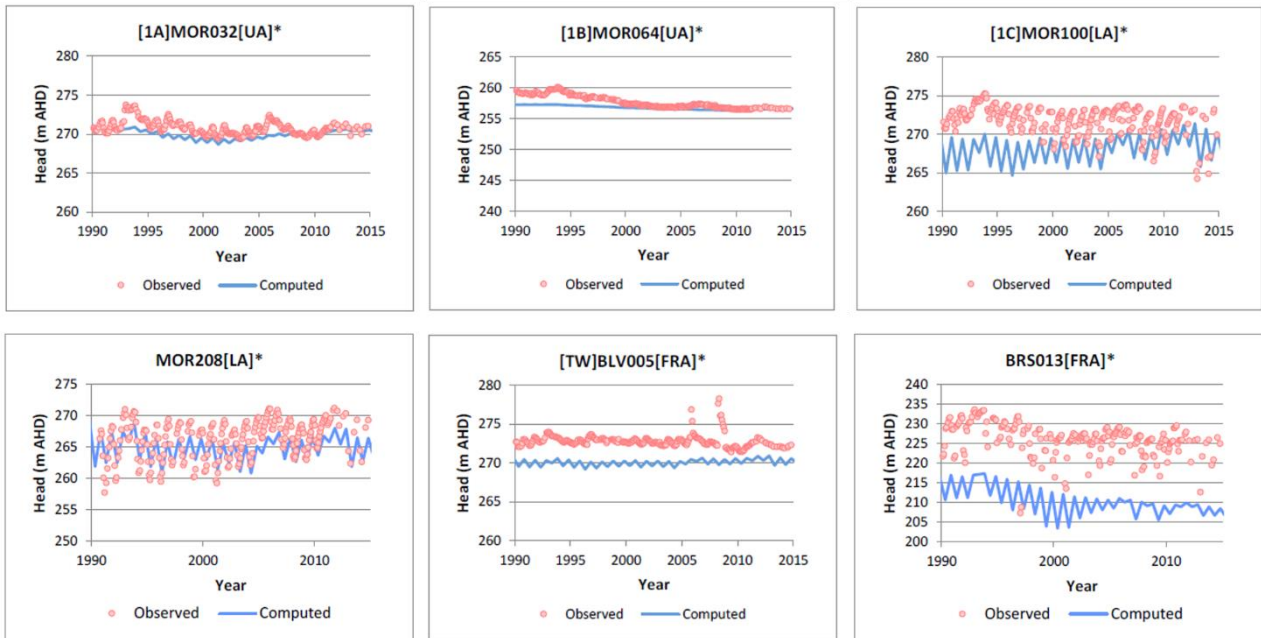


Figure 31. A selection of representative groundwater hydrographs identified by Li and Cranswick (2017) to capture overall Barossa PWR groundwater trends (from Li and Cranswick (2016)). ‘AHD’ refers to the Australian Height Datum (approximately equal to mean sea level). Subplot titles are the observation well identifiers.

Total groundwater storage within the Barossa PWR and its variability in time is estimated here using simulated heads from the groundwater model of Li and Cranswick (2016), together with calibrated aquifer storage property parameter values. Mathematically the amount of water stored in aquifers represented in a groundwater model is given by (e.g., Knowling et al., 2015):

$$\sum_{i=1}^n (S_y b)_i \Delta x \Delta y \quad (\text{unconfined aquifer})$$

$$\sum_{i=1}^n (S_s b H)_i \Delta x \Delta y \quad (\text{confined aquifer})$$

where S_y is the aquifer specific yield (-) (equivalent to ‘effective’ porosity); S_s is the aquifer specific storage (m^{-1}); b is the aquifer (saturated) thickness (m); H is the height of the potentiometric surface above the top of the (confined) aquifer (m); n is the number of model grid cells; $\Delta x \Delta y$ is the area of each model grid cell (here equal to $10^4 m^2$).

Figure 32 shows the time series estimate of total groundwater stored within both unconfined and confined aquifers within the Barossa PWR. The year-to-year variability represents an aggregated form of the hydrographs in Figure 31. For reference, 690 GL is equivalent to a water column of approximately 1.3 m height over the Barossa PWR area ($528 km^2$).

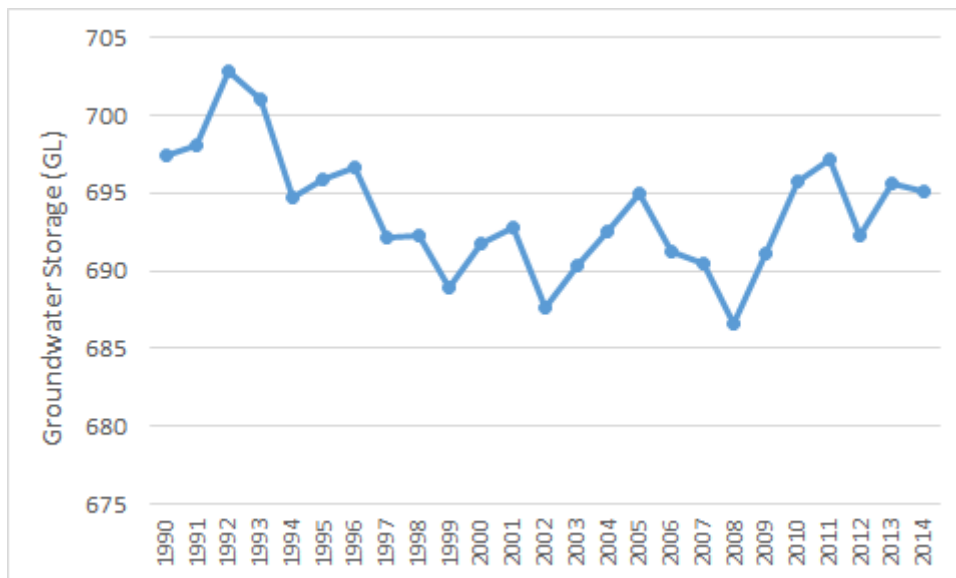


Figure 32. Time series estimates of total groundwater storage in the Barossa PWRA based on calibrated groundwater model of Li and Cranswick (2016).

3.10 Summary of Historical Water Consumption

The historical water consumption for the Barossa PWRA, Eden Valley and Barossa Valley regions are presented in the following sections. This includes surface water extraction (both licensed and unlicensed), groundwater extraction, and supply from the BIL and SA Water off-peak schemes. As the Eden Valley is not connected to any pipeline schemes with the exception of a small contribution of the SA Water off-peak scheme, water supply in this region comes almost exclusively from native sources.

Data on licensed and unlicensed surface water, and licensed groundwater in the Barossa PWRA was taken from multiple sources as detailed in Sections 3.6.1 and 3.6.2. The licensed surface and groundwater use data for Barossa and Eden Valley were extracted from WILMA, and are taken from Barossa PWRA, Marne & Saunders PWRA and Western Mount Lofty PWRA regions. Unlicensed surface water extraction, presumed to be used for stock and domestic purposes, is estimated from unlicensed farm dam capacity (as detailed in Section 3.6.1). The BIL and SA water off-peak water use data is from recorded usage as mentioned in Sections 3.2.1 and 3.2.2 respectively.

3.10.1 Barossa PWRA

The historical water use from 2008/09 to 2019/20 is shown in Figure 33. It is assumed that the full BIL capacity supplies the Barossa Valley region. For the Barossa PWRA, the area of vineyards that are in both the Barossa PWRA and Barossa Valley (74.9 km²) are divided by the total area of vineyards in the Barossa Valley (117.5 km²) to estimate that 64% of the BIL capacity supplies the Barossa PWRA. Similarly, as discussed in Section 3.2.3, it is estimated that around 40% of the Seppeltsfield vineyards lie within the PWRA, and hence 40% of the Bunyip supply is assumed to be attributed to this region.

Total water use ranges from 6.5 GL in a wet year (2010/11) to over 16GL in a very dry year (2018/19). It can be seen that there is an increasing trend in water use, with a greater proportion of this is coming from the external water supply sources in recent years. Use from surface water sources also appears to be decreasing, which may be due to reduced availability of this water source during drier years.

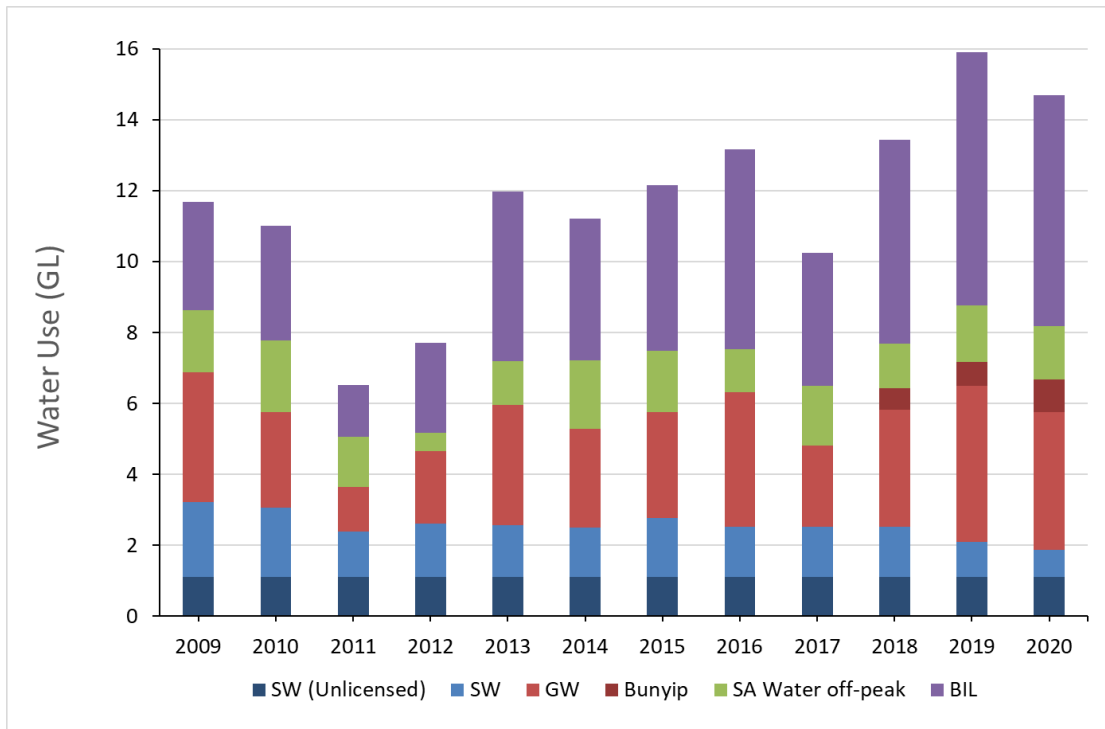


Figure 33. Observed water use in the Barossa Pwra from 2008/09-2019/20

3.10.2 Barossa Valley

The Barossa Valley water use from 2010/11 to 2019/20 is shown in Figure 34. The Barossa Valley has very similar year-to-year variability as the Barossa Pwra, which is expected as they are significantly overlapping regions. The water use ranges from 6GL (2010/11) to 20GL (2018/19). Less surface water and groundwater extraction is observed in the Barossa Valley than for the Barossa Pwra, and extraction from external sources is larger as the full use from these sources is assumed for the Barossa Valley.

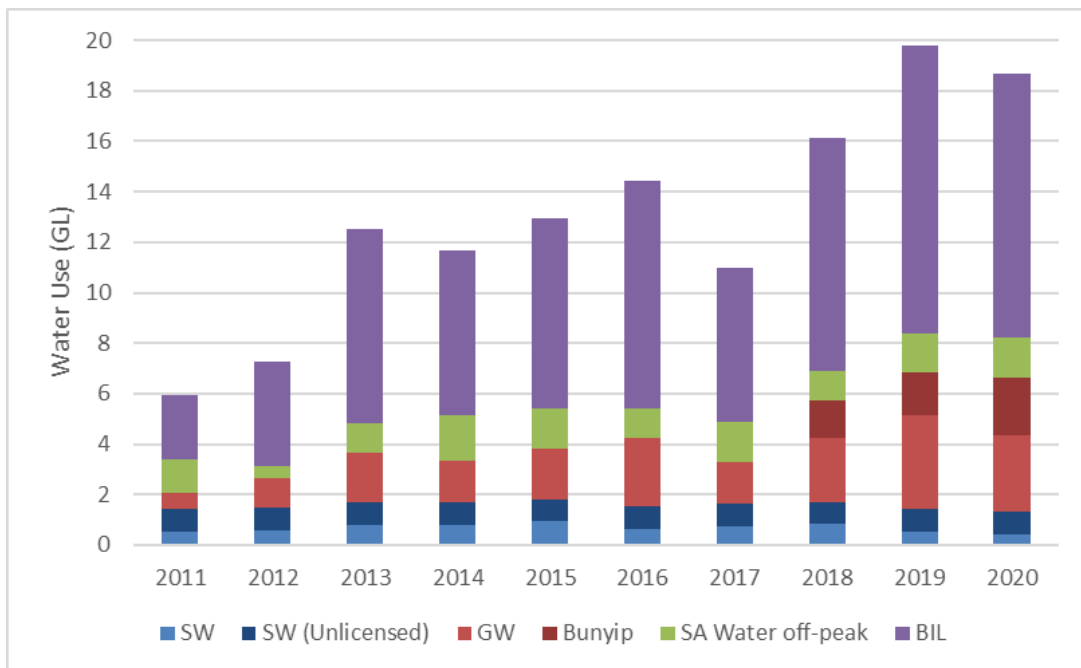


Figure 34. Observed water use in the Barossa Valley from 2010/11-2019/20

3.10.3 Eden Valley

The Eden Valley water use from 2010/11 to 2019/20 is shown in Figure 35. As expected, due to lack of external sources, there is a much larger proportional use of water from the native surface water and

groundwater sources compared to the other delineations. Water use ranges from 1.8 GL (2010-11) to 3.3GL (2016-17), and has some similarities to the year to year variability as the Barossa PWRA and Barossa Valley. As there is no supplementary pipeline in the Eden Valley, water use is limited by the quality and availability of native sources, so very dry years may not necessarily have the highest water use if this water was not available.

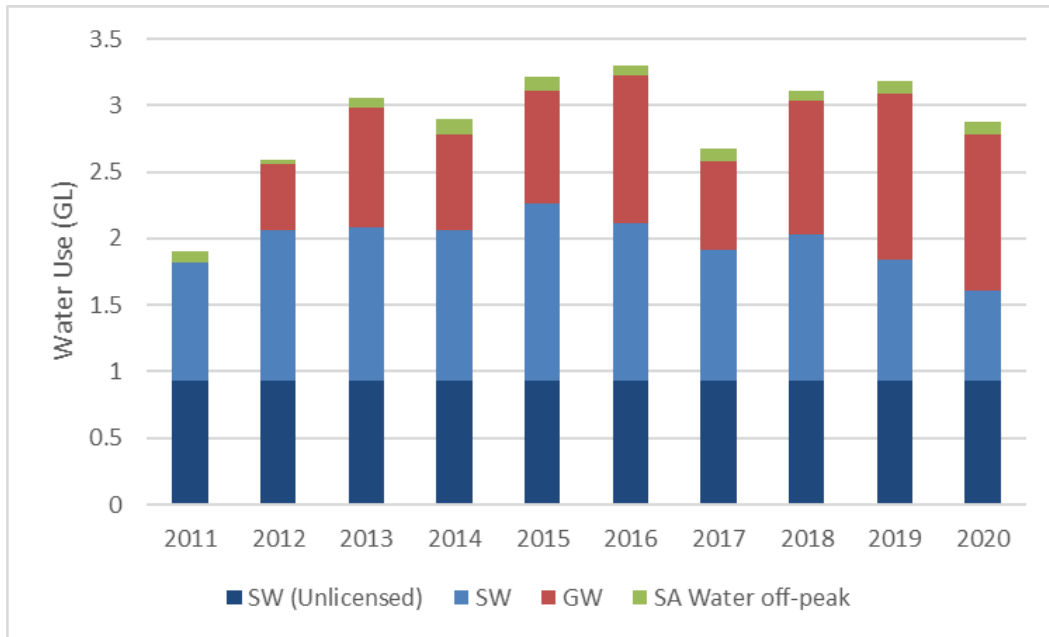


Figure 35. Observed water use in the Eden Valley from 2010/11-2019/20

3.11 Demand estimation

Human demand for water represents a key element of the overall system water balance, and two complementary methods for estimating demand are discussed here. Both methods explicitly seek to relate demand to climate variables, in the same manner that approaches to model surface water and groundwater supply (i.e. Source and MODFLOW) have explicit relationships with precipitation and potential evapotranspiration. The development of this relationship between climate and demand represents a critical foundation for subsequent climate stress tests. The theoretical basis for both demand models are described below.

3.11.1 Regression-based demand estimation

A simple water demand model has been developed that is driven by climate variables and calibrated to recent (2009-2020 for the Barossa PWRA, 2011-2020 for the Barossa and Eden Valleys) water use data. The conceptual basis for this model is that recent water consumption provides a quantitative basis for estimating actual demand in the region. By linking historical water consumption with climate variables, the model provides a basis for estimating demand (e.g., total or from imported sources) under plausible future changes in climate.

Mathematically the model takes the form:

$$D = \beta_0 + \beta_1(K_c PET - P) + \varepsilon$$

$$\varepsilon \sim N(0, \sigma)$$

where D is the irrigation water demand, β_0 and β_1 are the linear regression coefficients, K_c is a crop coefficient (a value of $K_c = 0.55$ was found to produce a best-fit) and ε is the 'residual' between the prediction and actual water use, which is assumed normally distributed. The $(K_c * PET - P)$ term constitutes an irrigation demand prediction based on annual climate factors and K_c only, assuming that the difference between the estimated

evapotranspiration and rainfall represents the irrigation demand. Note that a slightly stronger correlation between recent annual water use and demand can be achieved when considering only summer P and PET; however, as described in Section 2, the stress-test assessment to be conducted herein predominantly employs an annual temporal resolution. The demand model therefore requires P and PET inputs on an annual basis rather than on a seasonal basis.

We expect good agreement between estimated demand based on the regression model and recent water use (on which the estimated demand is calibrated). However, plausible climate futures are likely to encounter water resource limits that have only recently been encountered in reality (i.e., in 2013 and 2019, where BIL capacity was reached, as shown in Figure 14). Such dynamics mean that this simple demand regression model will require careful extrapolation when making demand estimates in the future. It is for these reasons that the uncertainty associated with the regression model is assessed. We therefore not only determine best-fit model regression coefficients, but also the stochastic model error term ε (given above), which can subsequently be used to explore demand uncertainty.

This regression relationship makes the following key assumptions:

- The effect of the two years where water resource limits were exceeded (i.e. 2013 and 2019) on regression parameters were relatively limited (this would be valid if the actual demand was only slightly greater than available water supply); and
- Historical demand behaviours will remain constant into the future such that the relationship between climate and demand remains 'stationary'.

In practice, the first assumption may mean that the actual regression slope is somewhat steeper than estimated here; in other words, this model may slightly underestimate demand sensitivity to climate. This is particularly because there may be an inverse yield response to compensate for decreased water availability, with yields well below the average in dry years indicating potentially significant 'latent' demands during those years (cf. Figure 5)

3.11.2 Process-based demand estimation

In order to contrast empirical water use demand estimates with daily irrigation demand estimates based on hydroclimate variables and biophysical processes and/or relationships, we adopt a recently developed wine grape irrigation demand model (Phogat et al., 2020). The two demand models are intended to be used in combination given their distinct natures, strengths and weaknesses.

The irrigation demand model of Phogat et al. (2020) employs the FAO-56 dual crop coefficient (DCC) approach (i.e., plant transpiration and soil evaporation are computed separately; Allen et al., 1998). The model runs on daily basis and treats each year independently (i.e. persistence from year-to-year in, for example, soil moisture stores or vine demand, is neglected). Despite its physical basis, the model (referred to herein as 'FAO-56 DCC') is relatively simple and easy to apply, particularly when compared to crop-soil models (e.g., Knowling et al., 2021).

The FAO-56 DCC model requires daily weather input variables including: rainfall, (reference) evapotranspiration, minimum relative humidity and wind speed. Several static model parameters were specified in order to reflect typical wine grape grower practices across each of the delineations, including 'management associated decisions' (MAD) related to soil water deficit to trigger irrigation during different stages of crop development, and 'available water' (AW) which is equivalent to AWHC following Robinson and Sandercock, 2014).

This model makes the following key assumptions:

- Irrigated viticulture is the primary demand; and

- The overall relationship between climate and irrigation behaviour will remain constant (i.e. no major changes in vineyard varieties, irrigation practices etc relative to the period from 2009-2020)

3.11.3 Results

In this section, results are presented for the Barossa PWRA (Figure 36), Barossa Valley (Figure 38) and Eden Valley (Figure 39). The mm to GL conversion in each plot assumes a constant area of vineyards within each delineation (87.2 km², 117.5 km² and 23.2 km² for the Barossa PWRA, Barossa Valley and Eden Valley delineations, respectively) for all sources. Note that the volumetric version of the models do not make any assumptions on the nature of the demand; however, conversion to (in the case of regression-based demand) and from (in the case of process-based demand) depth average estimates requires the assumption that demand is dominated by irrigated viticulture. The coloured bars represent the observed water use (as in Figure 33 to Figure 35), with the black line representing the regression-based demand, and the orange line representing the process-based demand (with stock added to the model results later on). The parameters used as a result of calibrating both the regression and process based models is summarised in Table 9.

Table 9. Summary of model parameters used for the Barossa and Eden Valleys

	Regression-based demand		FAO-56 DCC Model		
	β_0	β_1	AW (mm)	MAD initial (%)	MAD final (%)
Barossa PWRA	9.366	0.145	135	85	70
Barossa Valley	9.864	0.129	160	85	85
Eden Valley	2.485	0.902	160	85	80

Results for the Barossa PWRA (Figure 36 and Figure 37) show a good agreement between estimated demand based on the regression model and recent water use (on which the estimated demand was calibrated). The scatter about the regression line of best fit (Figure 37) likely reflects a combination of factors including inter-annual aspects of the hydrologic system, as well as changes in water user preferences, market demands, and so forth. While the estimated demand is unbiased in a first order sense over this time period, it can be seen that, due to the increased total water use over the last five years (2016 to 2020), estimated demand underestimates water use by approximately 1.0 GL on average over this latter period.

In contrast to the regression model, the FAO-56 DCC model displays significantly higher inter-annual variability, corresponding to different growing seasons, ranging from 0 mm (stock and domestic demand added in post to give 12.7mm) for wet years (2011) to 270 mm (283 including stock) for dry years (2013). The larger variability in irrigation demand based on the FAO-56 DCC model compared to the regression model is somewhat expected given the less aggregated nature of this model. Despite this, the year-to-year variability in irrigation demand between the two models shows consistent patterns. As expected, the average annual irrigation demand from the FAO-56 DCC model (121 mm) is similar to that obtained from the regression model (121 mm, excluding stock and domestic use), due to calibration of both models to historical water use data (average annual of 121 mm excluding stock and domestic use).

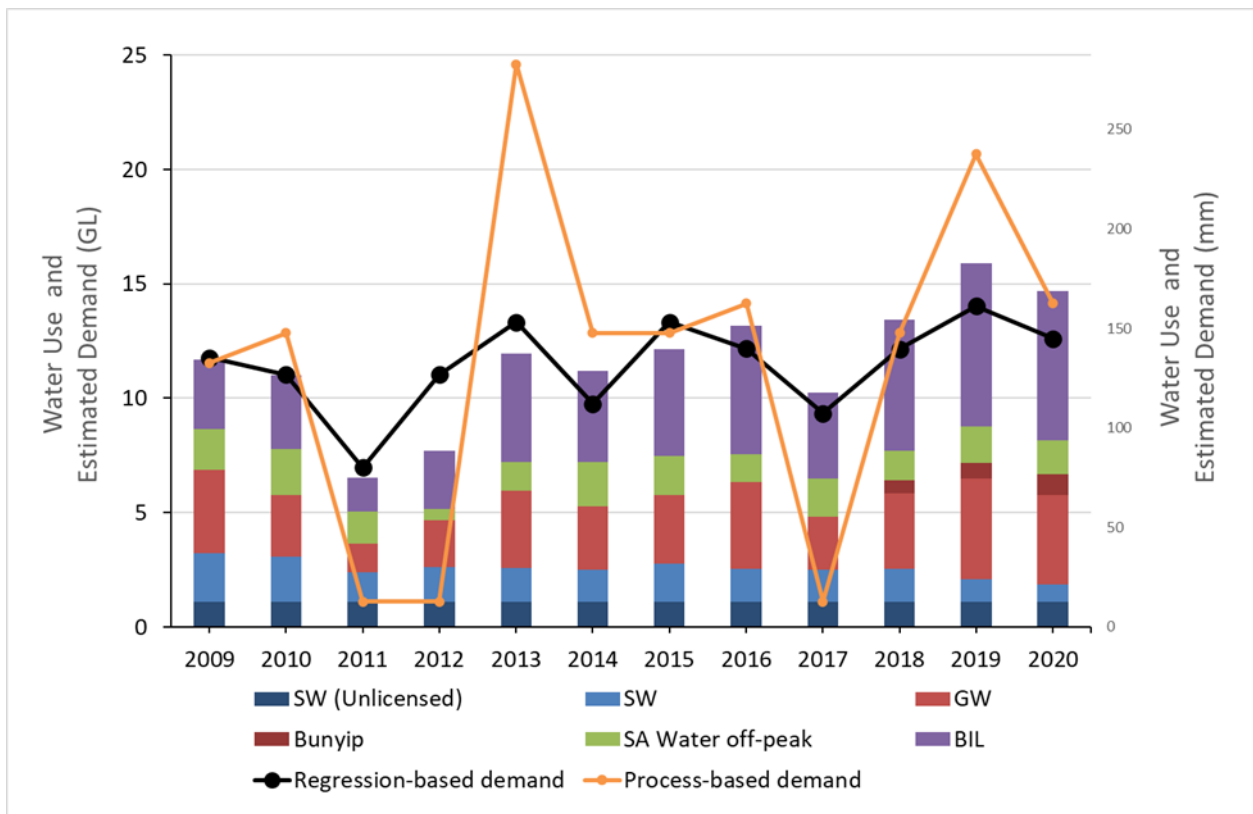


Figure 36. Comparison of recent water use from different sources (coloured bars) and estimated demand from regression model (black line) and FAO56-DCC model (orange line) shown as depths (mm; right vertical axis) and volumes (GL; left vertical axis) in the Barossa PWRA.

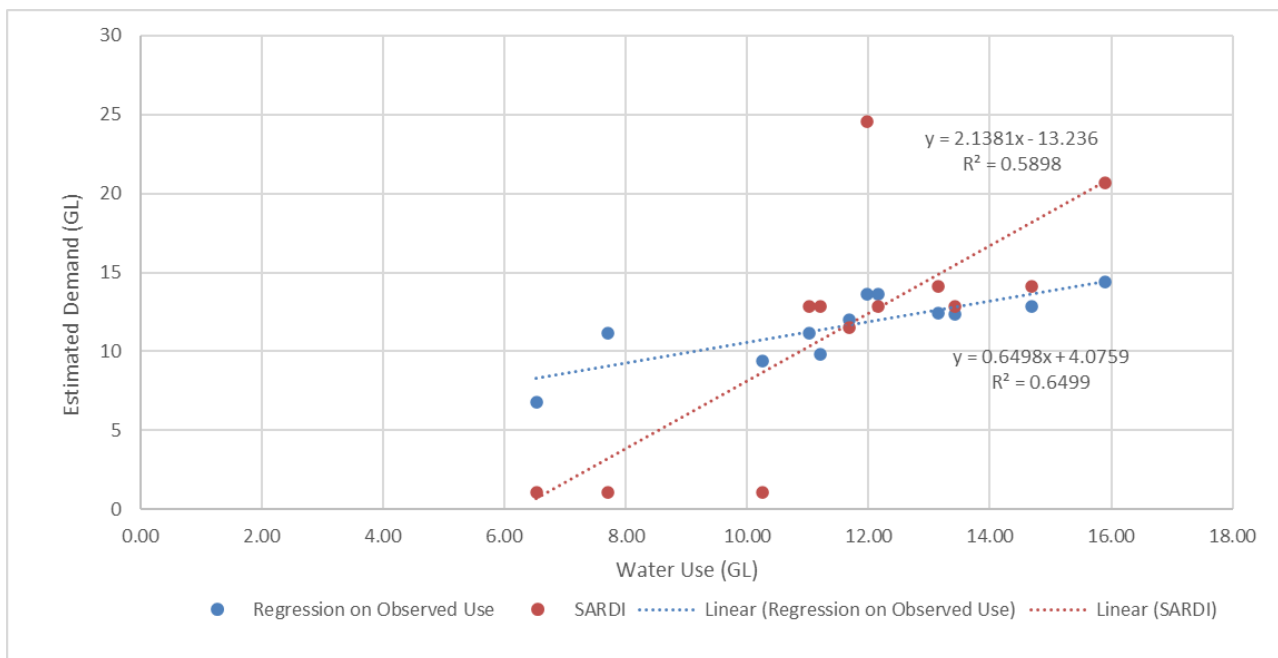


Figure 37. Comparison of regression on observed water use of the regression-based (blue) and process-based (red) model results. Figure 37 shows that for the Barossa PWRA, both models fit the average well (regression model R^2 of 0.65, and SARDI model R^2 of 0.59), although the regression based demand shows much lower sensitivity. The process-based model is much more sensitive to climate forcings, and thus has a larger range of estimated demand, which is much higher than use in dry years and lower than use in wet years. As the process-based model is a crop model, this could suggest that growers tend to irrigate more than necessary in wet years, and may have been unable to water as much as needed in dry years. Note that cases where the SARDI model

provides demand estimates that exceeds water use corresponds to the years where BIL capacity was reached (Figure 14).

To further explore possible differences between the regression model and the FAO-56 DCC model, an adjusted regression model was explored in which it was assumed that for the recent period, winegrape growers were actually pursuing a consistent yield target of 5 T/ha. Using crop water production relationships (Section 7.7) that assumes each ML/ha of water leads to an additional three tonnes of yield, the water demands associated with the difference between actual yield (Figure 5) for each year and the hypothetical 'target' yield could be calculated. This difference was added to the regression results, providing an approximate estimate of possible water demands had the growers sought to achieve consistent yields from one year to the next. Although the assumptions underpinning this analysis are very simplistic, it is interesting to note that the variance of the yield-adjusted regression in Figure 36 appears more similar to the FAO-56 DCC model compared to the standard regression results, providing some additional support for the notion that growers may have been adjusting yield targets to account for water limitations in dry years.

The results for the Barossa Valley and Eden Valley delineations are shown in Figure 38 and Figure 39. Similar to the Barossa PWRA, the regression-based model matches the average well, but can overestimate or underestimate demand in given years. The R^2 for the Barossa Valley regression is 0.53 and for Eden Valley it is $R^2=0.74$. In contrast, whereas by design the process-based model matches the averages well, the model is much more sensitive and has a larger amplitude of predicted demand compared to the regression-based model.

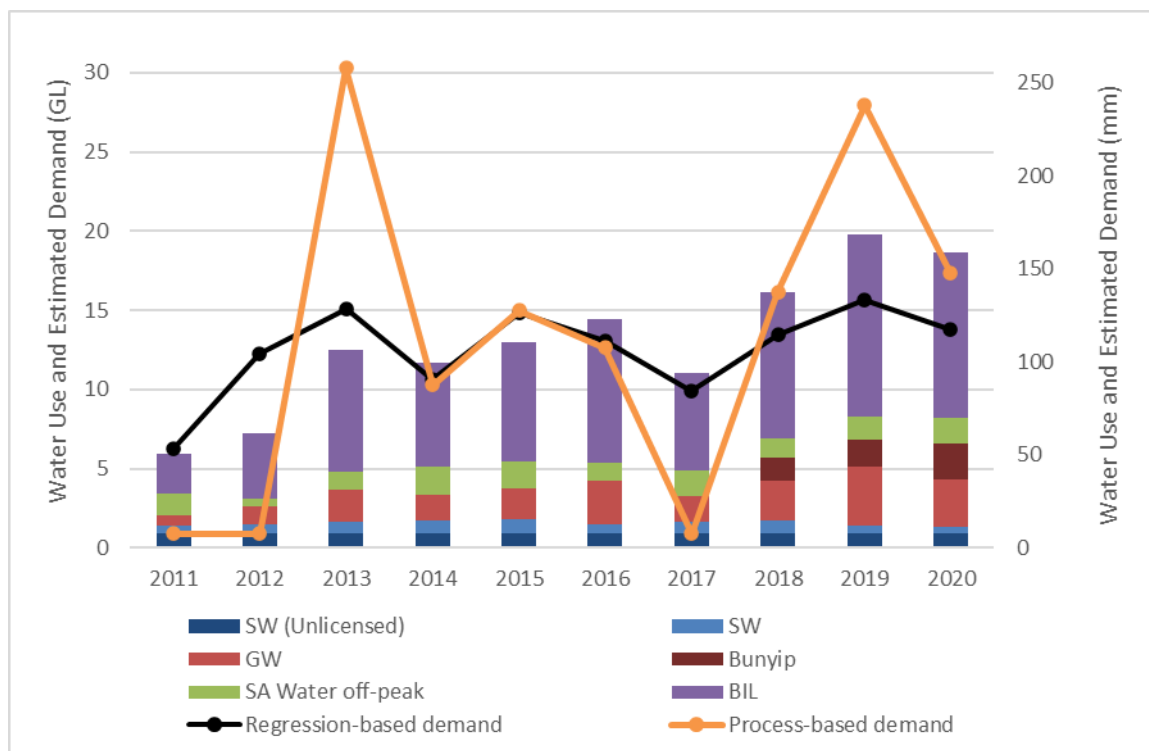


Figure 38. Comparison of recent water use from different sources (coloured bars) and estimated demand from regression model (black line) and FAO56-DCC model (orange line) shown as depths (mm; right vertical axis) and volumes (GL; left vertical axis) in the Barossa Valley

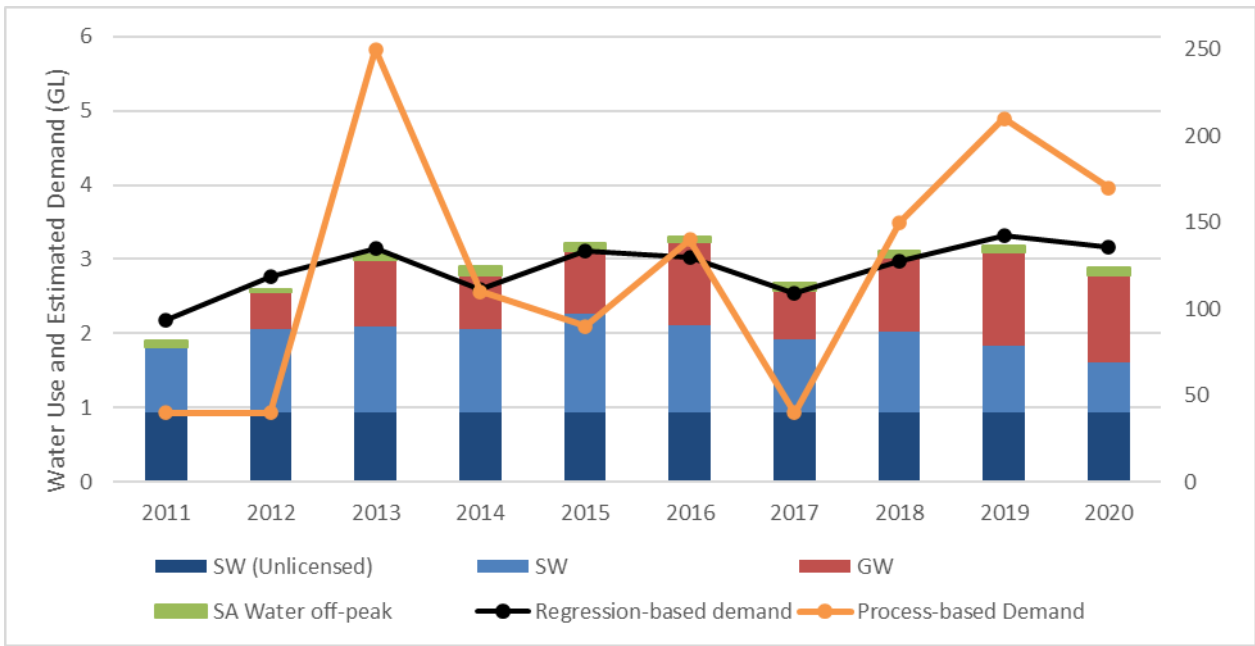


Figure 39. Comparison of recent water use from different sources (coloured bars) and estimated demand from regression model (black line) and FAO56-DCC model (orange line) shown as depths (mm; right vertical axis) and volumes (GL; left vertical axis) in the Eden Valley

4 Future climate stressors

In this section we take a multiple-lines-of-evidence approach to exploring possible future climate scenarios, defined in terms of the climate variables that have the potential to impact upon water supply and demand in the Barossa and Eden Valleys; namely, rainfall, potential evapotranspiration and temperature. The three primary lines of evidence are described first, followed by a summary of projections for each climate variable.

4.1 Sources of Climate Information

4.1.1 Climate Change in Australia (CCIA)

The Climate Change in Australia (CCIA; CSIRO and Bureau of Meteorology, 2015) report and web interface provides nationally consistent projections of future climate change for a broad range of atmospheric variables, and these have been presented for regions defined by Australia's natural resource management (NRM) delineations. The projections are based on a subset of the CMIP5⁴ suite of model simulations that have been determined to perform well over Australia.

The results presented in this report have been synthesized from the CCIA Report – Southern and South-Western Flatlands (East) (Hope *et al.* 2015). Projections for annual, seasonal and monthly data are available for 20-year time slices centred on 2030, 2050, 2070 and 2090, and are presented as changes relative to a 1986-2005 baseline. The projections are provided as median values and the 10-90th percentile range.

4.1.2 Climate Ready SA (CR-SA)

'Climate Ready SA' (CR-SA) is a dataset containing projections for large parts of South Australia, capturing information at the daily timescale for six separate climate variables: rainfall, temperature maximum, temperature minimum, areal potential evapotranspiration, solar radiation and vapour pressure deficit. The data includes two emissions pathways (RCP 4.5 and 8.5, representing 'intermediate' and 'high' greenhouse gas concentration pathways). The dataset has been divided into 'projections' spanning the period from 2006 to 2100, together with historical simulations from 1961 to 2005 that can support the development of a climatological baseline.

The data are derived from a subset of 15 general circulation models (GCMs) from the CMIP5 suite of model simulations, with the choice of GCMs selected based on their ability to capture climate drivers that are relevant to South Australia, including the Indian Ocean Dipole (IOD) and El Niño Southern Oscillation (ENSO). The GCM outputs were downscaled using a method known as 'Nonhomogenous Hidden Markov Modelling' that represents a statistical approach to adjust the large-scale climate model information into site-specific daily timeseries. This approach enables generation of multiple 'realisations' of historical and future weather, with each realisation reflecting expected climatic patterns, but with random day-to-day variations to capture real-world weather variability. In total there are 100 such realisations for each climate model and RCP, leading to a total of 1500 time series for each RCP.

Three stations within or close to the Barossa region were identified as having data relevant for this study: St Kitts [23360], Williamstown (Glen Gillian) [23756] and Rosedale (Turretfield Research Centre) [23343]. Of

⁴ The Coupled Model Intercomparison Project (CMIP) is a global collaborative scientific effort for collecting and analysing climate model outputs, and the CMIP outputs represent a critical data source on climate projections and other relevant information to inform the Intergovernmental Panel on Climate Change assessment process. CMIP Phase 5 (CMIP5) was compiled over the period 2010-2014, and was used to inform the Intergovernmental Panel on Climate Change's Fifth Assessment Report completed in 2014.

these, only the Williamstown station lies within the Barossa Valley PWRA (Table 26); the other two stations are within 5km of this region.

To inform stress testing, future changes are presented either as absolute values (e.g. mm rainfall, °C) or relative changes (e.g. percentage) relative to a baseline. Unless specified otherwise, a baseline of 1976-2005 is selected, representing a 30-year period consistent with the minimum length recommended by the WMO. Future changes were then assessed for 30 years windows centred on 2020 (i.e. the period 2006-2035, representing 'current' climate), 2035 (2021-2050) and 2050 (2036-2065) relative to this baseline.

For each station, emissions scenario, GCM and realisation the CR-SA data set provides time series of daily precipitation, PET, radiation and maximum temperature. These time series were spatially averaged by calculating the daily average across the three stations for each emissions scenario (historical, RCP 4.5 and RCP 8.5), GCM and replicate, giving 4500 daily time series of data.

Each of these 4500 time series are passed into the *foreSIGHT* software, where the specified rainfall, PET, radiation and maximum temperature attributes are calculated. For the historical scenarios, this is calculated for the baseline (1976-2005), and for the RCP 4.5 and RCP 8.5 scenarios, this is calculated for three future time slices (2006-2035, 2021-2050 and 2036-2065). This gives 1500 historical values for each attribute, and 1500 future attribute values for each RCP and time slice combination. For each attribute, RCP and time slice, the range of projections were derived by calculating the absolute or relative change for each attribute separately for each replicate. Repeating this for the 100 replicates and 15 GCMs leads to 1500 values of future change for each attribute.

Further information on this dataset can be found on the SA Climate Ready webpage (<https://data.environment.sa.gov.au/Climate/SA-Climate-Ready/Pages/default.aspx>), with a technical summary contained in the User Guide (Goyder Institute for Water Research, 2015).

4.1.3 NARClIM

NARClIM is a dataset developed by the NSW Government in partnership with the Climate Change Research Centre at the University of New South Wales, and contains projections for NSW, ACT, VIC and parts of the NT and SA—including the Barossa region. In the most recent version of NARClIM (NARClIM1.5) there are a range of climate variables available, both postprocessed (i.e. re-gridded) and bias corrected. The data includes two emissions pathways (RCP 4.5 and 8.5), capturing projections from 2006 to 2100, together with historical data from 1951 to 2005 to provide information to inform a historical baseline.

The data is derived from a subset of three CMIP5 GCMs (IPCC Fifth Assessment Report, 2014), each using two alternative configurations of the Weather Research and Forecasting (WRF) regional climate model. The selected GCMs are ACCESS1.0, ACCESS1.3 and CanESM2, which were chosen based on their performance in representing large-scale climate phenomena, such as ENSO, and as well as widely used metrics of climate variability. GCMs that performed poorly for the south-east Australian region were excluded and the remaining chosen models were selected to provide a spread of temperature and rainfall projections.

The regional climate models (RCMs) chosen for NARClIM1.5 are two variations of the WRF model. The two RCMs were selected from 36 combinations of physics schemes, and differ by their parametrisations of the planetary boundary layer, land surface and cumulus physics, micro physics, and short- and long-wave radiation physics. The two RCMs were selected from this larger set based on their comparative statistical independence from each other, and ability to capture climate variables of interest, such as temperature, precipitation and mean sea-level pressure and winds.

The two variables analysed in this report (precipitation and temperature) were both bias corrected. Studies have demonstrated the value of bias-corrected data for analysis of the climate change impacts of temperature and precipitation (Gross et al. 2016; Macadam et al. 2016). These climate variables were bias corrected towards the AWAP observational dataset (Argüeso et al. 2013; Evans & Argüeso 2014) using a

quantile matching technique (Piani et al., 2010). These corrections were applied to allow the fitted distributions of daily RCM output to match the fitted distributions of daily observations; these corrections were assumed to be independent of future climate change, and the same corrections were applied to the future data values.

The resolution of chosen data is the 10-kilometre south-east Australian NARClIM domain. To derive projections for the Barossa and Eden Valley region, a boundary was selected that incorporates six-by-seven 10 km² grid squares in the region. The latitude and longitude of the northwest and southeast extent of this region are represented by the points (-34.25, 138.75) and (-34.85, 139.25) respectively. This gives a total of 42 grid squares over the region.

Future changes are assessed for the same baseline and future windows, and procedure, as for the SA Climate Ready dataset.

4.2 Changes in Rainfall

Rainfall represents arguably the most critical climate control on both water supply and demand in the Barossa, driving surface and groundwater stores and fluxes as well as crop water requirements and other forms of demand. In this study we explore a range of rainfall ‘attributes’ capturing annual and seasonal rainfall totals, rainfall intermittency and a measure of rainfall extremes.

4.2.1 Annual and seasonal rainfall

The annual rainfall projections for the Barossa based on the Climate Ready SA product are shown in Figure 40 below, represented as percentage changes relative to the climatological baseline. Numerical values for annual and seasonal rainfall for each RCP and time slice are also summarized in Table 10, and include not only the Climate Ready SA dataset but also information from Climate Change in Australia and from NARClIM.

The results show a pattern of declining rainfall across most simulations, with greater declines for longer future time horizons and higher radiative forcings (i.e. RCP 8.5). These patterns were also generally present across the different approaches to developing the projections (i.e. CR-SA, CCIA, NARClIM), and for the different seasons. Equally importantly, there is a significant variation in individual modelling results, with a non-negligible number of simulations that show increasing trends across the various projection methods. For example while a significant majority of simulations showed declining trends for annual rainfall (e.g. the 25 to 75 percentile of the CR-SA projections ranged from -14% to -0.83%), the spectrum of projections (defined by the 2.5 to 97.5 percentile for CR-SA, the 10 to 90 percentile for CCIA and the full range of projections for NARClIM) ranged from a 23% decrease to a 5% increase. This range is due to a combination of representation concentration pathway uncertainty, climate model uncertainty (both GCM and RCM), methodological uncertainty (e.g. between statistical and dynamical downscaling) and stochastic ‘weather noise’. Moreover, the range is generally wider for longer future horizons and larger radiative forcings—a pattern that is repeated for other simulations.

The uncertainty limits play a particularly important role in system stress testing, as the focus of the stress test is to evaluate system performance under a broad range of plausible changes. For the case of annual and seasonal rainfall, the wide range of possible climate futures implies that stress tests need to consider the possibility of future increases to the total rainfall amount, even if the majority of projections suggest a future of declining rainfall totals. This issue will be discussed further in subsequent sections of this report.

Finally, the ‘projections’ for the period 2006-2035 encompass the current year (2021), and thus provide a reflection of the estimated current climate state relative to the climatological baseline. Both CR-SA and NARClIM have information for this time window, and are consistent in suggesting a median decrease of between 3.6 and 7.3% for total annual rainfall relative to the baseline (with the 25 to 75 percentile for CR-SA showing -7.0 to -0.83% change, and only the full uncertainty range containing projections of increasing rainfall). Whilst the intention of this report is not to conduct a formal climate change attribution analysis,

these results do strongly suggest that based on modelling estimates relative to the baseline, current-day rainfall would be expected to contain a small but significant climate change signal.

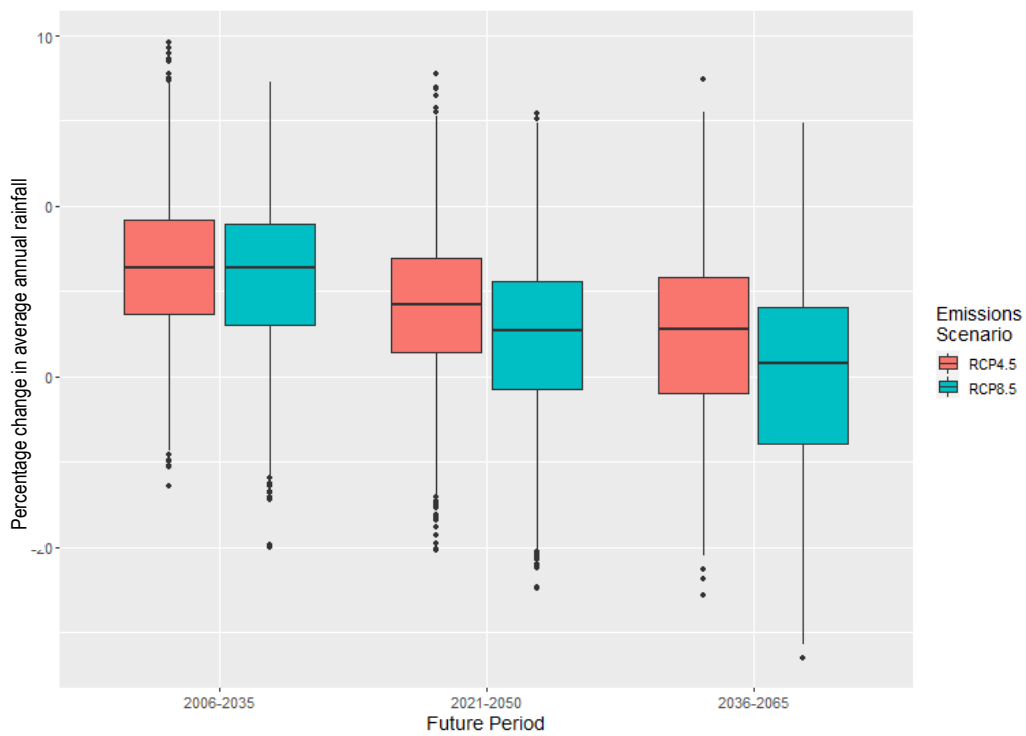


Figure 40. Annual changes in rainfall relative to a 1976-2005 climatological baseline. Each box-and-whisker plot represents the variability from 4,500 separate time series. The median value is represented by the horizontal black line, the boxes are bounded by the upper and lower quartiles. The upper whisker represents the values from the upper quartile to no further than $1.5 \times \text{IQR}$ (Inter Quartile Range). The lower whisker likewise extends to the value at most $1.5 \times \text{IQR}$. The dots above and below the whiskers represent outlying points.

Table 10. Percentage change of seasonal and annual precipitation averaged across all three stations in the Barossa. The median value, upper and lower quartile (25 to 75th percentile) and 2.5 and 97.5th percentile values are quoted.

Season	Percentile	Emissions Scenario	2020		2030	2035		2050		Range of future change
Line of Evidence:			CR-SA	NARClIM	CCIA	CR-SA	NARClIM	CR-SA	NARClIM	
DJF	Median	RCP4.5	-3.6	-12	0	-8.3	-9.4	-7.2	-10	-16 to 2
		RCP8.5	-4.0	-0.18	2	-7.7	-6.1	-9.8	-16	
	25-75%	RCP4.5 RCP8.5	-11 to 4.8 -12 to 4.0	NA	NA	-16 to -0.24 -14 to 0.092	NA	-17 to 1.5 -18 to -1.4	NA	-18 to 4.8
	2.5-97.5%*	RCP4.5 RCP8.5	-23 to 22 -23 to 22	-13 to -12 -19 to 33	-24 to 30 -14 to 19	-29 to 17 -27 to 17	-18 to 4.3 -9.2 to 23	-35 to 18 -31 to 17	-16 to 9.1 -27 to 11	-35 to 33
MAM	Median	RCP4.5	-4.5	2.9	-1	-3.8	-5.4	-5.4	-9.9	-9.9 to 2.9
		RCP8.5	-4.5	-3.9	-3	-5.2	-3.4	-6.9	-5.2	
	25-75%	RCP4.5 RCP8.5	-11 to 2.5 -11 to 2.8	NA	NA	-11 to 2.7 -13 to 2.1	NA	-12 to 2.5 -14 to 0.24	NA	-14 to 2.8
	2.5-97.5%*	RCP4.5 RCP8.5	-22 to 20 -24 to 18	-22 to 16 -20 to 5.9	-22 to 18 -22 to 23	-23 to 17 -25 to 15	-25 to 7.1 -21 to 3.3	-24 to 18 -27 to 14	-19 to 7.1 -30 to 4.9	-30 to 23
JJA	Median	RCP4.5	-1.6	-11	-6	-3.6	-10	-5.9	-13	-13 to 1.9
		RCP8.5	-1.5	-8.2	-5	-4.9	-5.1	-6.7	1.9	
	25-75%	RCP4.5 RCP8.5	-5.9 to 2.9 -5.5 to 1.8	NA	NA	-7.5 to 1.2 -8.7 to -1.3	NA	-11 to -0.39 -11 to -2.3	NA	2.9 to -11
	2.5-97.5%*	RCP4.5 RCP8.5	-12 to 12 -13 to 8.6	-17 to 9.4 -16 to 14	-16 to 6 -16 to 5	-11 to 14 -16 to 5.5	-20 to -4.7 -10 to 18	-17 to 10 -19 to 5.4	-27 to 5.7 -15 to 12	-27 to 18
SON	Median	RCP4.5	-6.7	-12	-5	-10	-17	-13	-25	-25 to -5
		RCP8.5	-7.9	-11	-7	-14	-10	-17	-18	
	25-75%	RCP4.5 RCP8.5	-12 to -1.7 -13 to -1.7	NA	NA	-16 to -5.2 -19 to -8.4	NA	-19 to -8.5 -24 to -11	NA	-24 to -1.7
	2.5-97.5%*	RCP4.5 RCP8.5	-20 to 8.9 -20 to 8.3	-27 to -3.6 -22 to 4.7	-20 to 10 -23 to 10	-25 to 5.4 -28 to 2.4	-31 to -3.2 -29 to -0.52	-28 to 1.2 -36 to -1.4	-32 to -12 -33 to 1.9	-36 to 10
Annual	Median	RCP4.5	-3.6	-7.3	-4	-5.7	-11	-7.2	-14	-14 to -2
		RCP8.5	-3.6	-4.7	-2	-7.3	-4.7	-9.2	-8.3	
	25-75%	RCP4.5 RCP8.5	-6.3 to -0.83 -7.0 to -1.1	NA	NA	-8.6 to -3.0 -11 to -4.4	NA	-11 to -4.2 -14 to -6.0	NA	-14 to -0.83
	2.5-97.5%*	RCP4.5 RCP8.5	-12 to 4.5 -14 to 4.3	-19 to -0.24 -9.0 to 4.4	-13 to 4* -13 to 5*	-15 to 2.8 -18 to 0.82	-23 to -3.4 -18 to 3.0	-18 to 1.6 -21 to -0.39	-19 to -8.2 -20 to 0.52	-23 to 5.0

* For NARClIM the values displayed in the 2.5-97.5% row is the minimum and maximum attribute values for the scenario; the CCIA report records 10th to 90th percentile uncertainty

4.2.2 Number of wet days

The total number of wet days per year is an important metric that represents the intermittency of rainfall (i.e. the sequencing of wet and dry days throughout the year), with CR-SA results shown in Figure 41 and numerical values shown in Table 11. Consistent with total annual rainfall, the results show a general pattern of declining trends, with the greatest declines for longer future horizons and greater radiative forcings. Also consistent with the total annual rainfall are a non-negligible number of projections showing increases in number of wet days, indicating that the possibility of wetter conditions cannot be ignored as part of future scenario evaluations.

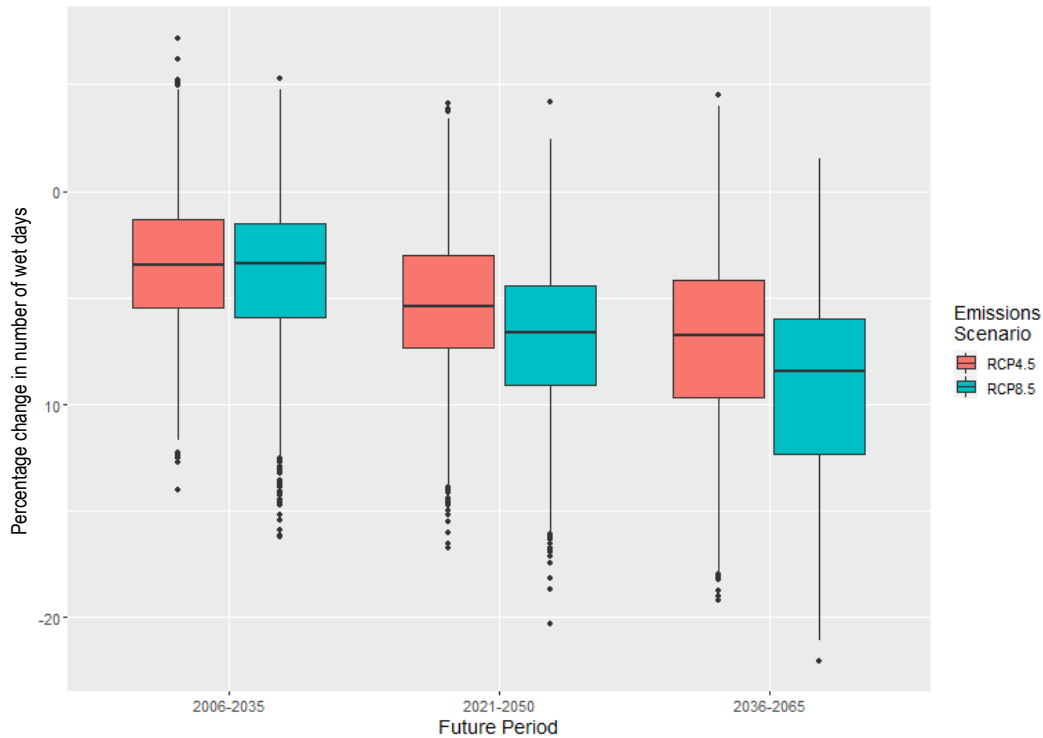


Figure 41. Percentage change in annual number of wet days (wet day threshold = 1mm) for RCP4.5 and RCP8.5 emission scenarios, relative to a 1976-2005 climatological baseline. See caption for Figure 40 for further details.

Table 11 – Percentage change in the annual number of wet days (wet day threshold = 1mm)

Percentile	Emissions Scenario	2020		2035		2050		Range of Future Change
		SA-CR	NARClIM	SA-CR	NARClIM	SA-CR	NARClIM	
Line of Evidence:								
Median	RCP4.5	-3.5	-8.7	-5.4	-8.1	-6.7	-13	-13 to -3.4
	RCP8.5	-3.4	-7.9	-6.6	-8.5	-8.5	-9.1	
25-75%	RCP4.5	-5.5 to -1.3	NA	-7.4 to -3	NA	-9.7 to -4.1	NA	-12 to -1.5
	RCP8.5	-5.9 to -1.5		-9.1 to -4.5		-12 to -6.0		
2.5-97.5%*	RCP4.5	-9.8 to 2.6	-15 to 3.1	-13 to 1.2	-20 to -6.1	-16 to 0.25	-20 to -8.7	-20 to 8.1
	RCP8.5	-12 to 2.1	-18 to 8.1	-15 to -0.9	-17 to 6.1	-18 to -2.1	-18 to 0.11	

* For NARClIM the values displayed in the 2.5-97.5% row is the minimum and maximum attribute values for the scenario

4.2.3 Daily extremes (99th percentile wet day rainfall)

The 99th percentile wet day rainfall is a commonly used method of climate extremes, and is presented in Figure 42. Although this is a common metric for extreme rainfall, it is noted that the 99th percentile wet day rainfall should not be interpreted as a genuine extreme rainfall day for flood estimation purposes, with events such as the 1% annual exceedance probability event (an event that is only exceeded on average once every hundred years) more commonly used to denote flood events. Nevertheless, the 99th percentile wet day rainfall is often used as a proxy for these more extreme events, and thus provides useful information on the possible magnitude of future change.

The projections show a distinctly different pattern to total annual rainfall or total number of wet days, with comparatively small declines over time, and a larger proportion of simulations with increasing trends. This suggests that declines in heavy rainfall days are likely to be less severe than other rainfall days, implying larger declines in light to moderate rainfall events relative to the total annual declines.

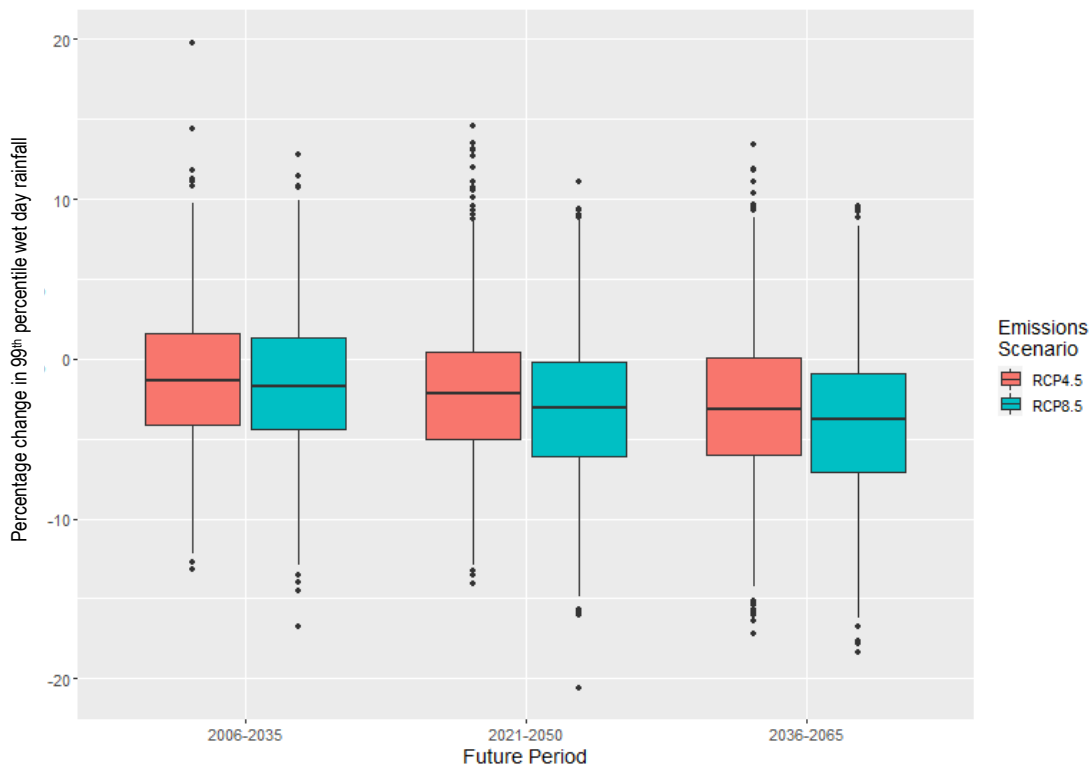


Figure 42 – Percentage change in annual 99th percentile wet day amount rainfall for RCP4.5 and RCP8.5 emission scenarios, relative to a 1976-2005 climatological baseline. See caption for Figure 40 for further details.

Table 12 – Percentage change in Annual 99th percentile wet day amount rainfall

Percentile	Emissions Scenario	2020		2035		2050		Range of Future Change
		SA-CR	NARClIM	SA-CR	NARClIM	SA-CR	NARClIM	
Median	RCP4.5	-1.3	-5.9	-2.2	-7.6	-3.2	-6.0	-6.2 to 0.98
	RCP8.5	-1.7	0.98	-3.1	0.13	-3.8	-6.2	
25-75%	RCP4.5	-4.2 to 1.6	NA	-5.0 to 0.47	NA	-6.0 to 0.05	NA	-7.1 to 1.6
	RCP8.5	-4.4 to 1.3	NA	-6.1 to 0.17	NA	-7.1 to -0.88	NA	

2.5-97.5%*	RCP4.5	-9.2 to 7.2	-14 to 19	-11 to 6.7	-14 to 16	-12 to 6.2	-9.7 to 9.5	-14 to 19
	RCP8.5	-9.8 to 7.2	-10 to 8.5	-11 to 5.8	-11 to 11	-13 to 5.0	-9.6 to 15	

* For NARClIM the values displayed in the 2.5-97.5% row is the minimum and maximum attribute values for the scenario

4.2.4 Rainfall seasonality

As well as changes in total rainfall volume, climate change is expected to have an effect on when rainfall occurs and the distribution of seasonal rainfall volume. The following metric is used to represent these changes in seasonality as regards to rainfall. The metric is the calculated from the ratio of rainfall in wet months to rainfall in dry months. The wet months are defined as April to September and dry months are October to March.

$$\text{Seasonality index} = \frac{\text{Sum of rainfall in simulation years (Wet Months)}}{\text{Sum of rainfall in simulation years (Dry Months)}}$$

The projections show an expected increase in seasonality. This is due to the decrease in precipitation in the dry months being greater than the decrease in the wet months, hence the percentage change in this attribute is increasing. Nevertheless there is large uncertainty in the estimates, with a substantial proportion of projections (~25%) showing a decrease in seasonality.

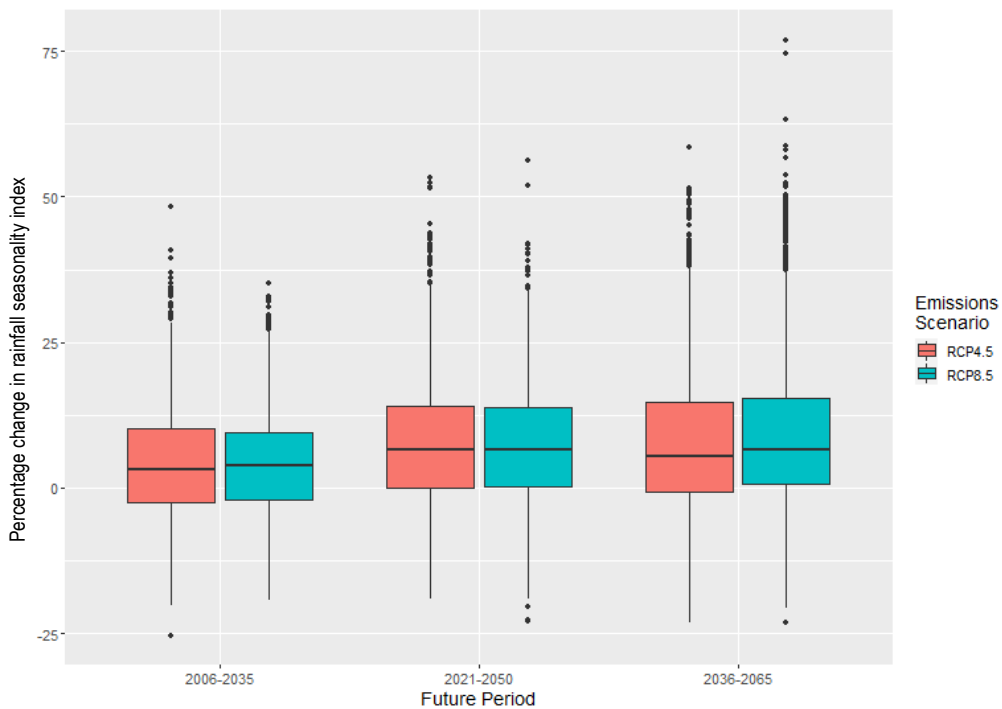


Figure 43. Percentage change in seasonality for RCP4.5 and RCP8.5 emission scenarios, relative to a 1976-2005 climatological baseline. See caption for Figure 40 for further details.

Table 13. Percentage change in seasonality from SA Climate Ready data

Percentile	Emissions	2020	2035	2050	Range of future change
Median	RCP4.5	3.2	6.4	5.5	3.2 to 6.6
	RCP8.5	3.7	6.4	6.6	
25-75%	RCP4.5	-2.5 to 10	0.07 to 14	-0.79 to 15	-2.5 to 15

	RCP8.5	-2.1 to 9.6	0.15 to 14	0.58 to 15	
2.5-97.5%	RCP4.5	-11 to 27	-9.5 to 34	-11 to 39	-12 to 44
	RCP8.5	-12 to 24	-12 to 30	-11 to 44	

4.3 Changes in Potential Evapotranspiration

Potential evapotranspiration represents the evaporative flux that would occur assuming an unlimited supply of water. The Climate Ready SA dataset presents results using Morton’s Areal Potential Evapotranspiration (APET), and the CCIA dataset uses Morton’s wet-environmental PET. Results from NARcliM were not available. Each of these contain different assumptions—including in terms of the relevant climate drivers that are used to calculate PET—and therefore the alternative lines of evidence cannot be contrasted in a genuine ‘like for like’ comparison. This is particularly the case given that Morton’s APET estimate uses different combinations of atmospheric variables and process representation compared to the Penman-Monteith FAO-56 estimate described elsewhere in this report.

Nevertheless the general sign of change between evapotranspiration estimates are likely be largely consistent, and the climate change analysis shows that there is significant consistency between projections, with almost all projections showing an increasing pattern of PET, with larger increases for longer future horizons and larger radiative forcings (Figure 44). At the annual scale, projections ranged from 1.4 to 9.5% increase in PET across all the projections, climate modelling methodologies and representative concentration pathways (Table 14).

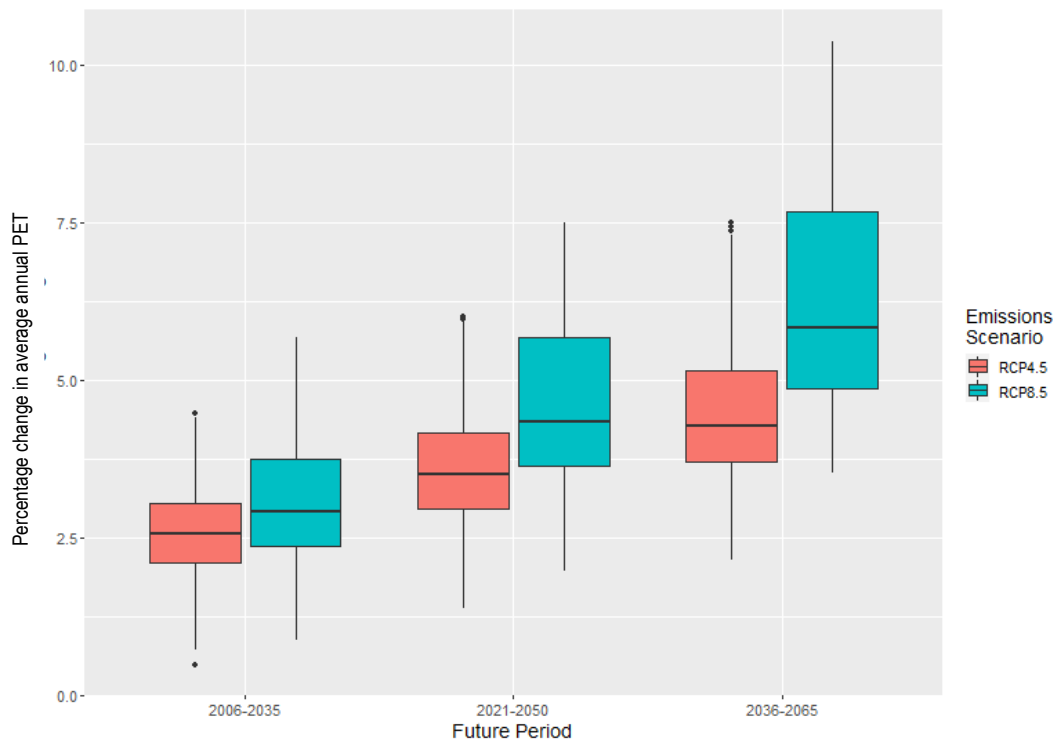


Figure 44. Percentage change in annual average PET for RCP4.5 and RCP8.5 emission scenarios, relative to a 1976-2005 climatological baseline. See caption for Figure 40 for further details.

Table 14. Percentage change in annual and seasonal PET

Season	Percentile	Emissions Scenario	2020	2030	2035	2050	Range of Future Change
--------	------------	--------------------	------	------	------	------	------------------------

Line of Evidence:			SA-CR	CCIA*	SA-CR	SA-CR	
DJF	Median	RCP4.5	2.1	2.6	2.9	3.5	2.1 to 5.0
		RCP8.5	2.5	2.4	3.7	5.0	
	25-75%	RCP4.5	1.5 to 2.7	NA	2.2 to 3.6	2.8 to 4.3	1.5 to 6.2
		RCP8.5	1.8 to 3.3		2.9 to 4.7	4.0 to 6.2	
	2.5-97.5%**	RCP4.5	0.47 to 4.2	0.6 to 3.5	1.0 to 6.0	1.5 to 7.4	-0.14 to 9.8
		RCP8.5	-0.14 to 5.0	1.8 to 4.1	0.6 to 7.1	1.5 to 9.8	
MAM	Median	RCP4.5	2.2	2.4	3.1	4.1	2.2 to 5.8
		RCP8.5	2.9	3.5	4.4	5.8	
	25-75%	RCP4.5	1.3 to 3.3	NA	2.1 to 4.3	2.8 to 5.1	1.3 to 7.4
		RCP8.5	2.0 to 3.8		3.2 to 5.6	4.7 to 7.4	
	2.5-97.5%**	RCP4.5	-0.02 to 5.0	0.5 to 5.6	0.5 to 6.1	0.9 to 7.1	-0.02 to 10
		RCP8.5	0.56 to 5.5	1.9 to 5.9	1.6 to 7.7	2.7 to 10	
JJA	Median	RCP4.5	2.5	4.5	3.7	4.6	2.5 to 6.3
		RCP8.5	2.9	5.0	4.5	6.3	
	25-75%	RCP4.5	1.8 to 3.1	NA	2.6 to 4.4	3.6 to 5.4	1.8 to 7.7
		RCP8.5	2.3 to 3.6		3.6 to 5.4	5.2 to 7.7	
	2.5-97.5%**	RCP4.5	0.9 to 4.1	1.3 to 8.8	1.4 to 5.4	1.8 to 6.9	0.9 to 10
		RCP8.5	1.3 to 5.7	3.7 to 9.5	2.3 to 8.0	3.6 to 10	
SON	Median	RCP4.5	3.5	2.2	4.8	5.9	2.2 to 7.7
		RCP8.5	3.9	2.3	5.7	7.7	
	25-75%	RCP4.5	2.8 to 4.2	NA	4.0 to 5.5	5.0 to 6.7	2.8 to 9.3
		RCP8.5	3.1 to 4.8		4.7 to 6.9	6.3 to 9.3	
	2.5-97.5%**	RCP4.5	1.6 to 5.4	0.9 to 4.2	2.5 to 6.9	3.2 to 8.3	1.6 to 12
		RCP8.5	1.5 to 6.3	1 to 4.9	3.0 to 8.9	4.4 to 12	
Annual	Median	RCP4.5	2.5	2.5	3.5	4.3	2.5 to 5.8
		RCP8.5	2.9	3	4.3	5.8	
	25-75%	RCP4.5	2.1 to 3.0	NA	3.0 to 4.2	3.7 to 5.2	2.1 to 7.7
		RCP8.5	2.4 to 3.7		3.6 to 5.7	4.9 to 7.7	
	2.5-97.5%**	RCP4.5	1.4 to 4.0	1.4 to 3.5	2.2 to 5.5	2.8 to 6.9	1.4 to 9.5
		RCP8.5	1.6 to 4.8	2.1 to 4.5	2.7 to 6.9	4.0 to 9.5	

*From CCIA Report – Southern and South-Western Flatlands (East). Baseline 1985-2006. 2030 future projection represents period 2020-2039.

**CCIA report records 10th to 90th percentile uncertainty

4.4 Changes in Temperature

4.4.1 Annual and Seasonal Changes to Daily Maximum Temperature

Changes in the daily maximum temperature are shown for the CR-SA analysis in Figure 45, with numerical results for all the lines of evidence and across all seasons given in Table 15. The results show a significant increase in temperature relative to the baseline, with slightly under a degree of warming already expected for 'current' climate relative to the 1976-2005 baseline (and presumably an even larger change relative to a 'pre-industrial' baseline), and increases in temperature by as much as 3.1°C by mid-century. Importantly, even for a relatively low radiative forcing scenario (RCP4.5), projections suggest a further 0.6-0.9°C warming over the next three decades relative to current climate, suggesting that further significant change can be anticipated for the Barossa region regardless of the emissions scenario.

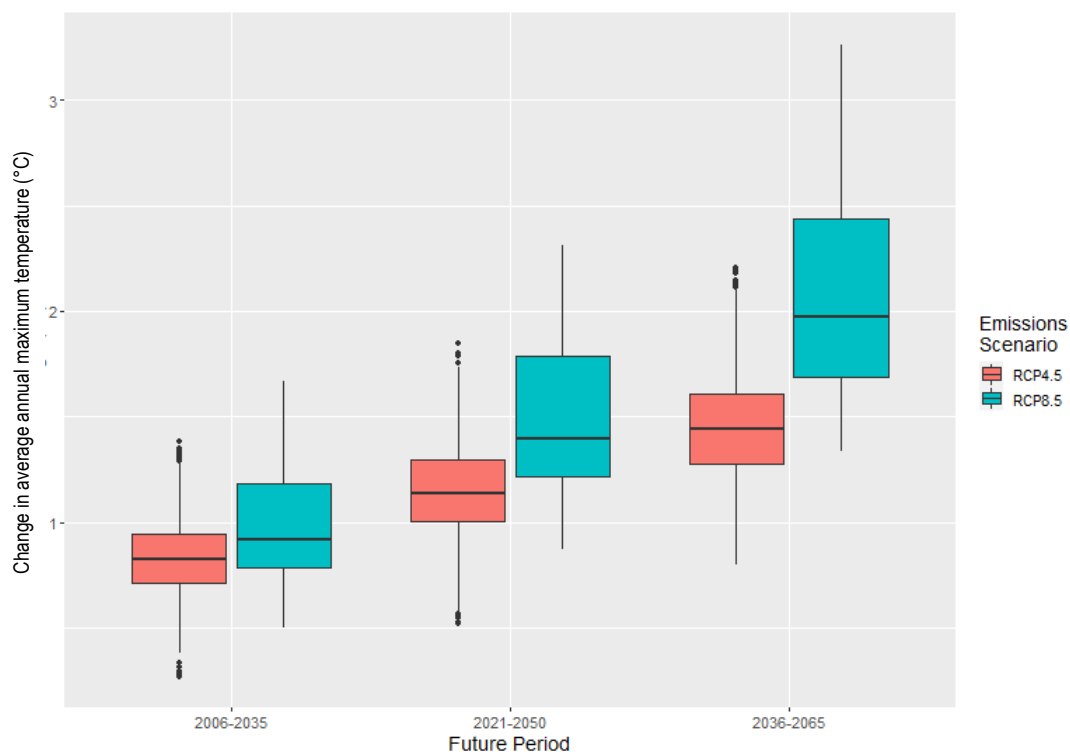


Figure 45. Percentage change in annual average maximum temperature for RCP4.5 and RCP8.5 emission scenarios, relative to a 1976-2005 climatological baseline. See caption for Figure 40 for further details.

Table 15. Relative change (°C) in annual and seasonal maximum temperature

Season	Percentile	Emissions Scenario	2020		2030	2035		2050		Range of future change
Line of Evidence:			SA-CR	NARCIIM	CCIA	SA-CR	NARCIIM	SA-CR	NARCIIM	
DJF	Median	RCP4.5	0.9	1.1	0.7	1.2	1.6	1.5	1.9	0.7 to 2.0
		RCP8.5	1.0	1.2	0.9	1.5	1.6	2.0	1.9	
	25-75%	RCP4.5	0.70 to 1.1	NA	NA	0.99 to 1.5	NA	1.3 to 1.8	NA	0.70 to 2.6
		RCP8.5	0.77 to 1.4			1.2 to 2.0		1.7 to 2.6		
	2.5-97.5%*	RCP4.5	0.33 to 1.7	0.22 to 1.9	0.4 to 1.3	0.59 to 2.4	1.1 to 1.9	0.89 to 2.9	1.3 to 2.1	0.23 to 3.8
		RCP8.5	0.33 to 1.9	0.23 to 1.8	0.6 to 1.3	0.73 to 2.7	0.89 to 2.1	1.2 to 3.8	1.4 to 2.6	
MAM	Median	RCP4.5	0.71	0.87	0.7	0.99	1.2	1.3	1.5	0.7 to 1.8
		RCP8.5	0.86	0.84	0.7	1.3	1.1	1.8	1.6	
	25-75%	RCP4.5	0.51 to 0.92	NA	NA	0.78 to 1.2	NA	1.0 to 1.5	NA	0.51 to 2.2
		RCP8.5	0.66 to 1.1			1.1 to 1.6		1.6 to 2.2		
	2.5-97.5%*	RCP4.5	0.12 to 1.4	0.26 to 1.2	0.3 to 1.1	0.31 to 1.8	0.79 to 1.6	0.55 to 2.1	1.0 to 1.7	0.12 to 3.0
		RCP8.5	0.28 to 1.7	0.56 to 1.5	0.4 to 1.3	0.55 to 2.3	0.64 to 1.9	0.98 to 3.0	1.3 to 2.1	
JJA	Median	RCP4.5	0.67	0.80	0.70	0.98	1.1	1.2	1.3	0.67 to 1.7
		RCP8.5	0.77	0.80	0.80	1.2	1.2	1.7	1.7	
	25-75%	RCP4.5	0.52 to 0.79	NA	NA	0.78 to 1.1	NA	1.0 to 1.4	NA	0.52 to 2.2
		RCP8.5	0.61 to 0.95			1.0 to 1.5		1.4 to 2.2		
	2.5-97.5%*	RCP4.5	0.26 to 1.0	0.61 to 1.1	0.4 to 1.0	0.46 to 1.4	0.84 to 1.5	0.66 to 1.8	1.1 to 1.9	0.26 to 2.6
		RCP8.5	0.38 to 1.4	0.46 to 1.2	0.6 to 1.2	0.72 to 2.0	0.95 to 1.5	1.2 to 2.6	1.5 to 2.1	

SON	Median	RCP4.5	1.0	1.1	0.9	1.4	1.6	1.8	2.3	0.9 to 2.3
		RCP8.5	1.2	1.2	0.9	1.8	1.6	2.4	1.9	
	25-75%	RCP4.5	0.85 to 1.2	NA	NA	1.2 to 1.6	NA	1.6 to 2.0	NA	0.9 to 2.8
		RCP8.5	0.96 to 1.4			1.5 to 2.1		2.1 to 2.8		
	2.5-97.5%*	RCP4.5	0.48 to 1.5	0.69 to 1.5	0.5 to 1.1	0.85 to 2.0	1.2 to 2.4	1.2 to 2.4	1.7 to 2.8	0.21 to 3.5
		RCP8.5	0.62 to 1.8	0.21 to 1.9	0.6 to 1.3	1.1 to 2.6	0.56 to 2.8	1.6 to 3.5	1.6 to 2.9	
Annual	Median	RCP4.5	0.82	0.91	0.7	1.1	1.3	1.4	1.8	0.7 to 2.0
		RCP8.5	0.92	1.0	0.8	1.4	1.4	2.0	1.8	
	25-75%	RCP4.5	0.71 to 0.94	NA	NA	1.0 to 1.3	NA	1.3 to 1.6	NA	0.71 to 2.4
		RCP8.5	0.79 to 1.2			1.2 to 1.8		1.7 to 2.4		
	2.5-97.5%*	RCP4.5	0.46 to 1.2	0.58 to 1.4	0.5 to 1	0.72 to 1.6	1.1 to 1.8	1.0 to 2.0	1.4 to 2.0	0.46 to 3.1
		RCP8.5	0.61 to 1.5	0.51 to 1.4	0.6 to 1.2	1.0 to 2.2	0.92 to 1.8	1.5 to 3.1	1.6 to 2.3	

* For NARClIM the values displayed in the 2.5-97.5% row is the minimum and maximum attribute values for the scenario; the CCIA report records 10th to 90th percentile uncertainty

4.4.2 Annual Number of Days Over 35°C

The annual number of days above 35°C represents a useful proxy for heatwave incidence, and is represented as percentage changes relative to the baseline. The baseline (1976-2005) number of days above 35°C has a median of 11.5 days with a 2.5% and 97.5% range of 3.3 days and 13.5 days, respectively, across the three stations. The results show a significant increase in the incidence of days over 35°C, with climate models already indicating current climate should have a median of 38-45% more hot days compared to the baseline, and with a significant number of projections showing the possibility of a doubling in the number of hot days by mid-century.

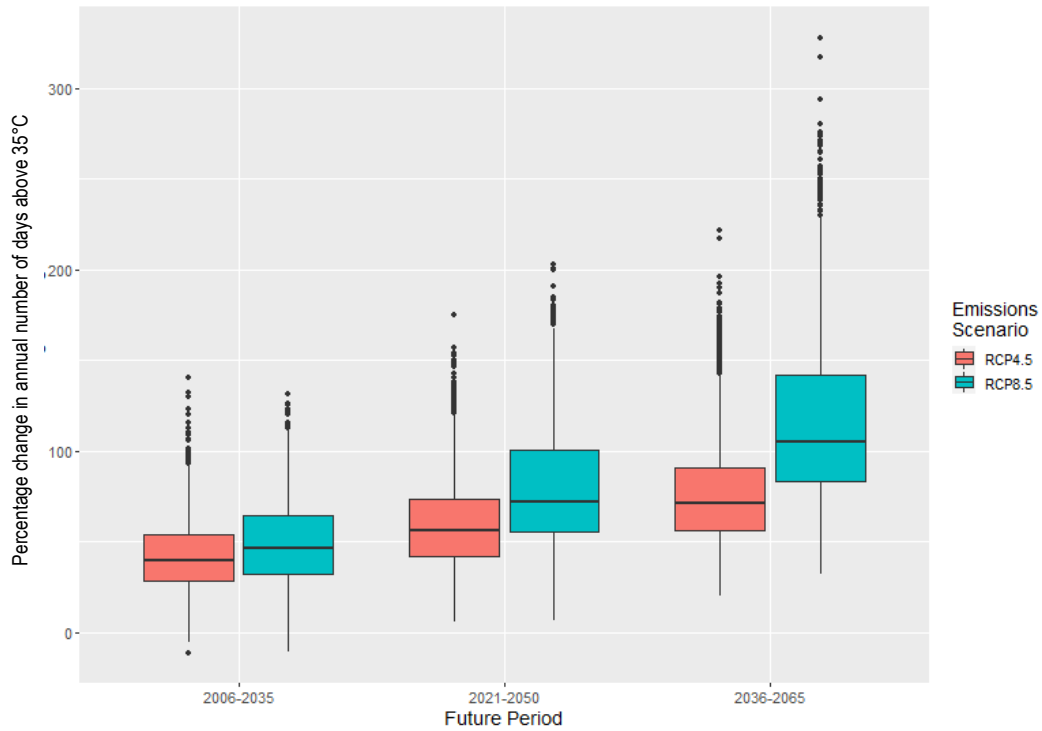


Figure 46. Percentage change in annual number of days above 35 degrees Celsius (as a percentage relative to the baseline) for RCP4.5 and RCP8.5 emission scenarios, relative to a 1976-2005 climatological baseline. See caption for Figure 40 for further details.

Table 16. Percentage change in annual in number of days above 35 degrees Celsius from SA Climate Ready data

Season	Percentile	Emissions	2020	2035	2050	Range of future change
Annual	Median	RCP4.5	39	56	71	39 to 110
		RCP8.5	47	72	110	
	25-75%	RCP4.5	28 to 54	42 to 73	56 to 91	28 to 140
		RCP8.5	32 to 64	55 to 100	83 to 140	
2.5-97.5%	RCP4.5	10 to 87	22 to 130	35 to 160	10 to 240	
	RCP8.5	12 to 100	30 to 160	54 to 240		

4.5 Selection of Scenarios for Stress Testing

4.5.1 Range of Projections

The preceding sections identified a range of changes to key climatic drivers of the Barossa and Eden Valley regions. The identification of the primary climate ‘attributes’⁵ for inclusion in the subsequent stress test is informed by *a priori* understanding of the most likely climatic drivers that would influence the key system performance metrics, as represented by the process representations embedded in the relevant system model(s). For the present study, the primary climate variables that serve as inputs to the integrated system model (see Figure 9 and Figure 10) are precipitation and potential evapotranspiration. Given that the Stella model runs at an annual timescale, and that the identified water security metrics (Table 4) are also generally represented at the annual timescale, we focus largely on annual statistics of these variables in the analysis. However, given the highly seasonal nature of many key processes—including but not limited to crop water demands—a seasonal metric for precipitation is also included which enables adjustment of the strength of the seasonal cycle. While it is not possible to integrate sub-annual changes directly into Stella, the individual component models operate at sub-annual scales, and it is possible to implement different relationships into Stella depending on the nature of any seasonal changes.

Therefore, a total of three attributes are selected for stress testing, and these are summarized in Table 17. To identify the range for stress testing, for each attribute the maximum and minimum value across the three lines of evidence (if available) are chosen to represent the range of likely change. For rainfall and PET, the range is extended to the next 5% increment on both sides of the projection range, and for seasonality this is decreased to the nearest 5% increment⁶. The bounds for stress testing, together with the perturbation increments, are also summarized in Table 17.

Table 17. Change in attribute estimated by various climate change lines of evidence, together with chosen bounds and perturbation increments used for climate stress tests

Climate attribute	Minimum Change (%)	Maximum Change (%)	Chosen Bounds (%)	Perturbation increments	Lines of Evidence
Mean annual total rainfall	-23	5.0	-25 to 10	5%	SA-CR, NARClIM, CCIA*
Annual average PET	1.4	9.5	0 to 10	5%	SA-CR, CCIA*
Rainfall seasonality	-12	44	-10 to 40	{-10, 0, +40}	SA-CR

4.5.2 Scenarios for Stress Testing

In addition to ‘stress testing’ the system across a broad spectrum of changes as depicted in Table 17, for part of the analysis it may be useful to provide a more deeper exploration of a small number of future climate scenarios. These ‘scenarios’ represent specific points on the exposure space, and in addition to the climatological baseline, we will consider the following scenarios:

Scenario 1: Moderate change. This scenario is based on the climate statistics over the previous decade (2011-2020). The perturbation values are also reasonably close to the median of the Climate Ready 2050 climate

⁵ The term ‘attribute’ is used in the *foreSIGHT* software to refer to statistics of climate variables. For example the ‘annual average PET’ or ‘99 percentile daily rainfall’ are both attributes.

⁶ The decrease in seasonality is because the visual treatment of seasonality is through taking ‘slices’ through the seasonality attribute, which is different to the approach to visualising the other attributes.

projections for RCP4.5, with this RCP representing a plausible greenhouse gas concentration scenario given recent commitments made at COP26.

Scenario 2: Severe change, strengthened seasonal cycle. This scenario is what could be described as an ‘unlikely worst case’ that focuses on the outer range of projections associated with RCP 8.5. Whilst it is increasingly recognized that RCP 8.5 represents an unlikely outcome even under ‘business as usual’ emissions scenarios (see Hausfather et al, 2020), the possibility that climate models underestimate other aspects of the uncertainty space—particularly changes to precipitation—cannot be discounted, and thus this represents a plausible ‘worst case’ outcome. This scenario also contains an enhanced seasonal cycle (relatively more winter rainfall and less summer rainfall).

Scenario 3: Severe change, weakened seasonal cycle. This is equivalent to Scenario 2, except it assumes a weakened seasonal cycle (relatively more summer rainfall and less winter rainfall).

Specific perturbations relative to the climatological baseline for each scenario are summarized in Table 18.

Table 18. Climate scenarios for further investigation, as a fractional change relative to the climatological baseline (1976-2005)

Climate attribute	Annual average precipitation	Annual average PET	Seasonal cycle of P
Baseline	1	1	1
Scenario 1: Moderate climate change	0.9	1.04	1
Scenario 2: Severe change & strengthened seasonality	0.8	1.1	1.4
Scenario 3: Severe change & weakened seasonality	0.8	1.1	0.9

5 Representing system connections under change

The system-wide response to climate stressors arises through the propagation of the climate signal through both the supply and demand elements of the Barossa water resource system. This was illustrated in Figure 9 and Figure 10, whereby key climate drivers are shown to influence different aspects of supply and demand through a complex set of pathways and interactions. In this section we focus on understanding the behaviour of these interactions under different climate forcings, with this to serve as the foundation for integration into the system dynamics model (Stella) to represent overall system behaviour under historical, current and future climates.

The ‘component models’ (eWater Source, MODFLOW and the regression and FAO-56 DCC demand models described in Sections 1 and 3) comprise the primary evidence base for understanding the relationships shown in Figure 9, with these models in turn having been calibrated to the historical record (see Section 3). The existing models are forced with perturbed climate conditions, based on the range of plausible changes to key climate attributes as described in Section 4 and summarized in Table 17. The connections are documented at the annual timescale (water year) to enable simpler representations of the influence of one component on another.

A straight forward approach to climate stress testing each of the key elements of the system diagram (Figure 9) is adopted here, whereby the baseline climate is perturbed by constant ‘change factors’ based on the ranges and increments described in Table 17. Whereas the annual attributes apply uniform change factors throughout the year, the ‘seasonal index’ applies different change factors throughout the year to alter the strength of the seasonal cycle, with index values below one representing weakened seasonality (relatively less winter rainfall and more summer rainfall compared to the baseline), and values greater than one representing enhanced seasonality (relatively more winter rainfall and less summer rainfall). Further details on the application of the scaling method are provided in the *foreSIGHT* manual (Devanand et al, 2020). The stress test is run using the baseline climate period determined from Section 4 (1976-2005). The following sub-sections describe each connection/link.

Finally it is noted that two modifications were made to the transient MODFLOW model of Li and Cranswick (2016) representing the period 1989 to 2015. First, model forcing variables—namely groundwater recharge and PET—were modified to represent baseline climate conditions. Second, MODFLOW solver settings were modified to enhance model stability, particularly when large climate perturbations are applied.

The results presented herein are for the Barossa PWRA, with equivalent sections for the Eden Valley and Barossa Valley presented in Appendices C and D.

5.1 System Dynamics Modelling

The approach to system dynamics modelling using Stella was described briefly in Section 2.2, and is built by mathematically describing relationships of each of the key links shown in Figure 10. These relationships are calibrated from the relevant component models, over the range of climate perturbations used for ‘stress testing’ as described in Table 17. In this section we aim to:

1. Develop regression models for system components (Stella model)
2. Show results from system components and regression models, with aim to:
 - a. Show how perturbations of inputs affects outputs
 - b. Show that the regression models perform well compared to component model results

The component stress test comprises multiple sets of 29-year simulations. The stress test outputs therefore comprises 696 data points (29 water years multiplied by 24 combinations of P and PET). For example, average annual streamflow, an output from the Source model, was found to be sensitive to the climate variables rainfall and PET. In Figure 47, the scatter of average annual rainfall against average annual rainfall and PET

can be observed, with the streamflow magnitude indicated by the infill colouring. As expected, streamflow increases with increase in rainfall and decrease in PET. From these, a regression can be plotted which captures the change in streamflow with relation to rainfall and PET. In this case, a non-linear bivariate regression was found to be most suitable, of the form $Q = c_1 + c_2P + c_3P^2 + c_4E$. Equivalent scatter plots of other perturbed variables are provided in Appendix E.

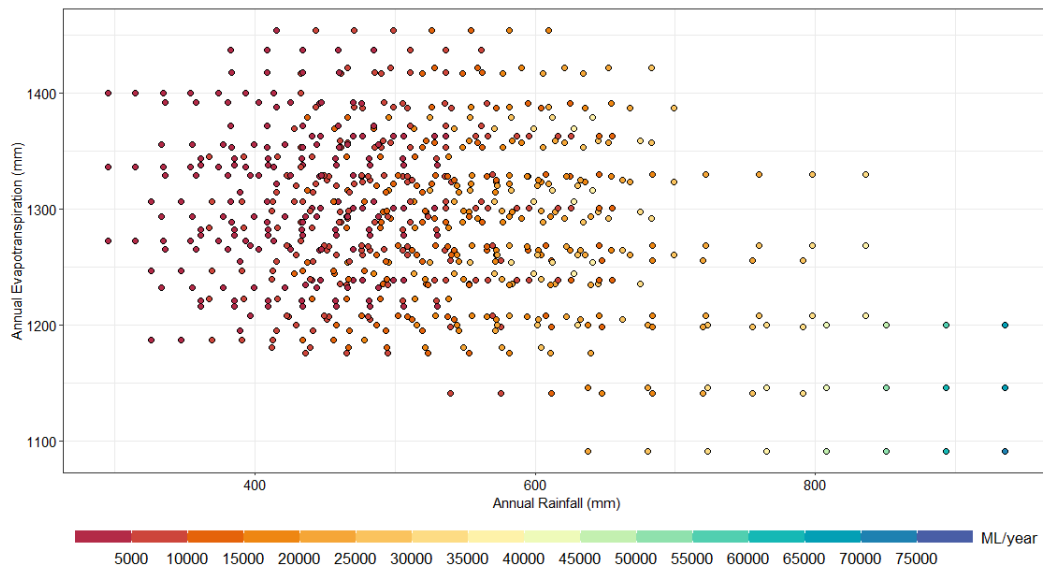


Figure 47. Scatter plots of streamflow outputs from Source as a result of the climate stress test. The axes are average annual rainfall and PET (mm), and the colour of the points represents the average annual streamflow in ML/year.

A majority of the other variables tested were also most sensitive to average annual rainfall, PET or both. Most of the groundwater components were also found to be sensitive to the size of the groundwater storage. Two extraction components (watercourse and farm dam extraction) were found to be very closely linked to their associated sources, streamflow and maximum farm dam storage, so were regressed against these parameters instead. However, groundwater storage, streamflow and watercourse extraction are all influenced by changes in rainfall and PET, so are sensitive to the stress test of P and PET. The regressions for the other variables are either linear or non-linear, and univariate or bivariate depending on what regression forms best captured the variable outputs.

In reviewing model performance, it was observed that calibrating Stella to individual years of record led to degraded performance when reviewing annual average statistics. However, the alternative—calibrating Stella only to annual average values—leads to the possibility that individual years are not adequately reflected in the system dynamics model, even though it is the individual years (and not the averages) that are the primary unit of operation within Stella. In order to improve the comparison between the component models and the regression relationships implemented in Stella, and to better represent changes to the averages while simultaneously preserving individual years, the average values of each of the 24 perturbation combinations of P and PET were also included in the calibration through a weighted regression. This expanded the regression to 720 individual data points for each relationship. Given the low ‘leverage’ of the average data points (given that they by construction were close to the centre of the data distribution), each of the ‘averages’ is given a weighting of 100^7 , while the other points were given a weighting of 1. The full data set was then regressed to obtain the relationship using weighted least squares. The effect of this weighting for various metrics can be observed in Appendix E: Weighted Plots.

⁷ Or 1000 for the link between groundwater ET and PET, given issues with the regression performance for the lower weighting

Table 19 summarises the relationships implemented in Stella for the Barossa PWRA, derived from regressing against the component model inputs and outputs. The results show strong R^2 values for most of the modelling elements, demonstrating reasonable regression performance.

Table 19. Regression form of component model results to be implemented into the Barossa PWRA Stella model. All output units are in ML, as are input units (except P and E, which are in mm) and R^2 values are presented in the right-most column. Variable abbreviations are as introduced in the system diagram in Figure 9.

Section	Metric	Component Model	Regression Relationship (all units in ML except for climate variables P and E (mm))	R^2
5.2	Streamflow	Source	$-19.4P + 0.089P^2 - 10.1E + 9930$	0.87
5.3.1	Baseflow	Source, Lyne-Hollick Filter	$-2.08P + 0.012P^2 - 1.87E + 1990$	0.84
5.3.2	Baseflow	MODFLOW	$(1.10 \times 10^{-8})S_{GW}^2 - 0.00939S_{GW} + 2180$	0.98
5.4	Maximum farm dam storage	Source	$30.3P - 0.0161P^2 - 2.47E - 4390$	0.81
5.5	Surface water use*	Source	$(-170 + 39.8 \ln Q) + (-11.8 + 0.71S_{DAM} - (8.3 \times 10^{-5})S_{DAM}^2 + (4.0 \times 10^{-9})S_{DAM}^3)$	0.72 (for watercourse) 0.95 (for farm dams)
5.6	Recharge	MODFLOW**	$63.8P - 22000$	0.86
5.7	Groundwater ET	MODFLOW	$-0.022S_{GW} + (2.1 \times 10^{-7})S_{GW}^2 + 0.38PET + 59100$	0.99
5.8.1	Demand	Regression on historical water use	$9400 + 156(0.0872)(0.55E - P) + N(0,1.65)$	0.65
5.8.2	Demand	SARDI crop model	$87.2(-191 - 0.22P + 0.34E)$	0.53

*Surface water use is represented in two ways in the Source model. This is by 'watercourse use' and 'farm dam use'. These are related to streamflow and maximum farm dam storage respectively, hence, there are two regression relationships considered, which are then added to form a relationship for surface water use. These sources are added as they are lumped as surface water use in the license data, so can be more easily compared if jointly considered as surface water use.

** As mentioned in Figure 9 we note that the relationship between P and R is derived not directly from the MODFLOW model, but rather from an external relationship defined by Li and Cranswick (2016) required for input to the MODFLOW model.

The following sections explore how the component models respond to perturbation of the climate variables rainfall and PET. A comparison of the variable representation from the component models and their corresponding representation in the system dynamics model is also presented. This is achieved by side-by-side performance plots from component model results and system dynamics model (Stella) results.

5.2 Annual average streamflow and climate

In this section we explore changes to streamflow metrics at Yaldara as a function of changes in annual rainfall and PET and the seasonality index. Yaldara was selected in this case as it represents the primary flow gauge representing streamflow in the Barossa PWRA, with the upstream catchment area comprising 70% of the Barossa PWRA. Annual average streamflow provides an aggregate measure of system response and is an important part of the overall water balance. The climate-streamflow relationship is also important as it is needed to calculate the three ecological metrics presented in Table 4. Assessment of the ecological metrics for current system configuration and changing climate is presented in Section 6.2.

Changes to the annual average streamflow at the Barossa Valley Gorge Zone outflow (Outlet Node 2 in Source) as a function of plausible changes to annual rainfall and PET are presented in Figure 48, including results from Source (left), and Stella (right). The streamflow for each combination of perturbed P and PET is presented both in absolute and relative terms compared to the baseline period (1976-2005). All results are

presented relative to the 1976 to 2005 baseline, with the recent 2011-2020 decade also denoted in the figure for reference purposes. Climate model projections from the two primary modelling lines of evidence are shown, comprising both individual model realisations and the results of various levels of model averaging.

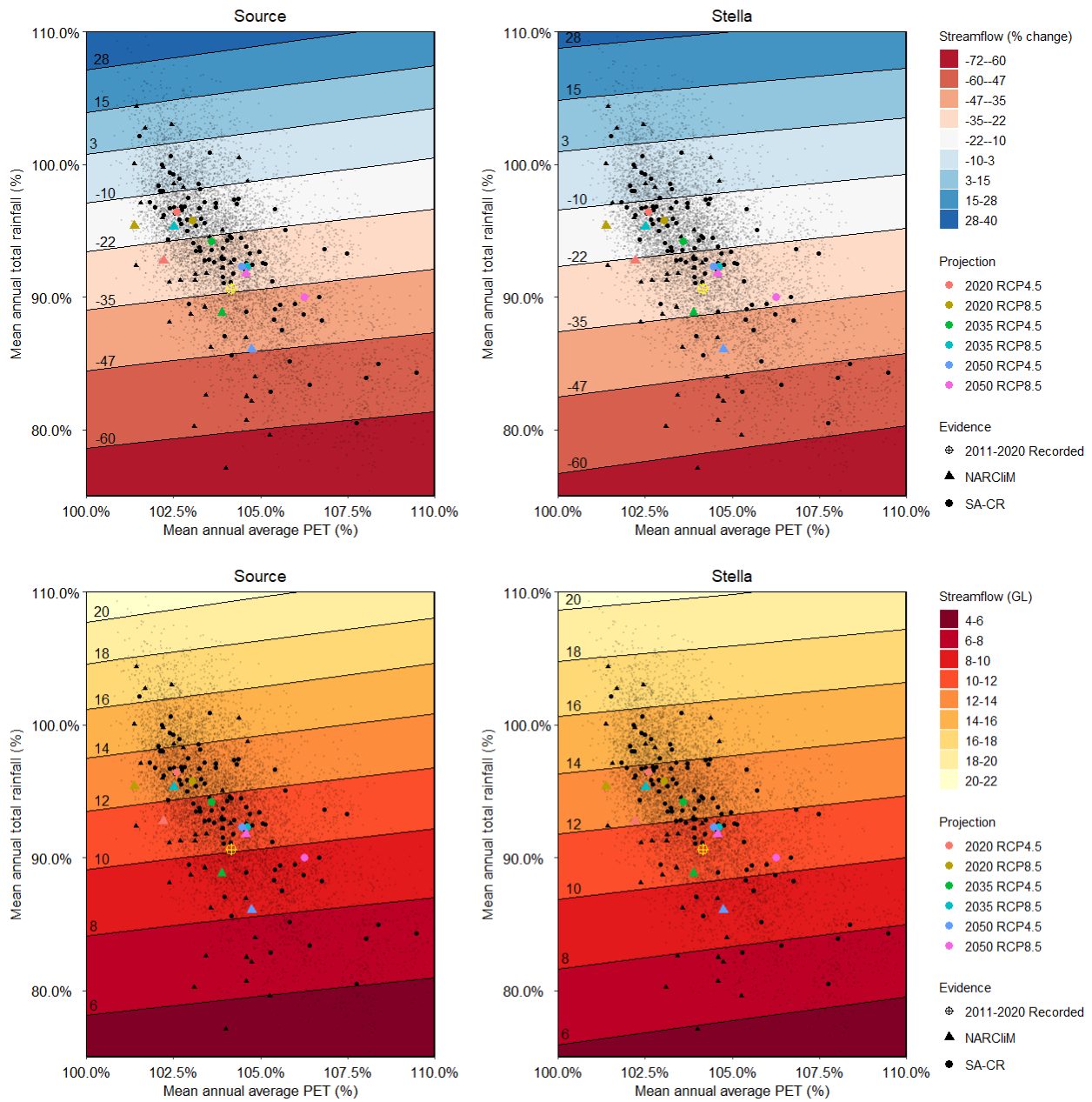


Figure 48. The performance space, both relative (upper panels) and absolute (lower panels) change, of streamflow at Outlet Node 2 (Barossa Valley Gorge Source outflow) from simple scaling, both from Source (left) and Stella (right) results. Climate projections are overlaid onto the plotting space - the faint grey dots represent the 9000 replicates from CR-SA, the small black circles represent the mean of each of the 15 SA-CR GCMs (15 models for 3 time slices and 2 emissions scenarios, 90 points), the small black triangles represent the mean of each of the 6 NARCIIM GCMs (36 points), and the coloured circles (SA-CR) and triangles (NARCIIM) represent the mean of all the data for each future time slice and climate emission scenario (6 each). The yellow circle with cross through it represents the average P and PET for the most recent decade (2011-2020) relative to the 1976-2005 baseline.

From Figure 48 it can be seen that both models follow the expected pattern of decreasing streamflow for an increase in PET and decrease in rainfall. It can be seen that the Stella results show a slightly smaller range of streamflow compared to the Source results; however overall, the models show very similar results with the Stella model slightly overestimating streamflow for a decrease in rainfall and increase in PET, and slightly underestimating streamflow for high rainfall and low PET.

From examining the mean absolute streamflow residuals (Figure 49), it can be seen that both models produce very similar results for most changes in rainfall and PET, although the Stella results are less accurate (i.e. larger errors) for extreme values.

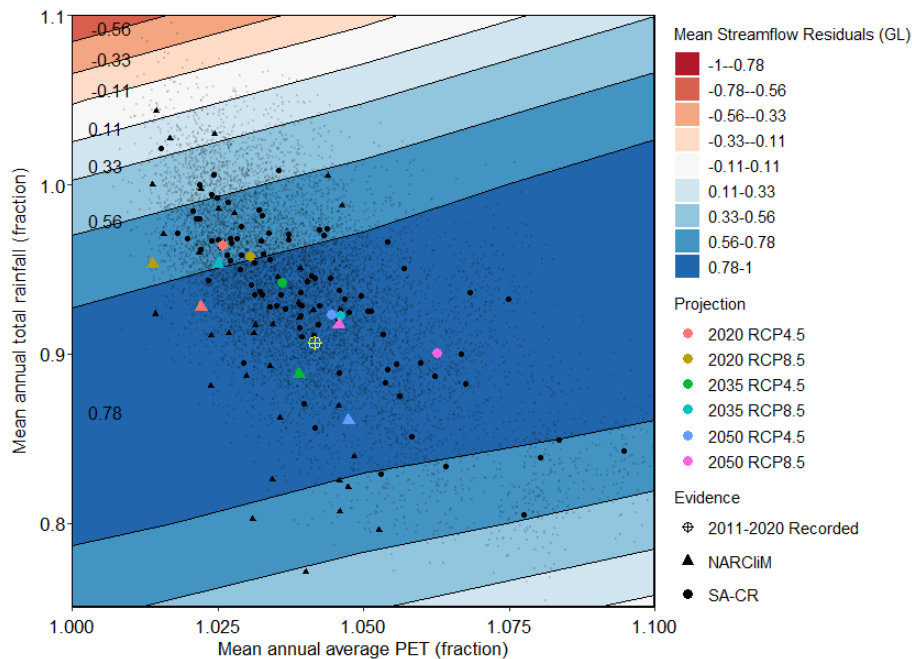


Figure 49. Residuals of the mean absolute streamflow values between Source and Stella

Differences between the models are likely to be due to the bivariate regression used in Stella being unable to capture the full variation and model complexity of the Source model. Despite this, from Figure 48 and Figure 49 it seems that application of the parametric relationship in Stella produces a very similar streamflow relationship to the Source model when applying simple scaling on P and PET.

The additional influence of seasonality is shown in Figure 50, for both a small decrease and a large increase in the strength of the seasonal cycle (left and right panels, respectively) relative to maintenance of the historical seasonal cycle (middle panel). The greatest reductions in streamflow occur for a decrease in the strength of the seasonal cycle, which is expected as this corresponds to relatively less rainfall in winter (where a larger proportion of rainfall is expected to be converted into runoff). In contrast, the impact on total annual runoff is lower for increases in the seasonal cycle.

Finally, as emphasised in Section 3.3.1, the Source model has a tendency to underestimate high flows and overestimate low flows. This may mean that the sensitivity to climate identified here slightly underestimates true sensitivity to climate. This issue has not been considered further in this work, and is highlighted as a limitation in Section 8.2.

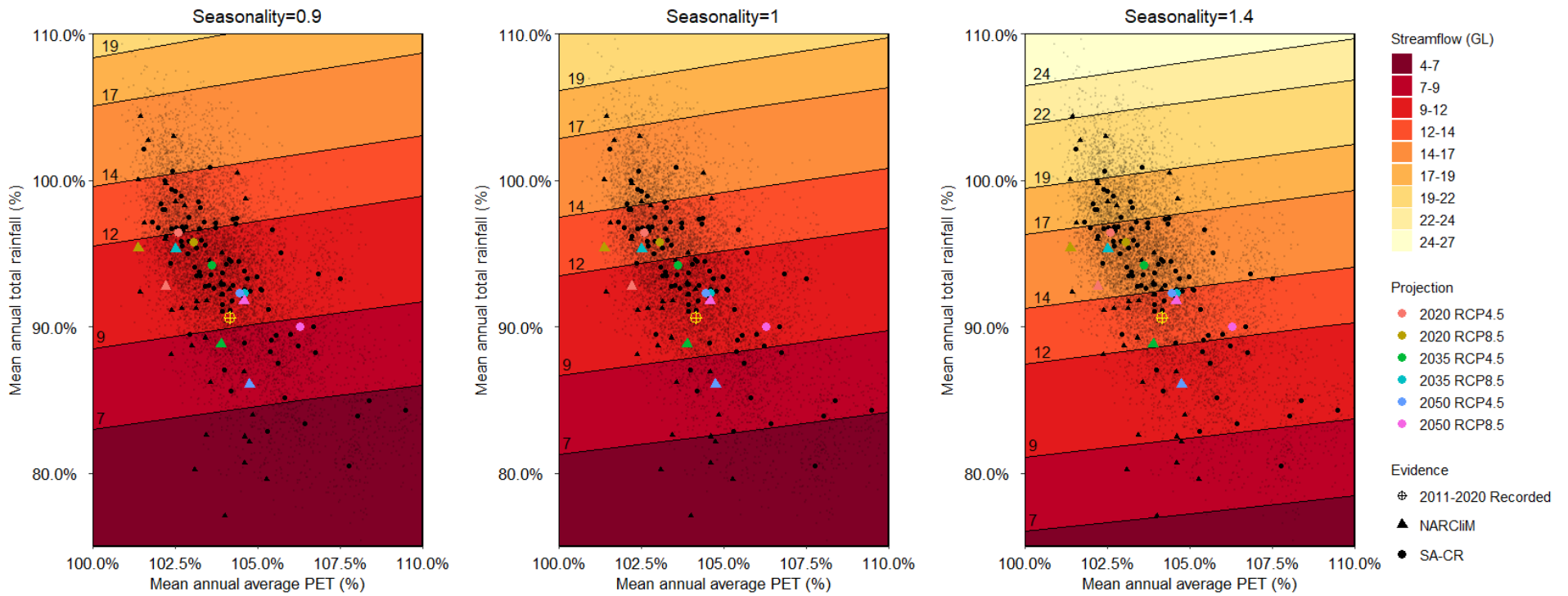


Figure 50: The performance space (absolute change only) replicated for a decrease in the strength of the seasonal cycle (i.e. relatively wetter summers and drier winters; left panel), the historical seasonal cycle (middle panel) and an increase in the strength of the seasonal cycle (additional drying in summer and wetting in winter; right panel).

5.3 Baseflow

As described in Section 3.3.2, two alternative approaches exist for estimation of baseflow—one derived from surface water modelling, and the other from groundwater modelling. Both are described here to enable comparison of results.

5.3.1 Baseflow from Source (Lyne-Hollick Filter)

The perturbed streamflow timeseries computed in Section 5.2.1 were passed through the Lyne-Hollick filter with $\alpha = 0.985$ to produce perturbed timeseries of baseflow. A bivariate regression as a function of P and PET was then fitted to the results.

The bivariate regression between rainfall, potential evapotranspiration and baseflow is implemented in the Stella model, with non-linear components for both P and PET. Figure 51 shows the sensitivity analysis conducted on the results from Source (left), and Stella (right). The value represented for each combination of perturbed P and PET is the mean annual baseflow/relative change in baseflow over the baseline period (1976-2005).

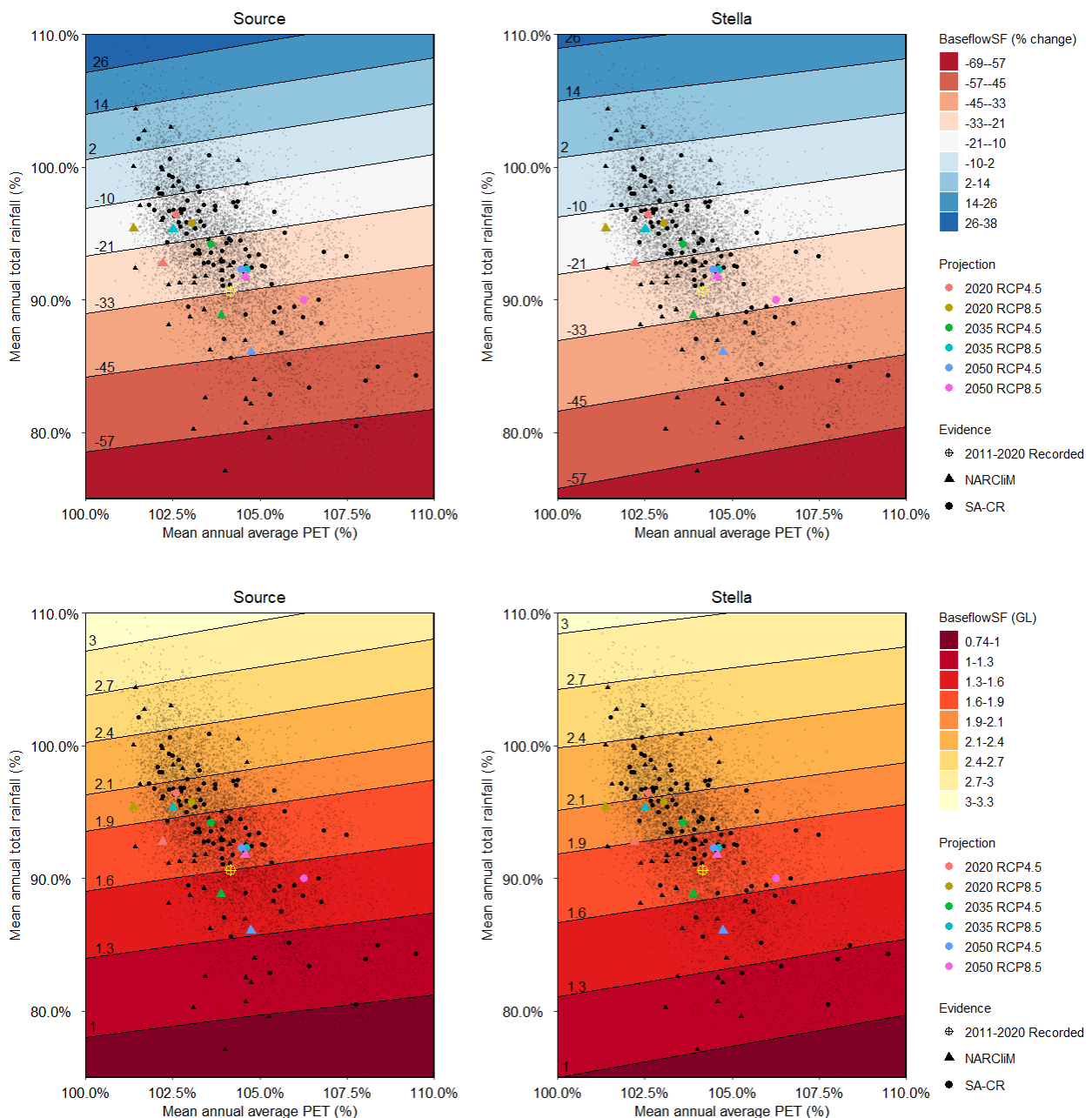


Figure 51. The performance space, both relative (upper panels) and absolute (lower panels) change, of baseflow from filtering streamflow at Outlet Node 2 (Barossa Valley Gorge Source outflow) from simple scaling, both from Source (left) and Stella (right) results.

The results for relative change in baseflow between Source and Stella show similar values for no change in P or PET, with Source having a greater range of change under different climate forcings compared to Stella. Source also has a greater range of absolute values, as observed for the streamflow metric. In particular, it can be seen from Figure 52 that the difference in absolute values is most apparent for extreme change in climate, with the extreme rainfall perturbations causing the most discrepancy. The residuals between the two models decrease for an increase in PET.

In interpreting these results, it's important to note that the difference in absolute baseflow between this figure and Section 3.3.2 is due to the difference in time frames, and the fact that in Section 3.3.2 the filter is applied to historic streamflow at Yaldara, and here is applied to Source downstream flow at Node Outlet 2 (the representative outlet of the Barossa PWRA).

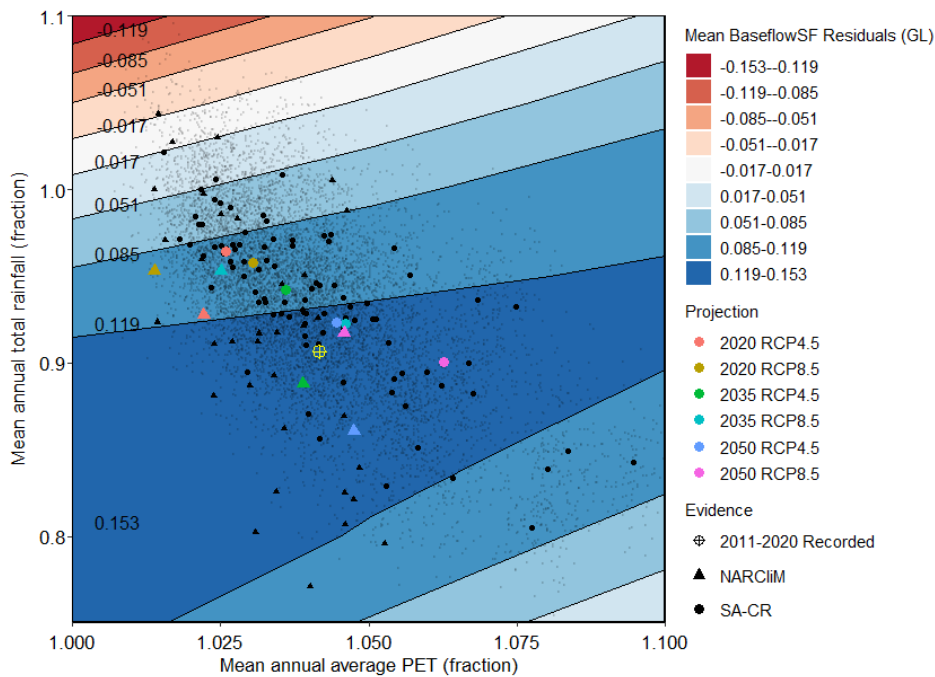


Figure 52. Residuals of the mean absolute Lyne-Hollick baseflow values between Source and Stella

The additional influence of seasonality on baseflow is shown in Figure 53. The greatest reduction in average baseflow occurs for a reduction in the seasonal cycle, which is expected as this corresponds to relatively less rainfall in winter. However, the smallest baseflow appears to occur for an increase in the seasonal cycle. This could be due to misrepresentation of baseflow when streamflow is run through the Lyne-Hollick filter, as we would expect change in baseflow due to seasonality to be similar to streamflow.

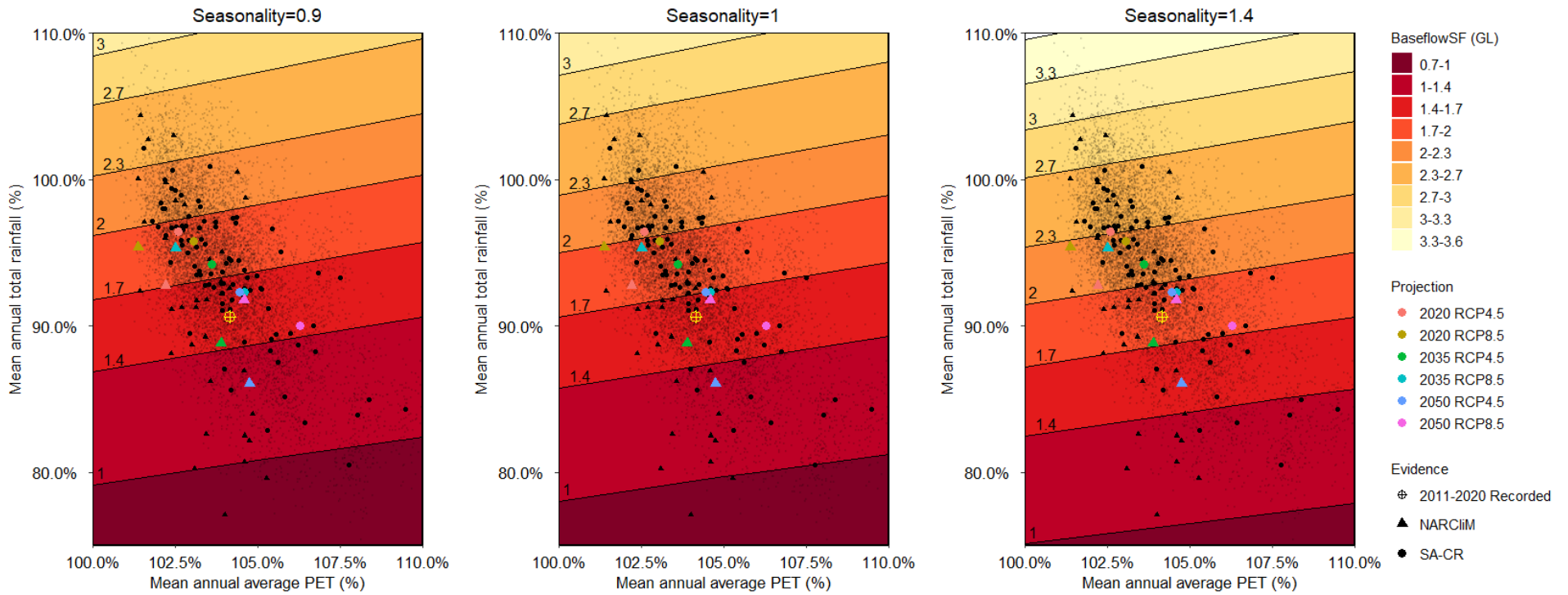


Figure 53: The performance space (absolute change only) replicated for a decrease in the strength of the seasonal cycle (i.e. relatively wetter summers and drier winters; left panel), the historical seasonal cycle (middle panel) and an increase in the strength of the seasonal cycle (additional drying in summer and wetting in winter; right panel).

5.3.2 Baseflow from MODFLOW

Here we explore MODFLOW-derived baseflow within the Yaldara gauge catchment (following the baseflow zones defined by Li and Cranswick [2016]) and its response to changes in P and PET. Figure 54 shows specifically the changes in average annual baseflow, in both absolute and relative terms with respect to the baseline period, as a function of plausible changes in P and PET from MODFLOW and Stella.

From the MODFLOW results it can be seen that baseflow increases with increasing P and decreasing PET. The change in baseflow with respect to P is much larger than that with respect to PET. The baseflow gradient with respect to P shows mild non-linearity, with highest sensitivity in baseflow at lower P values. The Stella results show similar baseflow trends with respect to P, but are much less sensitive to PET, especially for high rainfall perturbations.

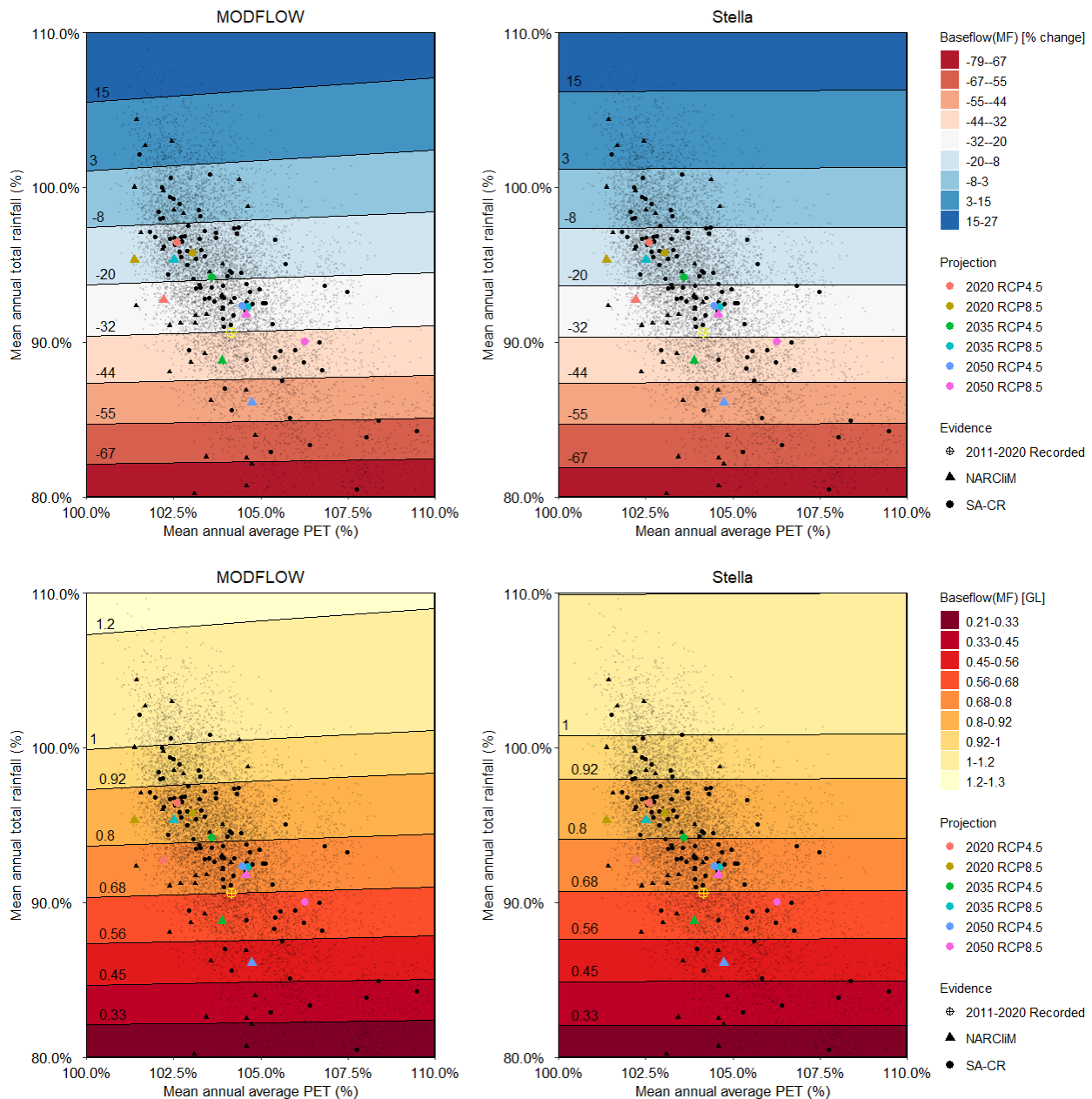


Figure 54. The performance space, both relative (upper panels) and absolute (lower panels), of baseflow at Yaldara from simple scaling, both from MODFLOW (left) and Stella (right) results.

Figure 55 shows the mean absolute baseflow Stella-MODFLOW residuals. It can be seen that the two models produce very similar results, with the largest difference between the models produced for high rainfall and low PET.

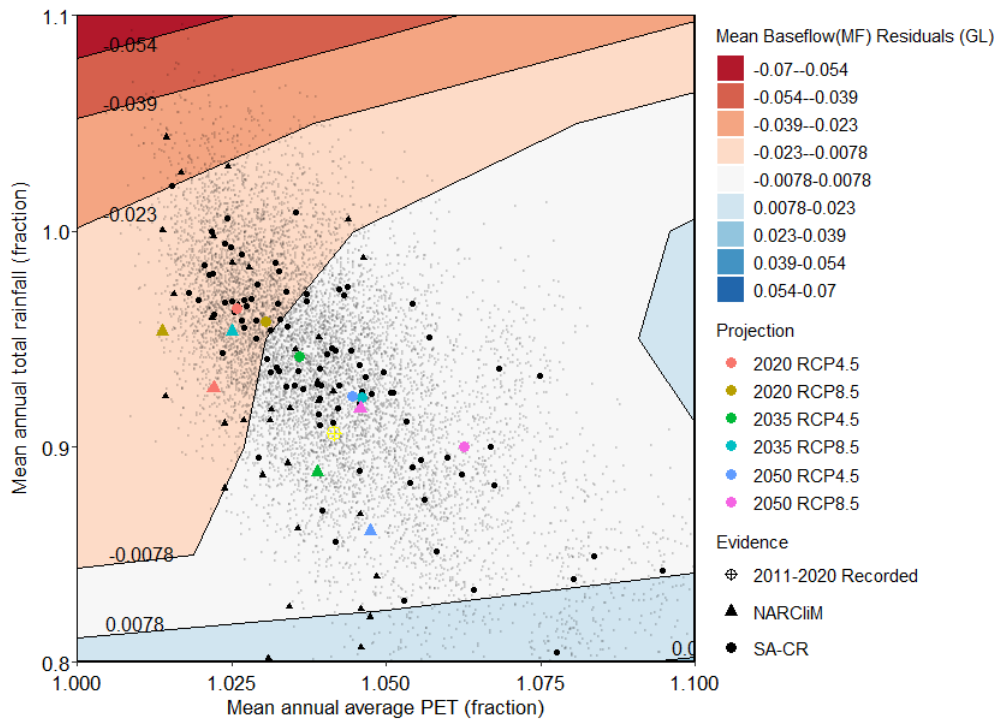


Figure 55. Residuals of the mean absolute baseflow values between MODFLOW and Stella

Discrepancy between the baseflow filter and MODFLOW model are expected due to the difference in models and has been previously observed in other studies such as those by Cranswick (2015) and Li and Cranswick (2016). As well as this, baseflow is recorded from Yaldara in the MODFLOW model, whereas the filter is run on Outlet Node 2 in Source (outflow from the Barossa Valley Gorge Zone), a node which is very close to the Yaldara gauging station but captures flows from a larger area, and hence produces a larger absolute result.

Finally, it is noted that baseflow as represented in MODFLOW is to a large degree driven by the relative influence of recharge (i.e. water into the aquifers) and extraction rates. A constant value of 2.7 GL/year was assumed for extractions throughout each of these simulations; however as highlighted in Section 5.6, recharge depends heavily on climate. As such, it is likely that transient (time-varying) groundwater dynamics may be present particularly for the more severe climate scenarios, as the rate of groundwater replenishment becomes insufficient to meet consumptive requirements. The results here are based on averaging over the simulation period and thus do not cover any issues associated with non-stationary groundwater dynamics; therefore, further investigation is warranted to explore the role of any transient groundwater behaviour.

5.4 Storage in farm dams and climate

The aggregate (lumped) behaviour of farms dams in the Barossa PWRA is explored here using the Source model, and these relationships are included in Stella for subsequent analysis. This section quantifies the relationship between the total water stored in all farm dams (S_{DAM}) as a function of annual P and PET as well as the seasonality of P. The annual maximum farm dam storage is used in this relationship to represent the farm dam storage before water extraction for consumption.

Based on Source results, the relationship included in Stella is a second degree polynomial in P and linear in PET, since an examination of responses from one-at-time perturbations in these climate variables indicated such a structure (not shown). S_{DAM} is the annual maximum total farm dam storage in ML. To ensure realistic range for S_{DAM} it is necessary to enforce the following bounds:

If $S_{DAM} > 8.25$ ML, $S_{DAM} = 8.25$ ML (farm dam capacity in model)

This parametric equation is implemented in the Stella model, and Figure 56 shows the sensitivity analysis conducted on the results from both Source (left), and Stella (right). The value represented for each combination of perturbed P and PET is the mean annual maximum farm dam storage/relative change in streamflow over the baseline period (1976-2005).

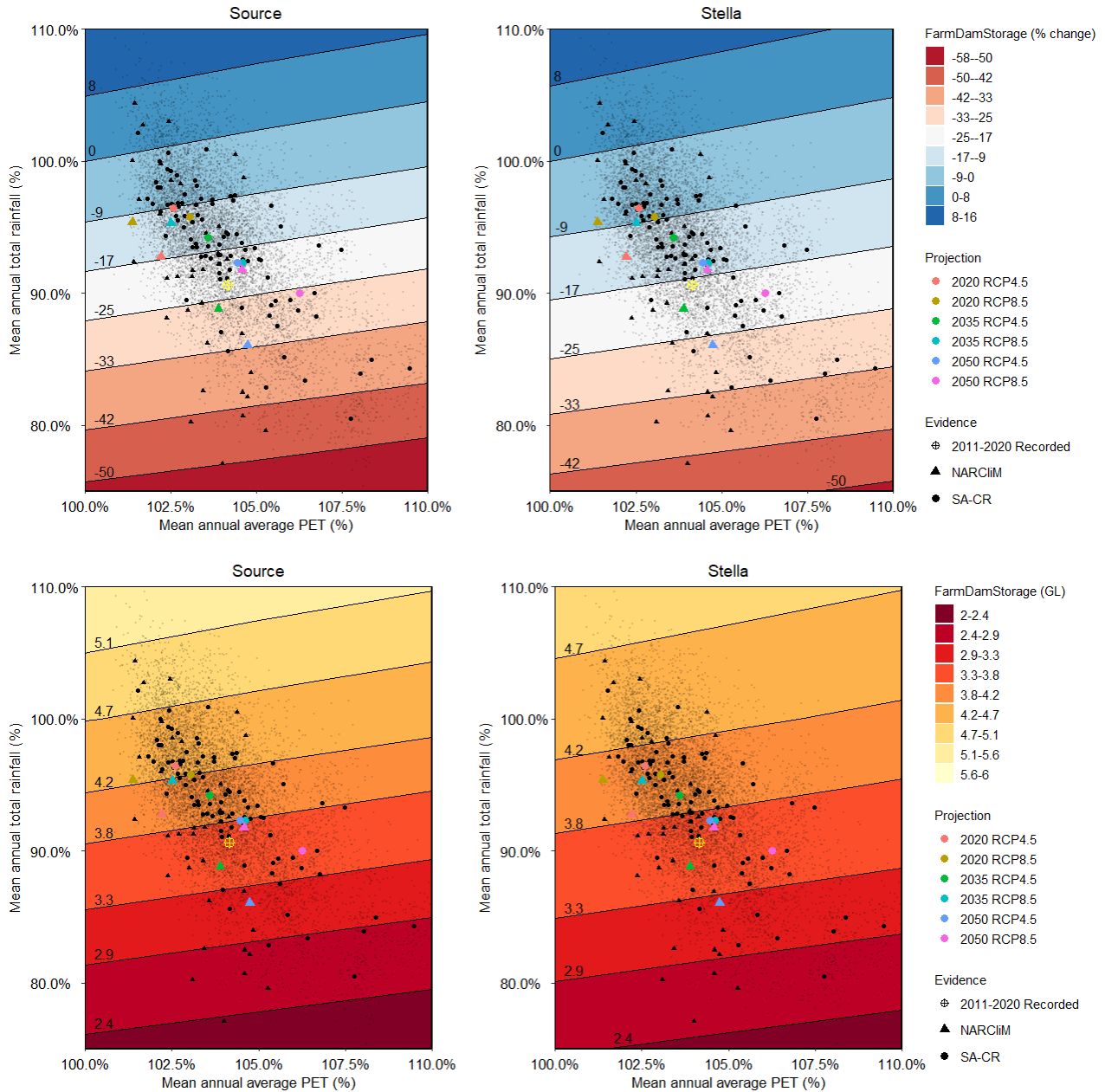


Figure 56. The performance space, both relative (upper panels) and absolute (lower panels) change, of maximum farm dam storage from simple scaling, both from Source (left) and Stella (right) results.

From Figure 56 it can be seen the annual average maximum level in the farm dam storages correspond to anticipated patterns, with maximum farm dam storage decreasing as rainfall decreases and PET increases. It can be seen that the Source results in general produce a higher range of percentage change than the Stella results. The Stella model is also more compressed for absolute maximum farm dam volume.

From examining the mean absolute maximum farm dam residuals (Figure 57), it can be seen that the models have some differences in absolute storage values. In particular, it can be seen that for an increase in rainfall, the models are much further apart (0.4 GL) than for a decrease in rainfall (0.1 GL). Although this is not ideal,

it is more important to capture behaviour for decrease in rainfall and increase in PET, as these are the scenarios which will have the greatest impact on water security.

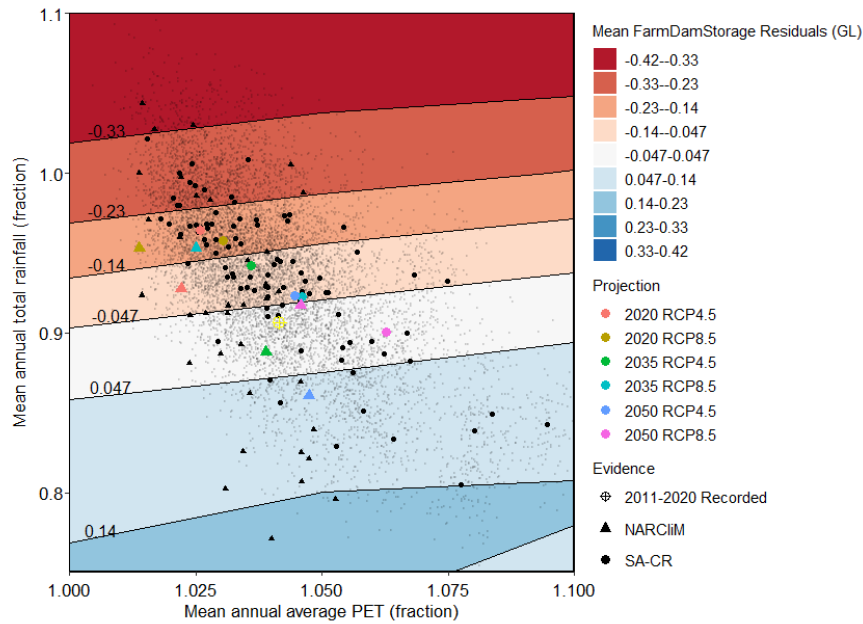


Figure 57. Residuals of the mean absolute maximum farm dam storage values between Source and Stella

The additional influence of seasonality is shown in Figure 58, for both a slight decrease and increase in the strength of the seasonal cycle (left and right panels, respectively) relative to maintenance of the historical seasonal cycle (middle panel). The greatest reductions in maximum farm dam storage occur for a reduction in the seasonal cycle, which is expected as this corresponds to relatively less rainfall in winter which then can be diverted to farm dams. For increases in the seasonal cycle, the annual maximum farm dam storage increases.

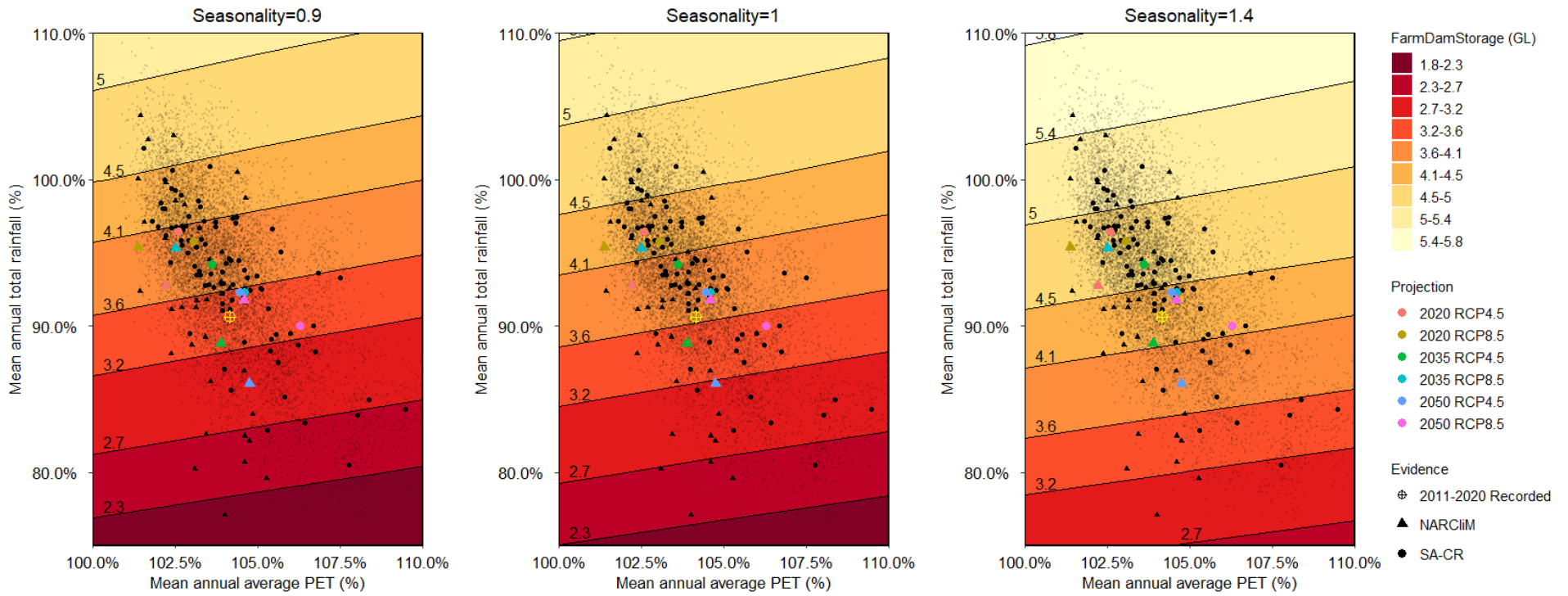


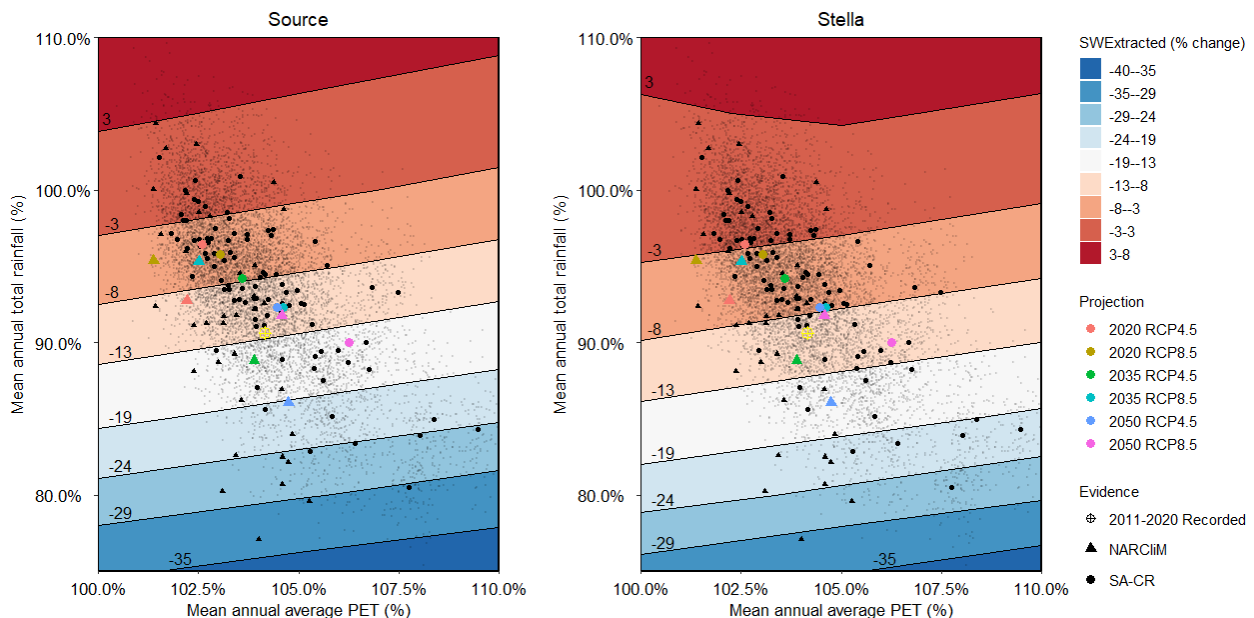
Figure 58. The performance space (absolute change only) replicated for a decrease in the strength of the seasonal cycle (i.e. relatively wetter summers and drier winters; left panel), the historical seasonal cycle (middle panel) and an increase in the strength of the seasonal cycle (additional drying in summer and wetting in winter; right panel).

5.5 Water use from surface water

Surface water use is calculated by combining extraction from farm dams and extraction from the watercourse (streamflow) in Source. The annual maximum total water stored in the dams (S_{DAM}) is calculated as a function of climate variables as described in the previous section (Section 5.4). The water extracted from the farm dams per water year is a function of this available storage. This relationship is quantified at the annual scale from the Source model simulations for representation in the system dynamics model. The farm dam and water extraction variables simulated using the eWater Source model is used to define the relationship. A third degree polynomial is fitted to model the variation in water use from farm dams with the maximum available annual storage in the farm dams.

The watercourse extraction is modelled using 37 'water user' nodes in the eWater Source model. The water course extractions are spatially distributed in reality, and are dependent upon the amount of water available in the stream at the points of extraction. Here we propose to model the total water course extractions in the Barossa PWRA as a lumped quantity in the annual scale system dynamics model. A simplified representation of the relationship between water course extraction and streamflow may be defined by modelling the lumped water course extraction as a function of the streamflow at the downstream gauging location at Yaldara. This relationship is quantified at the annual scale using the eWater Source model simulations. A linear relationship is fitted to the eWater Source simulations between U_{WC} (the annual volume of water used from the water course in ML), and Q (annual total streamflow at Yaldara in ML). Since the watercourse extractions form a small component of the water balance (up to 400 ML/year), this fitted simplified relationship is thought to be acceptable for use.

The outputs from the Stella and Source models at the annual water scale are then added together to get the total surface water extraction. Figure 59 shows the sensitivity analysis conducted on the results from Source (left), and Stella (right). The value represented for each combination of perturbed P and PET is the relative change in surface water extraction/mean annual surface water extraction over the baseline period (1976-2005).



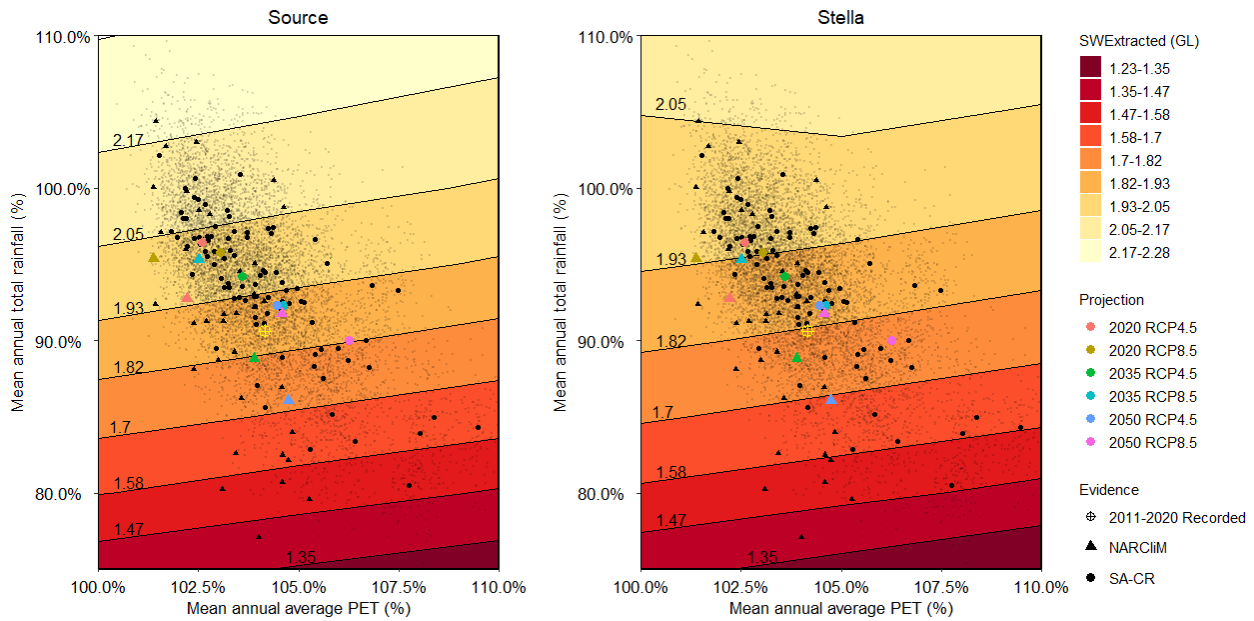


Figure 59. The performance space, both relative (upper panels) and absolute (lower panels) change, of surface water extraction from simple scaling, both from Source (left) and Stella (right) results.

It can be seen from Figure 59 that Stella and Source produce similar absolute changes for most perturbations, but they differ for extreme rainfall scenarios. This is due the Stella model not extracting the full supply of surface water if it is not required to meet demand in any given year. Hence less surface water is extracted for very wet years than predicted by the Source model. In general, the Stella results are lower than the Source results. As surface water is a combination from two different sources, it is difficult to pinpoint the origin of this error. Although not ideal, it is considered preferable to underestimate the surface water extractions as it is more conservative when assessing water security.

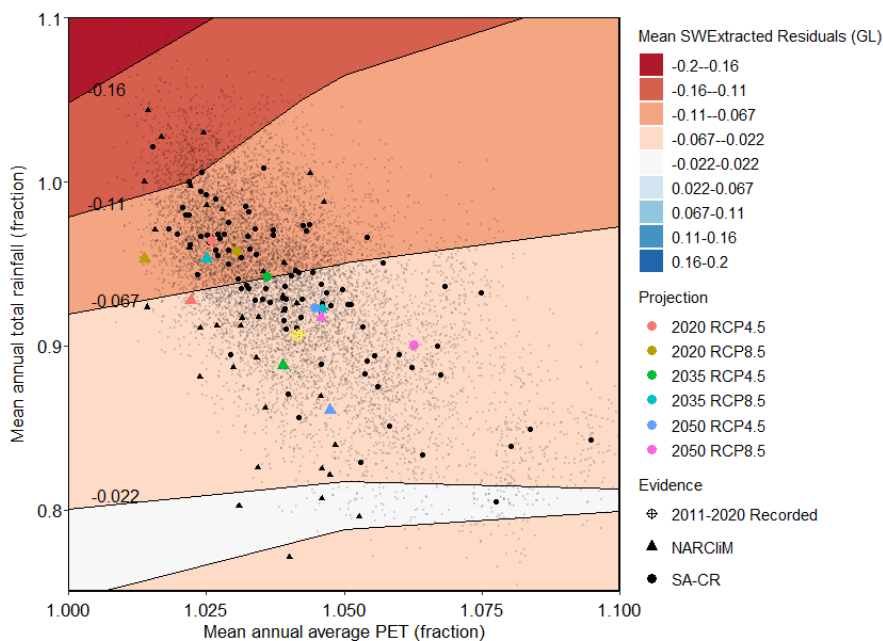


Figure 60. Residuals of the mean absolute surface water extraction values between Source and Stella

From the absolute residuals (Figure 60) there appears to be less of a difference in the models for the high rainfall region than the low rainfall region. The additional influence of seasonality is shown in Figure 61, for both a slight decrease and increase in the strength of the seasonal cycle (left and right panels, respectively) relative to maintenance of the historical seasonal cycle (middle panel). The greatest reductions in

watercourse extraction occur for a reduction in the seasonal cycle, which is expected as less water in streams and farm dams corresponds to less water that can be extracted. Increases in the seasonal cycle allow for more surface water available for extraction.

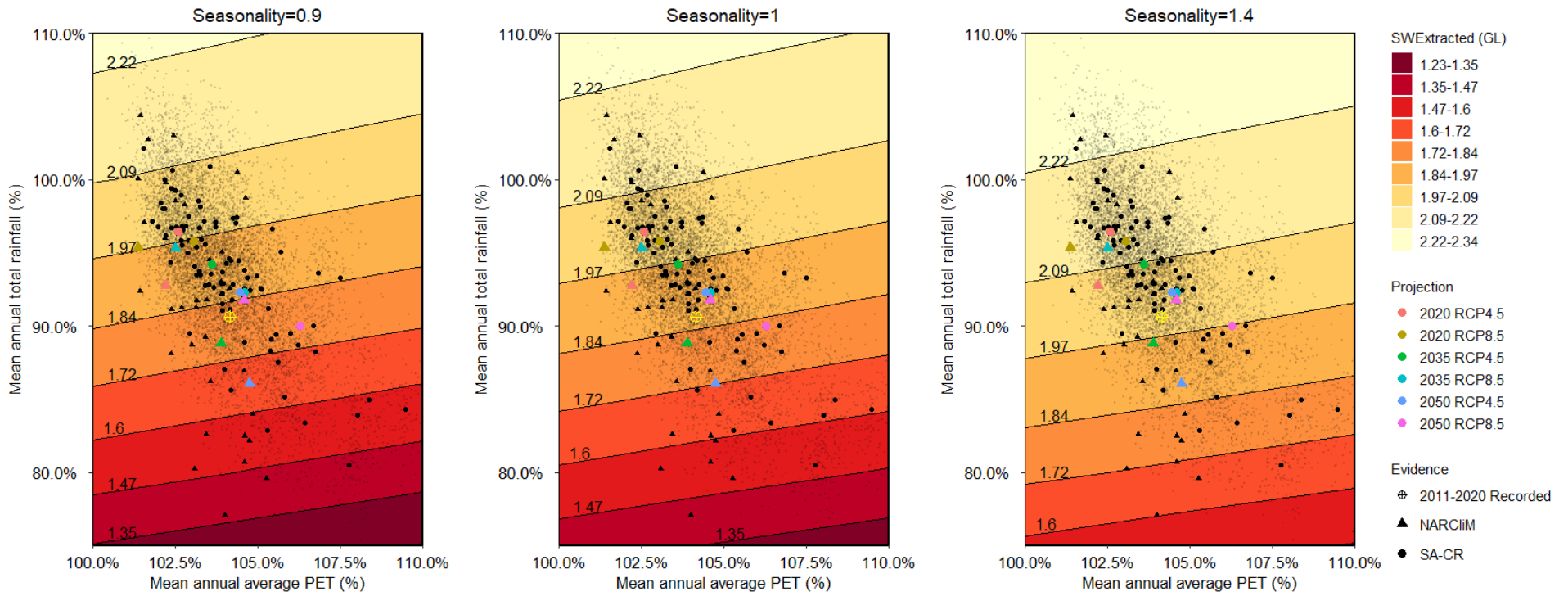


Figure 61. The performance space (absolute change only) replicated for a decrease in the strength of the seasonal cycle (i.e. relatively wetter summers and drier winters; left panel), the historical seasonal cycle (middle panel) and an increase in the strength of the seasonal cycle (additional drying in summer and wetting in winter; right panel).

5.6 Rainfall and groundwater recharge

Figure 62 shows the changes in groundwater recharge, in both absolute and relative terms with respect to the baseline period, as a function of plausible changes in P and PET from MODFLOW and Stella. As mentioned in Figure 9 we note that the relationship between P and R is derived not directly from the MODFLOW model, but rather from an external relationship defined by Li and Cranswick (2016) required for input to the MODFLOW model. As expected, it is seen that groundwater recharge increases linearly with respect to P and is insensitive to PET. The models also produce very similar results, with Stella results showing a smaller range of both absolute and relative change in recharge, as observed for the majority of Source regressions. Importantly, the recent decade shows recharge values of approximately 10.2 GL, which already is significantly below baseline levels.

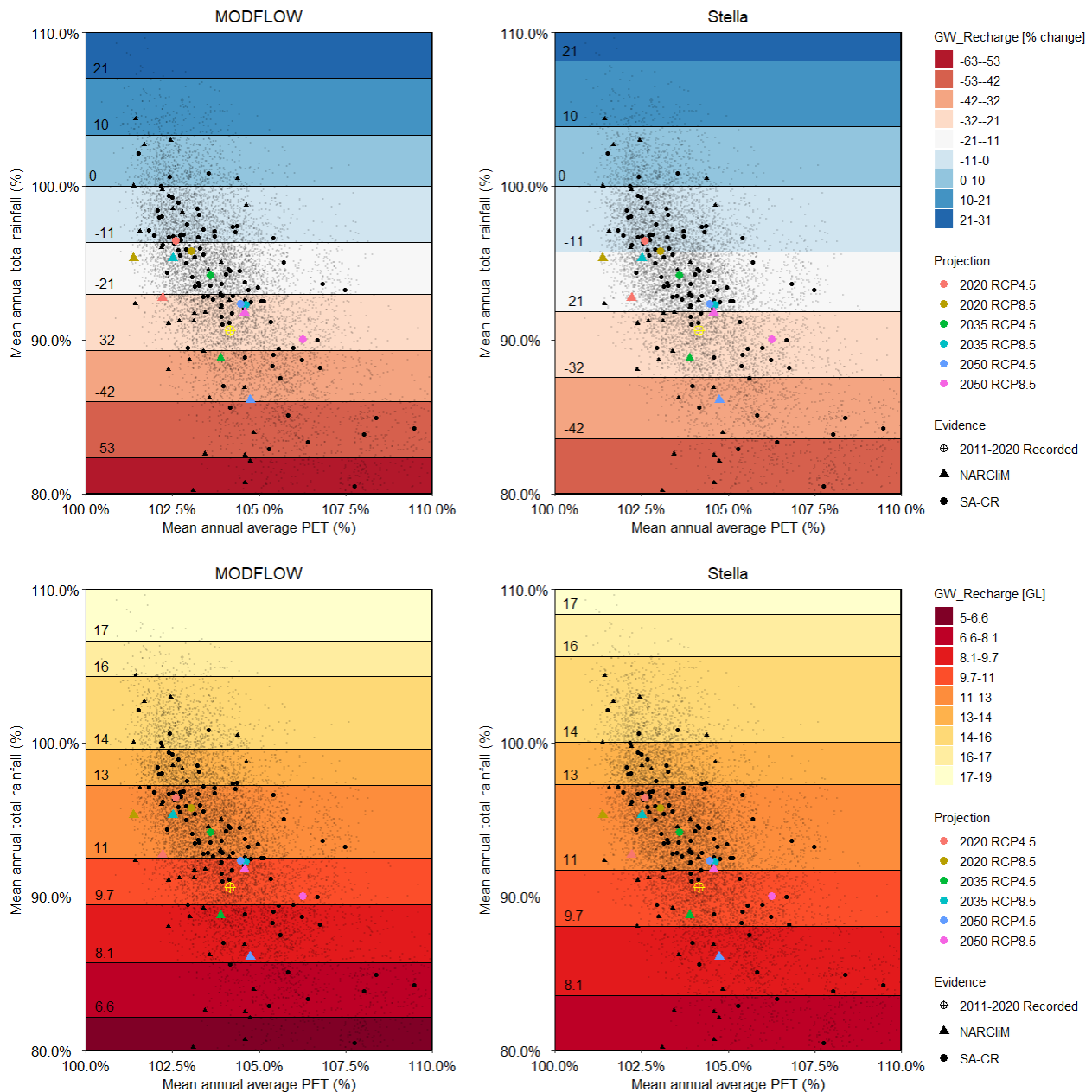


Figure 62. The performance space, both relative (upper panels) and absolute (lower panels) change, of groundwater recharge from simple scaling, both from MODFLOW (left) and Stella (right) results.

Figure 63 shows the mean absolute recharge Stella-MODFLOW residuals. This once again shows that the models produce fairly similar results, with the greatest changes between models observed for extreme values of rainfall.

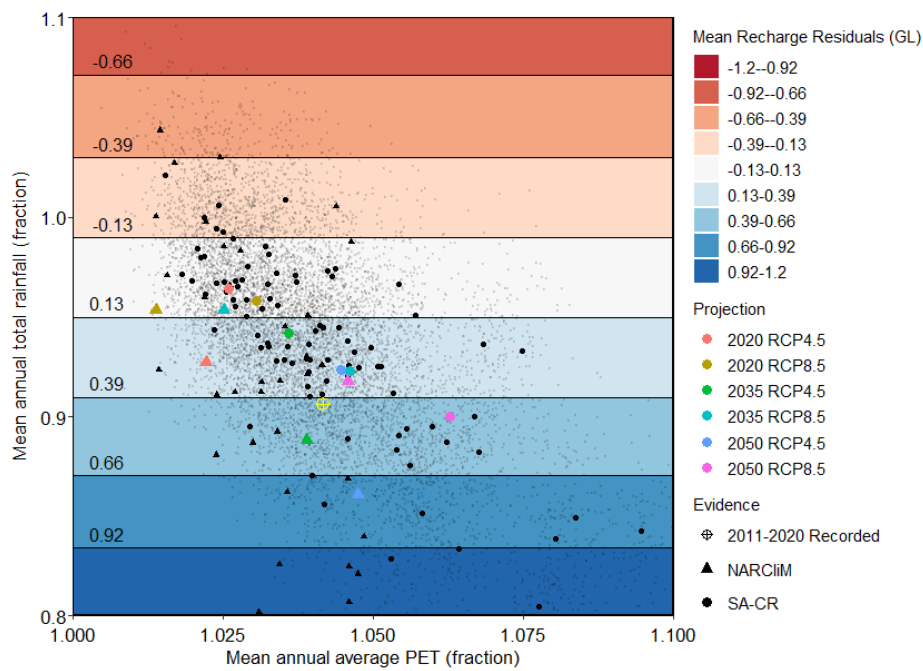


Figure 63. Residuals of the mean absolute recharge values between MODFLOW and Stella

5.7 Groundwater Evaporation

Figure 64 shows the changes in groundwater ET, in both absolute and relative terms with respect to the baseline period, as a function of plausible changes in P and PET from MODFLOW and Stella. As expected, groundwater ET is shown to increase with increasing P and PET. The gradient in groundwater ET is significantly larger with respect to P.

These results, when combined with recharge results, have important implications for water balance estimates. Assuming limited lateral flows outside of the Barossa PWRA delineation (see Section 3.5), and also assuming a steady state, the difference between recharge and evaporation represents the water available for both baseflow and for consumptive purposes. Thus, in the recent decade there was an average recharge of approximately 10.2 GL/yr (Figure 62) and average groundwater evapotranspiration is 6.7 GL/yr (Figure 64), leaving a residual of 3.5 GL/yr, which is insufficient to simultaneously maintain baseflows and consumptive requirements. This, in turn, suggests potential limitations to the steady state assumption, as already highlighted in Section 5.3.2.

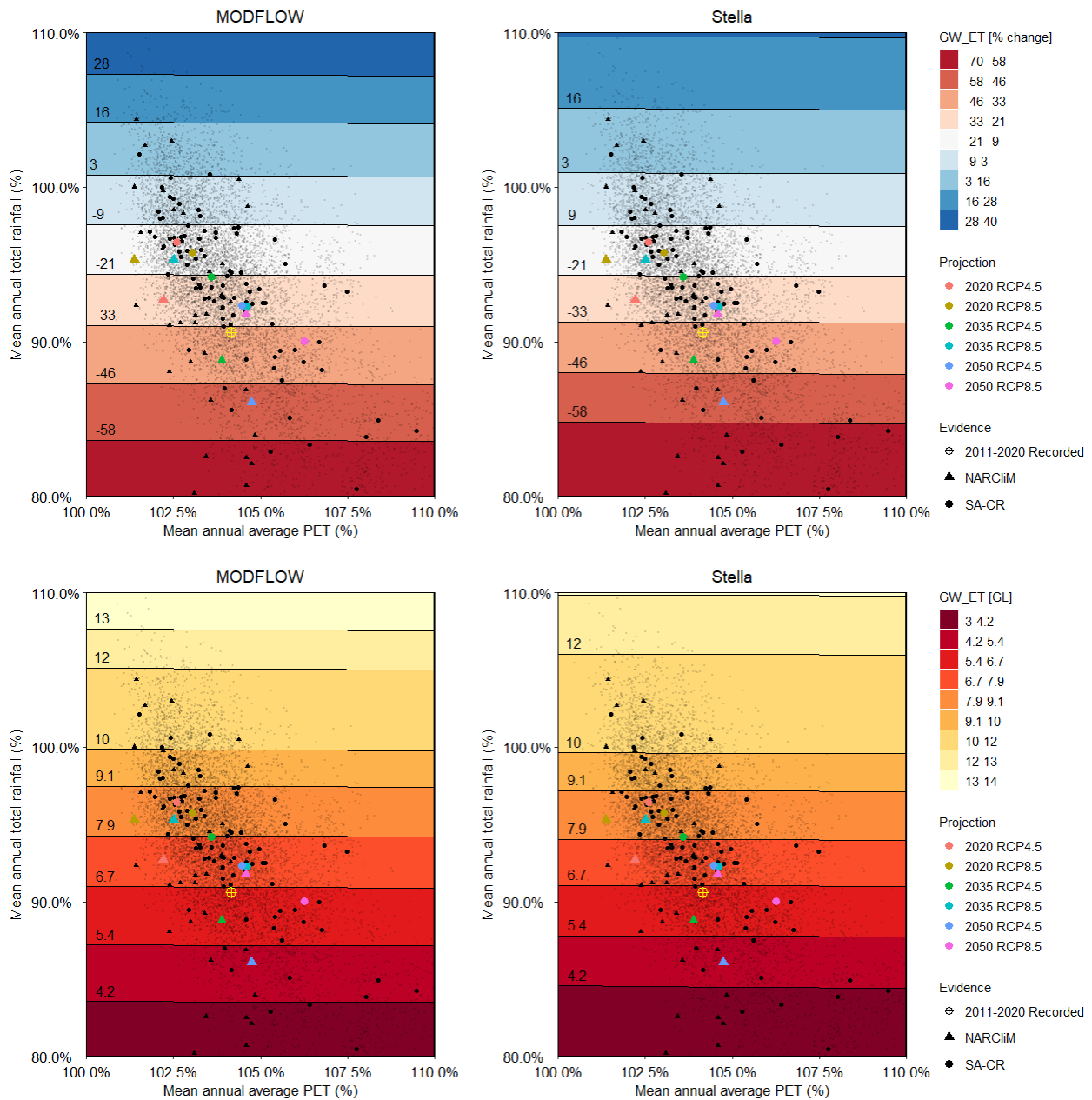


Figure 64. The performance space, both relative (upper panels) and absolute (lower panels) change, of groundwater evaporation from simple scaling, both from MODFLOW (left) and Stella (right) results.

Figure 65 shows the mean absolute groundwater ET Stella-MODFLOW residuals. It can be seen that the models produce similar absolute values, and there is no particular trend where the models disagree most.

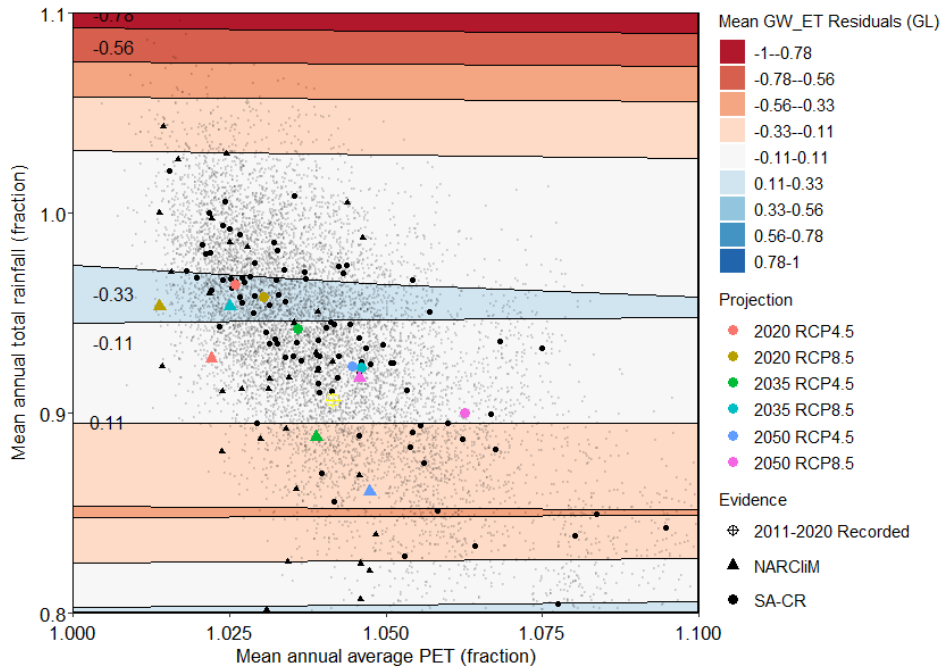


Figure 65. Residuals of the mean absolute groundwater evaporation values between MODFLOW and Stella

5.8 Groundwater Storage

Figure 66 shows the changes in groundwater storage volume, in both absolute and relative terms with respect to the baseline period, as a function of plausible changes in P and PET from MODFLOW and Stella. The expected pattern of increasing storage volume with increasing P and decreasing PET is evident, although the gradient in storage with respect to P is significantly larger than that with respect to PET (the storage gradient with respect to PET is barely visible). The storage gradient with respect to P displays non-linearity, with the steepest portion of the gradient occurring at low P values.

Note that initial groundwater storage is altered at the beginning of each Stella run in order to better match the observed storage levels in MODFLOW using the equation $S_{GW_i} = -2418100P_{pert}^2 + 5337.1P_{pert} - 2209.2$ where P_{pert} is the scaling factor applied to rainfall in a given sensitivity run. Another flux from the groundwater storage, lateral groundwater exchange, which is not presented here as it is a small portion of the water balance, nonetheless is implemented in Stella with the regression relationship $0.0013 \times S_{GW} - 881.9$.

The Stella results are very similar to the MODFLOW results and show very similar gradient with respect to P and PET, for both the absolute and relative change exposure spaces. Importantly, given a baseline storage value over the historical record varying approximately between 690-700 GL (Section 3.9), these results are highly suggestive of non-stationary behaviour in groundwater storage levels for more severe climate change forcings. The interpretation of absolute values in these results therefore need to be treated with caution given the methodological assumptions associated with 'fixed window' analysis.

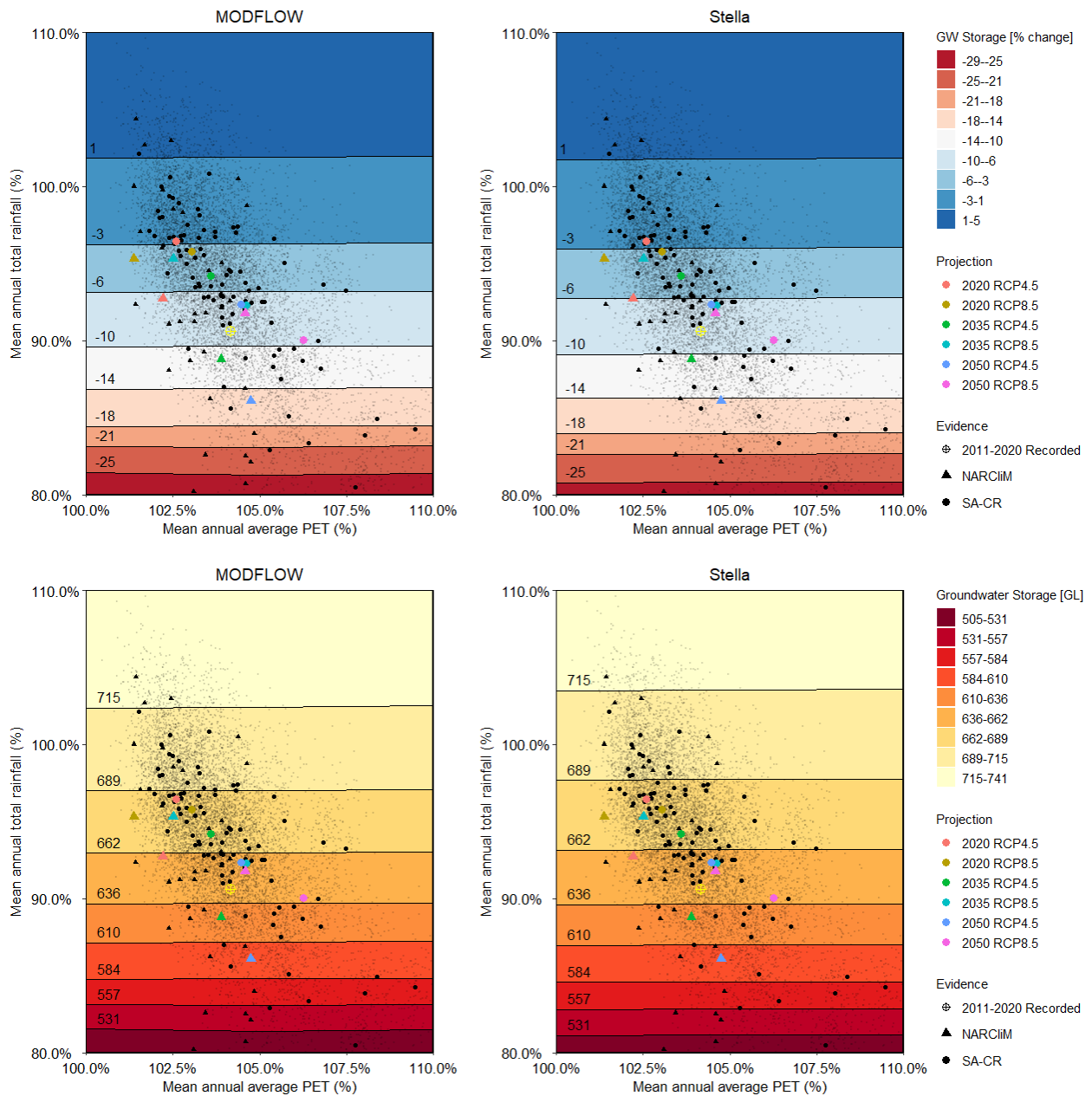


Figure 66. The performance space, both relative (upper panels) and absolute (lower panels) change, of groundwater storage from simple scaling, both from MODFLOW (left) and Stella (right) results.

Figure 67 shows the mean absolute groundwater storage Stella-MODFLOW residuals. Given the very large size of the GW storage, the residuals show that the models are very close, with the greatest difference for low rainfall and PET.

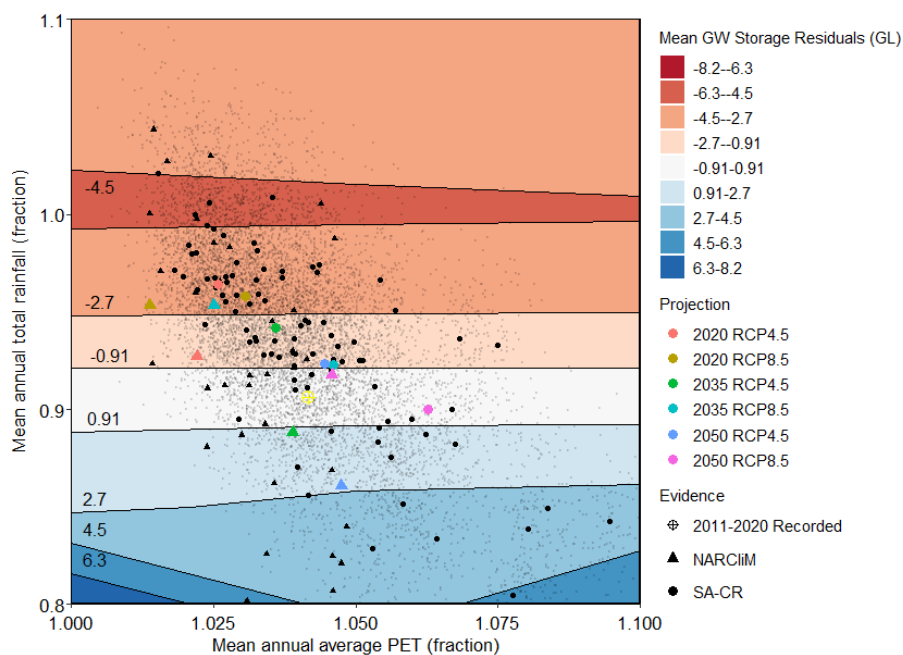


Figure 67. Residuals of the mean absolute storage values between MODFLOW and Stella

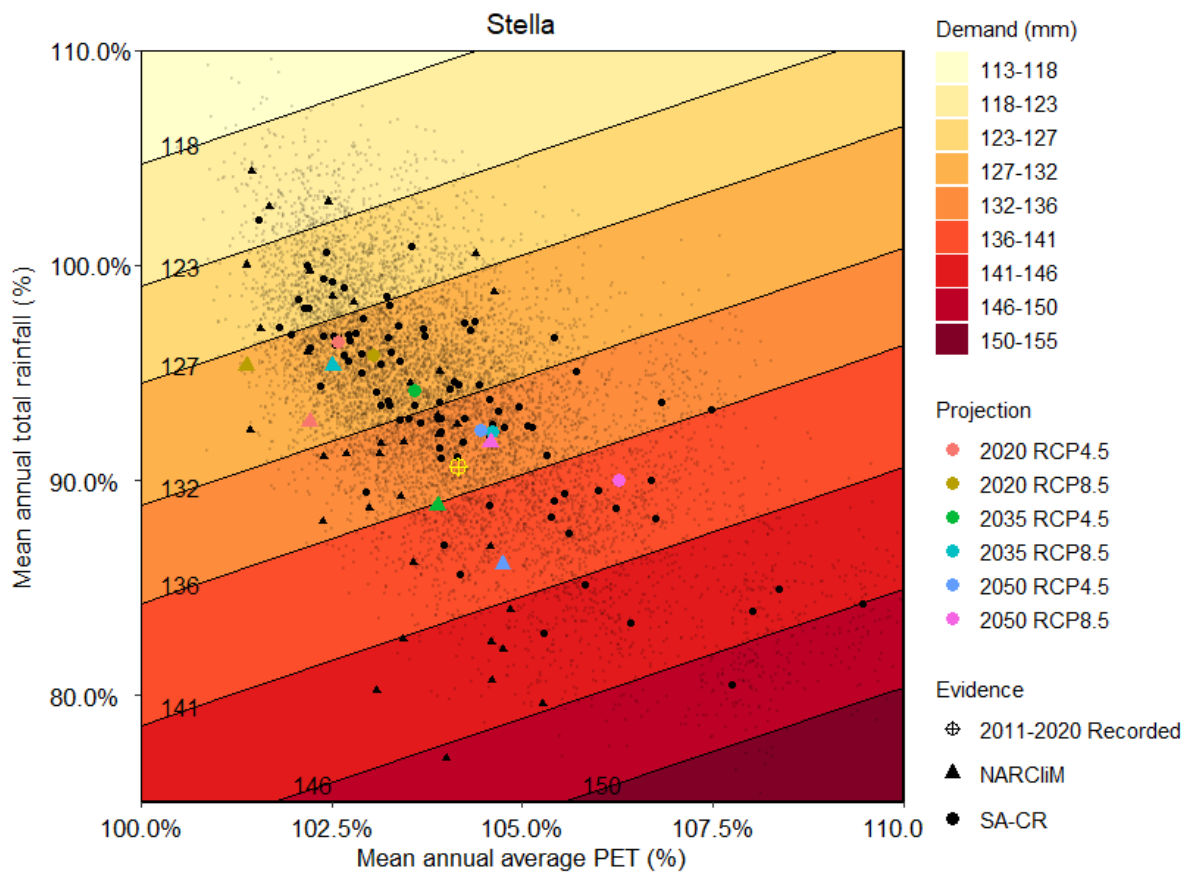
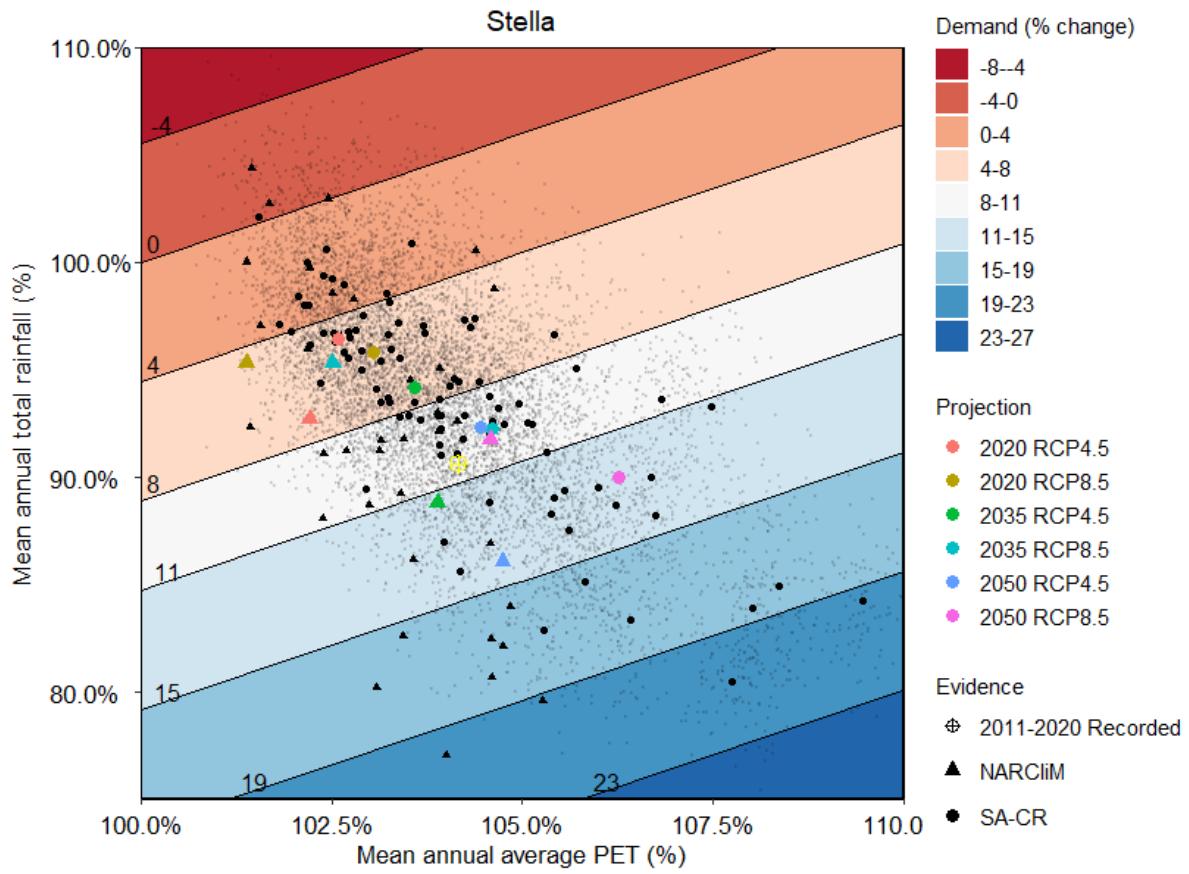
5.9 Irrigation demand

In this section, both irrigation demand models are stress-tested by perturbing P and PET via simple scaling with respect to the baseline period.

5.9.1 Regression Model

Here we stress test the demand regression model (Section 3.12). Due to their simplicity, the relationships underpinning the demand model were implemented directly in the Stella model (therefore no component model versus Stella comparisons are drawn below). A censored regression was also conducted, in which all years for which demand approached supply capacity (equivalent to an observed use in the Barossa PWRA of 12GL). The premise of the censored model is that for situations where observed usage approaches supply capacity, the actual demand may be greater than implied by the usage. Interestingly, the censored regression results were found to be consistent with the standard regression results, and as such the more complex censored approach was not implemented here. Instead, to address regression modelling uncertainty, an error term was introduced to simulate drivers of demand not captured by the simple regression model.

The results from Stella for absolute and relative change are presented in Figure 68. As expected, irrigation demand (and its percentage change) shows a linearly increasing trend with respect to increasing PET and decreasing P. As was discussed in Section 3.11.3, some evidence exists that growers were adjusting to lower availability in dry years by pursuing lower yield targets, and as such the regression model may be underestimating climate sensitivity of demand assuming that growers are aiming for consistent yields.



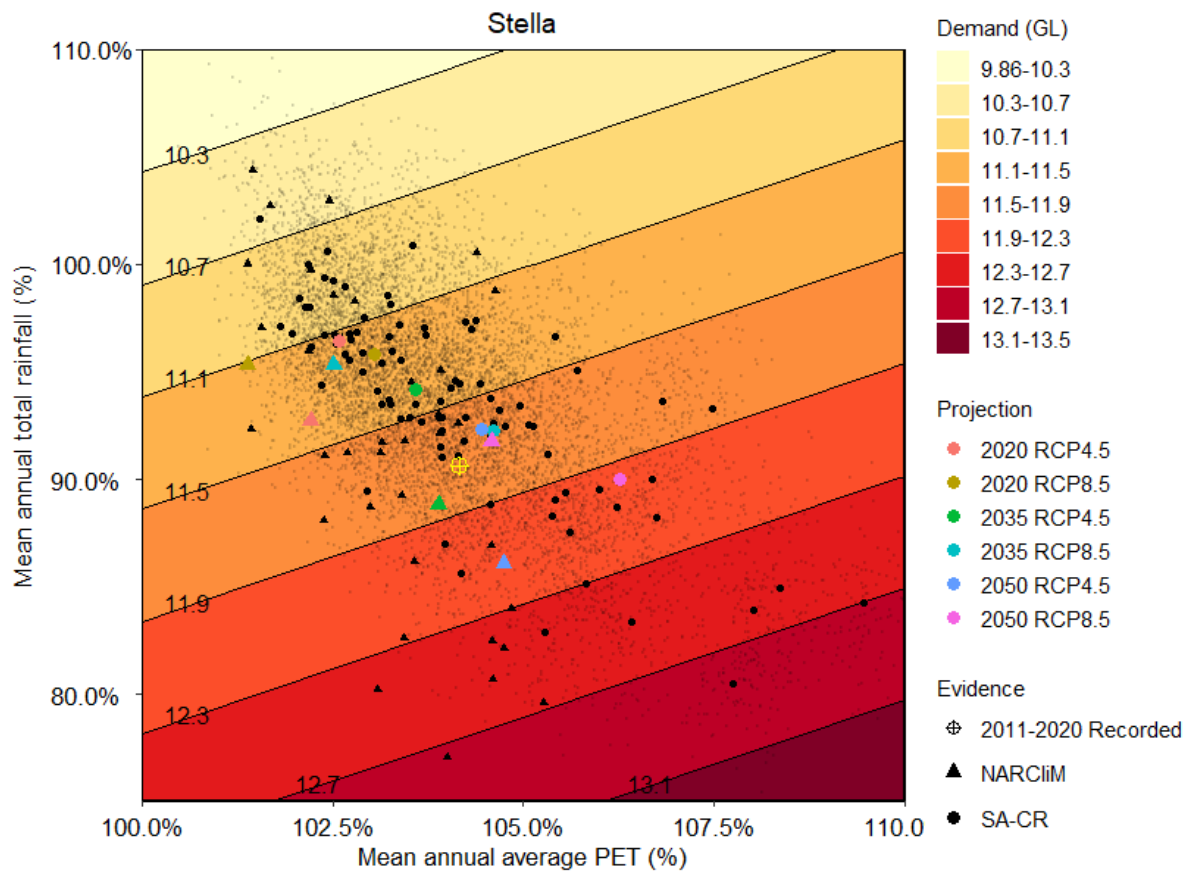


Figure 68. The performance space, both absolute (GL, bottom; mm, middle) and relative change (top), of regression-based demand from simple scaling, from Stella results.

5.9.2 FAO-56 DCC Model

We next stress test the FAO-56 DCC model (Section 3.11.2). We perturb both P and PET. We do not perturb minimum relative humidity – a climate variable that is an input variable to the FAO-56 DCC model. This was deemed appropriate due to the small influence on irrigation demand of increasing relative humidity based on the maximum CCIA projections for the SSWF-West Cluster, which suggests a maximum 3.2% absolute increase in RH by 2090 for RCP8.5 (Hope et al, 2015).

As expected, Figure 68 shows the absolute irrigation demand computed using the FAO-56 DCC model displays an increasing trend with respect to increasing PET and decreasing P. Compared to absolute demand from the regression model (Figure 68), the FAO-56 DCC model produces a larger gradient both with respect to P and particularly with respect to PET. The FAO-56 DCC model also has a much greater range of demand, for reasons discussed in Section 3.11 and 3.12.

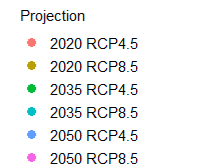
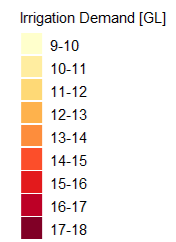
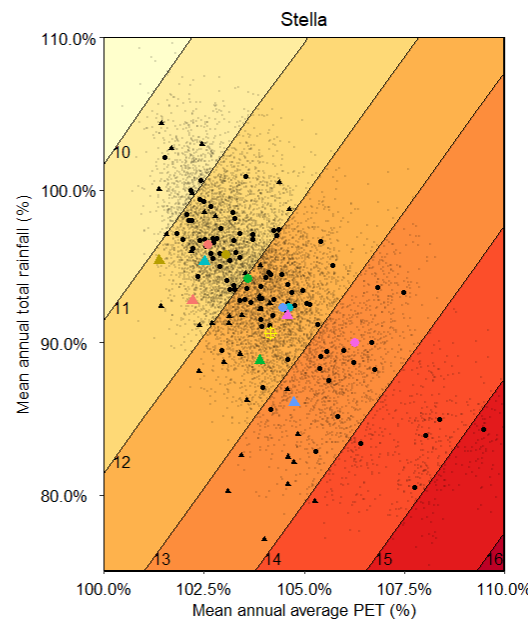
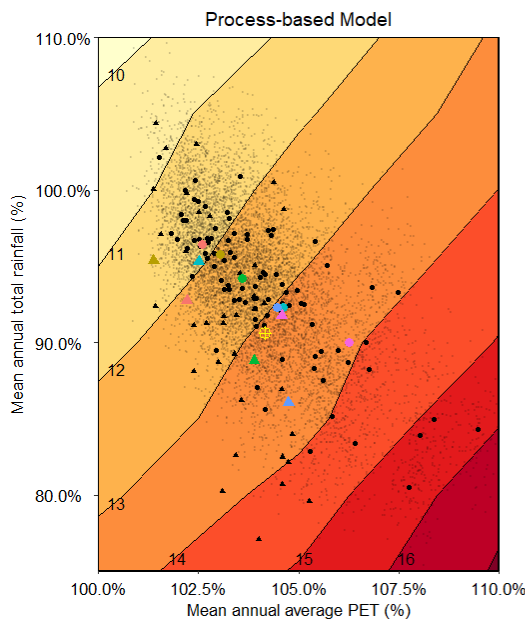
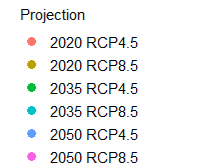
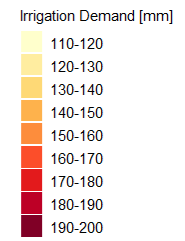
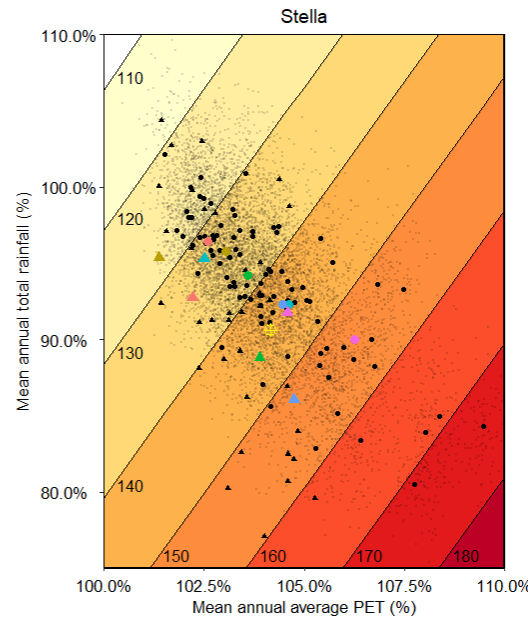
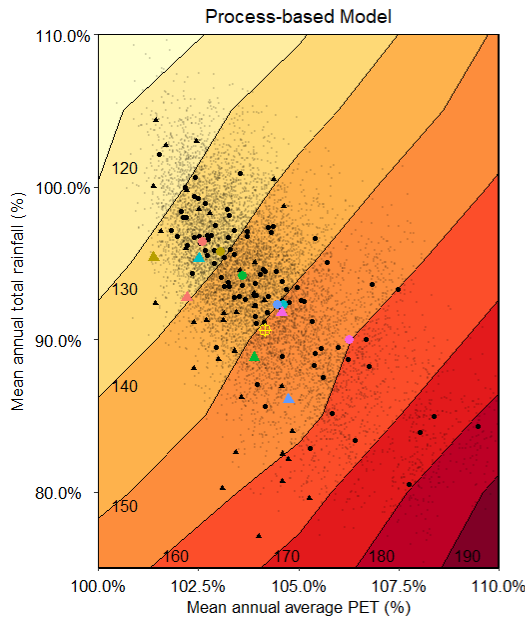
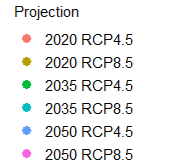
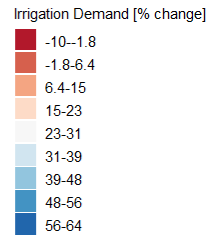
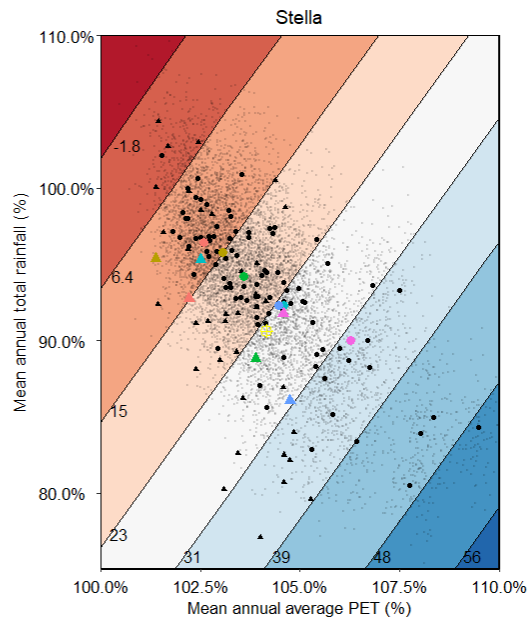
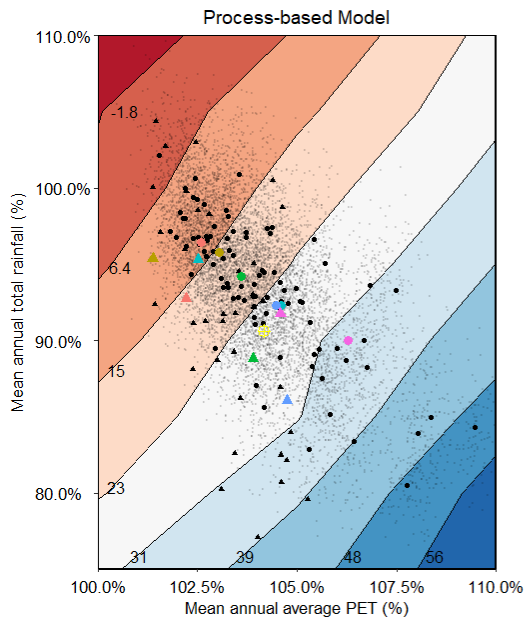


Figure 69. Performance space of relative (top) and absolute irrigation demand (mm middle; GL bottom). The performance space of absolute irrigation demand from the regression model is shown for comparative purposes.

The SARDI results and its implementation in Stella look fairly similar. The Stella results have much smoother contours, which is expected due to the nature of representing the model with a linear bivariate regression. The Stella model also has slightly steeper contours, but the average value for each perturbation combination of P and PET are comparable. It can be seen from the residuals of these models (Figure 70), that the difference is small (maximum 0.45 GL absolute difference).

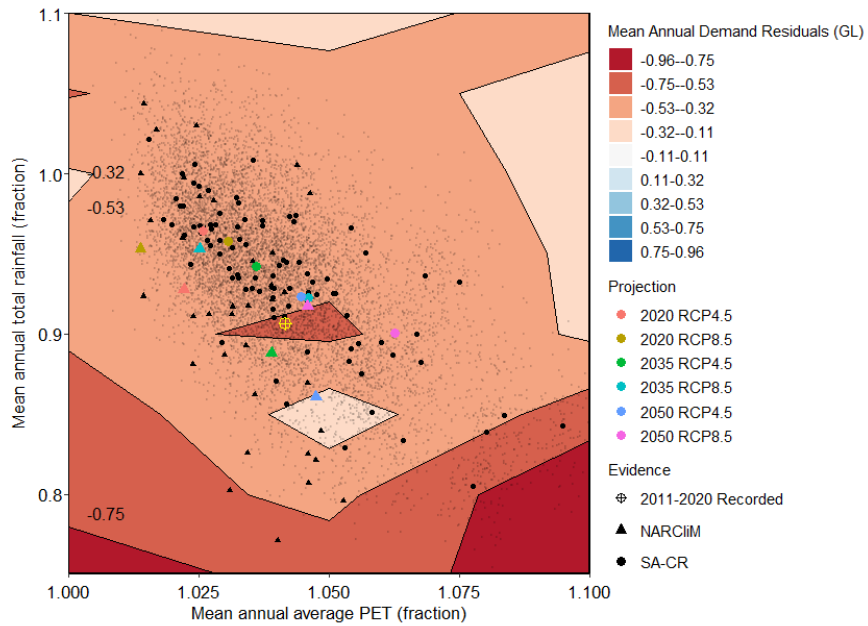


Figure 70. Mean Annual Demand Residuals (GL) between SARDI model and SARDI regression implemented in Stella

6 Current System Dynamics

In this section, the effect of plausible climatic change on current system dynamics is explored. System dynamics and performance are assessed using the performance metrics presented in Table 4. The water security metrics are first explored using the Stella system dynamics model (Figure 10), and the environmental flow metrics are subsequently explored purely from perturbed eWater Source model results.

Unmet demand is assessed in Stella by simulating the system's ability to meet estimated demand under various climate conditions. Estimated demand comes from both estimated vineyard irrigation requirements as well as stock and domestic use, and demand varies both year-to-year and with alternative climate conditions. The stock and domestic use is included in the observed use for the regression-based model, and is added within Stella to the process-based model regression as a constant. The adopted stock use is 1.1, 0.891 and 0.927 GL/year respectively for the three delineations (Barossa PWRA, Barossa Valley and Eden Valley).

Supply is derived from a combination of surface water, groundwater and external sources (BIL, SA Water off-peak and Bunyip pipelines). Surface water varies annually based on climate conditions, whereas groundwater and external sources are assumed constant and do not vary year-to-year or with climate. Groundwater extraction is kept constant, as extraction from this resource has been relatively stable in recent years, and there is some evidence that water quality limitations of the groundwater resource prohibit growers from further increasing groundwater utilisation. The assumed groundwater extraction is the average annual groundwater extraction over the more recent decade (3 GL, 2.1 GL and 0.9 GL for the Barossa PWRA, Barossa Valley and Eden Valley, respectively). The full imported water supply capacity is assumed to be available to the Barossa Valley (11 GL, 1.5 GL and 2 GL based on BIL capacity, SA Water off-peak averaged over the last decade, and reported Bunyip capacity, respectively). As discussed in Section 3.2, 64% of BIL is assumed to be supplied to the Barossa PWRA, as well as 40% of Bunyip. The full SA Water off-peak amount is assumed to be used in the Barossa PWRA. The Eden Valley has a small contribution from the SA Water off peak amount, but otherwise has no external sources. Finally, it is assumed that the stock and domestic use can be supplied for all delineations regardless of year-to-year and long-term climate conditions; this assumption may not hold particularly under the more severe climate conditions.

As described in Section 2.1, all environmental flow metrics are based on modelled streamflow from Source, at the outflow from the Barossa Valley Gorge (Yaldara) and Upper Flaxman Valley zones.

6.1 Water Security Metrics

As introduced in Table 4, four water security metrics are considered in this analysis. These include three metrics associated with unmet demand, where unmet demand is defined as the volume of annual demand that cannot be supplied through natural and external sources. This value fluctuates yearly based on estimated demand for that year (for both irrigation and non-irrigation uses), as well as surface water and groundwater availability. The unmet demand metrics are average unmet demand (GL), percentage of years for a given perturbation combination with unmet demand, and average unmet demand in years with unmet demand (GL). The fourth metric is the ratio of supply to demand that achieves a 90% system reliability, with a value of unity indicating that supply meets demand in 90% of years. The results are presented separately by delineation.

6.1.1 Barossa PWRA

Two alternative approaches were used to simulate current system demand dynamics: the first by using the regression model that was calibrated to usage over the recent decade, and the second that uses the results of a process-based model. Results from these two approaches are discussed below.

6.1.1.1 Water security metrics using regression-based model in Stella

The regression-based model with error term is implemented in Stella to obtain the unmet demand metrics, which is shown in Figure 71. The regression-based model produces no to very low unmet demand for the majority of climate scenarios. The climate scenario showing the recent decade (yellow 'bullseye') has around 3.5% of years with unmet demand. Given anecdotal information about difficulties in meeting total demand in the recent decade, this is expected to be a significant underestimation of actual demand. This is likely due to the assumptions of the regression model, that was trained based on the assumption that historical supply acts as a proxy for demand. The results for the average 2050 projections are also lower than expected, with also only 3.5% of years with unmet demand, and average unmet demand in those years of 1.5 GL.

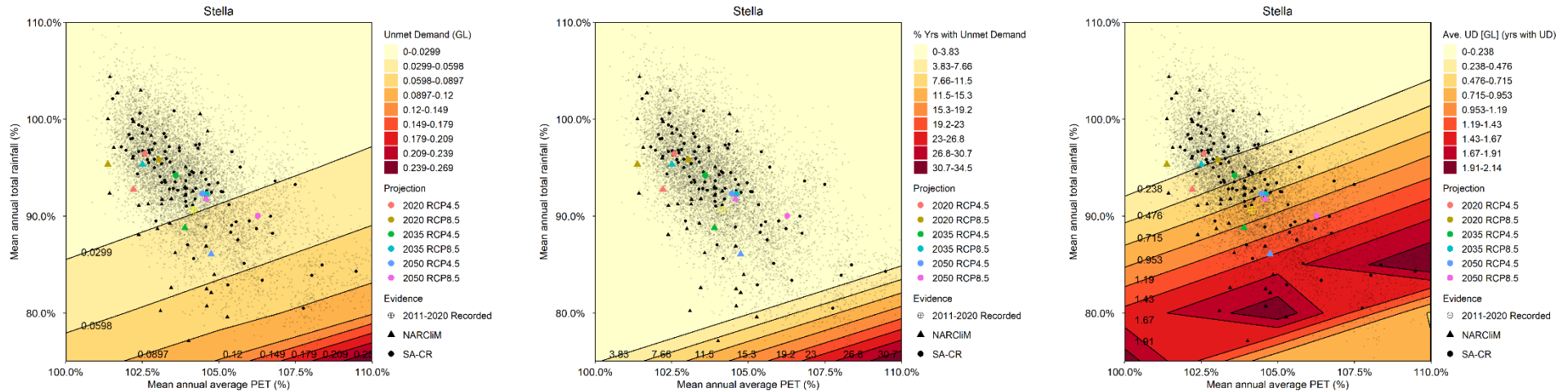


Figure 71. Unmet demand from regression-based model in Stella for the Barossa PWRA. Left to right: Average unmet demand [GL], percentage of years with unmet demand and average unmet demand in years with unmet demand [GL].

Figure 72 shows the ratio of supply on demand which corresponds to a 90% reliability. It can be seen that the line where supply is equal to demand is right on the edge of the most extreme future projections, and far past the 2050 average projections. As we know that the system has already exceeded its limits in recent years, it seems more reasonable that this white line should be closer to the high rainfall and low PET projections, and on the other side of the recent decade bullseye. Again, this is likely to be due to the assumptions of the regression model, which was calibrated on water usage over the recent decade, and thus would be expected to show reasonable performance over similarly dry climate conditions.

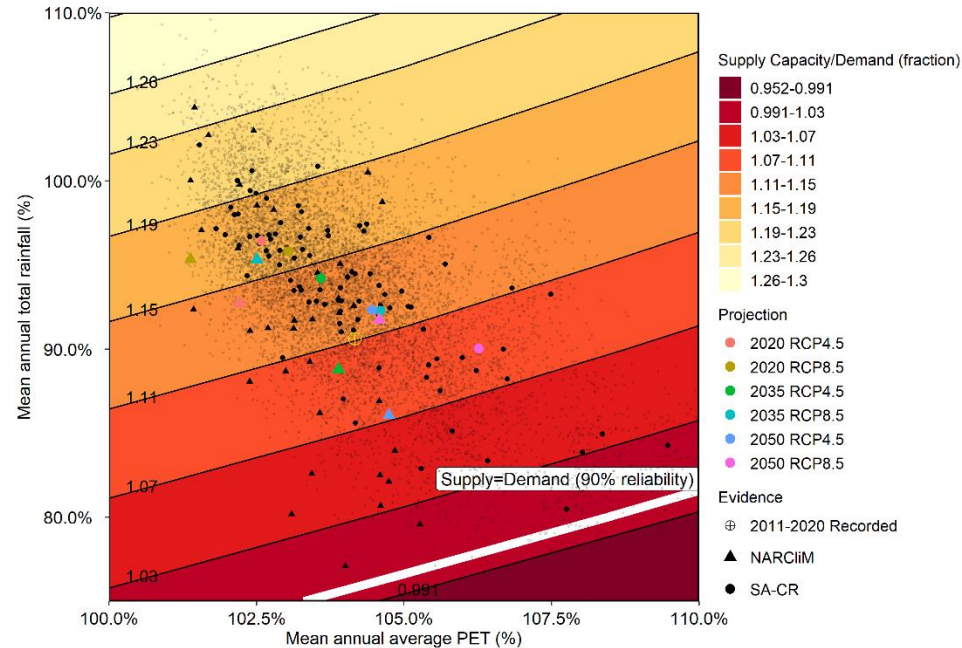


Figure 72. Ratio of supply on demand that corresponds to 90% reliability using the regression-based model in Stella for the Barossa PWRA. The white threshold line indicates the climate scenarios where supply is equal to demand.

6.1.1.2 Water security metrics using process-based model in Stella

An alternative approach to calculating unmet demand involves the use of a process-based demand model as shown in Figure 73. The process-based model results were employed in Stella using a linear bivariate regression. An error term was also applied within Stella to capture the year-to-year variability of demand in a manner consistent with the underlying FAO-56 DCC model. Quantile-quantile plots of the process-based model results and the process-based model regression with error term can be seen in Appendix E.

The process-based model is much more sensitive and predicts higher demand than observed use for some years in the calibration. The climate scenario for the recent decade shows around 30% of years with unmet demand (Figure 73, middle panel), which is closer to expectations based on anecdotal experience of severe water stress over the recent decade. This is likely due to the high demand in certain years caused by the large year-to-year variability in the FAO-56 DCC model results, with the demand from the FAO-56 DCC model far exceeding observed use during dry years, implying that use would have been greater in those years had supply been available. As the recent decade climate scenario sits within the middle of the future climate projections, the average 2050 scenario is not that far from the recent decade, with around 35% of years with unmet demand and 2.2 GL average unmet demand in these years.

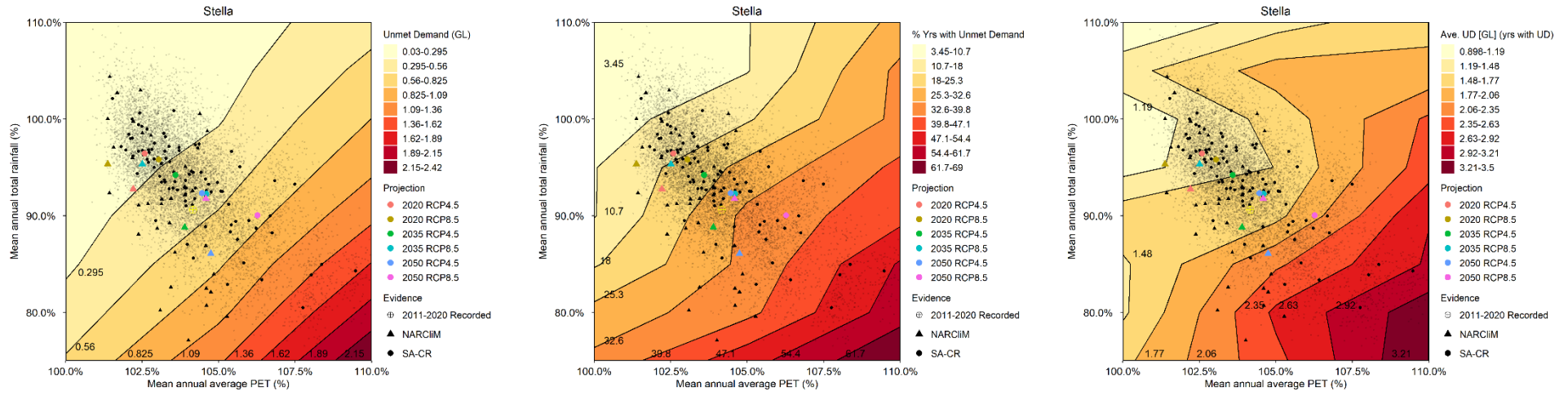


Figure 73. Unmet demand from process-based model in Stella for the Barossa PWRA. Left to right: Average unmet demand [GL], percentage of years with unmet demand and average unmet demand in years with unmet demand [GL].

Figure 74 shows the supply on demand ratio using the process-based model. It can be seen that the line where supply is equal to demand at least 90% of the time (corresponding to a system reliability of 90%) is to the top left of the recent decade climate scenario. In contrast, the 90 percentile of the ratio of supply to demand is equal to 0.88 based on the climate in the recent decade, implying that supply would need to be augmented by $1/0.88 = 14\%$ in order to have met the criteria of 90% reliability for the recent decade.

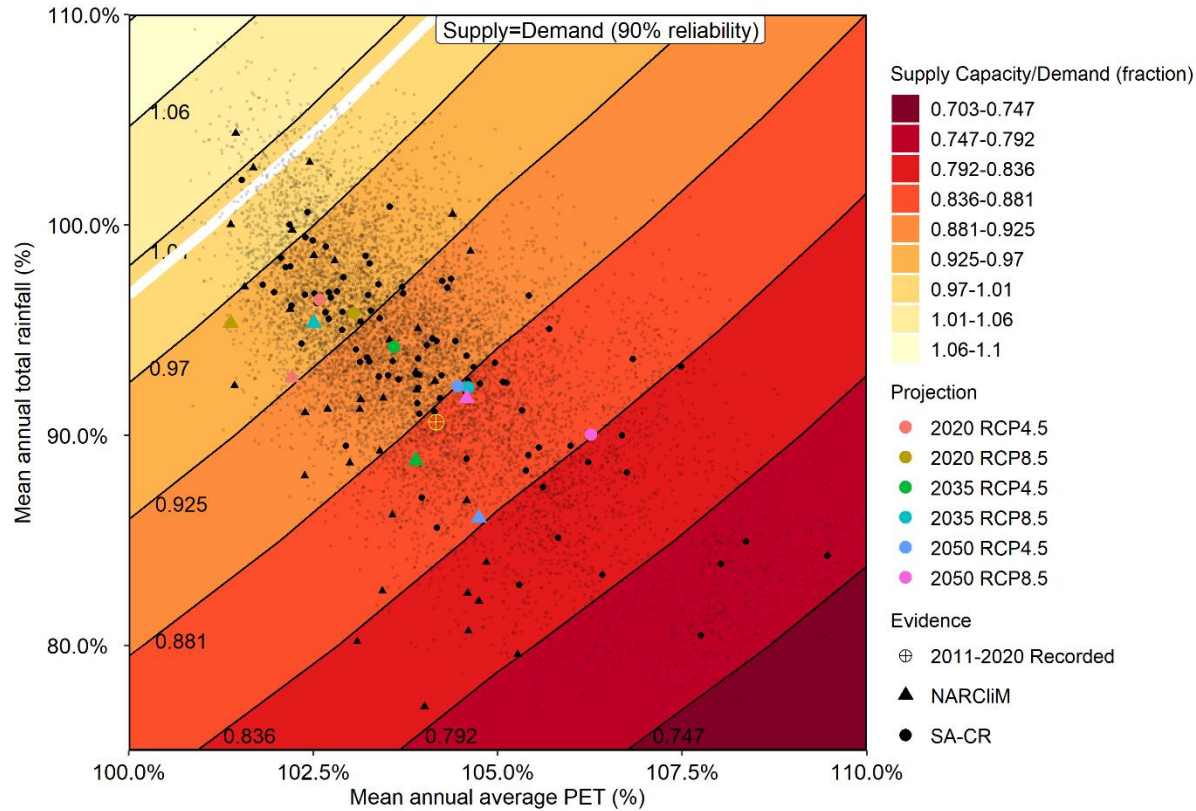


Figure 74. Ratio of supply on demand that corresponds to a 90% reliability using the process-based model in Stella for the Barossa PWRA. The white threshold line indicates the climate scenarios where supply is equal to demand.

All the previous plots focused on presenting information based on 30 year averages. Figure 75 shows the time series of demand (process-based model with error term) and supply (surface water, groundwater and external sources) from the system dynamics model. It can be seen that the demand changes from one year to the next as observed from the process-based model results, which gives confidence that the Stella model is representing this range well. The demand as well as the number of years with unmet demand is larger for the decreased rainfall and increased PET climate scenario, which is as expected.

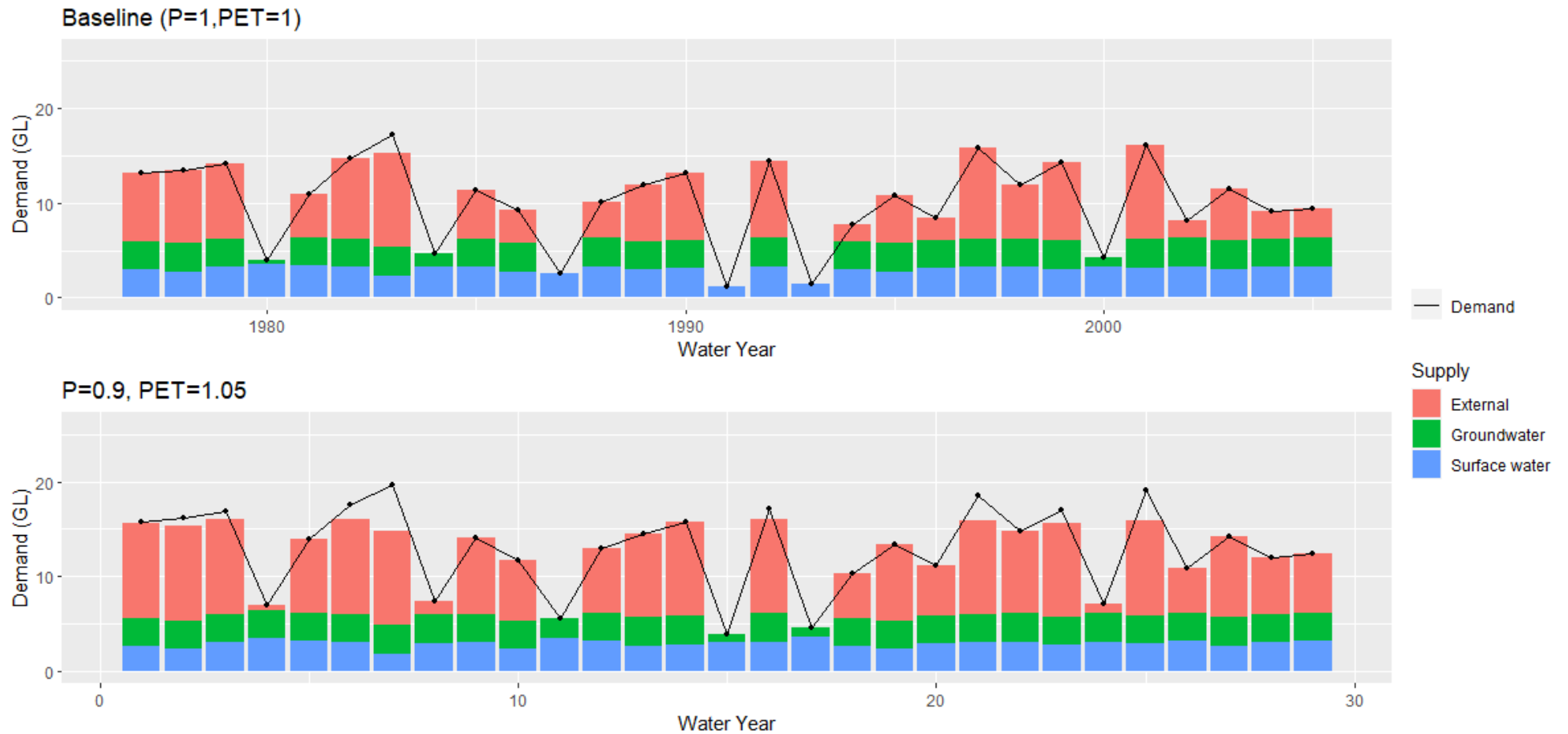


Figure 75. Time series of Stella supply and demand for the baseline case (PET=1, P=1) and a moderate climate change scenario (P=0.9, PET=1.05) for the Barossa PWRA.

In summary, the regression model produces much smaller and less variable demand than expected based on understanding that the system is experiencing severe water stress. Given the assumptions underpinning the regression model, use of the demand regression for analysis of the delineations and future pathways runs the risk of greatly underestimating demand, and thereby producing unreasonably low unmet demand for current and future scenarios. Therefore, for the remaining two delineations and for each of the future pathways, only the FAO-56 DCC model results (with a stochastic error term) will be used.

6.1.2 Barossa Valley

The Barossa Valley delineation shows a similar unmet demand to the Barossa PWRA, as shown in Figure 76. For the recent decade climate scenario, around 30% of years also have unmet demand, although the average volume of unmet demand in these years is higher. The average unmet demand in years with unmet demand for the 2050 average projections is around 4GL.

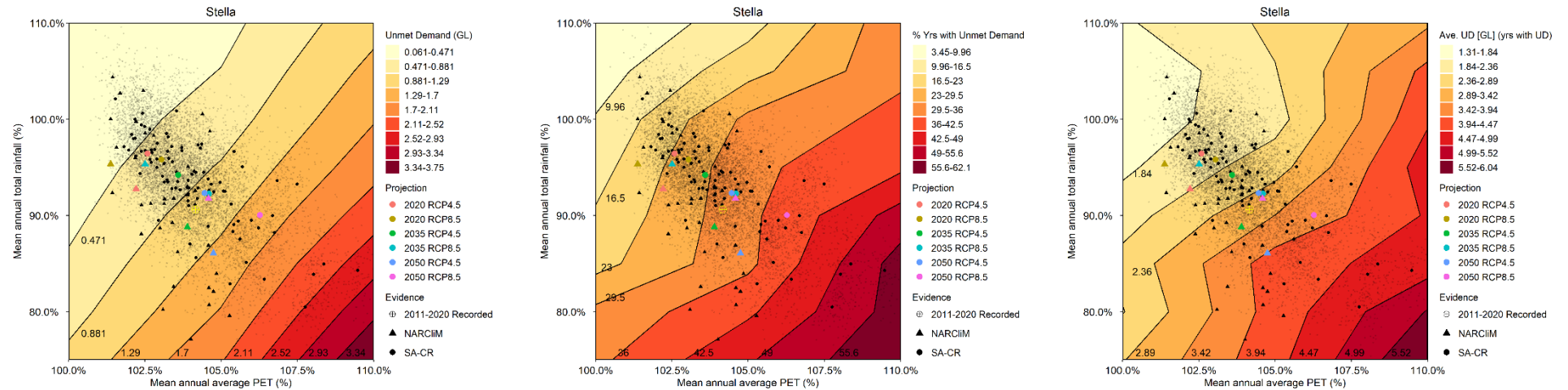


Figure 76. Unmet demand from process-based model in Stella for the Barossa Valley. Left to right: Average unmet demand [GL], percentage of years with unmet demand and average unmet demand in years with unmet demand [GL].

The ratio of supply and demand that corresponds to 90% reliability is represented in Figure 77. Given the high demand as well as unmet demand, it seems reasonable that the ratio of supply to demand at the 90% threshold is only achieved under a relatively small set of increasing rainfall projections.

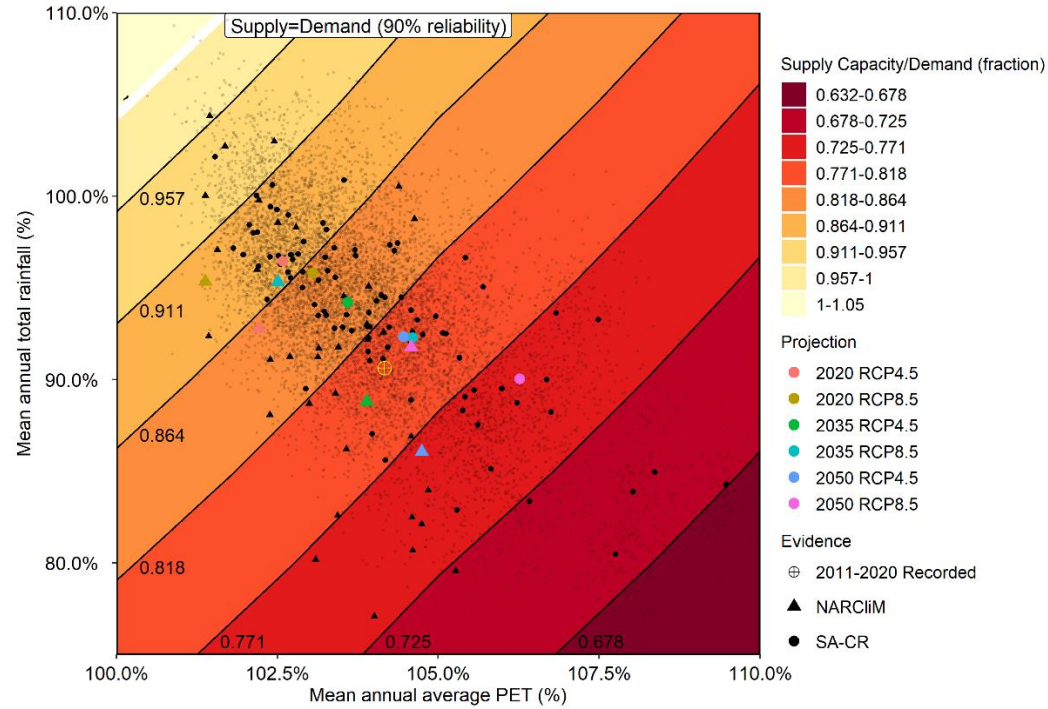


Figure 77. Ratio of supply on demand that corresponds to 90% reliability using the process-based model in Stella for the Barossa Valley. The white threshold line indicates the climate scenarios where supply is equal to demand.

The quantile-quantile plots of the process-based model results and regression in Stella can be seen in Appendix E. The time series plots in Figure 78 once again show the year-to-year variability expected from the process-based demand model. These results show that supply capacity in the Barossa Valley is even more limited by supply than in the Barossa PWRA.



Figure 78. Time series of Stella supply and demand for the baseline case (PET=1, P=1) and a moderate climate change scenario (P=0.9, PET=1.05) for the Barossa Valley.

6.1.3 Eden Valley

The unmet demand plots for the Eden Valley are shown below in Figure 79. Approximately 50% of years experience unmet demand under conditions experienced in the recent decade, which is much greater than the other two delineations. This is likely due to the lack of external supply in the Eden Valley. As all supply comes from groundwater and surface water, and surface water is variable based on climate, years with high demand are much more likely to cause unmet demand, especially due to the increased range of demand given by the SARDI model. The larger unmet demand seems reasonable, given that the region has no significant

external supply and has been struggling to meet demand in recent years without this external supply. The average volume of unmet demand in years with unmet demand is around 0.8GL for the recent decade and is around 1 GL for the the 2050 average projections.

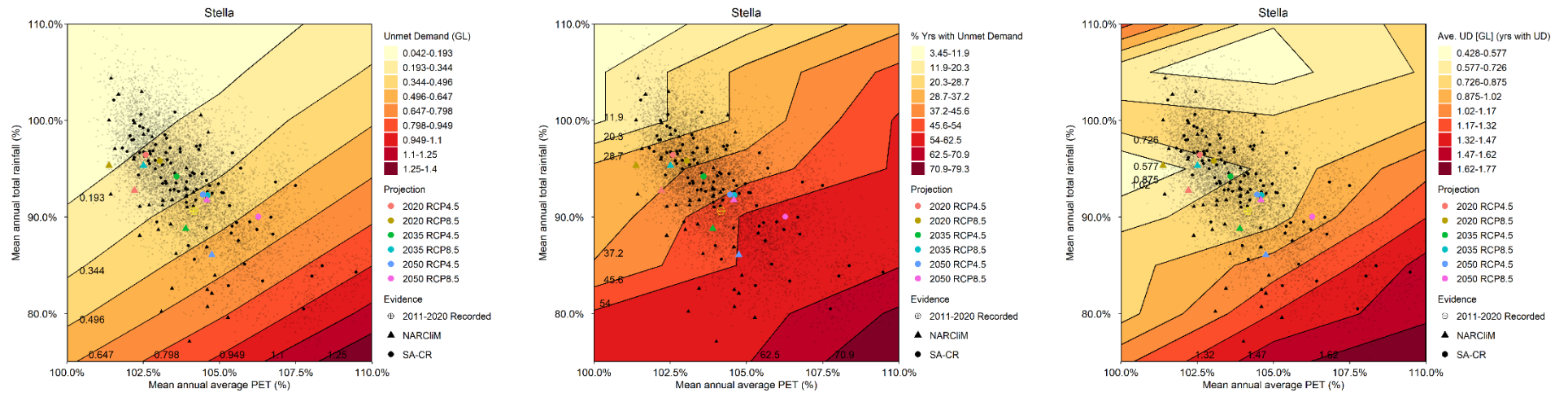


Figure 79. Unmet demand from process-based model in Stella for the Eden Valley. Left to right: Average unmet demand [GL], percentage of years with unmet demand and average unmet demand in years with unmet demand [GL].

The supply on demand plot (Figure 80) shows similar results to the unmet demand plot, with supply equal to demand only for the largest rainfall and lowest PET scenario.

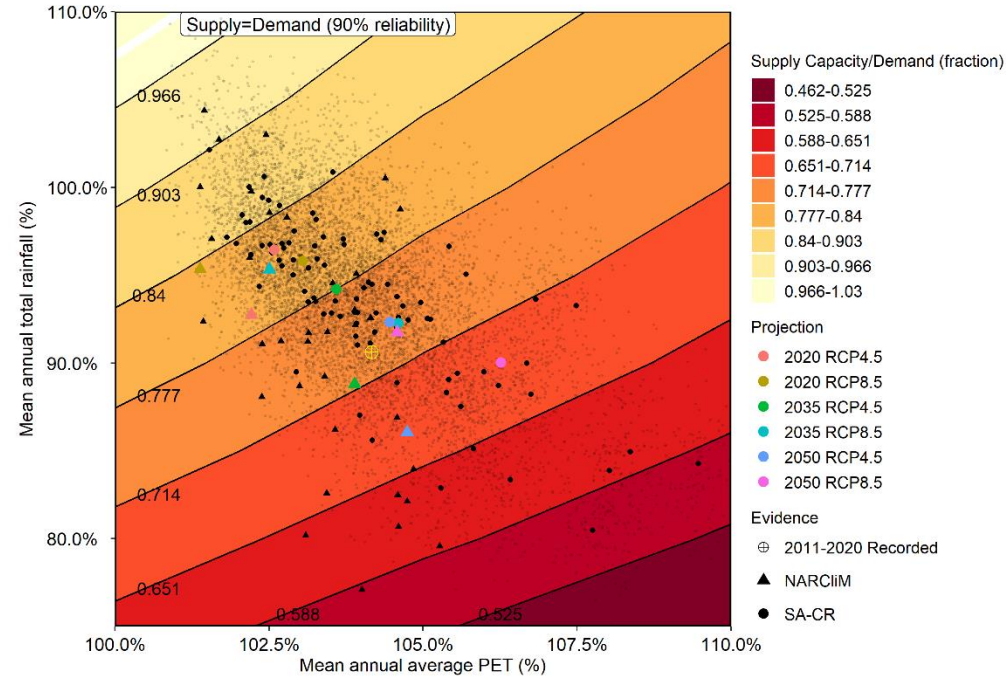


Figure 80. Ratio of supply on demand that corresponds to 90% reliability using the process-based model in Stella for the Eden Valley. The white threshold line indicates the climate scenarios where supply is equal to demand.

Quantile-quantile plots for the process-based model results and regression in Stella can be seen in Appendix E. The time series plots for the Eden Valley can be seen in Figure 81. Demand is variable as expected from the process-based model, and it can be seen that supply is also much more variable as licensed surface water extraction makes up a significant portion of the water balance, and is variable based on climate conditions.

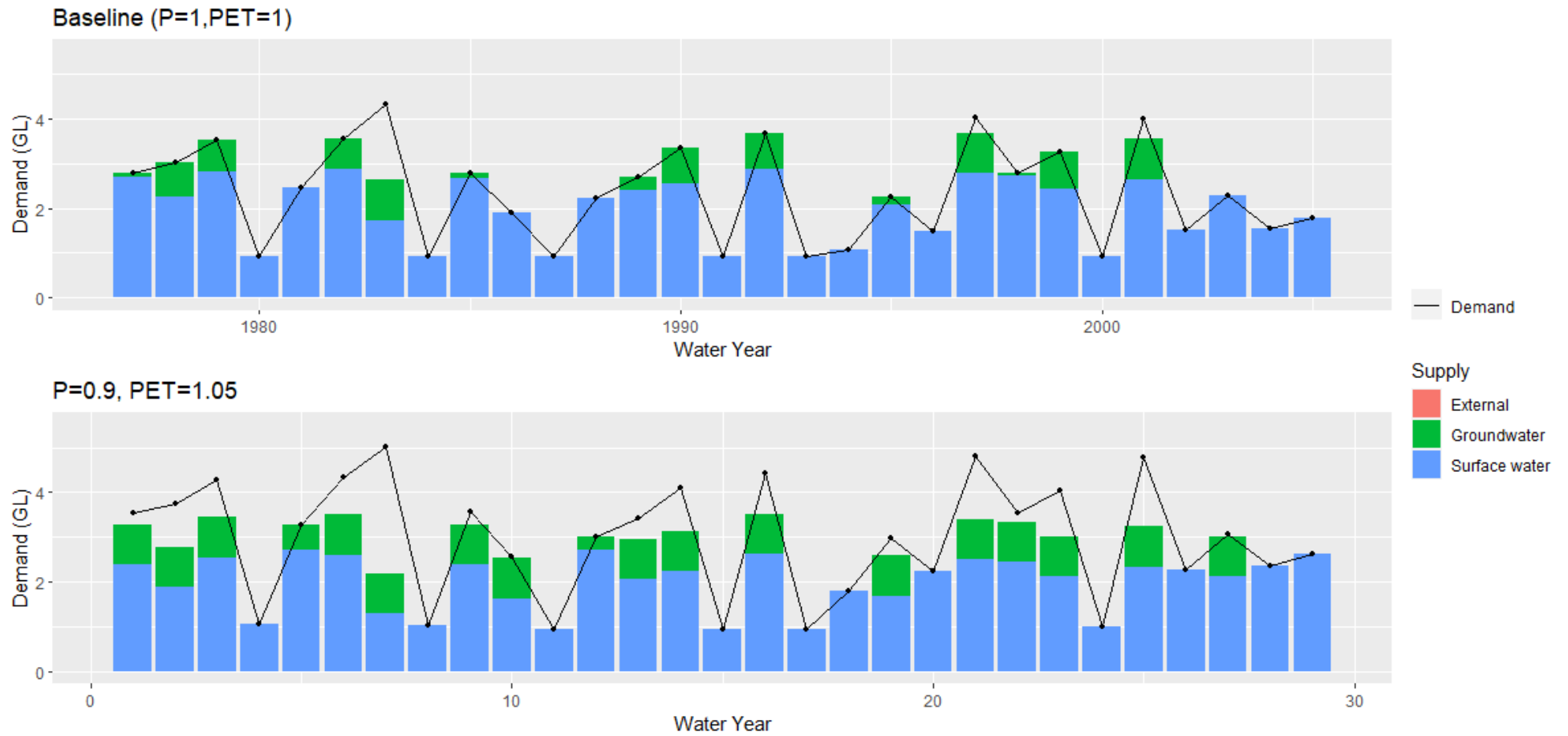


Figure 81. Time series of Stella supply and demand for the baseline case (PET=1, P=1) and a moderate climate change scenario (P=0.9, PET=1.05) for the Eden Valley.

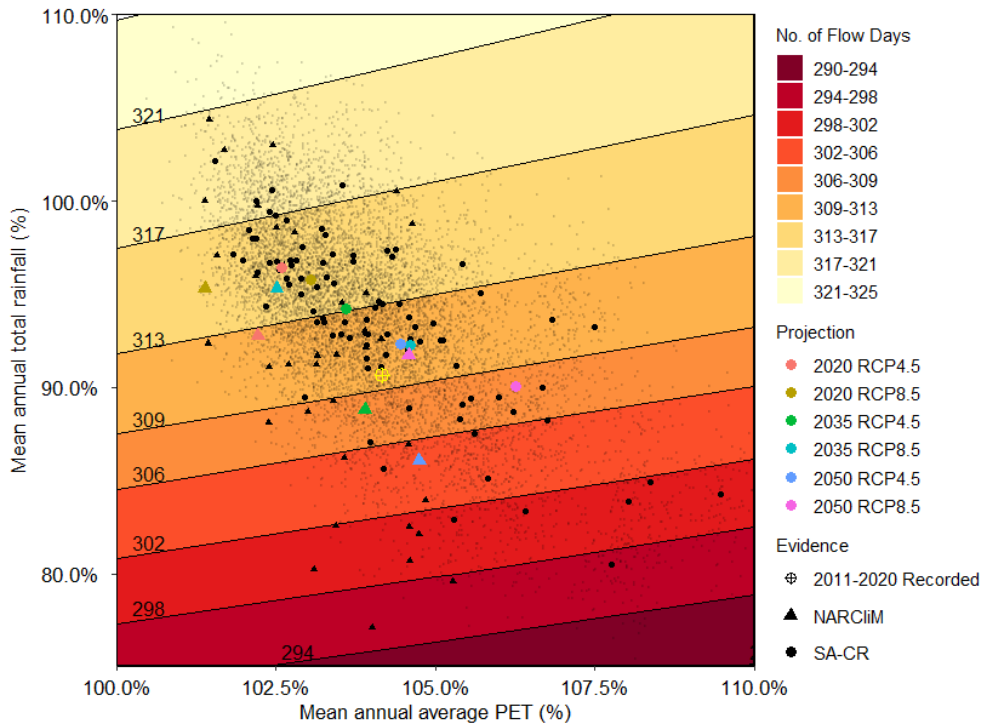


Figure 83. The performance space of the absolute change in the number of flowing days for the Barossa Valley Gorge Zone from simple scaling from Source results.

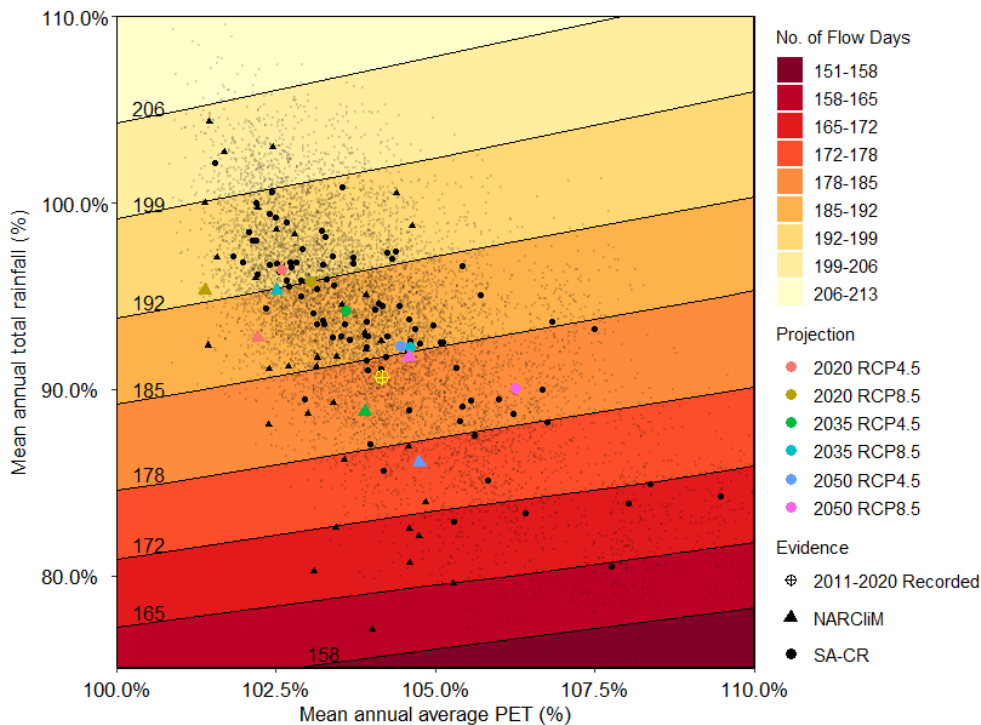


Figure 84. The performance space of the absolute change in the number of flowing days for the Upper Flaxman Valley Zone from simple scaling from eWater Source results.

6.2.2 Days over threshold flow

Each of the project zones has an associated threshold flow rate which indicates the volume of flow required to generate a flow depth of 12cm. This flow depth is considered a minimum flow depth for multiple ecological functions. The threshold flow value for the Barossa Valley Gorge is 0.374ML/day (Jones-Gill and Savadamuthu, 2014, p.57) The change in this metric is presented below in Figure 85. For the Upper Flaxman

Valley outlet the threshold flow value is 0.804ML/day. The change in this metric is presented below in Figure 86. These results again show much greater sensitivity for Upper Flaxman Valley, with number of days over threshold for that location varying from approximately 100 days under baseline climate conditions, down to about 55 days under more severe conditions. In contrast, sensitivity for the Barossa Valley Gorge is relatively low for this metric.

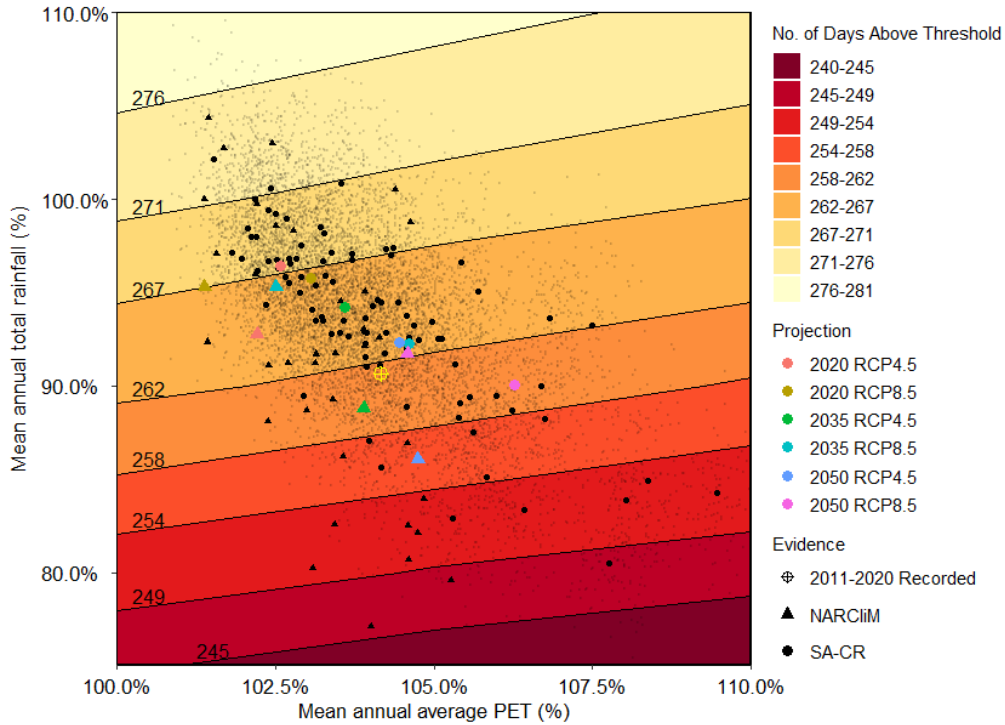


Figure 85. The performance space of the absolute change in the number of days over threshold flow for the Barossa Valley Gorge Zone from simple scaling from Source results.

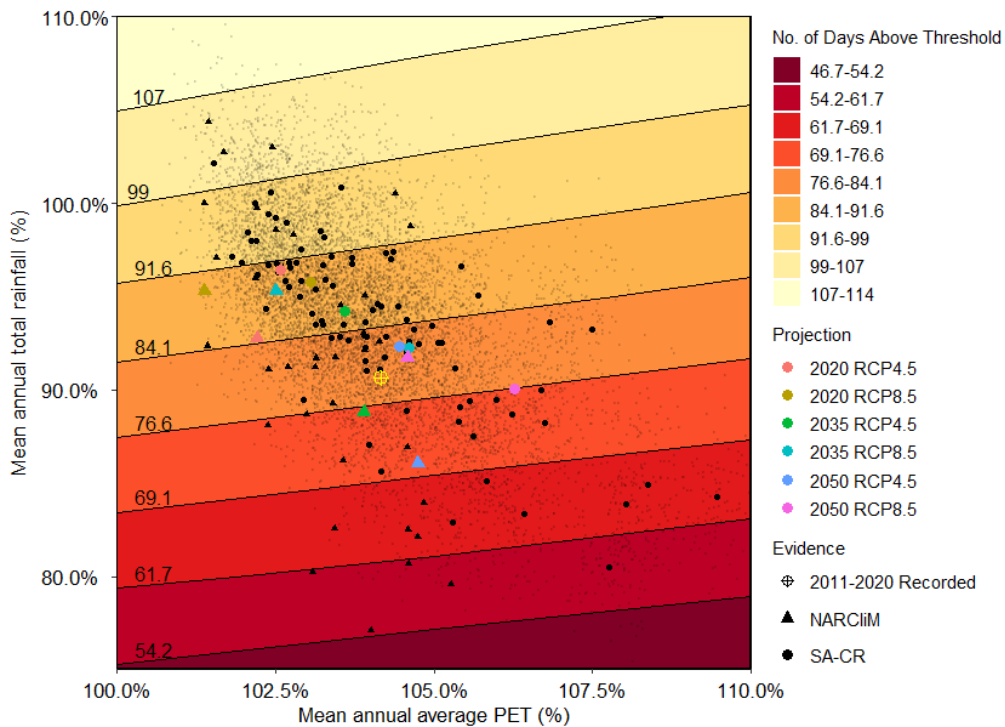


Figure 86. The performance space of the absolute change in the number of days over threshold flow for the Upper Flaxman Valley Zone from simple scaling from Source results.

6.2.3 Medium flow days

The medium flow days are defined as the number of days over the 50th percentile of daily flows, where flow is defined as greater than 0.05ML/day. The 50th percentile of daily flows for the Barossa Valley Gorge is 9.13 ML/day and the change in number of days larger than the 50th percentile value is given in Figure 87. The 50th percentile of daily flows for the Upper Flaxman Valley is 0.828 ML/day, and the change in number of days larger than the 50th percentile value is given in Figure 88. Interestingly, unlike the preceding results, the sensitivities for the Barossa Valley Gorge and Upper Flaxman Valley are more similar, with both locations showing a decrease in the order of 50 days between baseline climate conditions and a severe climate change scenario.

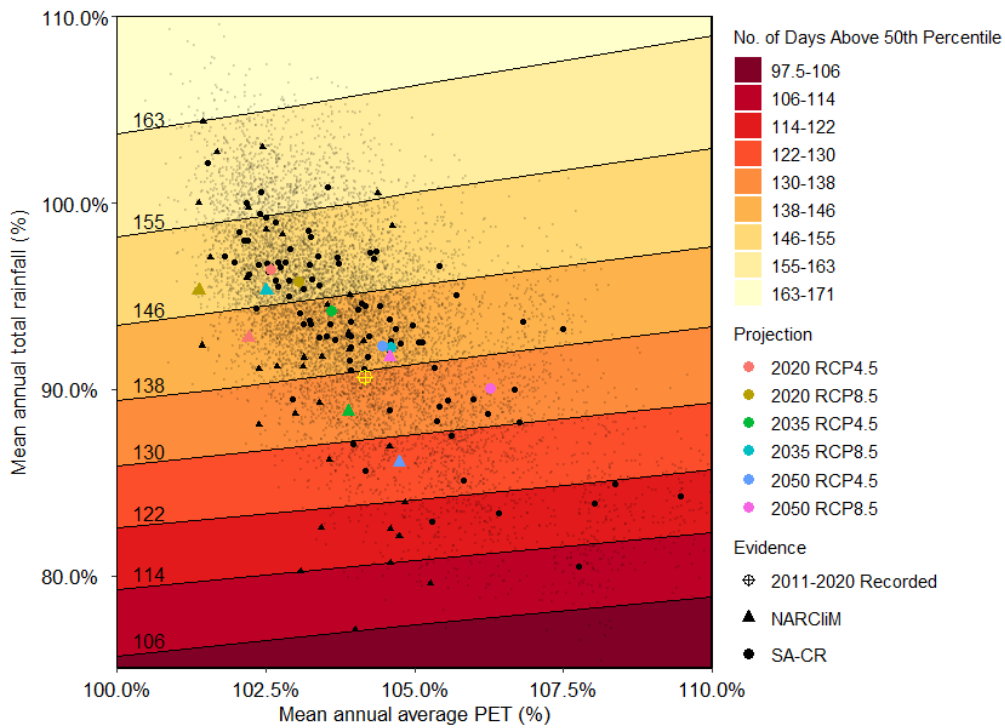


Figure 87. The performance space of the absolute change in the number of days over the 50th percentile daily flow for the Barossa Valley Gorge Zone from simple scaling from Source results.

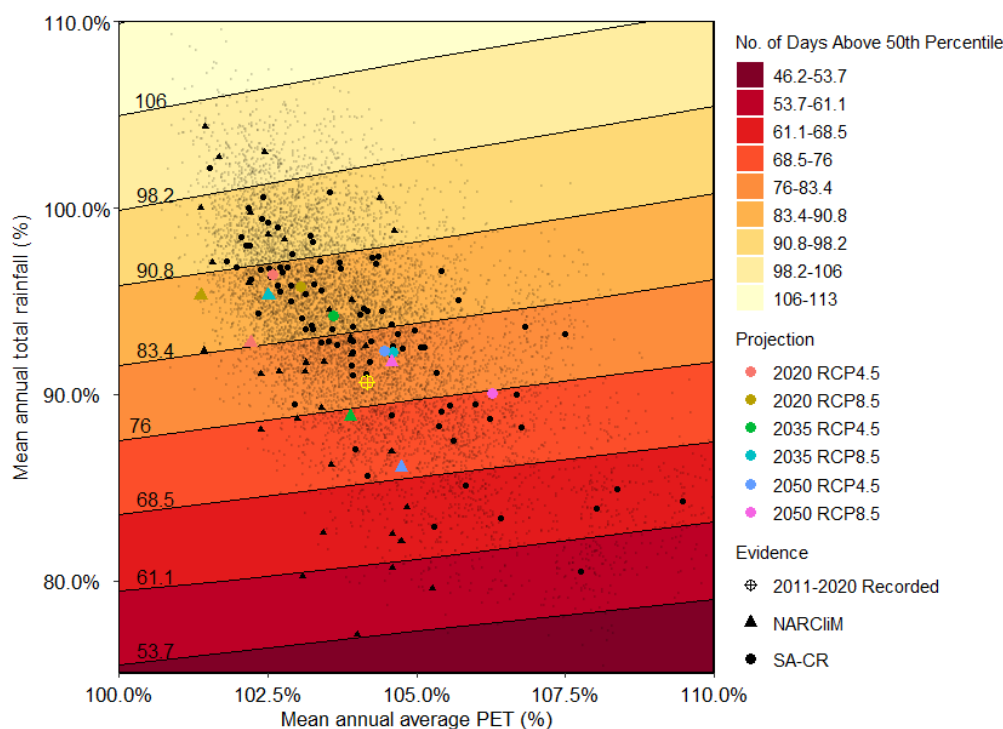


Figure 88. The performance space of the absolute change in the number of days over the 50th percentile daily flow for the Upper Flaxman Valley Zone from simple scaling from Source results.

6.2.4 Summary of ecological metrics

The preceding results showed varying degrees of sensitivity associated with climatic changes, with greater sensitivity for Upper Flaxman Valley compared with Barossa Valley Gorge. However, caution is required in interpreting the results. All metrics focus heavily on relatively low flows, in streams that are at least somewhat ephemeral. Moreover, significant groundwater-surface water interaction is known to exist in this region, with different parts of the stream network representing losing or gaining conditions. A core assumption of this modelling is that the future is reflective of historical conditions, which is not appropriate by design in a climate stress test. Finally, baseflow is likely to vary depending on factors such as recharge (which varies significantly with annual rainfall) and extraction rates (which will vary depending on assumed human behaviour); neither are explicitly included in the eWater Source model, and both will significantly alter the performance of the low flow metrics.

As a result of these uncertainties, further investigation is warranted in terms of likely responses of ecological flow metrics to a range of plausible climate scenarios and management options, that explicitly recognises issues associated with groundwater and surface water interactions.

6.3 Summary of Current System Dynamics

Table 20 summarises the water security and environmental flow metrics presented above for four time periods, corresponding to the recent decade (2011-2020), the 1976-2005 baseline, and a mid-range and high climate change scenario for 2050. These metrics are summarised for the driest year and average over the considered time period.

Table 20. Summary of water security and environmental flow metrics for four time periods: the baseline (1976-2005), the past decade (2011-2021), a 2050 mid-range climate projection (baseline perturbed by P=0.94 and PET=1.035), and a 2050 climate change stress test (baseline perturbed by P=0.8 and PET=1.075). Data for the driest year and average over time period are represented.

	Baseline* 1976-2005			Past Decade** 2011-2020			2050 mid-range climate change (Rainfall = 94%, PET = 103.5%)			2050 climate change stress test (Rainfall = 80%, PET = 107.5)		
	Eden Valley	Barossa Valley	Barossa	Eden Valley	Barossa Valley	Barossa	Eden Valley	Barossa Valley	Barossa	Eden Valley	Barossa Valley	Barossa
Average Over Period												
Groundwater use (GL/year)	0.28	1.7	1.98	0.908	2.10	3.01	0.45	1.8	2.25	0.66	2	2.66
Surface water use (GL/year)	2	1.6	3.6	1.98	1.57	3.55	2	1.7	3.7	1.8	1.6	3.4
Imported water (GL/year)	0	7	7	0.08	12.5	12.6	0	8.7	8.7	0	11.1	11.1
Total Use (GL/year)	2.22	10.3	12.6	2.97	16.2	19.1	2.43	12.3	14.7	2.44	14.5	16.9
Demand (GL/year)	2.3	10.5	12.8	2.82	13.2	16.0	2.7	13	15.7	3.4	17	20.4
Shortfall (GL/year) [§]	0.085	0.16	0.245	0.62	2.8	3.42	0.27	0.72	0.99	0.96	2.5	3.46
Number of days above threshold flow a year (Upper Flaxman)			200			Not modelle d			191			164
Driest Year[†]												
Groundwater use (GL/year)	0.9	2.1	3	1.25	3.73	4.97	0.9	2.1	3	0.9	2.1	3
Surface water use (GL/year)	1.7	1.5	3.2	1.84	1.42	3.26	1.5	1.4	2.9	0.78	0.92	1.7
Imported water (GL/year)	0	14.5	14.5	0.09	14.7	14.7	0	14.5	14.5	0	14.5	14.5
Total Use (GL/year)	2.6	18	20.6	3.18	19.8	23.0	2.4	18.3	20.7	1.7	17.8	19.5
Demand (GL/year)	4.3	21	25.3	4.87	27.9	32.8	4.8	24	28.8	5.5	28	33.5
Shortfall (GL/year) [§]	1.7	3	4.7	1.70	8.12	9.82	2.4	5.7	8.1	3.8	10.2	14
Number of days above threshold flow a year (Upper Flaxman) [#]			218			Not modelle d			206			174
Shortfall (% of years with shortfall)	10	10		40	30		38	28		66	50	

*As modelled using recorded climate data

**Water use data as recorded and modelled demand (from process-based model)

[§]Shortfall for each year in the recent decade was estimated as the predicted demand from the process-based model, minus the observed use.

[†]Driest baseline year was 1982/83; driest year in recent decade was 2018/19.

[#]Not necessarily the year with the smallest number of days over the threshold flow in the simulation.

From Table 20 it can be seen that the recorded total water use, both on average and in the driest year for the past decade (2011-2020), is more than the modelled total water use for the two climate change scenarios. This is partially due to water source limitation: groundwater use is capped at the average of the use in last decade [2011-2020] within the Stella model, and surface water availability decreases with worsening climate. However, it can also be seen that the water demand for the moderate climate change scenario is less than for the recent decade. Although the recent decade has similar average climate (compared to the baseline average) as the moderate climate change scenario, it is also possible that the model is underestimating demand.

This is a limitation of the simple scaling method used, as patterns of variability outside that of the baseline period are not considered. As the last decade was relatively dry, there are a greater percentage of extremely dry years in this period than in the baseline. Therefore, on average, the recent decade has a slightly higher water demand than the mid-range climate change scenario. This limitation is likely to be a particular issue when comparing extremes between the different scenarios.

7 Alternative System Configurations

7.1 Description of potential adaptive pathways

In order to address water security and sustain or enhance ecological outcomes, different pathways for system configuration and operation are explored. In addition to the ‘business as usual’ case (Section 6), four adaptive pathways are proposed, each with different drivers and including different system ‘interventions’ in order to achieve the pathway vision. The four identified pathways are:

- (1) enhanced infrastructure investment combined with existing behaviours;
- (2) sustainable economic growth including clean and green production systems;
- (3) healthy waterways through investment; and
- (4) maximum water availability and focus on production outcomes.

These pathways, and changes to current system configuration necessary to implement them, are detailed in Table 21, with a summary of each pathway provided in the following text.

Table 21: Summary of system pathways and changes to system configuration required to meet each pathway.

Element	Business as usual	1. Enhanced infrastructure investment and existing behaviour	2. Sustainable economic growth - clean and green production	3. Healthy waterways through investment	4. Maximum water availability and production outcomes
<i>Surface water</i>	Current dams in landscape	Current dams in landscape	High* impactful dams altered (2.685/0.73/1.96 GL capacity removed)	High & medium** impactful dams altered (3.664/1.21/2.46 GL capacity removed)	Current dams in landscape
<i>Groundwater extractions</i>	Groundwater use stable (3.0/2.1/0.9GL [†] [average over 2011-2020])	Groundwater use stable (3.0/2.1/0.9GL [†] [average over 2011-2020])	Groundwater use stable (3.0/2.1/0.9GL [†] [average over 2011-2020])	Groundwater use halved (supported by recycled water) (1.5/1.05/0.45GL [†] [average over 2011-2020])	Groundwater use grows to allocation (supported by micro-desalination and/or mixing with imported water) (8.0/6.3/3.7GL [†] [average over 2011-2020])

<i>Storages</i>	No recycled water storage	Existing dams & optimal regional recycled storages	High* impactful dams converted to covered off-storages (2.685/0.73/1.96 GL capacity [†])	High & medium** impactful dams converted to off-stream storages (3.664/1.21/2.46 GL capacity [†])	Existing dams & Optimal regional recycled storages
<i>Pipeline</i>	Existing BIL imported supply No Eden imported	Recycled water – Barossa (8 GL) Raw water to meet future Eden Valley demands (3.5 GL)	Recycled water – Barossa (8 GL) Raw water to meet future Eden Valley demands (3.5 GL)	Recycled water – Barossa and Eden valleys (up to 8 GL combined)	Recycled Water – Barossa (16 GL) Raw water to meet expanded future Eden Valley demands (5 GL)
<i>Investment in agricultural technology</i>	Existing	Existing	High-end efficiency investments	High-end efficiency investments	High-end efficiency investments
<i>Investments in sustainable agriculture practices[‡]</i>	Existing practice	Existing practice	Existing practice	Maximise soil carbon and water holding capacity	Existing practice
<i>Vineyard area</i>	Existing (87.2/117.5/23.2km ^{2†})	Existing (87.2/117.5/23.2km ^{2†})	Existing (87.2/117.5/23.2km ^{2†})	Existing (87.2/117.5/23.2km ^{2†})	Existing (87.2/117.5/23.2km ^{2†})
<i>Variety</i>	Existing	Existing	Existing	More drought tolerant (7% decrease in demand)	Existing
<i>Stock Watering</i>	Existing (no deficit) (1.1/0.89/0.93 GL [†])	Existing (no deficit) (1.1/0.89/0.93 GL [†])	Existing (no deficit) (1.1/0.89/0.93 GL [†])	Existing (no deficit) (1.1/0.89/0.93 GL [†])	Expanded x 50% (2.2/1.8/1.9 GL [†])

* High impactful dams are represented by Source model Sce1B. In total, 20 dams in the Barossa PWRA are deemed high impact (2.685 GL capacity removed)

** High and medium impactful dams are represented by Source model Sce1C. In total, 40 dams in the Barossa PWRA are deemed high and medium impact (3.664 GL capacity removed)

[†] Numbers refer to Barossa PWRA, Barossa Valley and Eden Valley, respectively

[‡] This includes carbon sequestration and other soil improvement practices, but excludes any technologies devoted primarily to achieving water use efficiency

7.1.1 Business as usual

In this scenario, no additional actions are taken to adapt to a changing climate, either at a farm or regional scale, nor are any specific actions taken to enhance the local environmental outcomes. Imported water continues to be available from the River Murray in the Barossa Valley but it is limited by both supply and infrastructure constraints based on infrastructure configuration as of 2020. In the Eden Valley, imported water is not available except for a small contribution from the SA Water off-peak system.

7.1.2 Pathway 1: Infrastructure investment supports existing industry and behaviours

The current area of vineyards and irrigation behaviours (including yield targets) are maintained at levels consistent with the recent decade. An additional 8 GL/year is imported for the Barossa Valley, and an addition 3.5 GL/year is imported to the Eden Valley. Existing dams continue to be utilised to capture surface water and balancing storage tanks are utilised to supply imported water. No specific actions are taken to enhance the local environmental outcomes and as a result environmental condition and overall amenity continue to degrade.

7.1.3 Pathway 2: Sustainable economic growth - clean and green production

The current area of vineyards and irrigation behaviours (including yield targets) are maintained at levels consistent with the recent decade. Volumes imported are sufficient to meet viticultural demand in future hot and dry years (2050s) for the current planted area. 20 strategically located medium and large dams,

predominantly in the upper reaches of the Barossa Valley, are converted to off-stream storages with an aggregate volume of 2.685 GL. Finally, water use efficiency on-farm is maximised, through precision irrigation and application of emerging agricultural technologies.

7.1.4 Pathway 3: Healthy waterways and soils

The current area of vineyards and irrigation behaviours (including yield targets) are maintained at levels consistent with the recent decade. 40 strategically located medium and large dams, predominantly in the upper reaches of the Barossa Valley, are converted to off-stream storages, with an aggregate volume of 3.664 GL. Viticultural outcomes are optimised through drought tolerant varieties, precision irrigation, mulching, increased soil carbon, canopy cooling and adoption of emerging agricultural technologies.

7.1.5 Pathway 4: Maximum water availability and expansion

This pathway focuses on maximising water availability, and in particular comprises an additional 16 GL to meet viticultural demand in Barossa Valley, and an addition 5 GL/year to the Eden Valley. Existing dams continue to be utilised to capture surface water, and groundwater consumption increases significantly up to the current amounts available under license. Water use efficiency on-farm is nevertheless maximised, through precision irrigation and application of emerging agricultural technologies. No specific actions are taken to enhance the local environmental outcomes.

The below sections focus on exploring the pathways in two delineations, the Barossa Valley and Eden Valley.

7.2 Pathway 1: Enhanced infrastructure investment

Pathway 1 is largely equivalent to 'business as usual', with the only difference being that additional imported water capacity is added to the external supply node within the model. This extra supply has a capacity of 8 GL and 3.5 GL for the Barossa Valley and Eden Valley respectively.

7.2.1 Water Security Metrics

7.2.1.1 *Barossa Valley*

Figure 89 (left column) shows the unmet demand for the Barossa Valley when implementing Pathway 1, while the right column shows the change in the three water security metrics compared to the current system (business as usual pathway). It can be seen that the additional external supply has a large impact on the system's ability to meet demand, reducing the number of years where demand is not met to zero for the 'recent decade' climate scenario. This increases up to 15% or more of years with unmet demand for the most extreme climate scenario, with an average unmet demand of 2GL in those years.

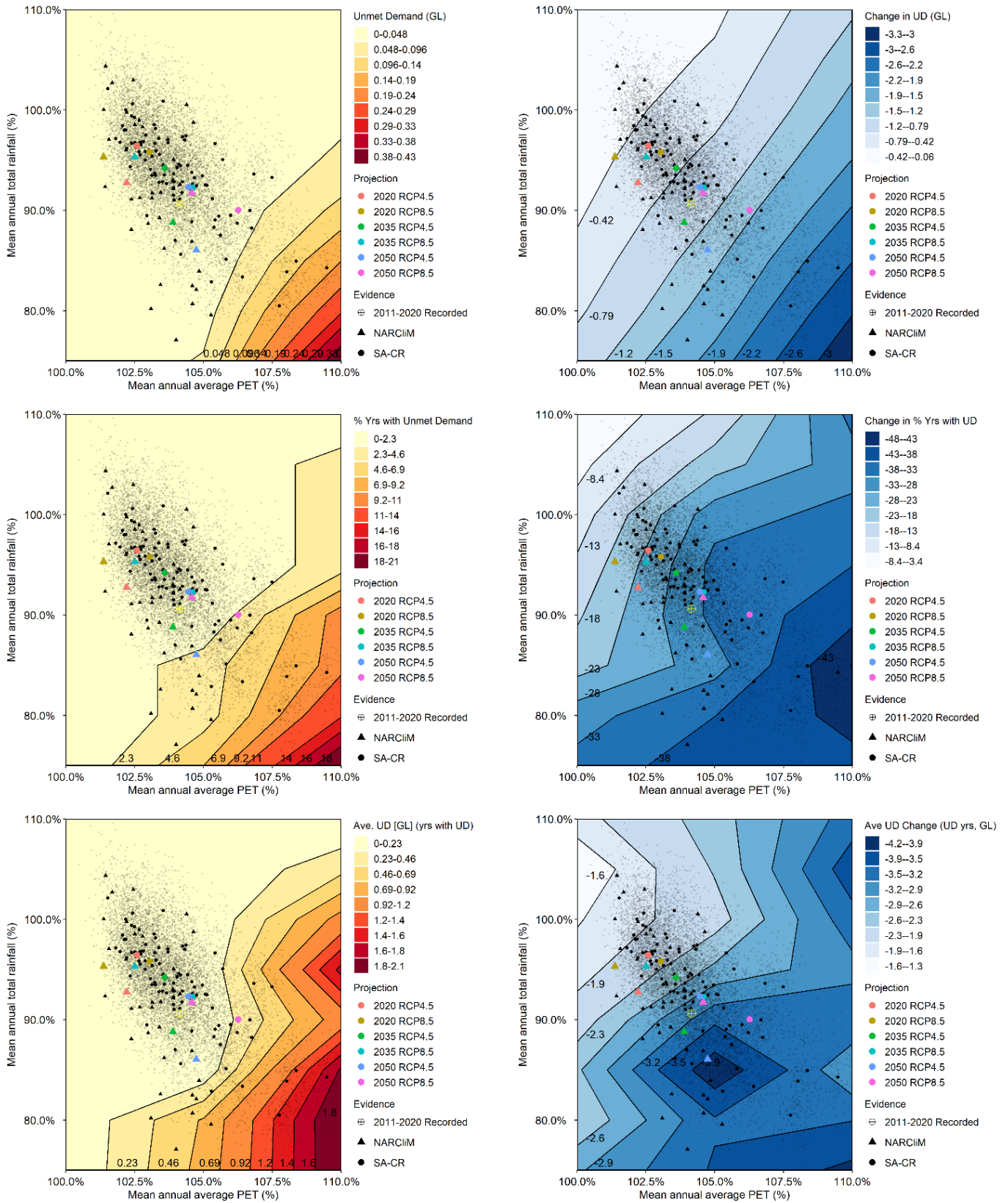


Figure 89. Left column - Unmet demand from process-based model in Stella for the Barossa Valley (Pathway 1). Top to bottom: Average unmet demand [GL], percentage of years with unmet demand, and average unmet demand in years with unmet demand [GL]. Right column - Difference between water security metrics in the left panel (Pathway 1) and the corresponding metrics for the current system (business as usual).

Figure 90 shows the ratio of supply to demand. It can be seen that for a 90% reliability, supply is meeting demand for most of the projections, and only for a few extreme projections is supply not equal to demand.

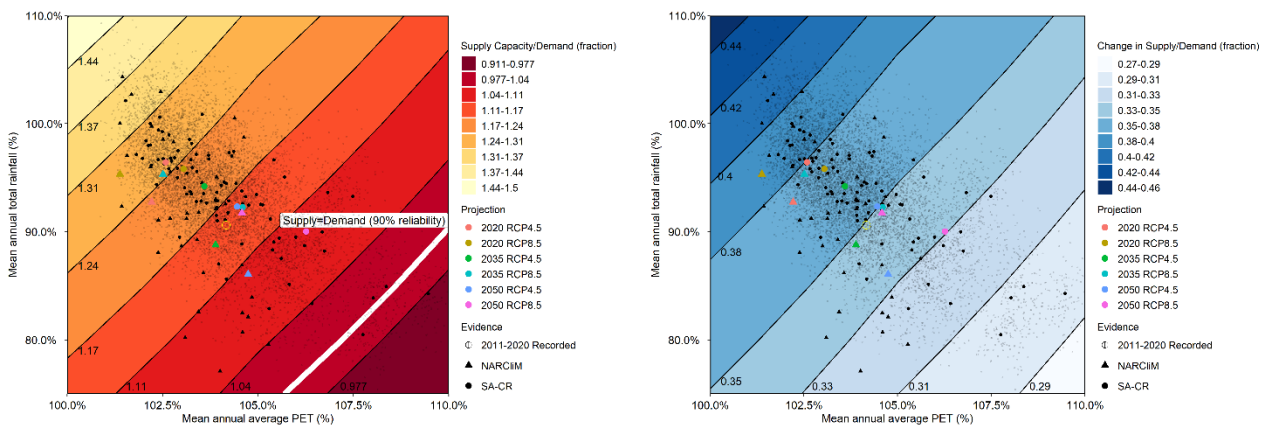


Figure 90. Left plot – Ratio of supply on demand that corresponds to 90% reliability using the process-based model in Stella for the Barossa Valley (Pathway 1). The white threshold line indicates the climate scenarios where supply is equal to demand. Right plot – the difference in the fraction of supply on demand between the current system (business as usual) and Pathway 1.

7.2.1.2 Eden Valley

The additional 3.5GL of external supply has a very significant impact on the ability to meet demand, which can be seen in Figure 91. This is expected, as the additional water volume is more than the current average annual use from native sources. This additional demand gives no unmet demand for the recent decade climate projection, up to 3.5% of years with unmet demand with an average annual unmet demand of 1.1GL for the most extreme climate scenario.

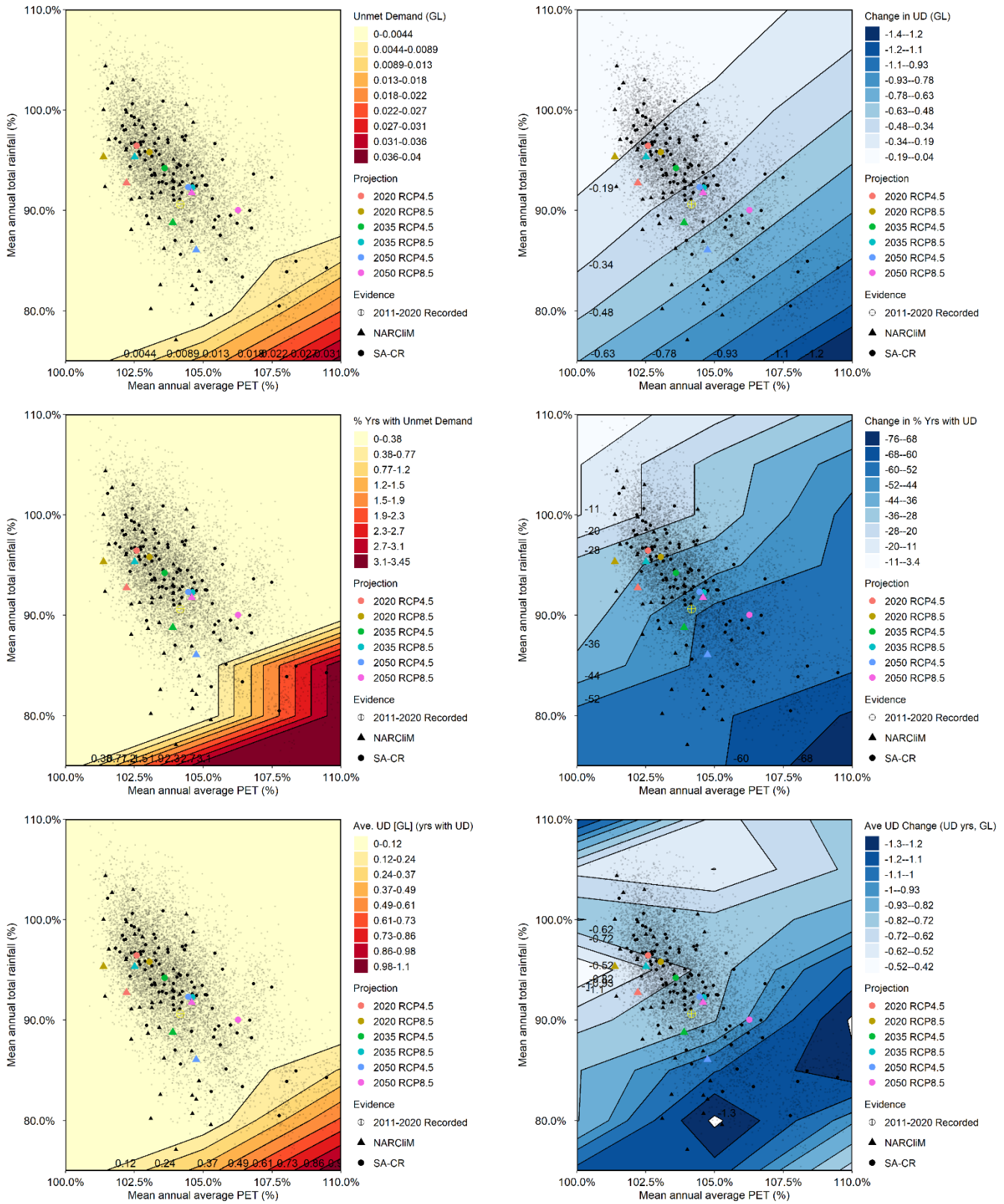


Figure 91. Left column - Unmet demand from process-based model in Stella for the Eden Valley (Pathway 1). Top to bottom: Average unmet demand [GL], percentage of years with unmet demand, and average unmet demand in years with unmet demand [GL]. Right column – Difference between water security metrics in the left panel (Pathway 1) and the corresponding metrics for the current system (business as usual).

It can also be seen that from Figure 92, for a 90% reliability, supply is greater than demand for all the perturbed climate scenarios.

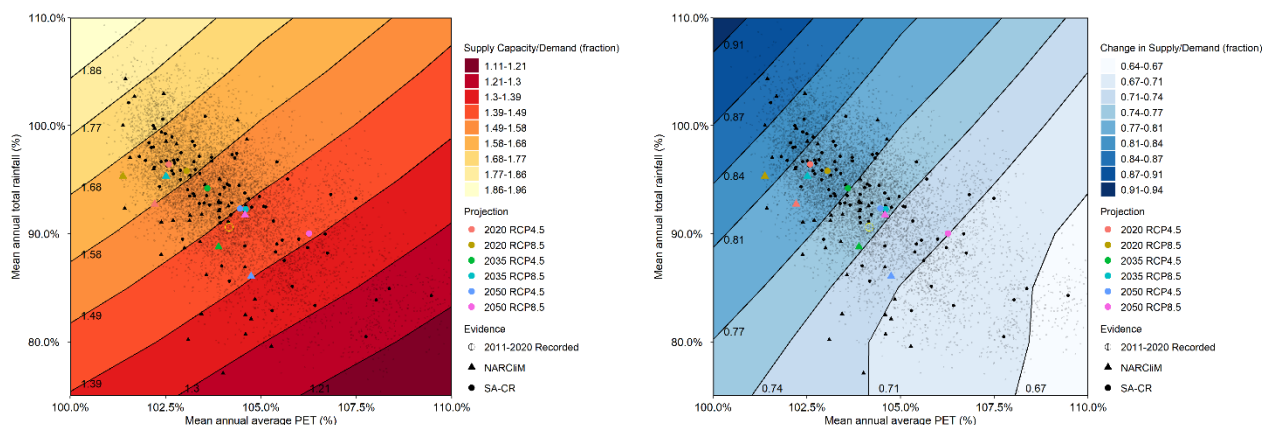


Figure 92. Left plot – Ratio of supply on demand that corresponds to 90% reliability using the process-based model in Stella for the Eden Valley (Pathway 1). The white threshold line indicates the climate scenarios where supply is equal to demand. Right plot – the difference in the fraction of supply on demand between the current system (business as usual) and Pathway 1.

In both valleys, the addition of external supply makes a significant impact on the ability to meet demand. A 90% reliability of supply can be achieved for almost all future climate scenarios in the Barossa Valley, and can be achieved for all scenarios in the Eden Valley. In both valleys, significant potential exists for increasing planted vineyard area and/or changing other elements of production (e.g. increasing yields per hectare) and still achieve a 90% reliability value under moderate levels of climate change.

7.2.2 Environmental Flow Metrics

As demand patterns from native sources (surface water and groundwater) were assumed to remain unchanged for this pathway, there is no change in the environmental flow metrics from the baseline case for either the Barossa Valley Gorge or Upper Flaxman Zones. See Figure 83 to Figure 88 for these metrics (Section 6.2).

7.3 Pathway 2: Sustainable economic growth

Pathway 2 involves increasing external demand while simultaneously converting high impact farm dams into an off-line balancing storage. For this pathway, an updated Source model with reduced farm dams was run (Barossa_Sce1B_his_V5.0.3.rsprj). This was implemented in the Stella model with new regression relationships for the components from Source, as well as addition of a balancing store which can hold the volume of the high impact dams that were taken off-line, and carry over additional external supply from wet to dry years.

The other feature of this pathway is the assumption that water use efficiency from adoption of precision agriculture technologies is implemented such that for any year drier than the baseline average (1976-2005), there is no change to water use efficiency, whereas under wetter-than average conditions water use efficiency change increased linearly from zero (average conditions) to up to 10% (wettest year in the baseline period). The water use efficiency benefits of precision irrigation technologies is capped at 10% for any perturbations that produce an annual rainfall greater than the wettest year in the baseline period. This modelling approach was based on anecdotal feedback that the capacity of agricultural technology to increase water use efficiency during dry years is likely to be limited.

7.3.1 Water Security Metrics

7.3.1.1 *Barossa Valley*

It can be seen from Figure 93 that taking the high impact dams offline and converting them to offline storages, as well as the introduction of precision irrigation technologies, further improves the number of years with unmet demand. Interestingly, although there are fewer years with unmet demand, the average unmet demand for years with unmet demand for the most extreme climate scenario is slightly higher at 2.1GL.

These results suggest that farm dams may be more effectively used as balancing stores for imported water from one year to the next, rather than as native surface water stores. However, there are several caveats to this conclusion: firstly, that anecdotal evidence suggests farm dams may currently already be used as balancing stores by individual growers, and that this is not included in current surface water modelling; and secondly, there are various balancing store configurations (e.g. seasonal balancing store versus interannual balancing store) and this study has not explored specific configurations in depth. This issue therefore warrants further investigation.

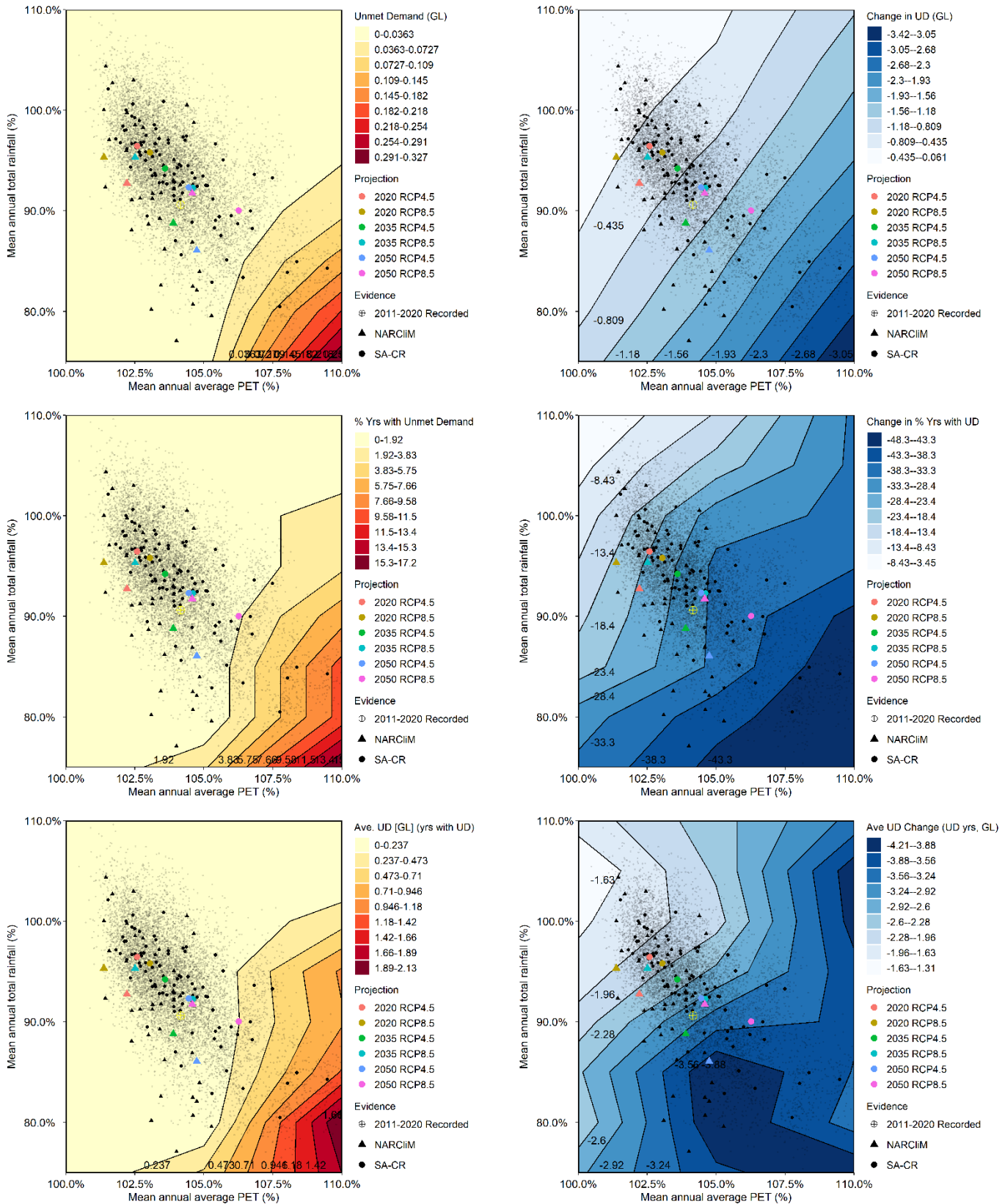


Figure 93. Left column - Unmet demand from process-based model in Stella for the Barossa Valley (Pathway 2). Top to bottom: Average unmet demand [GL], percentage of years with unmet demand, and average unmet demand in years with unmet demand [GL]. Right column – Difference between water security metrics in the left panel (Pathway 2) and the corresponding metrics for the current system (business as usual).

Figure 94 shows that for 90% reliability, supply exceeds demand for most climate scenarios.

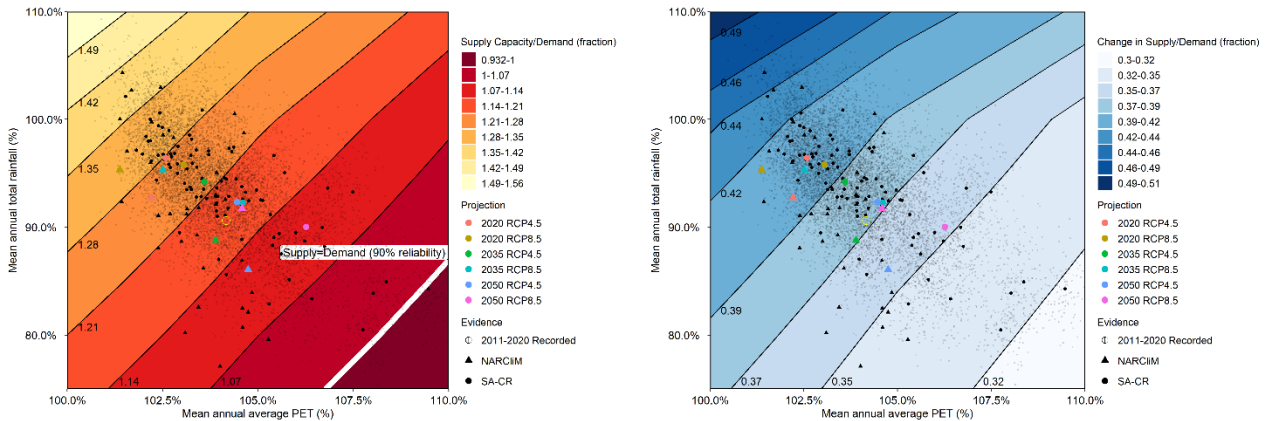


Figure 94. Left plot – Ratio of supply on demand that corresponds to 90% reliability using the process-based model in Stella for the Barossa Valley (Pathway 2). The white threshold line indicates the climate scenarios where supply is equal to demand. Right plot – the difference in the fraction of supply on demand between the current system (business as usual) and Pathway 2.

7.3.1.2 Eden Valley

Pathway 2 gives no unmet demand for the Eden Valley for any year in any climate scenario. From Figure 95 it can be seen that supply exceeds demand (for a 90% reliability) for all climate scenarios. As there is no unmet demand in this scenario, the supply also exceeds demand in all scenarios.

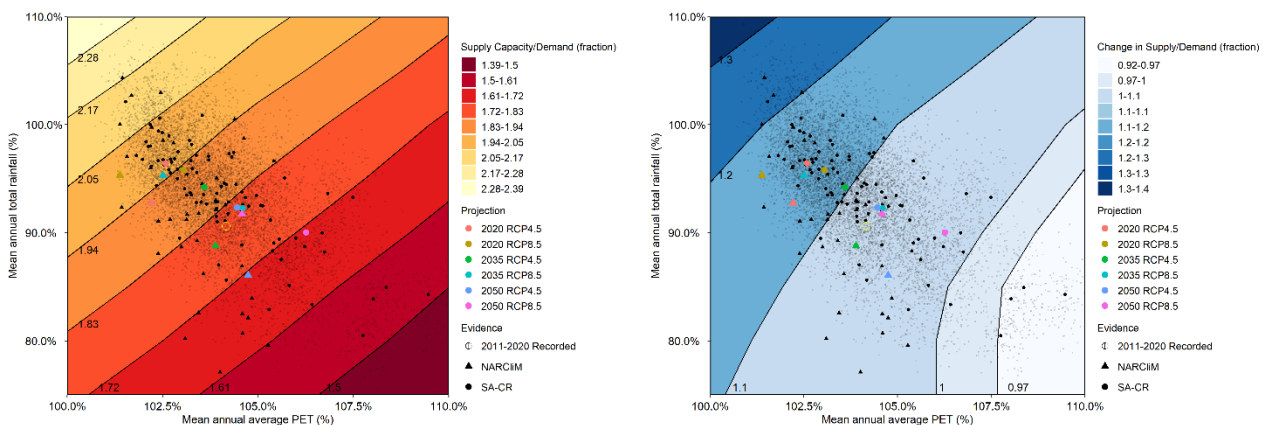


Figure 95 Left plot – Ratio of supply on demand that corresponds to 90% reliability using the process-based model in Stella for the Eden Valley (Pathway 2). The white threshold line indicates the climate scenarios where supply is equal to demand. Right plot – the difference in the fraction of supply on demand between the current system (business as usual) and Pathway 2.

7.3.2 Environmental Flow Metrics

The environmental flow metrics are positively affected by the removal of high impact dams. The following results are from outputs from the updated Scenario 1B Source model, for the outflows of the two locations of interest, the Barossa Valley Gorge and Upper Flaxman Valley zones.

7.3.2.1 Barossa Valley Gorge Zone

In comparison to the current system configuration, the removal of high impact dams has very little influence on the environmental flow metrics at the Barossa Valley Gorge zone outflow, as shown in Figure 96. Figure 96 shows the absolute value in days of the three metrics in the left column, while the right column shows the change in those metrics relative to the current system (business as usual pathway). In particular, it can be seen that in the first row of Figure 96, the number of flow days a year increases marginally between the current system and system with high impact dams removed. This increase is approximately one flowing day for all climate scenarios. The number of days a year above threshold flow can be seen in the second row of Figure 96. This increases by around two days for all climate projections between the current system and

Pathway 2 (second row, right panel). The number of flow days over medium flow a year is calculated based on the 50th percentile flow for the current system (9.13 ML/day) and can be seen in the third row of Figure 96. It can be seen from the right panel that this increase is roughly between two and three days above medium flow a year across the climate scenarios compared to the current system.

Based on these results, it is concluded that benefits of removal of high impact farm dams appear to be marginal at this location.

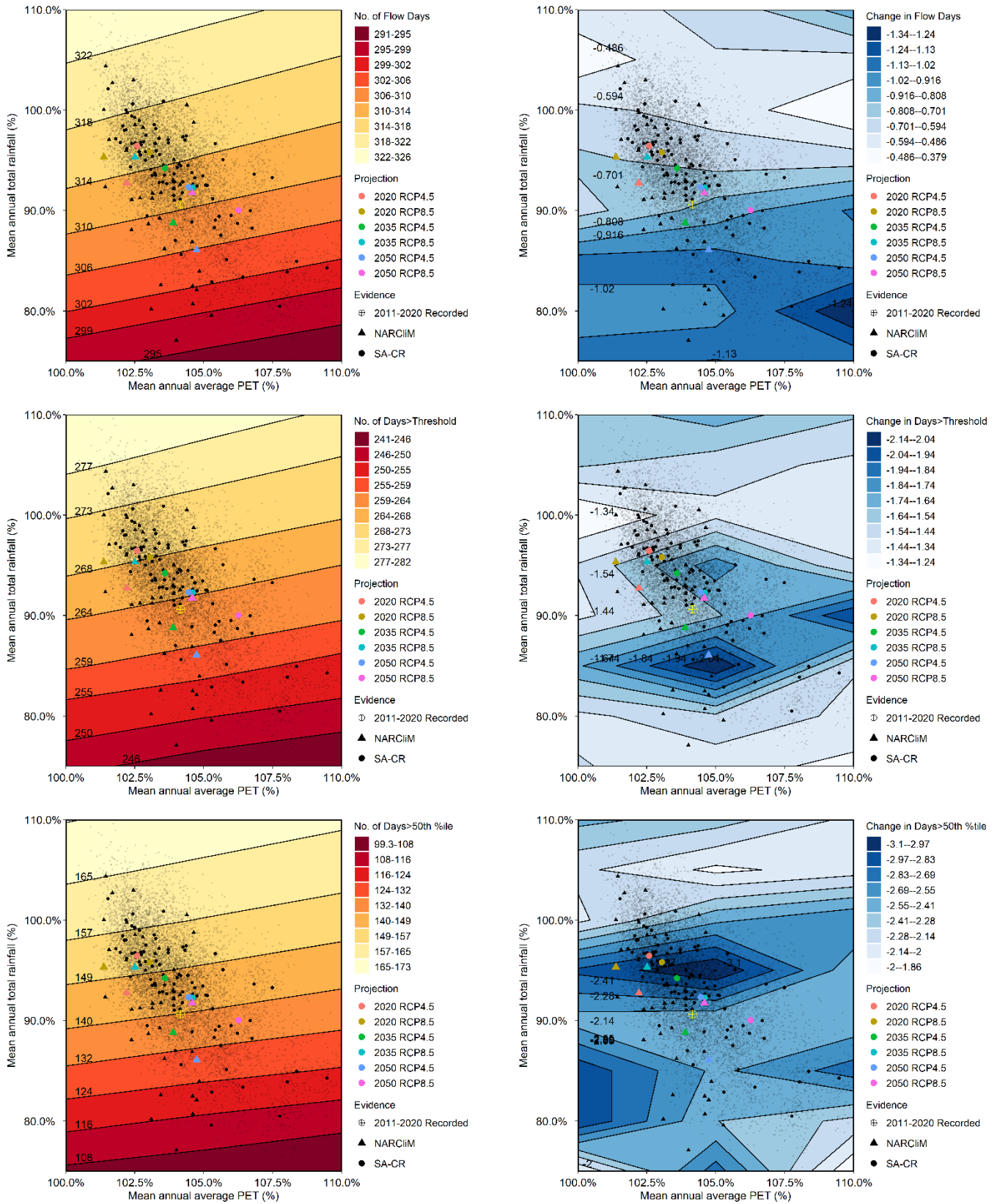


Figure 96. The performance spaces of environmental flow metrics for the Barossa Valley Gorge Zone from simple scaling from Source results (Pathway 2 – removal of high impact dams). Left column – Top to bottom: number of flow days; number of days above threshold flow; and the number of days over the 50th percentile flow (for the current system configuration this is 9.13 ML/day). Right column – Difference between environmental flow metrics in the left panel (Pathway 2) and the corresponding metrics for the current system (business as usual).

7.3.2.2 Upper Flaxman Valley Zone

There is a more significant change in the environmental flow metrics for the Upper Flaxman Valley than the Barossa Valley Gorge zone, which can be seen in Figure 97. Between the current system and Pathway 2, the increase in number of flow days a year ranges from 12 to 15 extra flowing days depending on the climate scenario (first row, right panel of Figure 97). From the second row of Figure 97 it can be seen that the number of days above threshold flow also increases, by around 10 days a year from the current system to Pathway 2. There is also around a 10 day a year increase in flows above the 50th percentile from the current system to Pathway 2 (third row, right panel of Figure 97).

Although there are significantly greater improvements in flows at the Upper Flaxman Zone outflow compared to the Barossa Valley Gorge Zone outflow, these improvements are still fairly small, especially considering the change in flow days projected by climate stressors. For example, in the first row of Figure 97, although there is up to 15 extra flow days a year due to the removal of high impact dams, the change from the baseline to a moderate climate change projection is around 13 less flow days, and to an extreme climate projection is around 40 fewer flow days. This suggests that while conversion of high-impact dams to off-line storages may yield environmental benefits, they are likely to require supplementation with other strategies (e.g. active environmental flow management and groundwater extraction limits) to achieve full stream restoration benefits.

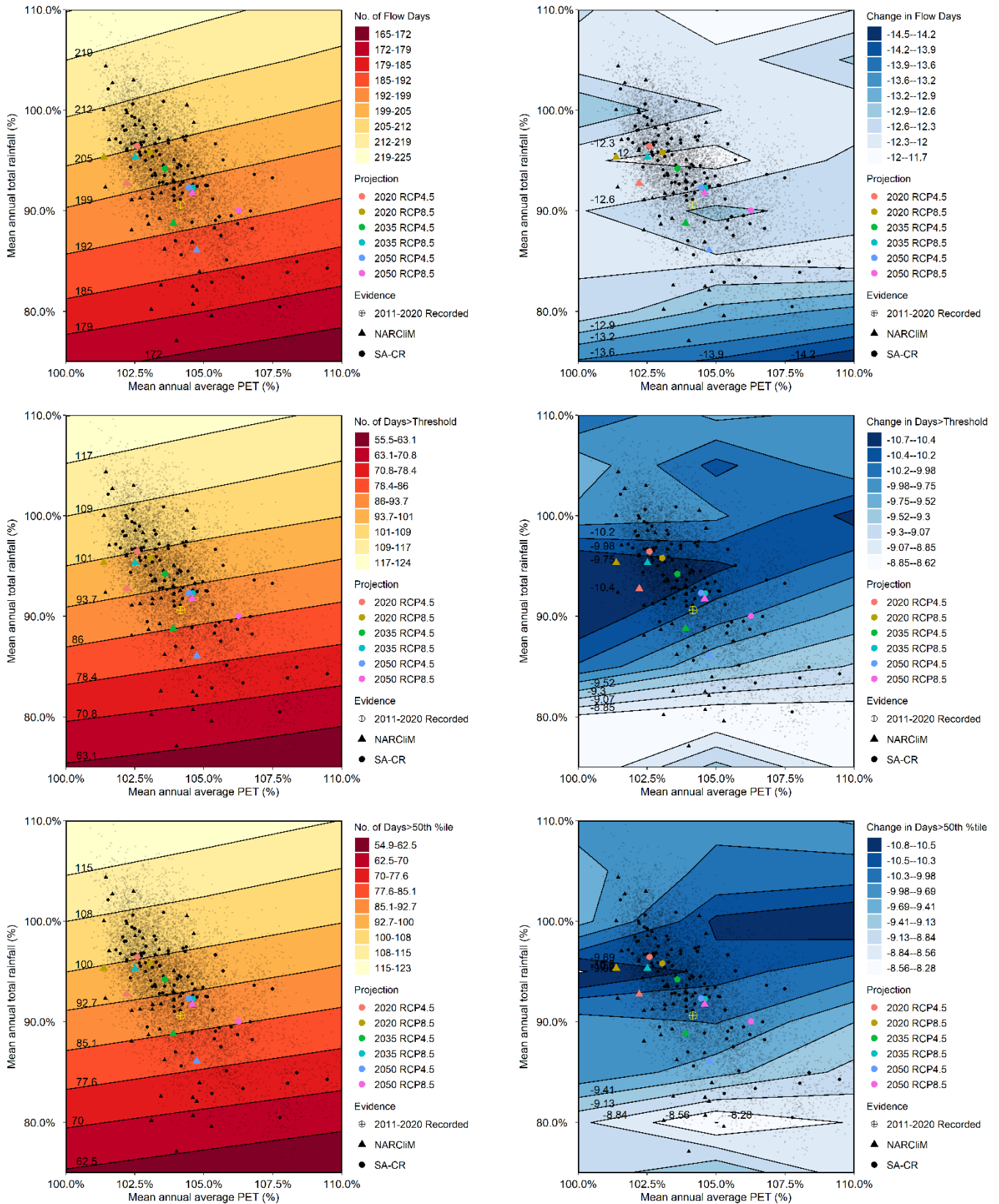


Figure 97. The performance spaces of environmental flow metrics for the Upper Flaxman Valley Zone from simple scaling from Source results (Pathway 2 – removal of high impact dams). Left column – Top to bottom: number of flow days; number of days above threshold flow; and the number of days over the 50th percentile flow (for the current system configuration this is 0.828ML/day). Right column – Difference between environmental flow metrics in the left panel (Pathway 2) and the corresponding metrics for the current system (business as usual).

7.4 Pathway 3: Healthy waterways through investment

As well as removal of high impact dams, Pathway 3 also involves removal of medium impact farm dams. For this pathway, an updated Source model with reduced farm dams was run (Barossa_Sce1C_his_V5.0.3.rsproj). This was implemented in the Stella model with new regression relationships for the components from Source, as well as addition of a balancing store. Pathway 3 also has additional external supply, which is 8GL between the two regions. This is divided 70/30 Barossa Valley/Eden Valley, giving 5.6 and 2.4GL additional external supply respectively to the two valleys.

Water use efficiency outcomes from precision agriculture technologies are implemented in the same way as for Pathway 2. There is also an additional 5% increase in demand efficiency through the use of more drought tolerant species. Groundwater abstraction in the region is halved in relation to the last decade average.

7.4.1 Water Security Metrics

7.4.1.1 *Barossa Valley*

It can be seen from Figure 98 that although the demand efficiency and offline storage capacity is increased compared to Pathway 2, the ability to meet water security metrics is negatively impacted by the reduction in pipeline size and the decrease in groundwater abstraction. Pathway 3 shows around 5% of years with demand unmet for the recent decade climate scenario, to around 23% of years with demand unmet for the most extreme climate scenario. This extreme climate scenario has an average unmet demand in those years of 3.5GL.

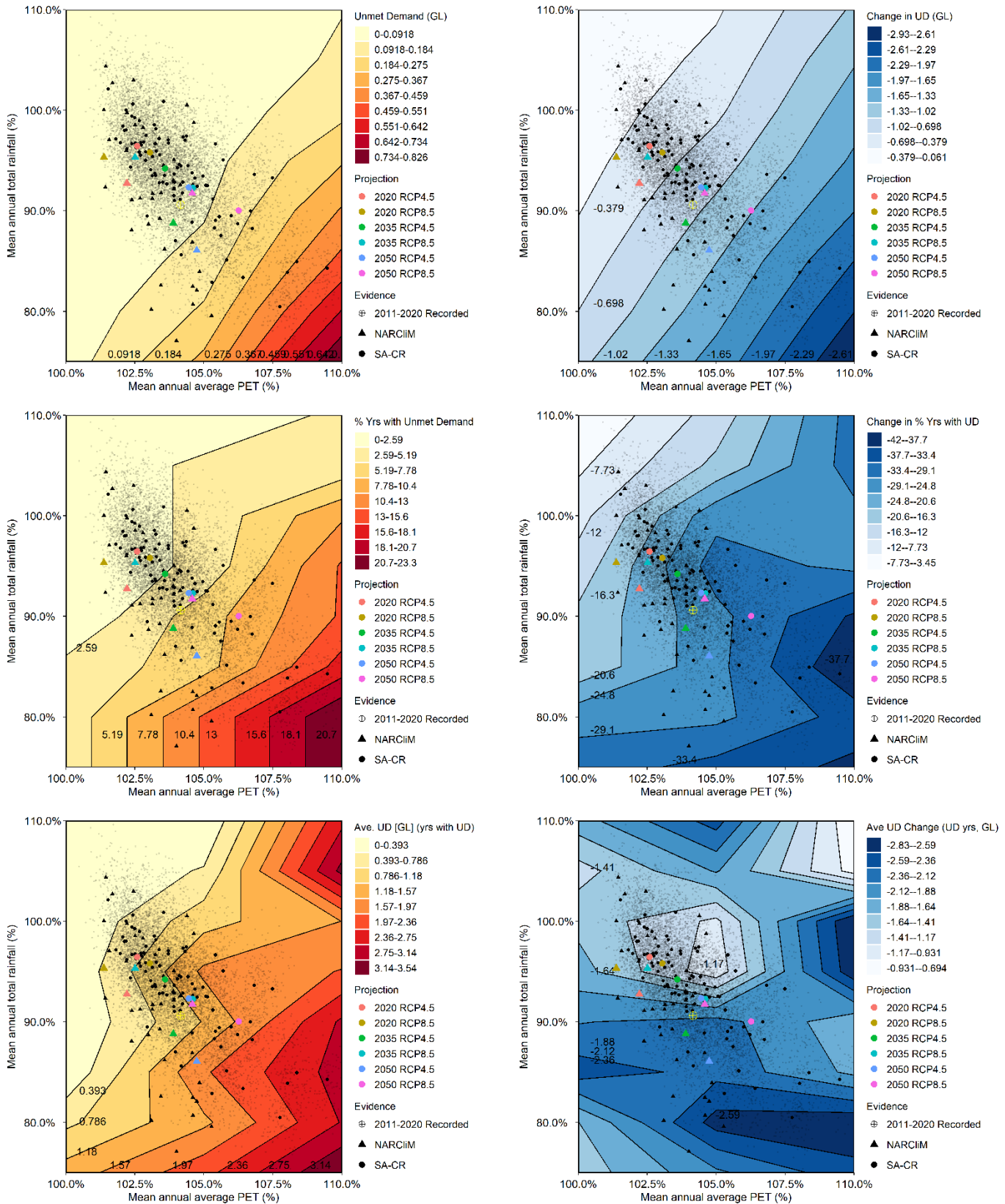


Figure 98. Unmet demand from process-based model in Stella for the Barossa Valley (Pathway 3). Top to bottom: Average unmet demand [GL], percentage of years with unmet demand, and average unmet demand in years with unmet demand [GL]. Right column – Difference between water security metrics in the left panel (Pathway 3) and the corresponding metrics for the current system (business as usual).

It can be seen that for a 90% reliability, demand exceeds supply for many of the 2050 projections, and is not met for a majority of the more severe climate scenarios.

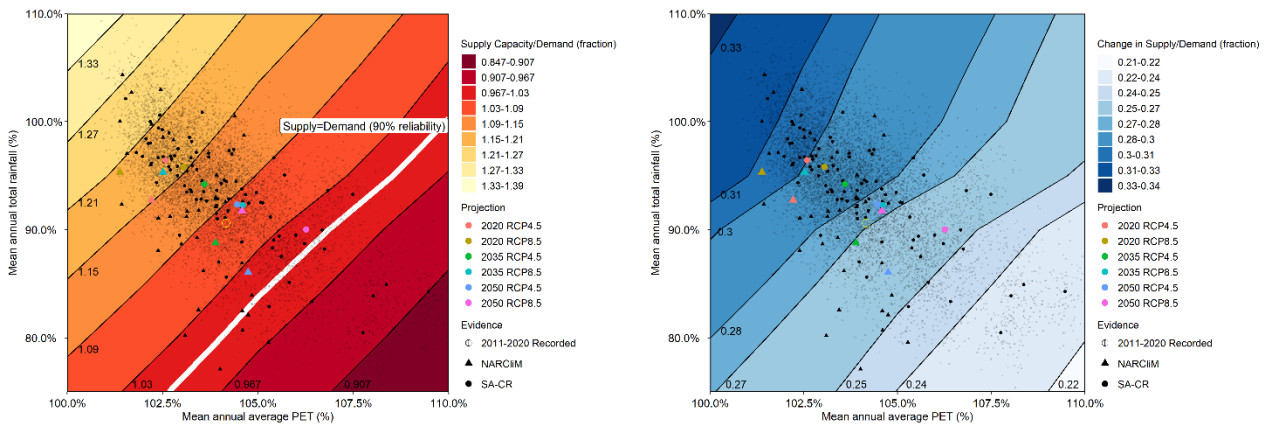


Figure 99. Left plot – Ratio of supply on demand that corresponds to 90% reliability using the process-based model in Stella for the Barossa Valley (Pathway 3). The white threshold line indicates the climate scenarios where supply is equal to demand. Right plot – the difference in the fraction of supply on demand between the current system (business as usual) and Pathway 3.

7.4.1.2 Eden Valley

The Eden Valley is also affected by the reduction in pipeline size and groundwater extraction, but still has a relatively small unmet demand, even for the most extreme climate scenario (Figure 100). The most extreme climate scenario shows around 0.82 GL of average unmet demand in the 3.3% of years where demand is not met.

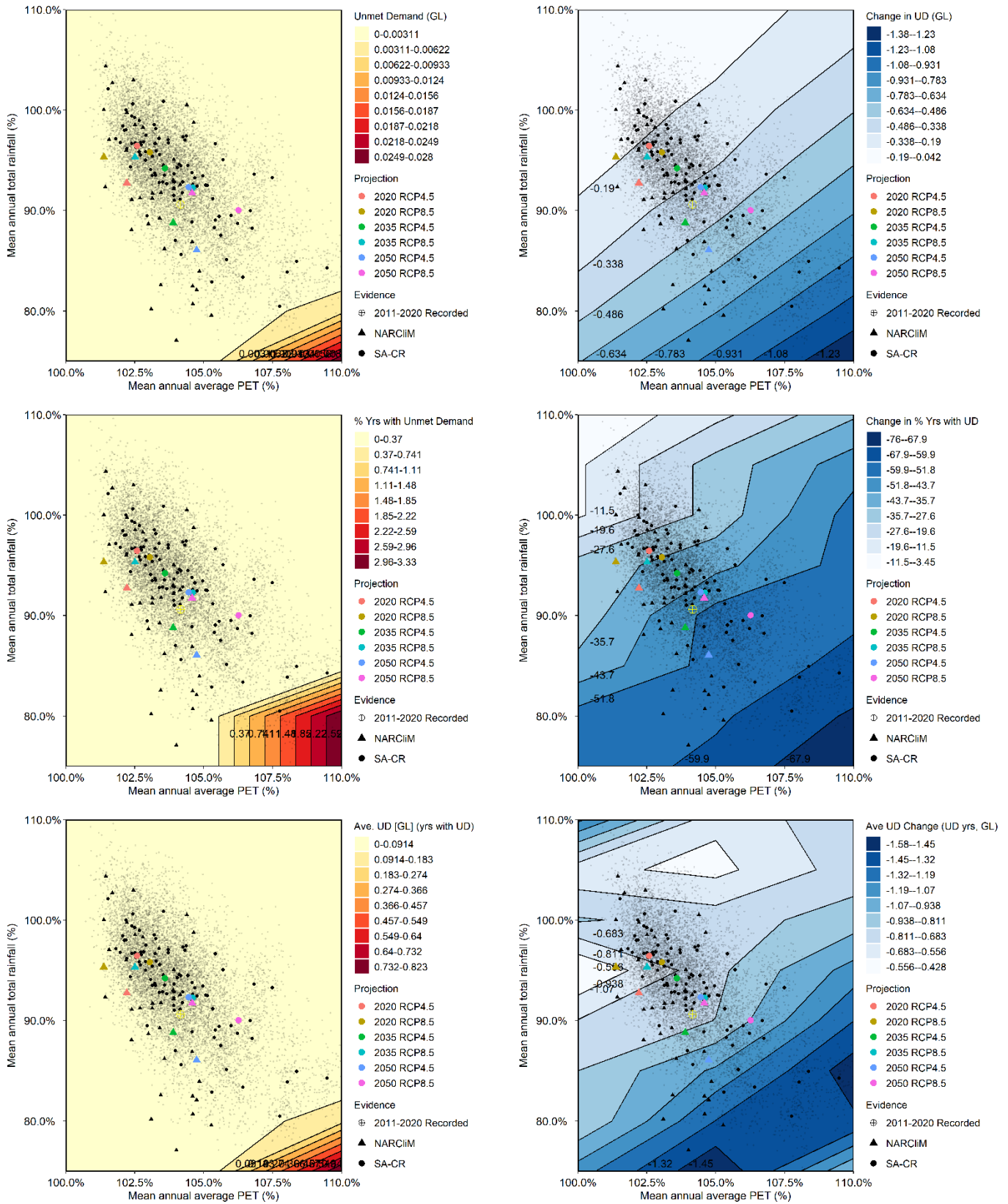


Figure 100. Left column - Unmet demand from process-based model in Stella for the Eden Valley (Pathway 3). Top to bottom: Average unmet demand [GL], percentage of years with unmet demand, and average unmet demand in years with unmet demand [GL]. Right column - Difference between water security metrics in the left panel (Pathway 3) and the corresponding metrics for the current system (business as usual).

It can be seen from Figure 101 that for 90% reliability, supply exceeds demand for all climate scenarios.

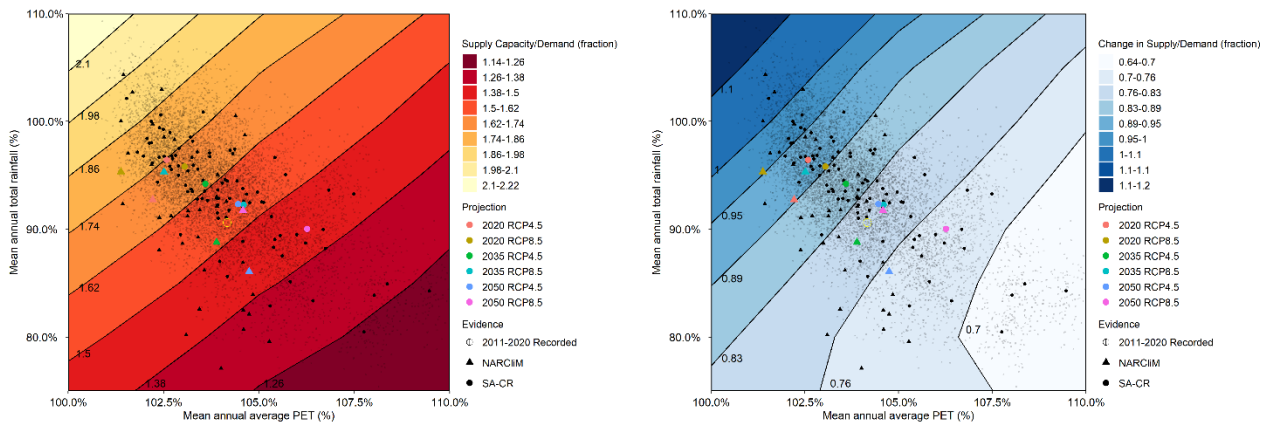


Figure 101. Left plot – Ratio of supply on demand that corresponds to 90% reliability using the process-based model in Stella for the Eden Valley (Pathway 3). The white threshold line indicates the climate scenarios where supply is equal to demand. Right plot – the difference in the fraction of supply on demand between the current system (business as usual) and Pathway 3.

7.4.2 Environmental Flow Metrics

The environmental flow metrics are positively affected by the removal of high and medium impact dams. The following results are from outputs from the updated Scenario 1C Source model, for the outflows of the two locations of interest—the Barossa Valley Gorge and Upper Flaxman Valley zones. It is noted that the changes to groundwater extractions are not reflected in the environmental flow metrics presented here, which are derived using the eWater Source model. This represents a significant limitation of the environmental flow work, and is discussed further in Section 8.2.

7.4.2.1 Barossa Valley Gorge Zone

In comparison to the current system configuration, it can be seen from Figure 103 that the removal of high and medium impact dams has very little influence on the environmental flow metrics at the Barossa Valley Gorge Zone outflow. The number of flow days a year increases marginally between the current system and system with high and medium impact dams removed (first row, Figure 103). This increase is by less than two flowing days for most climate scenarios compared to the current system. This increase is also only around one extra flowing day at most compared to the results as a result from implementing Pathway 2 (only high impact dams removed) (Figure 96). The number of days a year above threshold flow increases by around three days a year for all climate projections between the current system and Pathway 3 (second row, Figure 103). The number of flow days over the median annual flow is calculated based on the 50th percentile flow for the current system (9.13 ML/day). It can be seen from the third row of Figure 103 that this increase is roughly four days above medium flow a year compared to the current system.

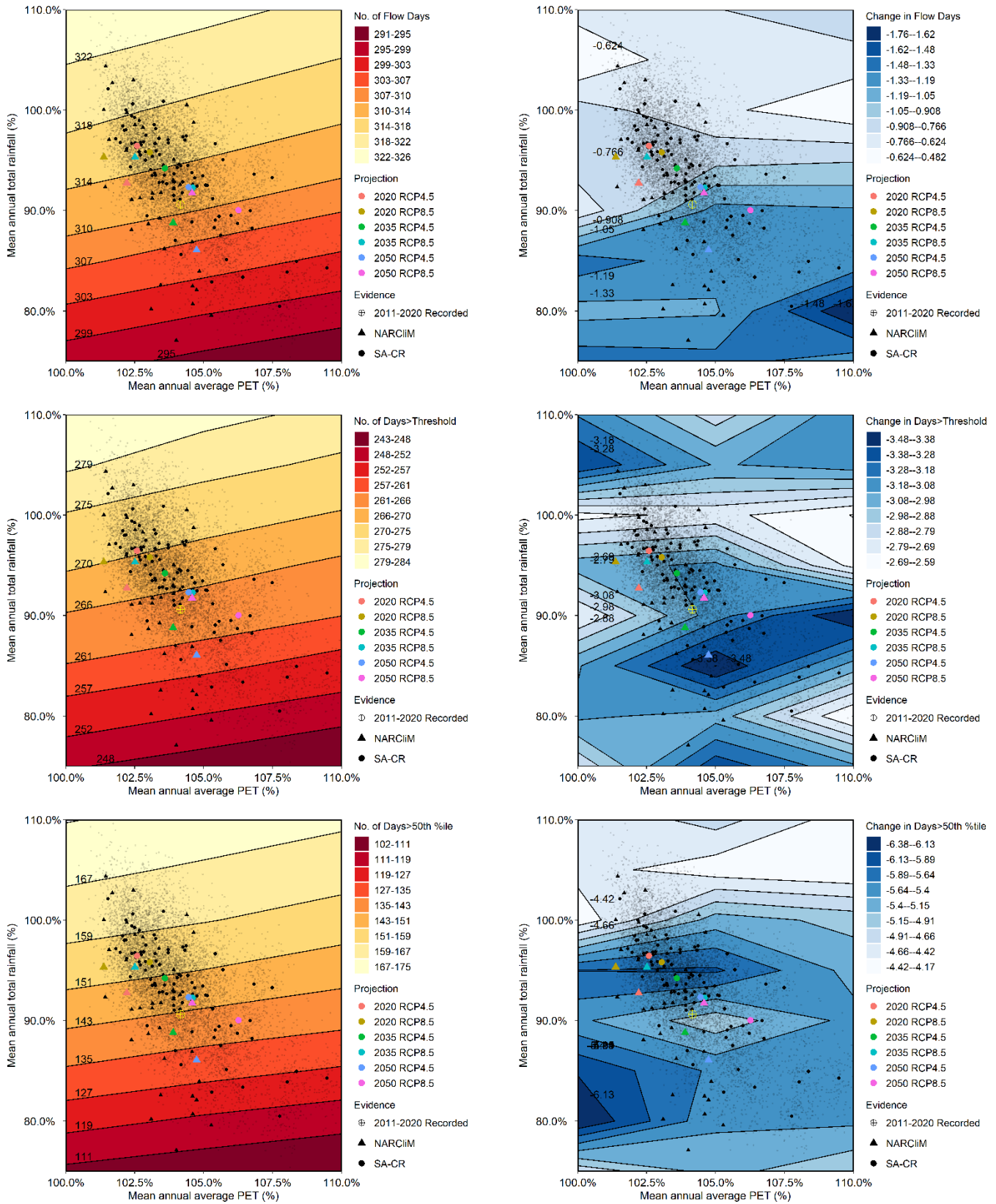


Figure 102. The performance spaces of environmental flow metrics for the Barossa Valley Gorge Zone from simple scaling from Source results (Pathway 3 – removal of high and medium impact dams). Left column – Top to bottom: number of flow days; number of days above threshold flow; and the number of days over the 50th percentile flow (for the current system configuration this is 9.13 ML/day). Right column – Difference between environmental flow metrics in the left panel (Pathway 3) and the corresponding metrics for the current system (business as usual).

7.4.2.2 *Upper Flaxman Valley Zone*

Consistent with Pathway 2, there is a much more significant change for Pathway 3 in the environmental flow metrics for the Upper Flaxman Valley compared to the Barossa Valley Gorge zone. Between the current system and Pathway 3 (first row of Figure 103), there is increase in number of flow days a year is around 19-22 extra flowing days, compared to the 12 to 15 extra flowing days for Pathway 2 (Figure 97). The number of days above threshold flow also increases (second row of Figure 103) by around 17-20 days a year from the current system. This is around a seven day increase from the result of implementing Pathway 2 (Figure 97). There is also around a 16-21 day a year increase in flows (third row of Figure 103) above the 50th percentile from the current system and an increase in 10 flowing days from Pathway 2 (Figure 97).

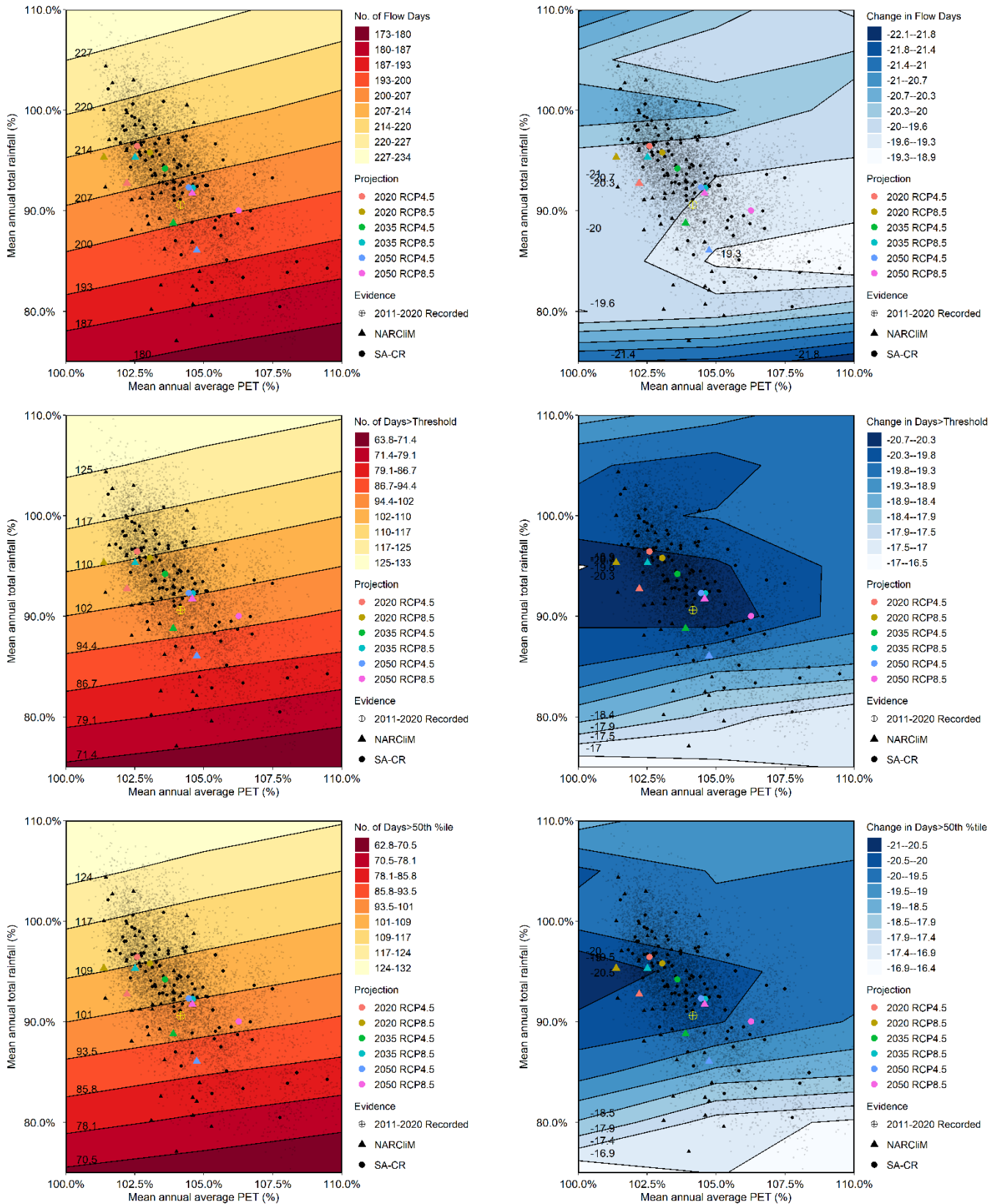


Figure 103. The performance spaces of environmental flow metrics for the Upper Flaxman Valley Zone from simple scaling from Source results (Pathway 3 – removal of high and medium impact dams). Left column – Top to bottom: number of flow days; number of days above threshold flow; and the number of days over the 50th percentile flow (for the current system configuration this is 0.828ML/day). Right column – Difference between environmental flow metrics in the left panel (Pathway 3) and the corresponding metrics for the current system (business as usual).

7.5 Pathway 4: Maximum water availability and production outcomes

Pathway 4 involves a large addition of imported water, as well as significant increase in groundwater abstraction to the allocation amount. Water use efficiency derived from investment in precision agriculture technologies is also implemented as with Pathway 2 and 3. Moreover, stock and domestic demand increases to 1.5 times the current use, although the 50% increase is not assumed to be supplied by unlicensed water extraction. This significant increase in available water supplies to meet demand allows for expansion of vineyards, either in terms of yield or planted area, which will be explored below.

7.5.1 Water Security Metrics

7.5.1.1 Barossa Valley

First the pathway is tested without increasing yield or planted area. This gives no unmet demand, as expected due to the large increase in water supply.

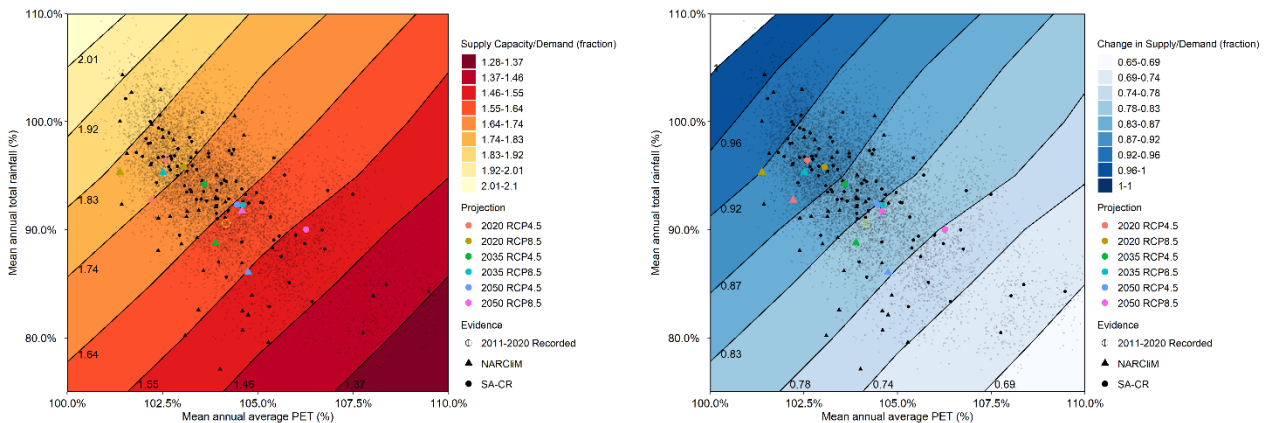


Figure 104. Left plot – Ratio of supply on demand that corresponds to 90% reliability using the process-based model in Stella for the Barossa Valley (Pathway 4, no increase in planted area). The white threshold line indicates the climate scenarios where supply is equal to demand. Right plot – the difference in the fraction of supply on demand between the current system (business as usual) and Pathway 4.

The planted area is then increased within the model until the supply equal demand line (90% reliability) is met for an extreme climate projection (Figure 105). This resulted in being able to support a 1.35 times increase in vineyard area in the Barossa Valley while exceeding 90% reliability for the majority of climate scenarios.

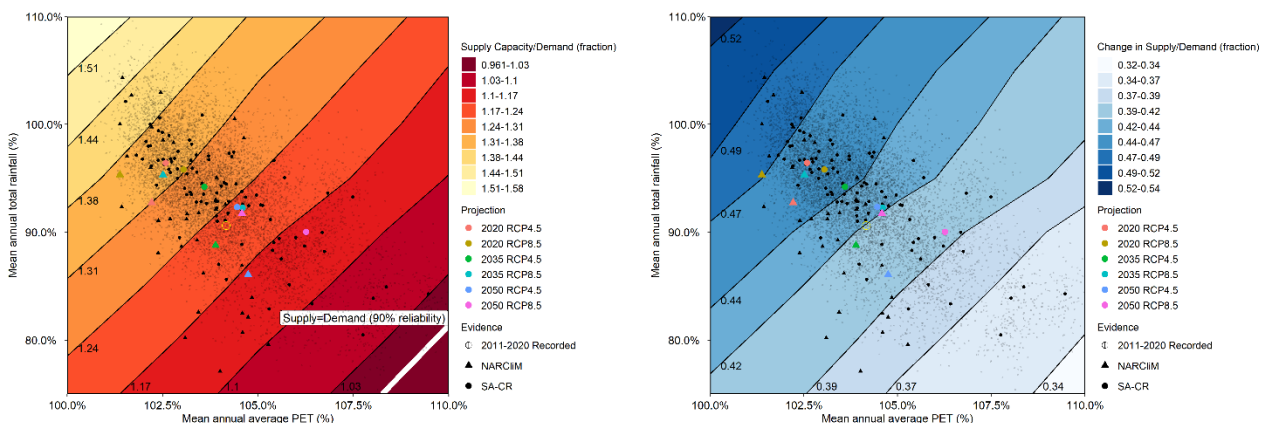


Figure 105. Left plot - Ratio of supply on demand that corresponds to 90% reliability using the process-based model in Stella for the Barossa Valley (Pathway 4, 1.35 times increase in planted area – 158.6 km²). The white threshold line indicates the climate scenarios where supply is equal to demand. Right plot – the difference in the fraction of supply on demand between the current system (business as usual) and Pathway 4.

A 2 tonne/ha increase in yield was also considered, where each extra tonne corresponds to 33mm of additional water demand. It can be seen from Figure 106 that for 90% reliability, this can be supported by the system.

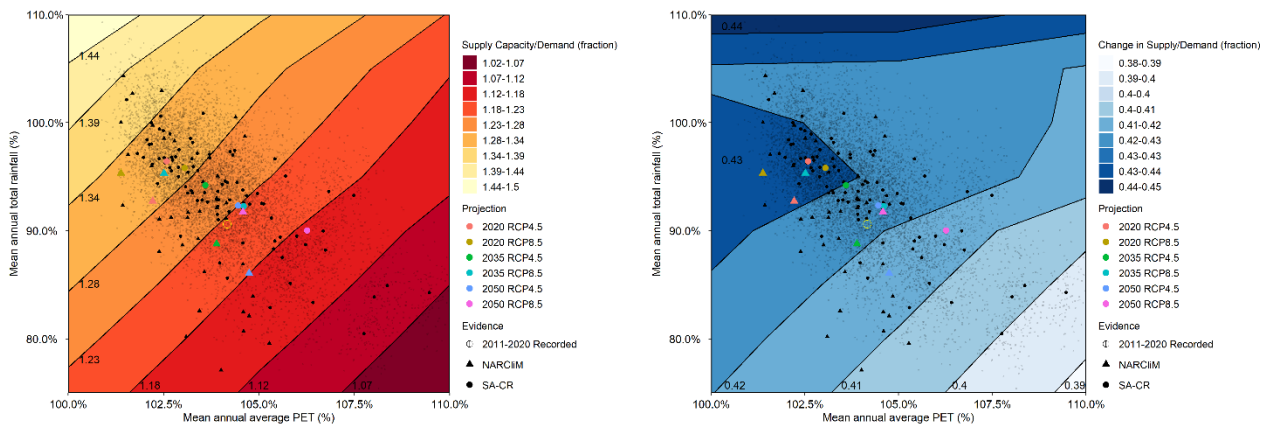


Figure 106. Left plot - Ratio of supply on demand that corresponds to 90% reliability using the process-based model in Stella for the Barossa Valley (Pathway 4, no increase in area, 2 tonne yield increase). The white threshold line indicates the climate scenarios where supply is equal to demand. Right plot – the difference in the fraction of supply on demand between the current system (business as usual) and Pathway 4.

7.5.1.2 Eden Valley

Likewise with the Barossa Valley region, there is no unmet demand when no increase in area is supplied, as seen in Figure 107.

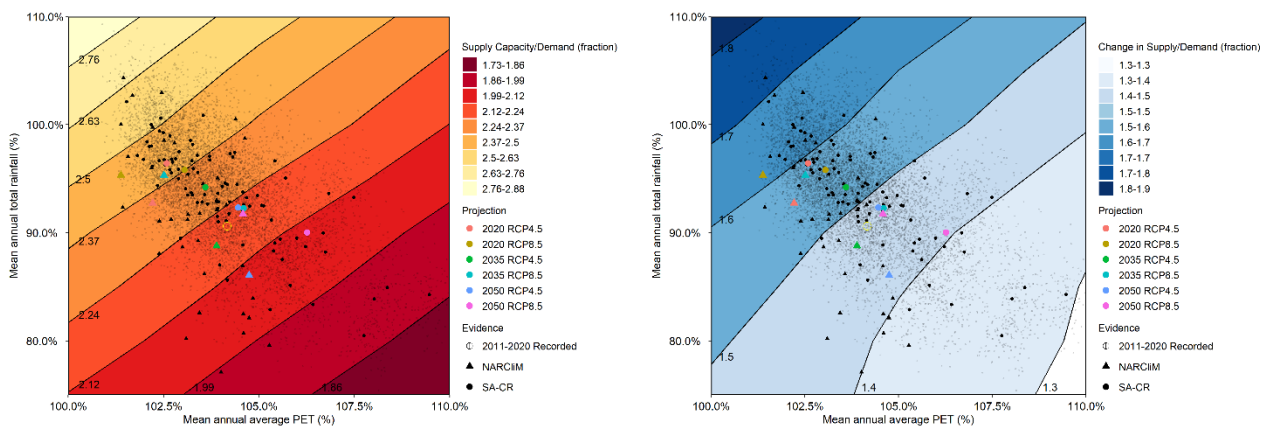


Figure 107. Left plot - Ratio of supply on demand that corresponds to 90% reliability using the process-based model in Stella for the Eden Valley (Pathway 4, no increase in planted area). The white threshold line indicates the climate scenarios where supply is equal to demand. Right plot – the difference in the fraction of supply on demand between the current system (business as usual) and Pathway 4.

As shown in Figure 108, in the Eden Valley, a 2.05 times increase in vineyard area can be sustained when considering 90% reliability and a severe, but not the most extreme, climate scenario.

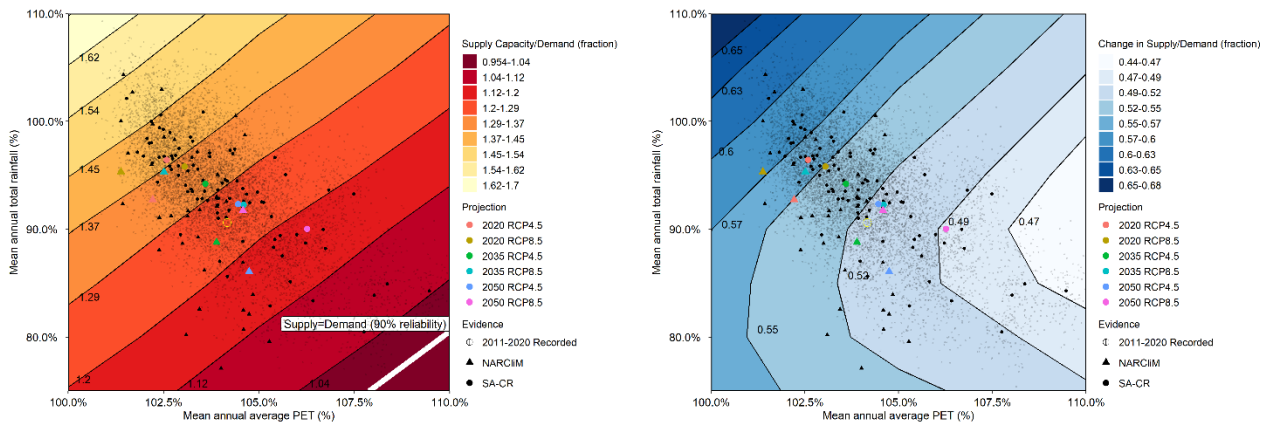


Figure 108. Left plot - Ratio of supply on demand that corresponds to 90% reliability using the process-based model in Stella for the Eden Valley (Pathway 4, 2.05 times increase in planted area – 47.6 km²). The white threshold line indicates the climate scenarios where supply is equal to demand. Right plot – the difference in the fraction of supply on demand between the current system (business as usual) and Pathway 4.

A 2 tonne/ha yield increase was also applied to the Eden Valley model. This increase in yield can easily be supplied by the additional water introduced in Pathway 4.

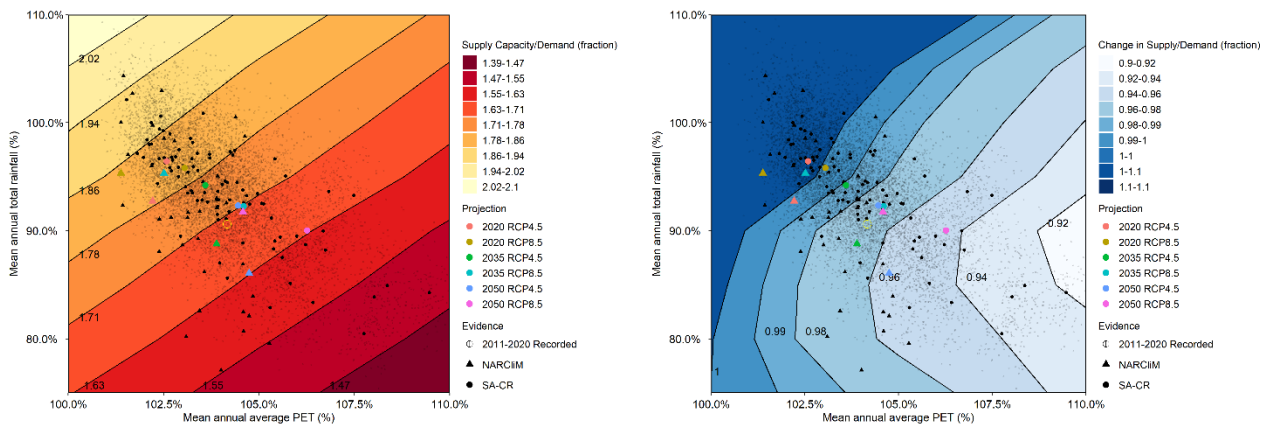


Figure 109. Left plot - Ratio of supply on demand that corresponds to 90% reliability using the process-based model in Stella for the Eden Valley (Pathway 4, no increase in area, 2 tonne yield increase). The white threshold line indicates the climate scenarios where supply is equal to demand. Right plot – the difference in the fraction of supply on demand between the current system (business as usual) and Pathway 4.

7.5.2 Environmental Flow Metrics

There is no change in the environmental flow metrics from the baseline case due to changes made in Pathway 4 for either the Barossa Valley Gorge and Upper Flaxman Zones. See Figure 83 to Figure 88 for these metrics (Section 6.2).

7.6 Pathway summary

A summary of key performance metrics for all pathways and several representative climate change scenarios is presented in Table 22. All pathways provide improvement to reliability of water security in the Barossa Valley, and the capacity for vineyard expansion while achieving a 90% reliability (and assuming no other system changes other than those articulated in the pathway) is also described, with increased capacity roughly corresponding to the additional imported volumes. In contrast, none of the pathways have a large impact on the outflow from the Barossa Valley Gorge Zone (end of system).

Table 22. Summary of pathway results for Barossa Valley

Element	Business as usual	1. Enhanced infrastructure investment and existing behaviour	2. Sustainable economic growth - clean and green production	3. Healthy waterways through investment	4. Maximum water availability and production outcomes
<i>Reliability* (baseline)</i>	90%	≥97%	≥97%	≥97%	≥97%
<i>Reliability* (mid-range climate projection)</i>	70%	≥97%	≥97%	95%	≥97%
<i>Reliability* (worst case)</i>	45%	85%	90%	79%	≥97%
<i>Capacity to change planted area** (baseline)</i>	-4%	37%	41%	29%	95%
<i>Capacity to change planted area** (mid-range climate projection)</i>	-20%	15%	18%	6%	63%
<i>Capacity to change planted area** (worst case)</i>	-35%	-3%	-1%	-13%	33%
<i>Number of days above threshold flow† (baseline)</i>	272	272	273	275	272
<i>Number of days above threshold flow† (mid-range climate projection)</i>	261	261	262	264	261
<i>Number of days above threshold flow† (worst case)</i>	245	245	246	248	245

*Water supply reliability has been calculated as '1 – percentage of years with unmet demand'. Note: as reliability is calculated relative to a 30-year climate sequence, it is not possible to estimate reliability values greater than 97%.

**This metric is calculated based on an assumption of 90% reliability, and that other system attributes (e.g. yield targets and/or other types of water demand) are held constant.

† Barossa Valley Gorge zone.

Presenting the same analysis for Eden Valley (Table 23) shows that the introduction of imported water has a significant impact on ability to meet water security, with all pathways achieving high reliability. This table also highlights potential changes to planted area that can be achieved for the different pathways and climate scenarios while achieving a 90% reliability. Pathways 2 and 3 also allow for increase in environmental flows at the Upper Flaxman Valley Zone outlet, which is located within the Eden Valley delineation, although these increases are somewhat dwarfed by the decrease in environmental flows caused by the more severe climate projections.

Table 23: Summary of pathway results for Eden Valley

Element	Business as usual	1. Enhanced infrastructure investment and existing behaviour	2. Sustainable economic growth - clean and green production	3. Healthy waterways through investment	4. Maximum water availability and production outcomes
<i>Reliability* (baseline)</i>	90%	≥97%	≥97%	≥97%	≥97%
<i>Reliability* (mid-range climate projection)</i>	70%	≥97%	≥97%	≥97%	≥97%
<i>Reliability* (worst case)</i>	45%	97%	≥97%	≥97%	≥97%
<i>Capacity to change planted</i>	-9%	77%	115%	98%	163%

<i>area** (baseline)</i>					
<i>Capacity to change planted area** (mid- range climate projection)</i>	-27%	48%	80%	53%	120%
<i>Capacity to change planted area** (worst case)</i>	-50%	15%	45%	20%	81%
<i>Number of days above threshold flow† (baseline)</i>	99	99	109	119	99
<i>Number of days above threshold flow† (mid- range climate projection)</i>	80	80	90	99	80
<i>Number of days above threshold flow† (worst case)</i>	54	54	63	71	54

*Water supply reliability has been calculated as ‘1 – percentage of years with unmet demand’. Note: as reliability is calculated relative to a 30-year climate sequence, it is not possible to estimate reliability values greater than 97%.

**This metric is calculated based on an assumption of 90% reliability, and that other system attributes (e.g. yield targets and/or other types of water demand) are held constant.

† Upper Flaxman Valley Zone.

7.7 The importance of yield assumptions

In all the simulations described thus far in the report, irrigation behaviour dynamics are assumed to remain at levels consistent with the most recent decade. As shown in Figure 5, yields have decreased from in the order of 7 tonnes per hectare in the early 2000s, to in the order of 4 tonnes per hectare on average in the last decade (down to 2 tonnes per hectare in 2020). The drivers for these changes to yield have not been clearly documented, but are likely to involve some combination of changes in varieties (e.g. Figure 4), ‘premiumisation’ (i.e. targeting higher value fruit, which is often associated with imposing greater water stress on the vine), and limitations due to water scarcity. The low yields in 2019 and 2020 both correspond to particularly dry years of record, and may suggest the important role of water scarcity on yield outcomes.

An important question, therefore, is the extent to which water scarcity has been a driver of the decline in recent years, and thus the extent to which an increase in water availability would lead to an increase in yield targets. Although there is no available evidence on likely grower response to increased water availability, there is evidence in the literature on likely changes to irrigation demand for a change in yield. This is often encapsulated in ‘crop water production’ relations or functions, which express mathematically the response of a crop to irrigation applied over the growing season in terms of its yield (Helweg, 1991).

Whilst to our knowledge there is no information available on crop water production functions tailored to Barossa or Eden Valley viticulture, several studies (e.g. Payan et al, 2011; Williams and Hymann, 2017; and Stevens et al, 2010) find typical yield changes in the order of 2-5 tonnes/ha for each additional ML of water. Converting this to total water demand in the Barossa and Eden Valleys (by multiplying these estimates by planted area), leads to an increase in demand ranging from 2.4 to 5.9 GL (Barossa Valley) and from 0.5 to 1.2 GL (Eden Valley) for each additional tonne of yield. These numbers are indicative only, and have not been derived from the unique context of the Barossa and Eden Valleys; nevertheless, they show the potential significant role of irrigation strategy on total water demand, and that assumptions related to yield targets are likely to have a significant bearing on sizing of any imported water sources.

8 Conclusions

This report presents the outcomes of a climate ‘stress test’ of water resources in the Barossa and Eden Valleys, both now and over the next 30 years to the year 2050, in order to inform work towards a water security strategy for the region. The stress test focused on three key elements:

- Current and projected future availability of native water resources (surface water and groundwater) under current and changing climate conditions;
- Current and projected future demand for water, with a particular focus on irrigation demands from the viticultural industry; and
- Implications of a set of possible adaptation pathways identified as part of the Barossa and Eden Valley water security strategy.

The analysis presented in this report has sought to use best-available data and models for the region, including a number of models that have been developed over a period of many years by various domain experts from both the Department of Environment and Water (DEW) and the South Australian Research and Development Institute (SARDI). Building on this foundation, the primary contribution of this report has been the integration of numerous existing models and datasets into a systems analysis framework that combined multiple sources of knowledge on all primary water sources (surface water, groundwater and imported water) and demands (focusing primarily on irrigated viticulture). The integrated analysis framework was designed to represent system dynamics under change, and for situations where significant uncertainties were identified, a ‘multiple lines of evidence’ approach was adopted.

The primary findings of the study are summarised next, followed by a brief overview of key assumptions and limitations.

8.1 Summary of Results

8.1.1 Recent system dynamics

Recognising the long-term (30-year) future horizon associated with the water security strategy, a review of key changes over the last few decades is useful to provide insight into the possible scope and scale of future change. A description of the multi-faceted nature of changes occurring in the system have been provided in the main report, with several key aspects summarised below:

- Population in the Barossa Valley has increased by 20% since 2005, representing an annualised growth rate of 1.2% which is slightly below the national average over this period.
- The irrigated viticulture industry represents the primary demand for water, far outstripping other demands (e.g. municipal and stock watering) at the regional level. Since the early to mid-2000s, the region has undergone what is referred to as the ‘fifth boom cycle’ of the Australian wine industry. Between 2001 and 2021 the planted area across the Barossa and Eden Valley regions has increased by 53%, with the majority of this increase occurring over the period from 2001-2009 (5% annualised growth), and much slower increases from 2010-2021 (0.3% annualised growth). The planted varieties have also shifted, with the most notable change being an increase in shiraz in the Barossa Valley, offset by a decrease in the proportion of white winegrape varieties.
- The most significant challenges to water supply volumes over this period came from external water sources, most notably the Barossa Infrastructure Limited Scheme (constructed in 2001/02 with initial capacity of 7 GL/yr, and growing to a capacity of 11 GL/yr from 2018-19 onwards), but also including the Bunyip Scheme (approximately 2 GL/yr). These pipeline systems exclusively serve the Barossa Valley region, with Eden Valley only having access to the SA Water off-peak pipeline (annual capacity approximately 0.12 GL).

- The total number and capacity of licensed farm dams have been relatively stable over the recent decade due to prescription of water resources, with a total farm dam capacity of 14.34 GL across Barossa and Eden Valleys. However a 10% reduction in rainfall over the recent decade relative to a 1976-2005 climatological baseline has meant that total surface water extractions have decreased by more than 50% of this period, and native surface water supplies thus represent a small and diminishing water source for both the Barossa and Eden Valley regions. For example in 2019/20, the total surface water supply was estimated to be 2.9 GL across the two regions, or just 20% of total dam capacity.
- In contrast to surface water, groundwater extractions have more than tripled over the last decade, with a maximum extraction of 5 GL in 2018/19 across the combined Barossa and Eden Valley regions. Whilst the sustainability of groundwater extraction was not assessed in this report, modelling results showed significant sensitivity of groundwater recharge to climate conditions, with total recharge in the recent decade approximately 28% below the climatological baseline; moreover, net recharge (groundwater recharge minus groundwater evapotranspiration fluxes) was well below the average annual groundwater extraction for at least some years in the recent record.

These changes, taken together, highlight increasing trends in water demands at a time of decreasing surface water supplies, with groundwater extractions (for both Barossa and Eden Valleys) increasing to potentially unsustainable levels, and imported water sources (Barossa Valley only) frequently being near or at their capacity. Moreover, it is not clear the extent to which the slowdown in growth in vineyard area over the recent decade is causally related to the decrease in availability of supply or whether it is related to other drivers (e.g. changes in varieties and/or 'premiumisation' drivers).

8.1.2 Projected climate changes

A detailed review of climate projections have been assessed using three lines of evidence (Climate Change in Australia, Climate Ready-SA and NARCLiM), and these are presented relative to a climatological baseline of 1976-2005. Significant consistency exists amongst the majority of projections for a drier and hotter future climate; however there is a large degree of uncertainty regarding the magnitude of future changes, and a minority of projections were also identified that suggest an increase in precipitation relative to the baseline.

The primary variables analysed in this report comprise annual average precipitation and potential evapotranspiration, as these two have a dominating influence on the water balance. A third variable (the strength of the seasonal cycle of precipitation) was also analysed in key sections, given the seasonal nature of both the hydrology and the irrigation cycle. Given the focus on climate 'stress testing', the emphasis of the climate change assessment has been placed on understanding the *range* of projections, rather than focusing on a single median projection that may not be reflective of the climate that will actually be experienced over the coming decades. This is designed to enable decision makers to investigate the extent to which possible adaptive pathways are suitable under a broad range of plausible future changes.

Based on this, the projection ranges over the coming 30 years are as follows:

- Average annual precipitation: -23% to +5%
- Average annual potential evapotranspiration: +1.4% to +9.5%
- Rainfall seasonality (positive values representing a strengthening of the seasonal cycle, implying wetter winters and drier summers): -12% to +44%

The projections indicate a general pattern of larger changes for greater climate forcings (i.e. RCP 8.5 versus RCP 4.5), and for longer future horizons (i.e. windows centred on 2050 compared with either windows centred on 2035 or 2020). Other precipitation variables that were investigated but not included in the system model include the number of wet days, which was found to have projected changes that are consistent with those for annual average precipitation, and the 99% daily precipitation, which was found to have smaller decreases relative to annual average precipitation. Temperature was also analysed and showed median

increases of 1.5°C (RCP4.5) and 2.0°C (RCP 8.5) by 2050 relative to the 1976-2005 climatological baseline, but with increases as much as 3.1°C for the worst-case scenario. Moreover, changes to the averages were also found to lead to large increases in the frequency of days above 35°C.

Interestingly, the recent decade (2011-2020), which on average had 10% less annual total precipitation and had 4% greater potential evapotranspiration than the climatological baseline, is very similar in terms of these variables compared to mid-range projections for 2050, and drier than mid-range projections for the earlier time slices. This highlights that the recent decade was significantly drier than what might have been expected based on climate change alone in the recent decade, and provides a reasonable guide as to what might be expected in future decades. However, this must also be viewed relative to the significant variability in the projections, and the fact that each of the climate scenarios considered here were based on 30 year averages rather than just a decadal average. As such, adaptation efforts should consider the possibility of future decades that may be either significantly drier or wetter than the recent decade.

8.1.3 Current system performance and the role of adaptive pathways

An integrated system model that combines features of both supply (including surface water, groundwater and imported water) and demand (focusing on irrigated viticulture but also including assumptions for stock and domestic consumption) was developed, and this model was used to simulate the range of plausible climate forcings on system performance for both 'business as usual' conditions and four possible adaptive pathways.

The four adaptation pathways were as follows:

- **Pathway 1 – Enhanced infrastructure investment and existing behaviour**, whereby vineyard area and irrigation behaviours are maintained at historical levels but an additional 8 GL and 3.5 GL of water is imported to the system for Barossa and Eden Valleys, respectively.
- **Pathway 2 – Sustainable economic growth with clean and green production**, which is similar to Pathway 1 but where 20 strategically located medium and large dams are converted to off-stream storages.
- **Pathway 3 – Healthy waterways through investment**, in which 40 strategically located medium and large dams are converted to off-stream storages, groundwater use is halved, and with an additional 8 GL of imported water across the combined Barossa and Eden Valley systems.
- **Pathway 4 – Maximum water availability and production outcomes**, in which an additional 16GL and 5GL of water is imported to the system for Barossa and Eden Valleys, respectively, and where groundwater use is more than doubled to its maximum allocation.

This analysis was undertaken for both the Barossa and Eden Valley delineations, and performance was represented considering a range of water security and ecological (environmental flow-based) metrics.

8.1.3.1 Water security

The 'business as usual' pathway suggested that overall system reliability was approximately 90% for baseline climate conditions for both the Barossa and Eden Valley delineations, with this decreasing to 45% under the 'worst case' climate scenario for both delineations. Not surprisingly, the greatest improvement to system reliability occurred for Pathway 4, with reliability estimates greater than 97% regardless of the climate change scenario assuming current planted area and irrigation strategies. Presented differently, assuming current irrigation strategies (e.g. yield targets), it would be possible to expand planted area by 63% and 120% in Pathway 4 under a mid-range climate projection for Barossa and Eden Valley, respectively.

Interestingly, the next highest performance pathway from a reliability perspective is Pathway 2, in which 20 medium and large dams are converted to an off-stream balancing store. This is despite the farm dams no longer being available to supply surface water from native sources as with Pathway 1. This suggests that careful utilisation of dams to provide year-to-year balancing storage may provide useful dividends from both

a water security and environmental flow perspective; however it is cautioned that this is an indicative result only, and that the design and management of balancing stores are likely to be much more complex than represented in the Stella modelling framework. Overall, Pathway 2 enables an increase in planted area by 18% (Barossa Valley) and 80% (Eden Valley) under mid-range climate change projections.

Lastly, Pathways 1 and 3 have the lowest reliability of the adaptive pathways, although both are significantly more reliable than 'business as usual'. These pathways have broadly similar reliability metrics, with Pathway 1 being slightly more reliable than Pathway 3 in the Barossa Valley, and slightly less reliable in Eden Valley. The two pathways enable a small increase in planted area for the Barossa Valley, and a larger increase of approximately 50% in Eden Valley.

8.1.3.2 Environmental flows

Environmental performance was assessed at two locations: Barossa Valley Gorge, and Upper Flaxman Valley. In reviewing these results, it is noted that processes leading to environmental flows are highly heterogeneous, with different drivers and effects at different portions of the stream network. As such, these results should be treated as indicative only given the limited spatial detail of the assessment.

In all cases, the greatest environmental response occurs at Upper Flaxman Valley (see Table 23), with the benefits at Barossa Valley Gorge (Table 22) difficult to ascertain from the modelling outputs presented herein. Focusing on Upper Flaxman Valley, the primary benefits are associated with Pathways 2 and 3, in which 20 and 40 strategically located medium and large dams are converted to off-stream storages, respectively. For a mid-range climate projection, Pathways 2 and 3 lead to an additional 10 and 19 flow days above threshold, with results broadly similar for other climate scenarios.

An important result is that for the most environmentally focused pathway (Pathway 3), the number of days above threshold for a mid-range climate projection is equivalent to the number of days above threshold under 'business as usual' for the baseline climate scenario. Thus, at best, conversion of 40 medium and large dams are able to compensate for the effects of the mid-range climate scenario relative to the climatological baseline, and thus are unable to achieve further ecosystem restoration benefits to address other elements of human modification of the system. These results strongly indicate that environmental flow recovery is likely to require a multi-pronged strategy that also considers reduction in groundwater extractions (noting also the identified sensitivity of groundwater recharge to climate forcings) as well as potentially more active environmental flow releases.

8.2 Assumptions and Limitations

Whilst every effort has been made to utilise best-available data and scientific understanding, any modelling study inevitably relies on a number of assumptions. This is particularly the case for a climate stress test, given the future-oriented nature of the investigation, which necessitates the use of models in situations that are well outside of their calibration domain. Extensive scientific literature is now available summarising modelling limitations associated with 'non-stationary' conditions, and in most cases there are high levels of uncertainty associated with the key processes that need to be represented and how these might be implemented in a revised modelling framework. This means that, in many cases, there is no easy 'fix' to address many of the modelling limitations.

To this end, the approach developed here is to provide transparency about key assumptions and possible limitations associated with the analysis in this report, and these have been summarised in Table 24 and discussed further in the context of the water security strategy in the subsequent text. These assumptions and limitations are not exhaustive, but represent those that have the potential to have a material impact on key results.

Table 24: Key assumptions made in this report, and their limitations

Assumption	Basis for assumption	Limitations
Surface water sensitivity to climatic changes (climate 'elasticity') is correctly estimated.	The eWater Source model performs well on standard calibration metrics. Moreover, streamflow elasticity to rainfall is approximately 3:1, which is consistent with typical elasticity values in similar catchments.	As shown in Section 3.3.1, Source appears to underestimate flow in wet years and overestimate flow in low years. Thus elasticity may be slightly underestimated. To our knowledge, differential split sample model evaluation methods have not yet been applied to Source and thus it is not well understood how well this model performs under change scenarios.
Baseflow estimates from surface water are realistic	Standard base flow approaches (e.g. Lyne-Hollick filter) were applied to the data, with the parameter estimated through a comparison with other estimation methods (e.g. tracer studies).	The significant surface water / groundwater interactions mean that groundwater levels will play a large role in baseflow. The assumptions are thus only valid under 'steady state' groundwater assumptions, in which the distribution of gaining and losing stream reaches is consistent with what occurred during the Source calibration. This assumption is unlikely to be the case for combined high extraction / severe climate change scenarios, and may not be valid for more moderate extraction and climate change scenarios. Moreover, a number of differences can be observed between surface water and groundwater-based estimates of baseflow, and these warrant further investigation.
Barossa Valley Gorge and Upper Flaxman Valley are good indicator sites to represent processes associated with environmental flow dynamics	Barossa Valley Gorge and Upper Flaxman Valley were provided to represent the end-of-system flows as well as an important zone for ecosystem health, respectively.	The high levels of stream heterogeneity may not reflect all key system dynamics associated with environmental flows.
Validity of fixed window analysis rather than transient analysis	Fixed-window approaches are useful to work out risk profiles that rely on probability calculations at a particular point in time. The results of fixed-window analysis is likely to be appropriate for situations where there is limited temporal dependency.	Groundwater storage in particular has significant year-to-year dependency, and so this element is not well-suited to fixed-window analyses. This is particularly likely to be the case for more extreme climate scenarios, as the rate of groundwater replenishment becomes insufficient to meet consumptive requirements.
Recharge dynamics adequately represented by the groundwater model	MODFLOW has been developed for the Barossa PWR using best-available information at the time including using chloride mass balance method and other groundwater data for model calibration	Recharge is anticipated to be extremely sensitive to climatic changes, is difficult to estimate accurately, and thus remains highly uncertain. Moreover, several key processes that could influence recharge rates (including irrigation behaviour in heavily irrigated areas, as well as the possible future utilisation of managed aquifer recharge) have not been included in the modelling presented herein.

<p>Annual total rainfall and potential evapotranspiration, as well as rainfall seasonality, are the ‘stressors’ that are most critical for the Barossa and Eden Valley systems</p>	<p>The highly seasonal nature of the hydrology, and the focus in this report on water balance considerations, means that annual-scale rainfall and evapotranspiration, together with a measure of the seasonal distribution of rainfall, are likely to have the largest control on key metrics.</p>	<p>The assumption has not been explicitly tested (for example by perturbing other attributes like number of wet days and extremes), and this may have an impact on several metrics. This is likely to be particularly relevant for environmental flow metrics that depend on the full hydrograph.</p> <p>However overall, within the context of the water security strategy, the role of other attributes are likely to be ‘second-order’ compared to the annual totals and the seasonal cycle.</p>
<p>Baseline perturbation using ‘climate scaling’ is an adequate approach for estimating future risk</p>	<p>Climate scaling is an approach of multiplying the historical record (in this case 1976-2005) by climate change ‘factors’ that represent plausible future changes. This ensures that the hydrological realism of the time series is maintained.</p>	<p>A limitation of scaling is that patterns of variability outside that of the baseline period are not considered. This is likely to be a particular issue for extremes, and for this reason estimates of reliability above a threshold of approximately 90% (representing three years out of the 30 year window not meeting the system performance criteria) should be treated with caution.</p>
<p>Total water consumption over the recent decade across all water sources provides a reasonable reflection of actual irrigation demand.</p>	<p>Historical behaviour provides a strong indicator for actual irrigation water requirements.</p>	<p>This assumption is particularly pertinent with the regression approach to demand estimation. Water usage for at least several years in the recent decade was equivalent to water source capacity, and thus actual demand may be somewhat higher than historical demand particularly for those years where water usage was equal to system capacity. Evidence for this includes the reduction in yield trends over recent decades, with particularly low yields during the years 2019 and 2020 which were very dry. Eden Valley, which has not had access to imported water, in particular is likely to have substantial ‘latent’ demand that is not reflected in the recent usage figures.</p> <p>It should be noted that whilst the FAO-56 dual crop model is less influenced by this assumption, the initial calibration of the model to historical average usage means that historical usage is still expected to have some influence on model results.</p>
<p>Changes to soil management (e.g. carbon sequestration) are not likely to materially affect water demand</p>	<p>Soil management strategies, when aggregated to the regional scale, are likely to have a ‘second-order’ influence on water balance considerations compared to the processes considered in the Stella model.</p>	<p>Quantitative models that describe the role of soil management (e.g. intercrop plantings, or carbon sequestration) on irrigation demands were not incorporated in the analysis. The extent to which soil management will have a material impact on the water balance is generally not known.</p>
<p>Role of water pricing on demand</p>	<p>Using demand models that focus on recent behaviour (in the case of the regression</p>	<p>Pricing is likely to be a key determinant on utilisation of imported water sources. The analysis herein does not consider water pricing and thus</p>

has not been considered	model) or assumed crop water requirements (in the case of the FAO-56 dual crop model) is a 'business as usual' approach and assumes that growers will pay what is required to meet existing vineyard demands.	the role of price as a possible enabler or limiter of demand is unclear.
Growers prioritise water sources in the order of surface water, groundwater and imported water	Surface water, when available, is generally of low salinity and cost effective, and thus is assumed to be utilised first. Groundwater is generally poorer quality based on historical usage (which is reasonably stable) is assumed to be used at a steady rate. Imported water, which is the most expensive water source, is only utilised when other sources are exhausted.	Grower behaviours are likely to be more variable and complex than assumed here, and there may be other reasons why growers may choose to use imported water sources in preference to surface water or groundwater.
Additional imported water will not drive an increase in groundwater demand	Good quality additional imported water sources are likely to be used in preference to poorer quality groundwater resources	If imported water is of a quality that exceeds quality requirements, growers may choose to 'shandy' this water with additional groundwater to save costs. Therefore it is plausible that an increase in imported water could lead to a simultaneous increase in groundwater consumption. At the time of writing, nothing further is known about the possibility of this dynamic.
Medium- and high-impact farm dams can be converted to inter-annual balancing storages with 100% efficiency	This is unlikely to be valid given the complexity of balancing stores, but provides an upper limit on the likely benefits of balancing stores from a water security perspective	Balancing stores are complex and may need to be designed to store water to address within-year (seasonal) variability as well as year-to-year variability. Moreover, benefits in this report are based on the assumption that individual farm dam owners do not already use their dams for balancing storages, as this was the assumption in the eWater Source model. This is unlikely to be the case.

8.2.1 Future water security

Given the relatively limited influence of surface water and groundwater for the Barossa Valley water balance, and that native water sources are being used at their capacity in both valleys, the impact of imported water is likely to be the key factor determining future water utilisation, as well as any associated water security issues.

A key limitation in this report is that water pricing was not considered as a driver of demand; instead, the approach taken in this report relied heavily on grower behaviour over the recent decade, and physical vine water requirements based on the FAO-56 dual crop coefficient model. It is almost certain that prices of imported water will have a material impact on demand, and this therefore is an area requiring further investigation.

Prices are only one consideration related to future water demands, and changes to planted area and grower strategies (e.g. yield targets) are also likely to have a material impact on demand. Estimates of yield sensitivity to irrigation rates presented in this report are approximate and have not been developed for the unique circumstances of the Barossa and Eden Valleys. Yield sensitivity results should therefore be considered to be indicative only. Other factors, such as the influence of wide-spread adoption of 'precision' irrigation technologies and/or carbon sequestration or other types of soil 'improvement' have highly uncertain impacts on water demands, and thus also have not been considered in any level of detail. Finally, there are a large number of possible changes that have not been anticipated in the adaptive pathways described herein (e.g. urban encroachment, industrial expansion, or changes in cropping mix away from viticulture, or a decline in the global demand for wine); each of these changes may have material impacts on future water security.

Decisions by growers related to the utilisation of alternative water sources have been treated in a sequential fashion, in which growers utilise available surface water resources first, followed by groundwater and then imported water sources. In practice, grower decisions are likely to be highly heterogeneous, and will be affected by multiple drivers. The nature of any contractual arrangements associated with additional imported water sources may also influence the hierarchy of demands. These factors are immaterial when considering total system reliability (which only depends on the total available water irrespective of source), but may matter when considering other factors including but not limited to environmental outcomes.

The capacity of the modelling framework developed in this report to represent system performance under high levels of reliability represents another modelling caveat. The 'climate scaling' method involved perturbation of the 1976-2005 baseline climate, and thus is not able to accurately represent reliabilities above about 90% (representing only three 'failures' in the 30 year record). Stochastic methods are available to get further insight on system behaviour for higher reliability situations; however these have not been implemented in this study.

Finally, the conversion of medium- and high-impact dams to balancing stores is treated in a highly simplistic manner, and assumes both that these dams will be used exclusively to address inter-annual variability (and not within-year variability), and that the dams are not currently used as balancing stores. Both these assumptions are unlikely to be correct; however more information on the proposed usage of the dams is required in order to more accurately simulate the behaviour of these structures.

If further information becomes available in any of the areas described above, it is likely that this information can be incorporated in the Stella modelling framework and used as part of future climate 'stress tests'. Thus, the framework remains flexible to incorporate improved system understanding over time.

8.2.2 Ecological outcomes

Streamflow elasticity, groundwater recharge and baseflow dynamics are all highly sensitive to changing climates, and are of critical importance in designing approaches for maintaining and/or enhancing aquatic ecosystem performance. The compartmentalisation between 'surface water' and 'groundwater' as largely separate systems (with different modelling representations) is likely to be increasingly problematic given the highly coupled nature of the systems, and the interconnected impacts of climate change on both systems. Baseflow dynamics in particular are likely to be very sensitive to surface/sub-surface interactions, and the efficacy of possible strategic interventions (e.g. low flow bypasses, removal of in-stream farm dams, changes in extractive limits) cannot be fully understood without considering possible interactions. The possible underestimation of streamflow elasticity in Source may also have a significant bearing on low flow dynamics.

In considering future changes to low flows, there are multiple additional couplings between human behaviour and groundwater that have not been considered in this work. For example, given the extensive nature of irrigation in the Barossa Valley in particular, changes to irrigator behaviour (possibly driven by changes to imported water resources) could materially impact upon recharge in those regions. This, however, depends heavily on how irrigation is applied; for example efforts to flush salts through the soil profile may

lead to recharge, whilst optimising irrigation rates to align closely to plant water requirements may not materially influence groundwater stores. Managed aquifer recharge, which has not been addressed in this report, provides another example of human interventions that may materially impact groundwater stores, and thence baseflows and associated ecological outcomes.

Each of the factors described above becomes of increased importance in situations where future changes (for example climatic changes, land use changes and/or changes in irrigator behaviour) diverge substantially from the historical situation, since it is in these cases that the models (which have been calibrated to historical data) may misrepresent key processes. Developing monitoring strategies that identify possible departures between observed system behaviour and simulated outcomes therefore represents a critical strategy for ensuring strategic initiatives are well-aligned with actual system behaviour.

8.2.3 Future Research

In any study of this nature, there are avenues for developing improved understanding system dynamics under change. Priority areas of future research as they relate to the water security strategy include the following:

- From a water balance perspective, there is significantly more uncertainty associated with demand-side processes compared to supply-side processes. In particular, whilst supply-based models (eWater Source and MODFLOW) have a long history of application in the Barossa and Eden Valleys, most of the demand models were developed specifically for this study. Further investigation of regional demand, including the drivers of change in viticulture irrigation demand but potentially also considering other types of land use change, is therefore likely to deliver significant benefits. This would ideally include changes to irrigation and soil management strategies, which form part of the water security strategy but have not been represented quantitatively in this analysis. Coupling physical processes with economic drivers—and in particular the link between demand and water pricing—represents a critical area of uncertainty that would benefit from further investigation. Various other areas of investigation such as the role of balancing storages, the impact of sustainability practices and/or drivers of water source prioritisation also may become relevant depending on the policy questions to be addressed.
- From an ecological perspective, improved understanding and representation of the interaction between surface water and groundwater dynamics, particularly under conditions of change, can be expected to yield benefits in order to better understand how interventions can enable stream restoration benefits. This work can be coupled with investigations into multi-pronged options for environmental flow restoration, including the combined implications of farm dam and groundwater extraction policies. Identification of a small set of key environmental performance indices will also improve monitoring and enable policy responses. Given the high level of heterogeneity with the region, and the important role of irrigated agriculture on the water balance in key sub-regions, it is likely that improved spatial understanding of regional dynamics will support optimum interventions.

Importantly, and as highlighted earlier in this section, the processes of change (so-called ‘non-stationarity’) are likely to lead to numerous violations of the modelling assumptions, given that most models have been calibrated to ‘stationary’ historical climate conditions. However, identifying the precise nature of the deficiencies is challenging, and pre-empting all possible issues is infeasible. As such, it is recommended that a monitoring strategy be developed that is designed to identify not only changes to system dynamics, but also helps identify deficiencies in the capability of models to represent those dynamics. This can be used as an early indicator of when key assumptions underpinning water security and/or environmental flow assessments need to be reassessed.

Finally, it is recommended that research continues into the utility and continued development of ‘systems’ approaches to support the development of strategies and adaptive solutions, while simultaneously supporting the operationalisation of elements of the framework and tools where benefits are identified.

9 Acknowledgements

We would like to acknowledge the generosity of staff at both the Department of Environment and Water, as well as the South Australian Research and Development Institute, for providing data, models and advice to support the project. In particular, we would like to thank Volmer Berens, Kumar Savadamuthu, Daniel McCullough and Tom Stewart from the DEW surface water team; Juliette Woods from the DEW groundwater team; and Paul Petrie and Vinod Phogat from SARDI. We would also like to acknowledge the support of Ariella Helfgott from Collaborative Futures for coordinating expert insights on vineyard water demands, and for helping align work with the Barossa strategic foresighting work. Finally, we'd like to acknowledge the support and coordination of Peta Brettig and Ashley Kingsborough from the DEW water strategy team, without whom this project would not have gone nearly as smoothly as it has.

Appendix A: Key areas and area/depth/volume conversions used in this report

Information on water fluxes and stores are commonly presented either in terms of a depth or volume, and from a water balance perspective there are advantages in converting between these units. Table 25 documents the areas of the relevant regions and a conversion between volume and depth for ease of use to understand the numbers. For an area A in km^2 a volume of 1 GL corresponds to a depth of $1000/A$ mm. Equivalently, 100 mm depth of water over an area A in km^2 corresponds to a volume of $0.1 \times A$ GL.

Table 25. Relevant areas in the region and a conversion between depth and volume

Name of the Region or Component	Area in km^2 (1 ha = 0.01 km^2)	Depth in mm corresponding to volume of 1 GL	Volume in GL corresponding to 100 mm depth
Key regional delineations			
Barossa GI Zone	1666	0.6	166.6
Barossa PWRA	491	2.0	49.1
Area of the Barossa PWRA draining to Yaldara (streamflow gauging station)	376	2.7	37.6
Barossa Valley Wine Region	561	1.8	56.1
Eden Valley Wine Region	605	1.7	60.5
Primary vineyard areas			
Vineyards for Barossa GI†	140.7	7.1	14.1
Vineyards inside the Barossa PWRA	87.2	11.5	8.7
Vineyards inside the Barossa Valley Wine Region	117.5	8.5	11.8
Vineyards inside the Eden Valley Wine Region	23.2	43.1	2.3
Vineyards inside both the Barossa Valley Wine Region and the PWRA	74.9	13.4	7.5
Vineyards inside both the Eden Valley Wine Region and the PWRA	12.3	81.3	1.2
Areas connected to pipelines			
Area connected to Barossa Infrastructure Limited (BIL) pipeline (Assumed 80%* of the vineyard area in the	94	10.6	9.4

Barossa Valley Wine Region is connected to BIL)			
Area connected to SA Water pipeline (Assumed all vineyards are connected to SA water pipeline)	140.7	7.1	14.1
Area of Seppeltsfield vineyards (~20 km ² as per rough GIS layer estimates and region map**)	~20	50	2.0

† Total estimated vineyard area based on GIS layer across the Barossa GI using data provided by DEW on 14/10/2020.

* The options consultation report note that BIL services 75% of the growers in the Barossa Valley. A slightly higher number is used here (80%) for the percentage of vineyard area connected to BIL assuming that large growers would be connected to BIL.

** <https://barossawine.com/wp-content/uploads/2017/12/Barossa-Wine-Region.pdf>

Appendix B: Primary Hydrological Data Sources

Table 26. Rainfall stations in the key project delineations

Station ID	Station Name	Period of Record ¹	Latitude	Longitude	Mean & standard deviation of annual rainfall (on water year ² basis) in mm	
					1900/1901 to 2019/2020	1980/1981 to 2019/2020
23300	Angaston ^B	1889 -	-34.5018	139.0466	554 & 110	535 & 111
23302	Collingrove ^E	1889 -	-34.55	139.0833	589 & 122	536 & 113
23305	Greenock ^B	1882 -	-34.46	138.93	525 & 108	510 & 108
23309	Lyndoch ^B	1887 -	-34.5964	138.8733	548 & 110	533 & 108
23318	Tanunda ^B	1870 -	-34.5071	138.9637	546 & 108	535 & 108
23373	Nuriootpa PIRSA ^B	1996 -	-34.4761	139.0056	503 & 104	487 & 108
23725	Keyneton	1889 -	-34.5569	139.1338	529 & 118	499 & 116
23756	Williamstown (Glen Gillian) ^B	1951 -	-34.6603	138.9262	713 & 137	706 & 132
23752	Williamstown ^B	1880 -	-34.6508	138.8780	636 & 124	649 & 128
23302	Collingrove ^E	1874 - 1973	-34.5500	139.0833	541 & 131	442 & 97
23312	Nuriootpa ^B	1882 - 1997	-34.4747	138.9928	500 & 103	488 & 109
23313	Lyndoch (Pewsey Vale) ^E	1889 -	-34.6167	138.9833	723 & 146	641 & 126
23317	Stockwell ^B	1886 - 1998	-34.4364	139.0542	489 & 109	473 & 120
23321	Nuriootpa Comparison ^B	1952 - 1999	-34.4767	139.0047	505 & 104	487 & 107
23363	Rowland Flat 4 ^B	1882 - 1987	-34.5833	138.9333	577 & 110	547 & 114
Community gauge	Heggies Vineyard ^{E,3}	1935 - 2016	-34.595	139.03	749 & 158	734 & 181

¹ Based on site establishment and closure dates. The time period outside this operational period is infilled in the SILO patched point data that is used for the modelling.

² Wateruse year is from 1 July to 30 June, for comparison with wateruse data over the same period.

³ Date for years 2017 to 2020 at this site is not available, so the time series was infilled using data from nearby gauge 23725 for these years.

^B Gauge is in the Barossa valley wine region. ^E Gauge is in the Eden valley wine region.

Table 27. Summary of neighbouring rainfall stations

Station ID	Station Name	Period of Record	Latitude	Longitude	Mean & standard deviation of annual rainfall (on water year basis) in mm	
					1900/1901 to 2019/2020	1980/1981 to 2019/2020
23307	Kapunda	1889 -	-34.3412	138.9155	488 & 96	479 & 94
24509	Dutton	1980 -	-34.3515	139.1289	-	440 & 105
24525	Palmer	1889 -	-34.853	139.1607	409 & 105	379 & 110
24573	Truro	1889 -	-34.4085	139.1274	493 & 118	501 & 119

¹ Based on water years 1910-11 to 2019-20

Table 28. Stations in the key project delineations from which FAO56 PET is estimated

Station ID	Station Name	Period of Record ¹	Latitude	Longitude	Mean & standard deviation of annual PET (on water year basis) in mm	
					1900/1901 to 2019/2020	1980/1981 to 2019/2020
23300	Angaston ^E	1889 -	-34.5018	139.0466	1204 & 53	1219 & 61
23302	Collingrove ^E	1889 -	-34.55	139.0833	1192 & 53	1208 & 60
23305	Greenock ^B	1882 -	-34.46	138.93	1226 & 52	1241 & 60
23309	Lyndoch ^B	1887 -	-34.5964	138.8733	1245 & 50	1266 & 56
23318	Tanunda ^B	1870 -	-34.5071	138.9637	1229 & 52	1247 & 59
23373	Nuriootpa PIRSA ^B	1996 -	-34.4761	139.0056	1224 & 56	1248 & 64
23725	Keyneton ^E	1889 -	-34.5569	139.1338	1199 & 53	1215 & 60
23752	Williamstown ^B	1880 -	-34.6508	138.8780	1205 & 51	1226 & 58
23312	Nuriootpa ^B	1882 - 1997	-34.4747	138.9928	1228 & 56	1248 & 64
23313	Lyndoch (Pewsey Vale) ^E	1889 -	-34.6167	138.9833	1155 & 52	1165 & 60
23317	Stockwell ^B	1886 - 1998	-34.4364	139.0542	1229 & 53	1245 & 61

23321	Nuriootpa Comparison ^B	1952 - 1999	-34.4767	139.0047	1223 & 56	1246 & 64
-------	--------------------------------------	-------------	----------	----------	-----------	-----------

Appendix C: System connections under change for the Barossa Valley region

This section details the system connections under change for the Barossa Valley region. Table 29 summarises the key regression relationships that have been created from the component model results (Source and the two demand models).

Table 29. Regression form of component model results to be implemented into the Barossa Valley Stella model. All output units are in ML, as are input units (except P and E, which are in mm) and R² values are presented in the right-most column.

Metric	Component Model	Regression Relationship (all units in ML except for climate variables P and E (mm))	R ²	Comments
Streamflow	Source	$-2.67P + 0.0822P^2 - 10.3E + 6100$	0.84	Although the same recorded streamflow node as for the Barossa PWRA is used, slightly different streamflow is produced due to slightly different climate forcings. Overall a fairly good match with similar reduced range in absolute and relative change due to smoothing effect of regression.
Baseflow	Source, Lyne-Hollick Filter	$1350 - 0.731P + 0.0108P^2 - 1.87E$	0.81	Stella results are on average lower than the Source results, especially for low rainfall and high PET scenarios.
Maximum farm dam storage	Source	$13.6P - 0.00796P^2 - 1.04E - 1910$	0.77	Similar results between two models with reduced absolute and relative change bounds due to smoothing.
Surface water use	Source	$(-122 + 30.9 \ln Q) + (-6.98 + 0.910S_{DAM} - (3.80 \times 10^{-4})S_{DAM}^2 + (7.16 \times 10^{-8})S_{DAM}^3)$	0.71 (for Q) 0.93 (for S _{DAM})	Similar results, with larger difference between models for high rainfall scenarios; this is due to SW not being extracted in the Stella model if it is not needed to meet demand.
Demand	Regression on historical water use	$9780 + 129(0.1175)(0.55E - P) + N(0,2.59)$	0.58	Maximum demand for highest PET and lowest rainfall case – around 14.6 GL.
Demand	SARDI crop model	$117.5(-274 - 0.246P + 0.398E)$	0.49	Good comparison between models, Stella much smoother. Models furthest away for low rainfall and high PET scenarios. Larger demand than from the regression model. Larger demand than for the PWRA.

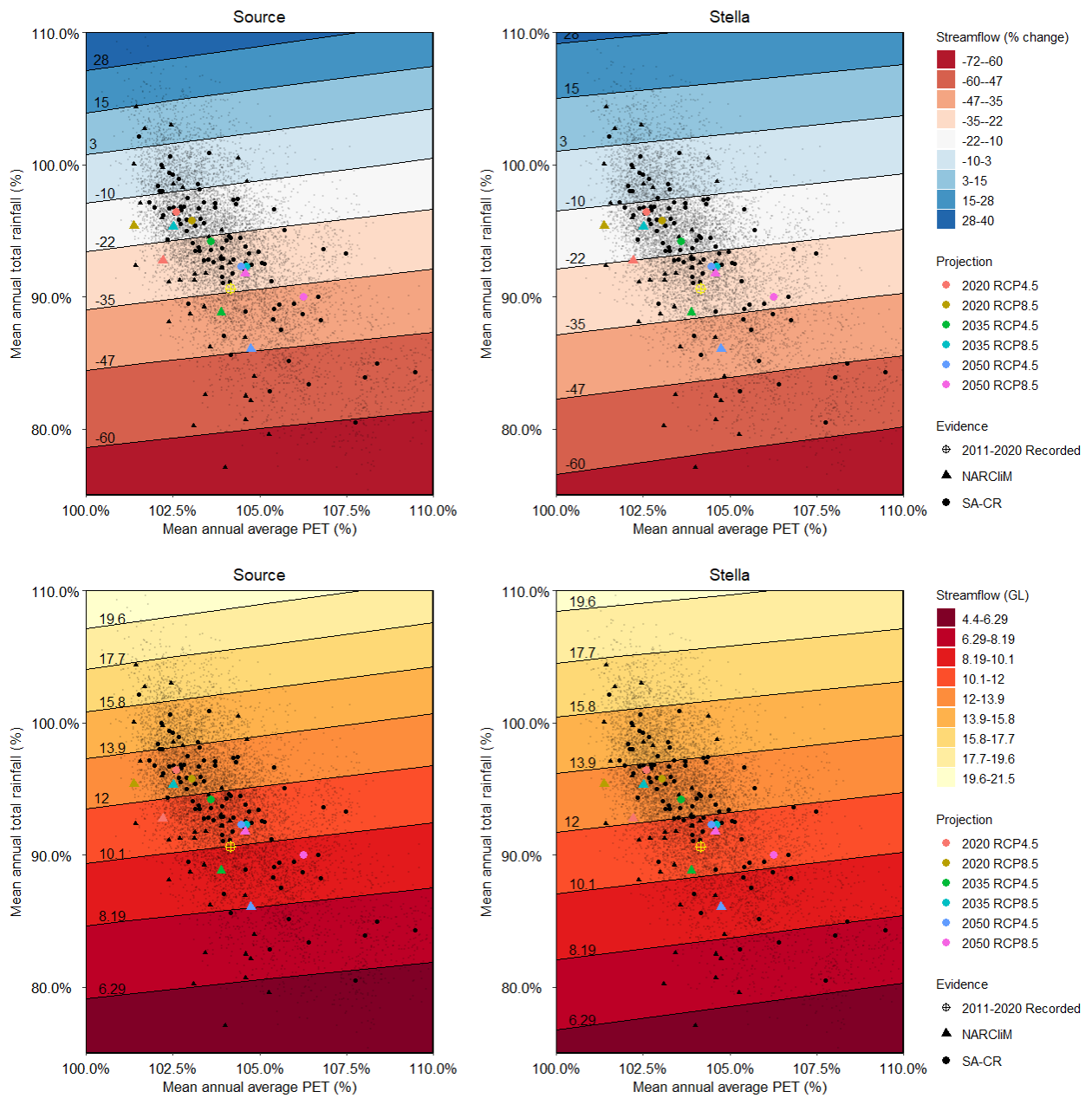


Figure 110. The performance space, both absolute and relative change, of Streamflow at Outlet Node 2 (Barossa Valley Gorge Source outflow) from simple scaling, both from Source (left) and Stella (right) results.

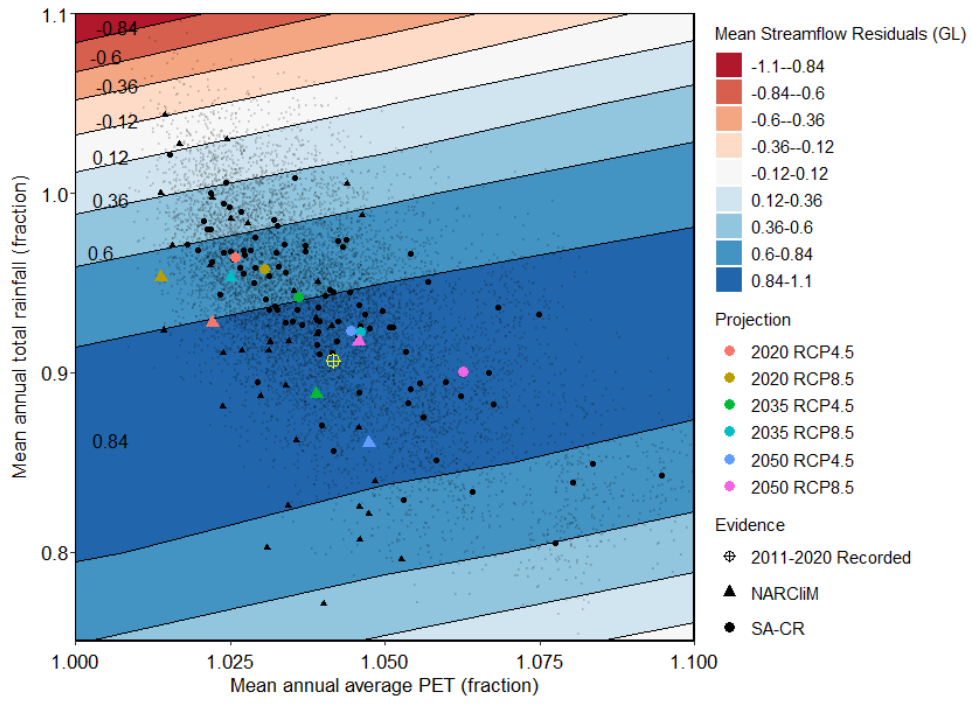


Figure 111. Residuals of the mean absolute streamflow values between Source and Stella

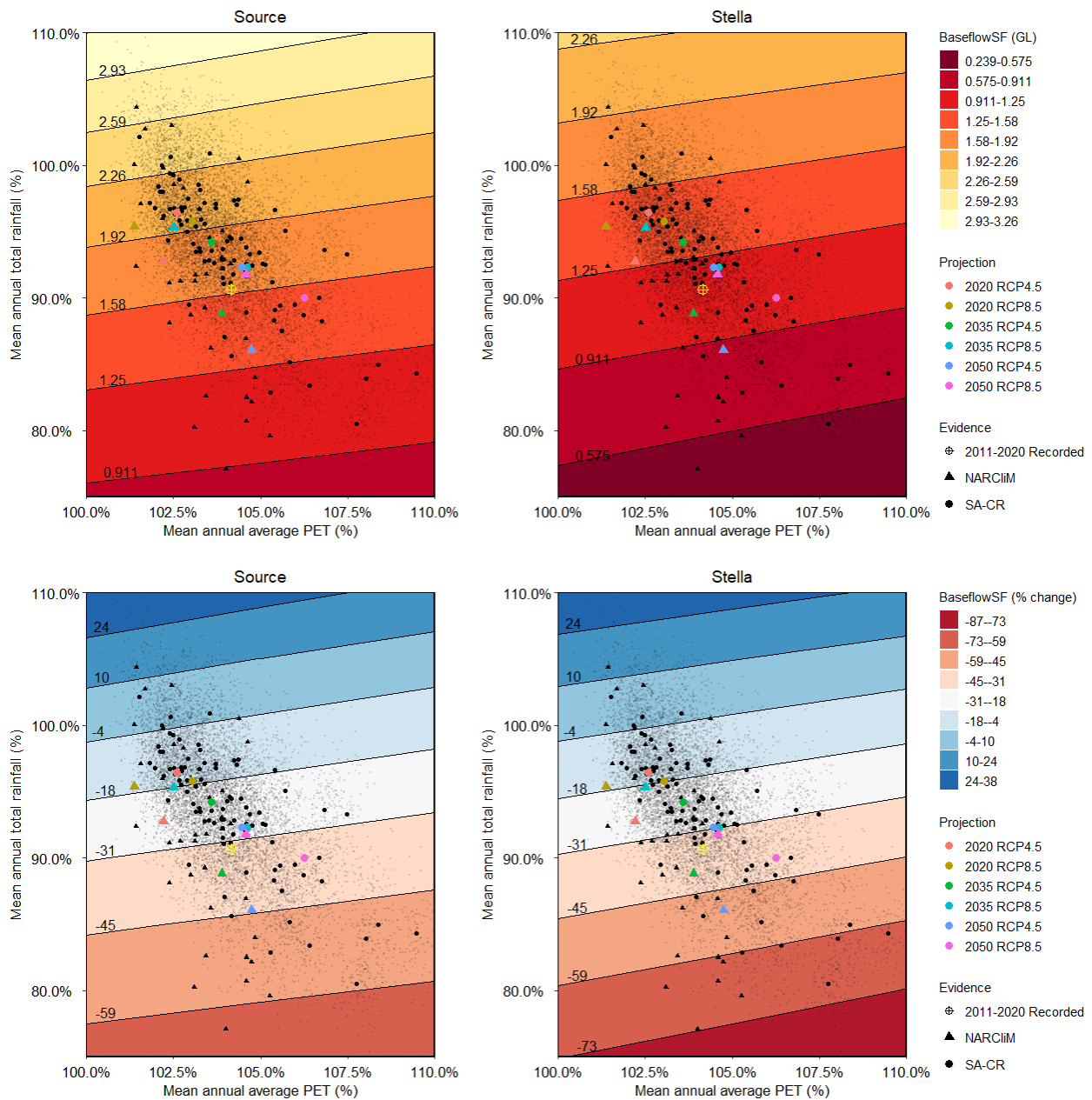


Figure 112. The performance space, both absolute and relative change, of Baseflow from filtering Streamflow at Outlet Node 2 (Barossa Valley Gorge Source outflow) from simple scaling, both from Source (left) and Stella (right) results.

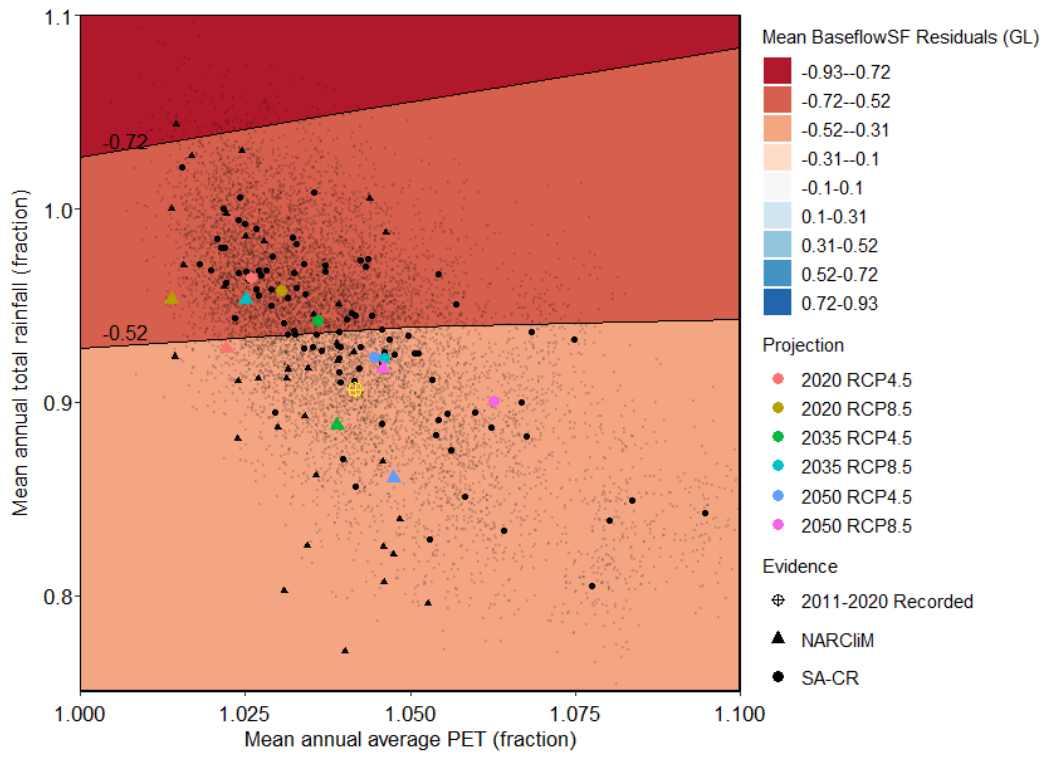


Figure 113. Residuals of the mean absolute baseflow values between Source and Stella

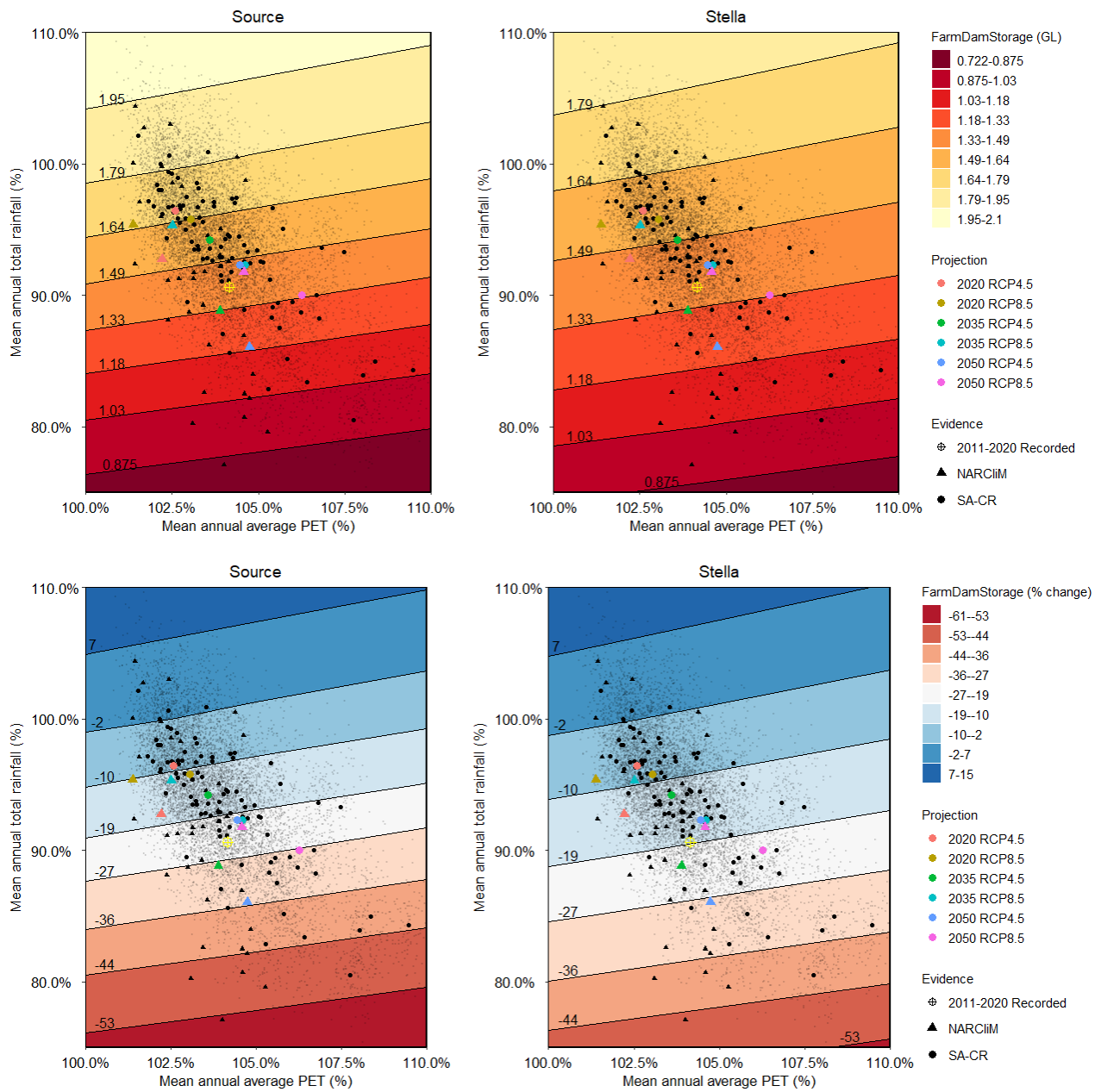


Figure 114. The performance space, both absolute and relative change, of average maximum farm storage from simple scaling, both from Source (left) and Stella (right) results.

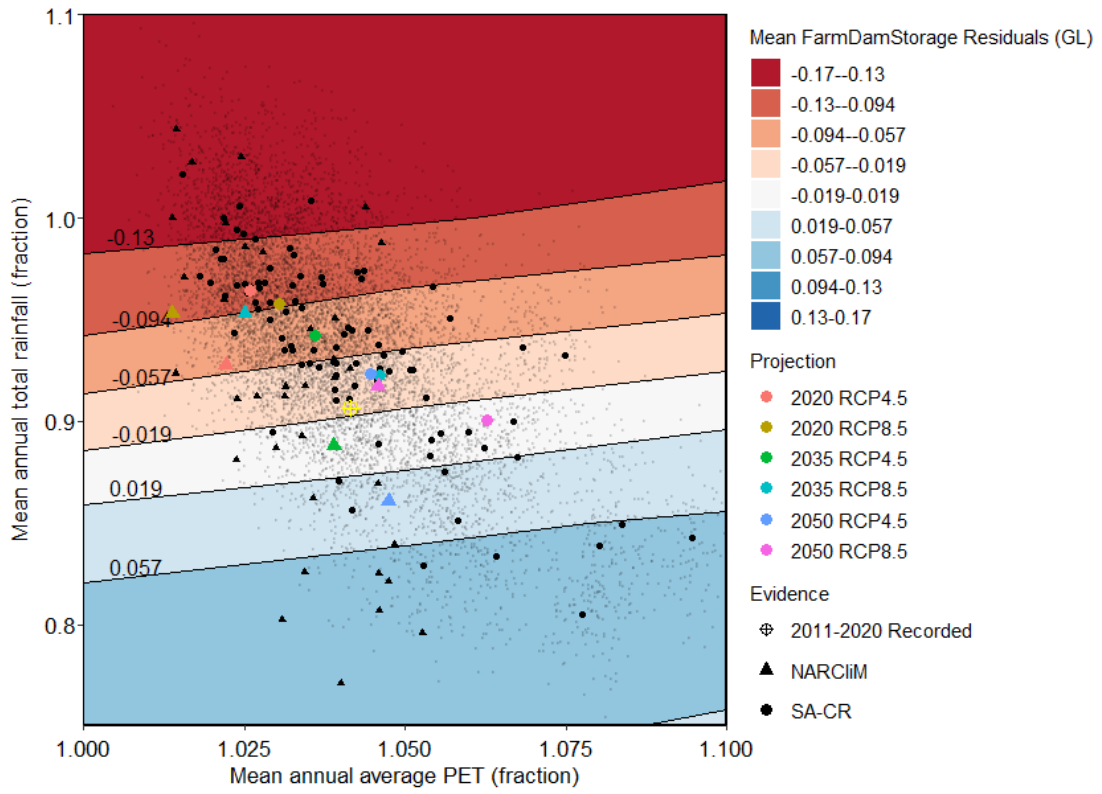


Figure 115. Residuals of the mean absolute maximum farm dam values between Source and Stella

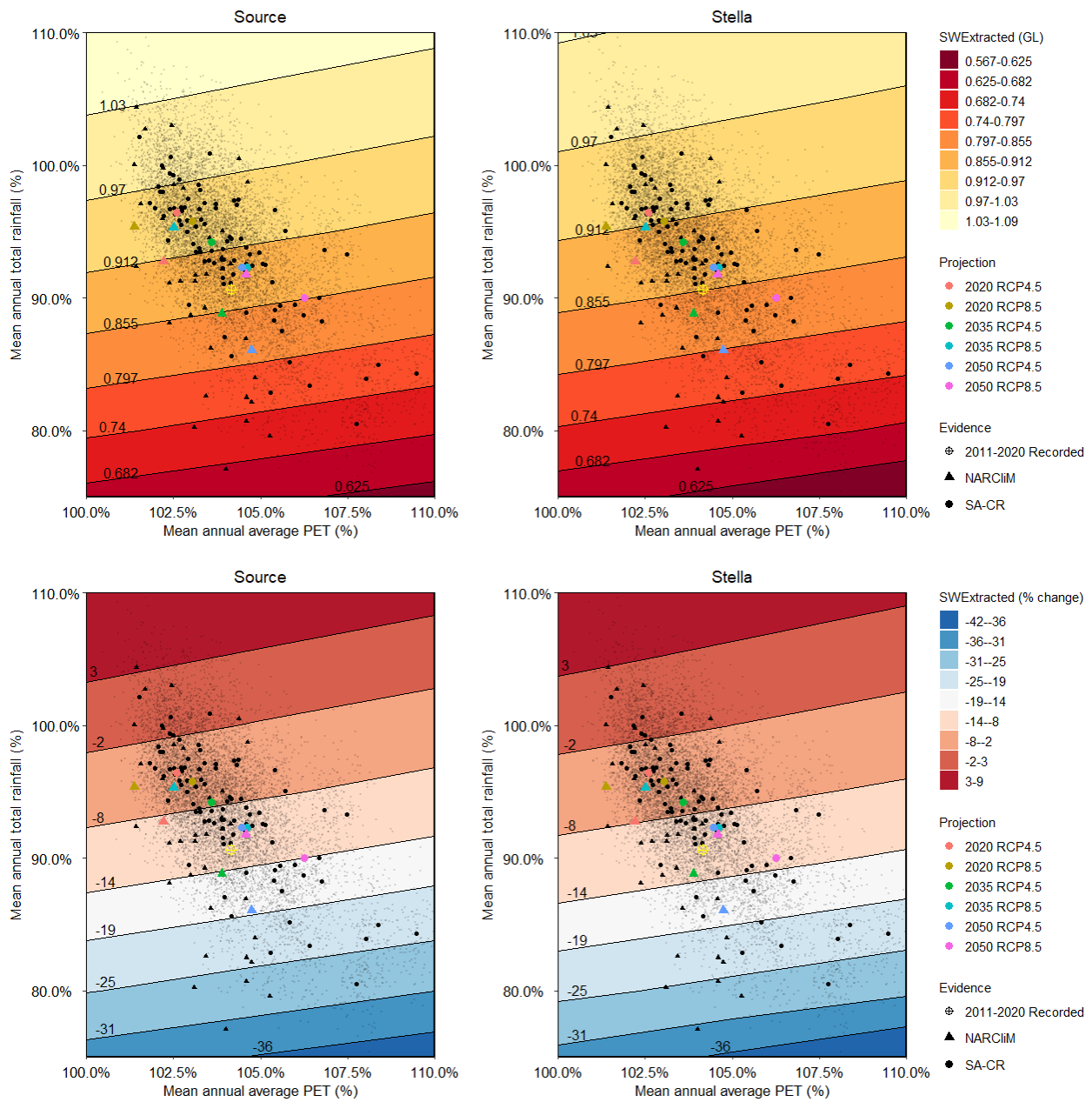


Figure 116. The performance space, both absolute and relative change, of average surface water extraction from simple scaling, both from Source (left) and Stella (right) results.

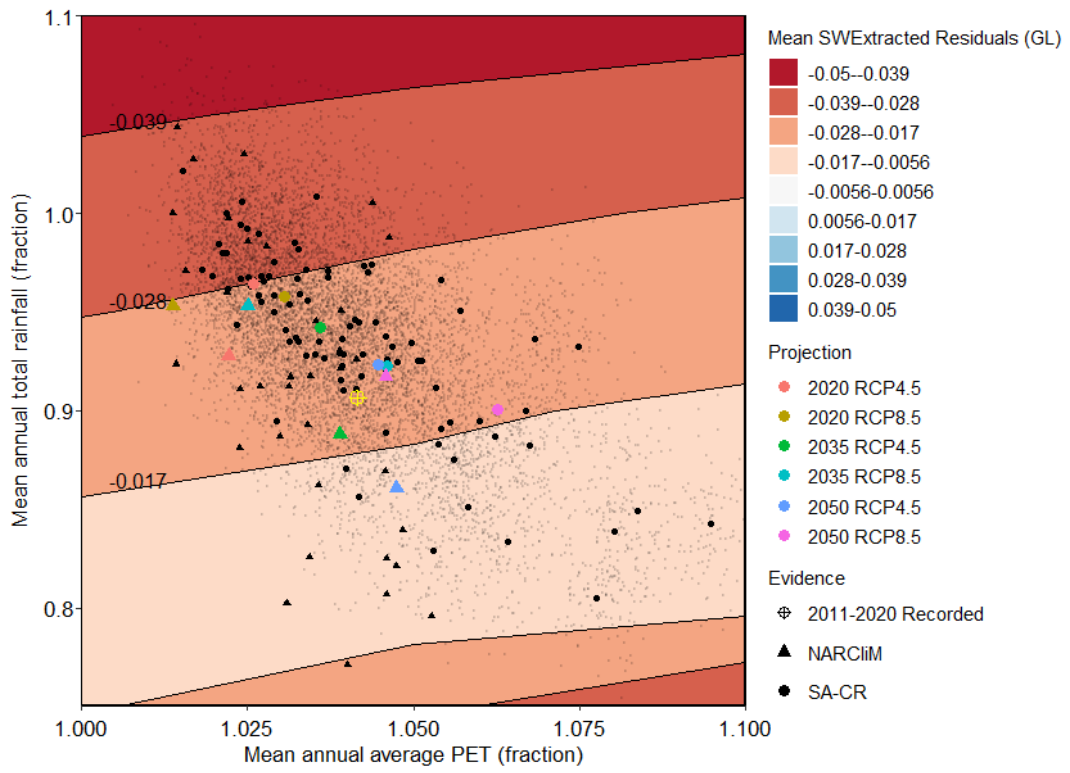
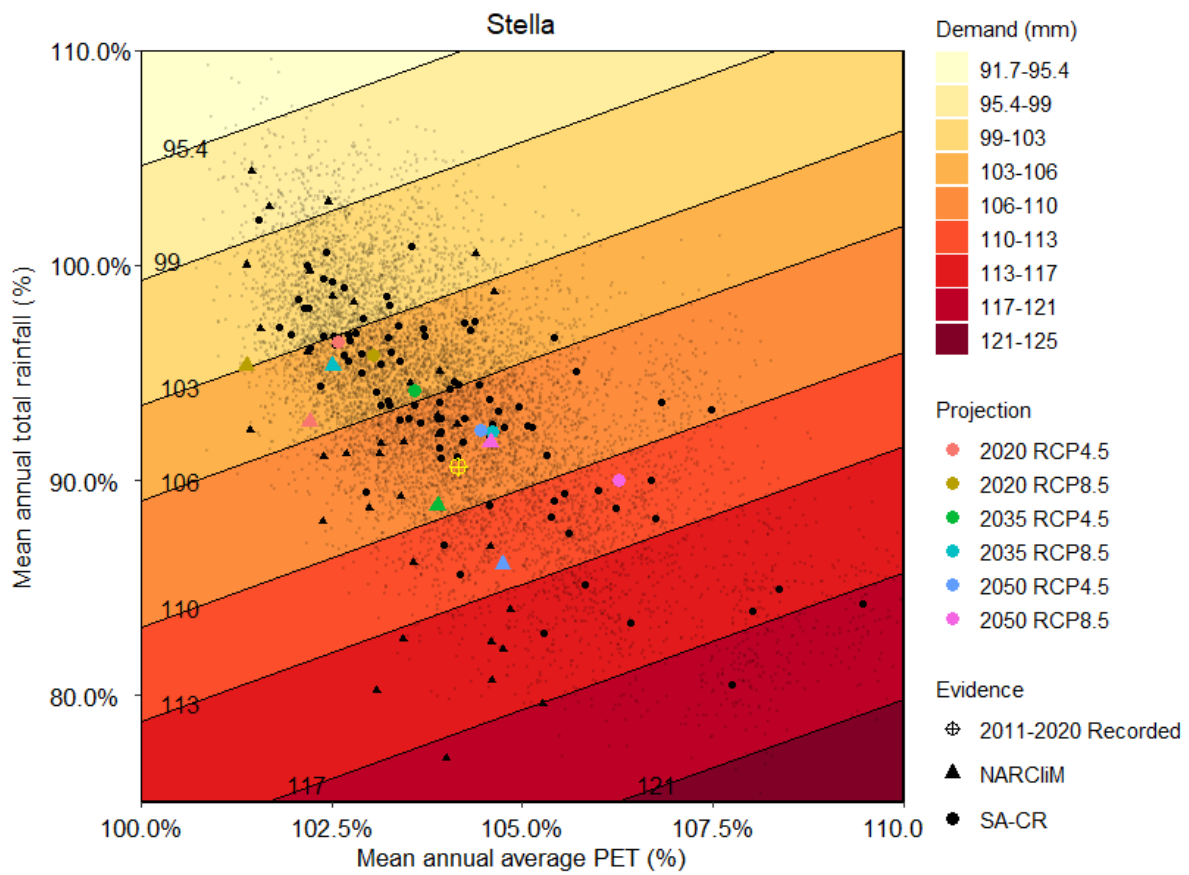
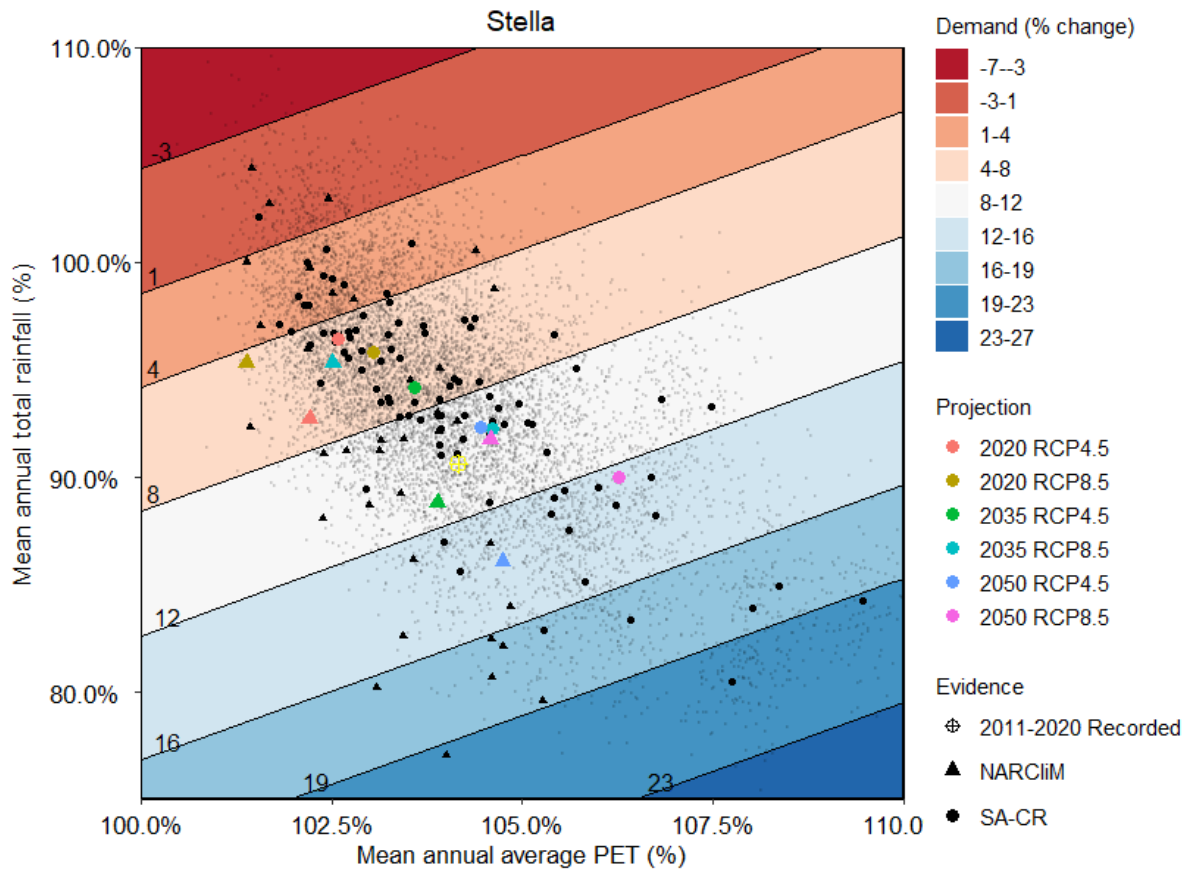


Figure 117. Residuals of the mean absolute surface water extraction values between Source and Stella



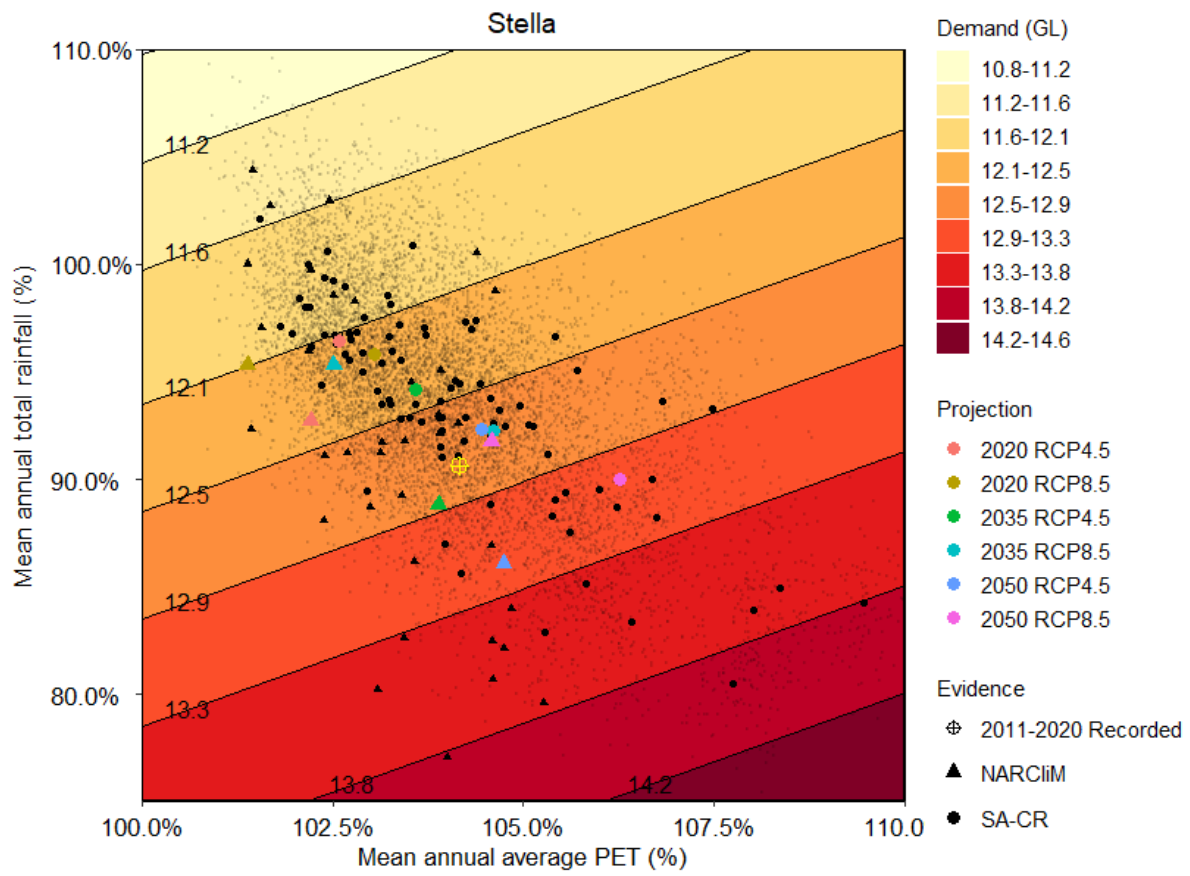


Figure 118. The performance space, both absolute (GL, bottom; mm, middle) and relative change (top), of regression-based demand from simple scaling, from Stella results.

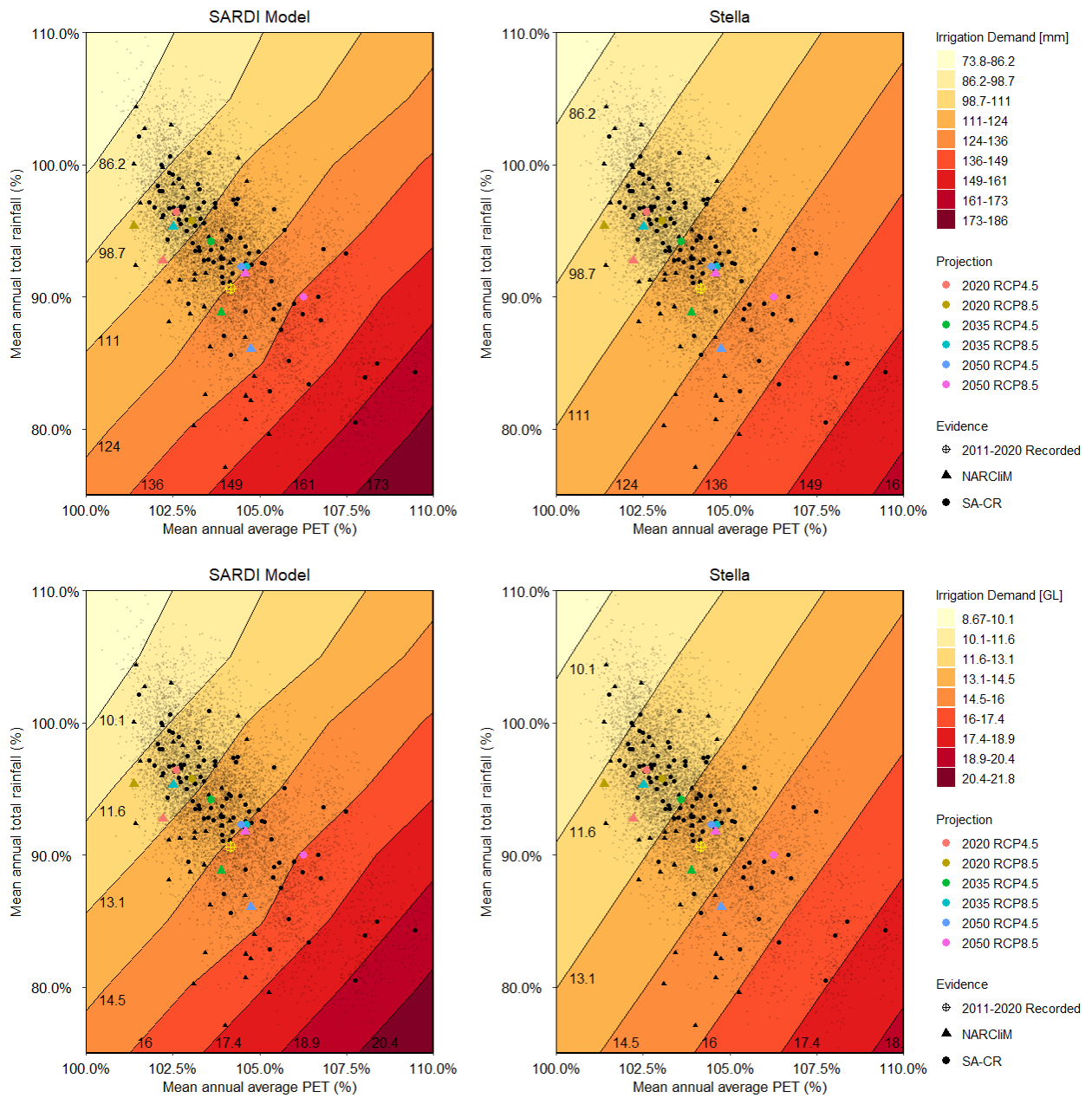


Figure 119. Performance space of absolute irrigation demand (mm top; GL bottom). The performance space of absolute irrigation demand from the regression model is shown for comparative purposes.

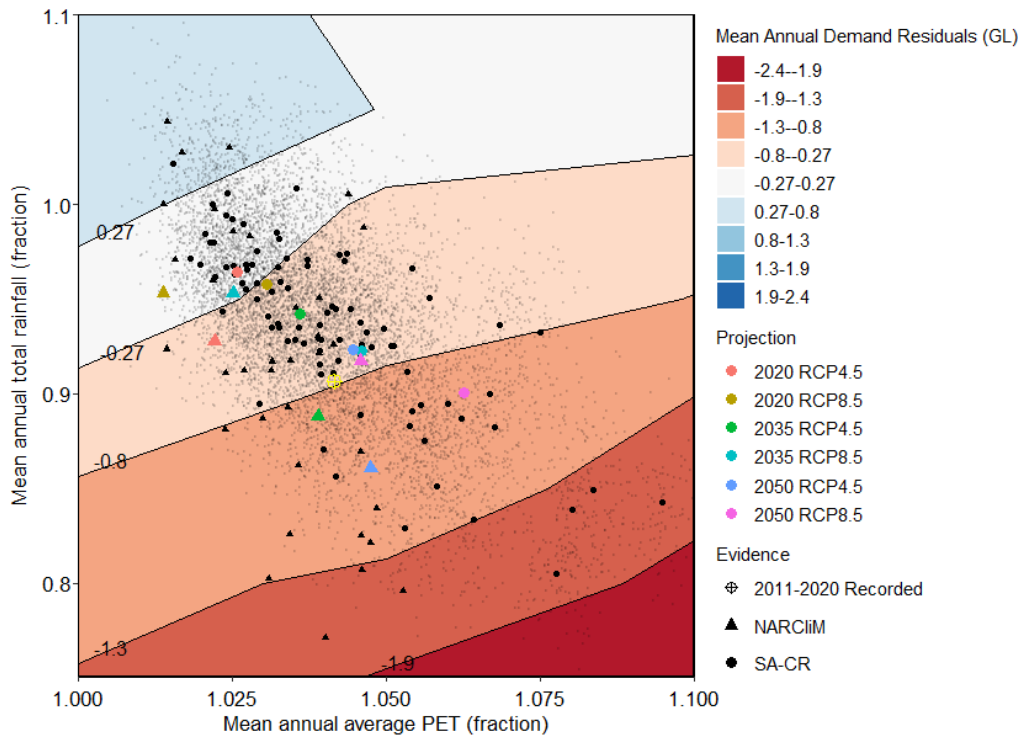


Figure 120. Mean Annual Demand Residuals (GL) between SARDI model and SARDI regression implemented in Stella

Appendix D: System connections under change for the Eden Valley region

This section details the system connections under change for the Eden Valley region. Table 30 summarises the key regression relationships that have been created from the component model results (Source and the two demand models).

Table 30. Regression form of component model results to be implemented into the Eden Valley Stella model. All output units are in ML, as are input units (except P and E, which are in mm) and R² values are presented in the right-most column.

Metric	Component Model	Regression Relationship (all units in ML except for climate variables P and E (mm))	R ²	Comments
Streamflow*	Source	$-6.64P + 0.130P^2 - 16.3E + 6660$	0.82	Models match well, reduced range due to smoothing observed from the Stella results.
Maximum farm dam storage	Source	$27.4P - 0.0137P^2 - 2.30E - 4290$	0.76	Good agreement between the models, but reduced range from Stella results due to smoothing.
Surface water use	Source	$(-45.7 + 8.29 \ln Q) + (-7.19 + 0.617S_{DAM} - (5.23 \times 10^{-5})S_{DAM}^2 + (2.38 \times 10^{-9})S_{DAM}^3)$	0.70 (for Q) 0.98 (for S _{DAM})	Similar results for most scenarios, expect for high rainfall. Like the other two delineations, SW is not extracted in Stella if it is not required to meet demand.
Demand	Regression on historical water use	$2570 + 90.3(0.0232)(0.55E - P) + N(0,0.226)$	0.73	Much smaller demand than for the Barossa PWRA and Barossa Valley. This is expected as this delineation has by far the smallest current demand.
Demand	SARDI crop model	$23.2(-270 - 0.198P + 0.375E)$	0.43	SARDI regression is more sensitive and gives a larger demand for the most extreme conditions than the regression model – around 4.3GL.

*Streamflow is aggregated from the outflow nodes of the Upper Jacobs Creek, Upper Tanunda Creek, Upper Angaston Creek, Duck Ponds Creek and Lower Flaxman Valley Zones. Note that baseflow is not included here as the streamflow is an aggregation of five different outflow locations, so applying the filter does not make sense.

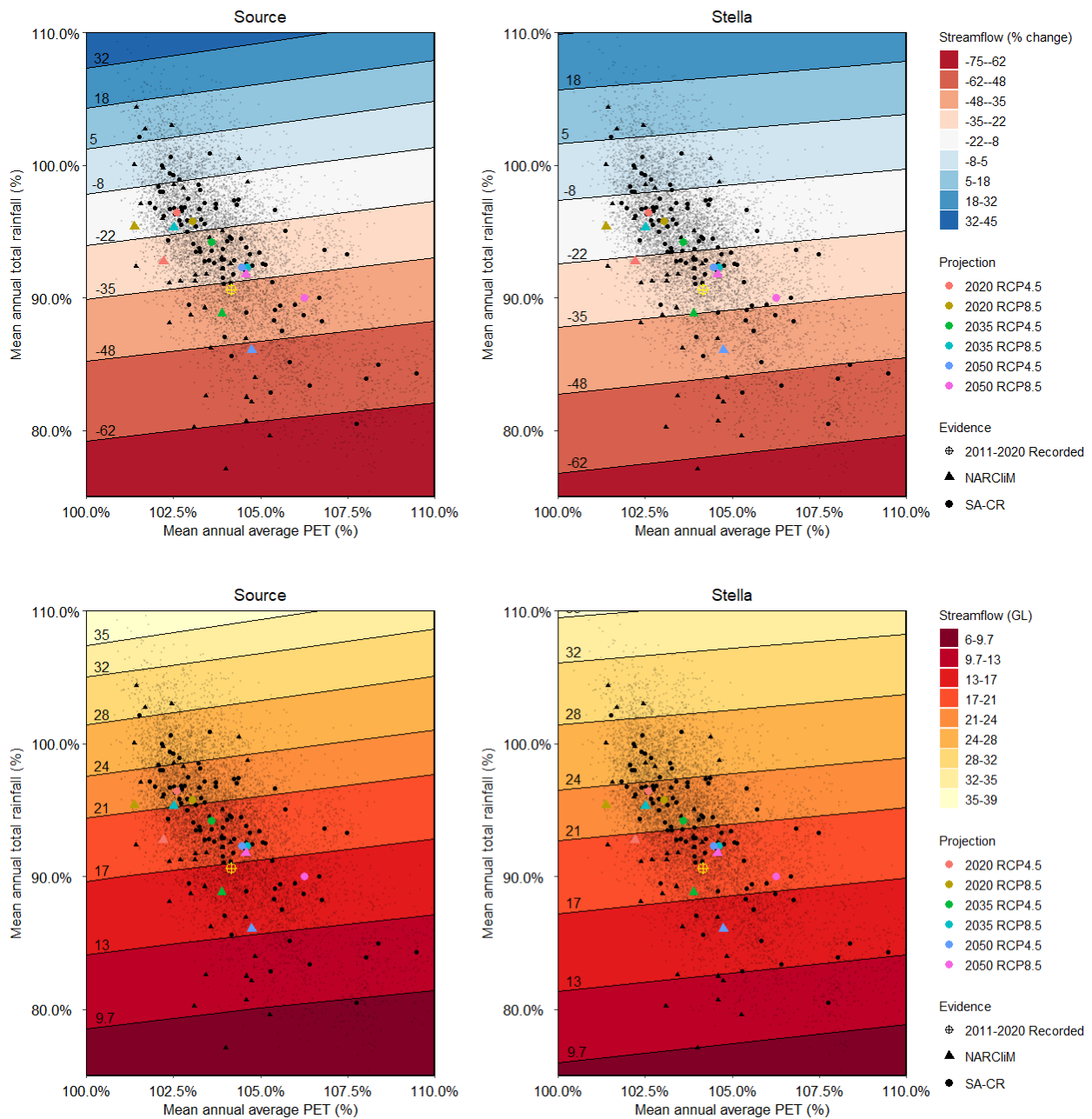
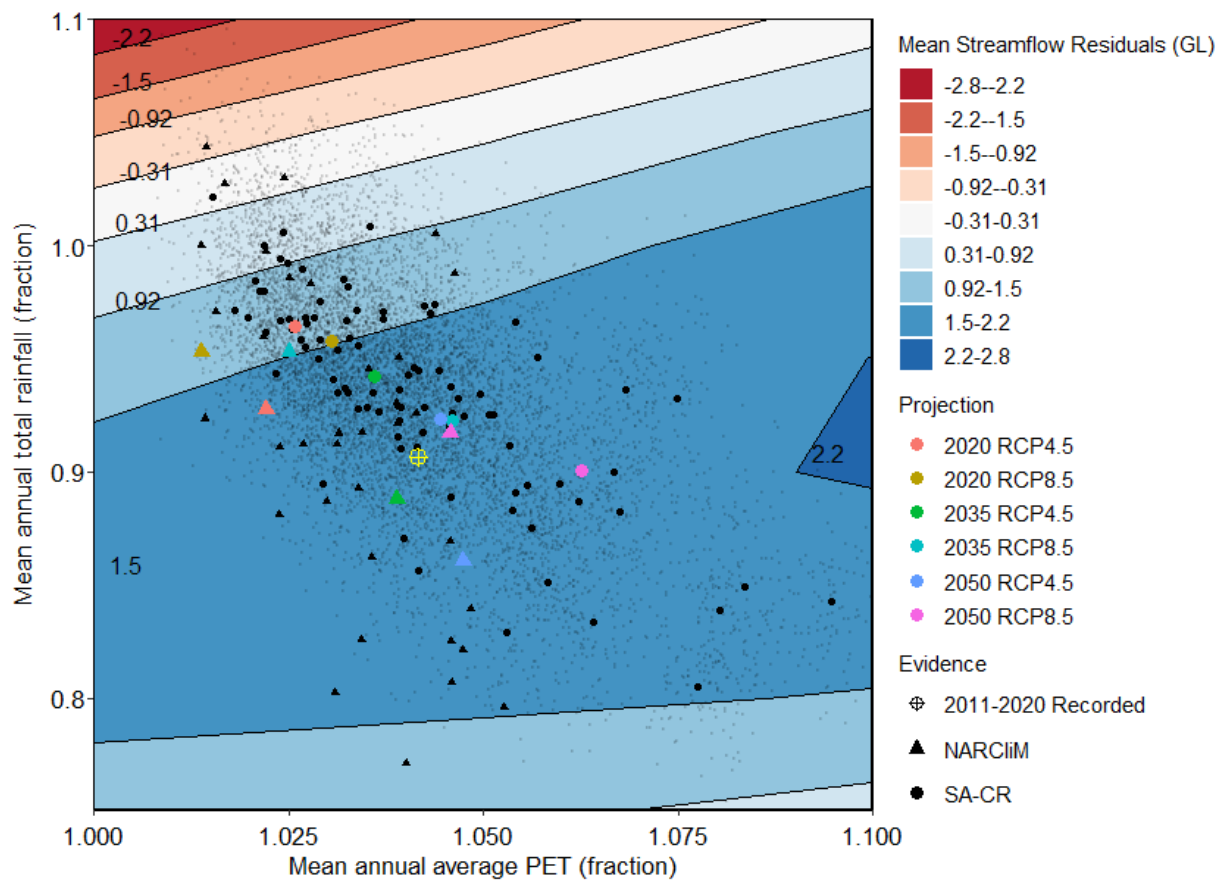


Figure 121. The performance space, both absolute and relative change, of average streamflow aggregated from five outflows from the Eden Valley from simple scaling, both from Source (left) and Stella (right) results.



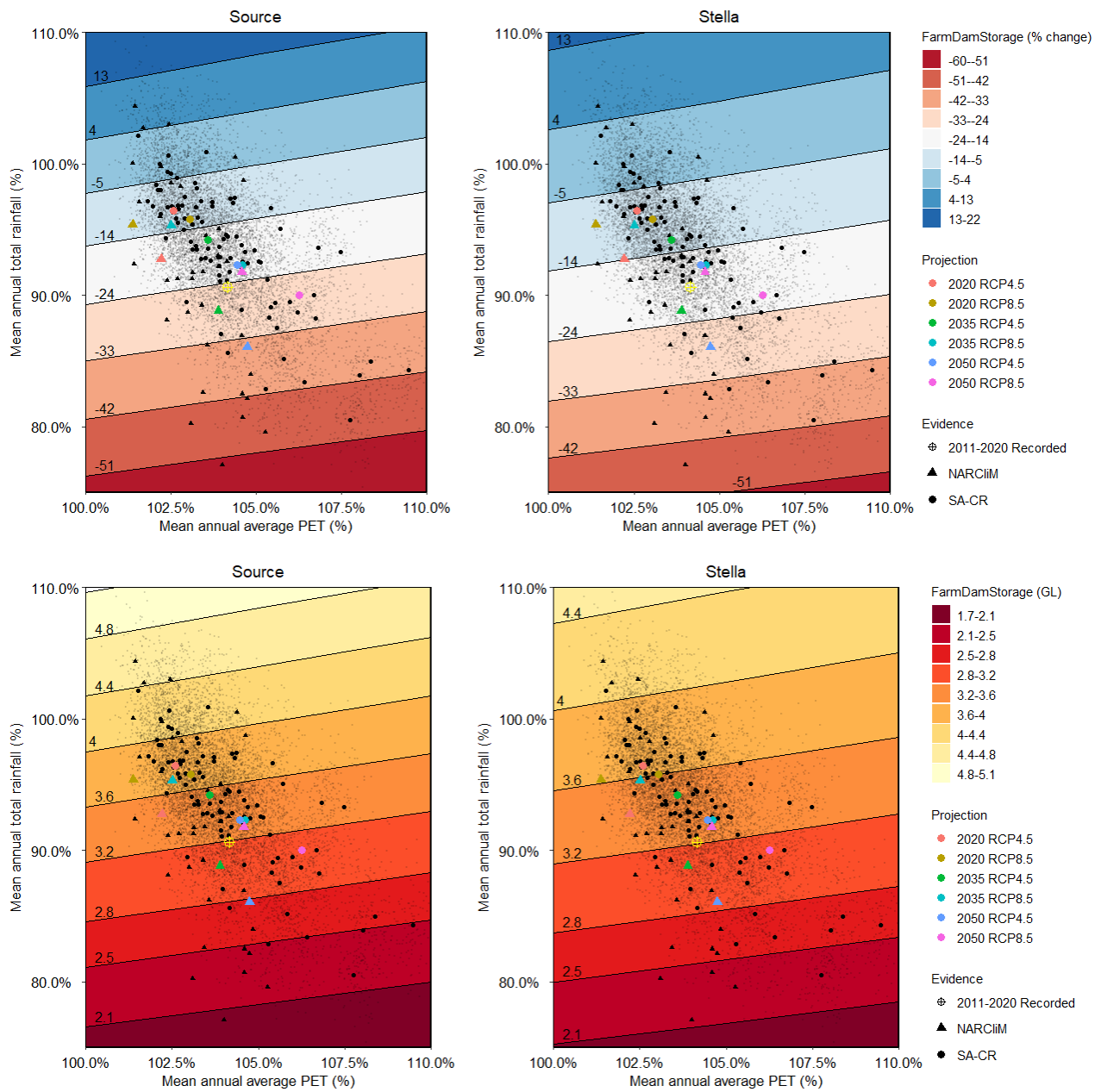
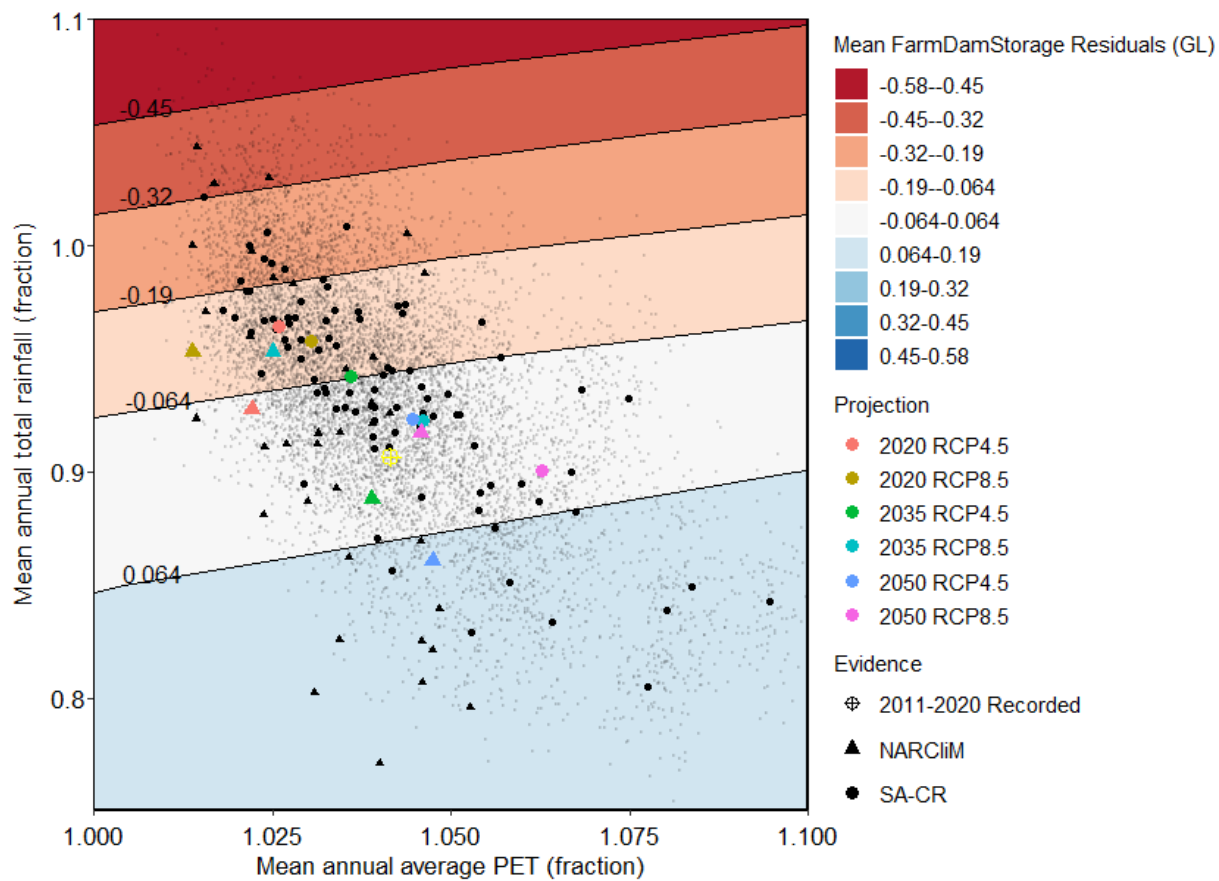


Figure 122. The performance space, both absolute and relative change, of average maximum farm storage from simple scaling, both from Source (left) and Stella (right) results.



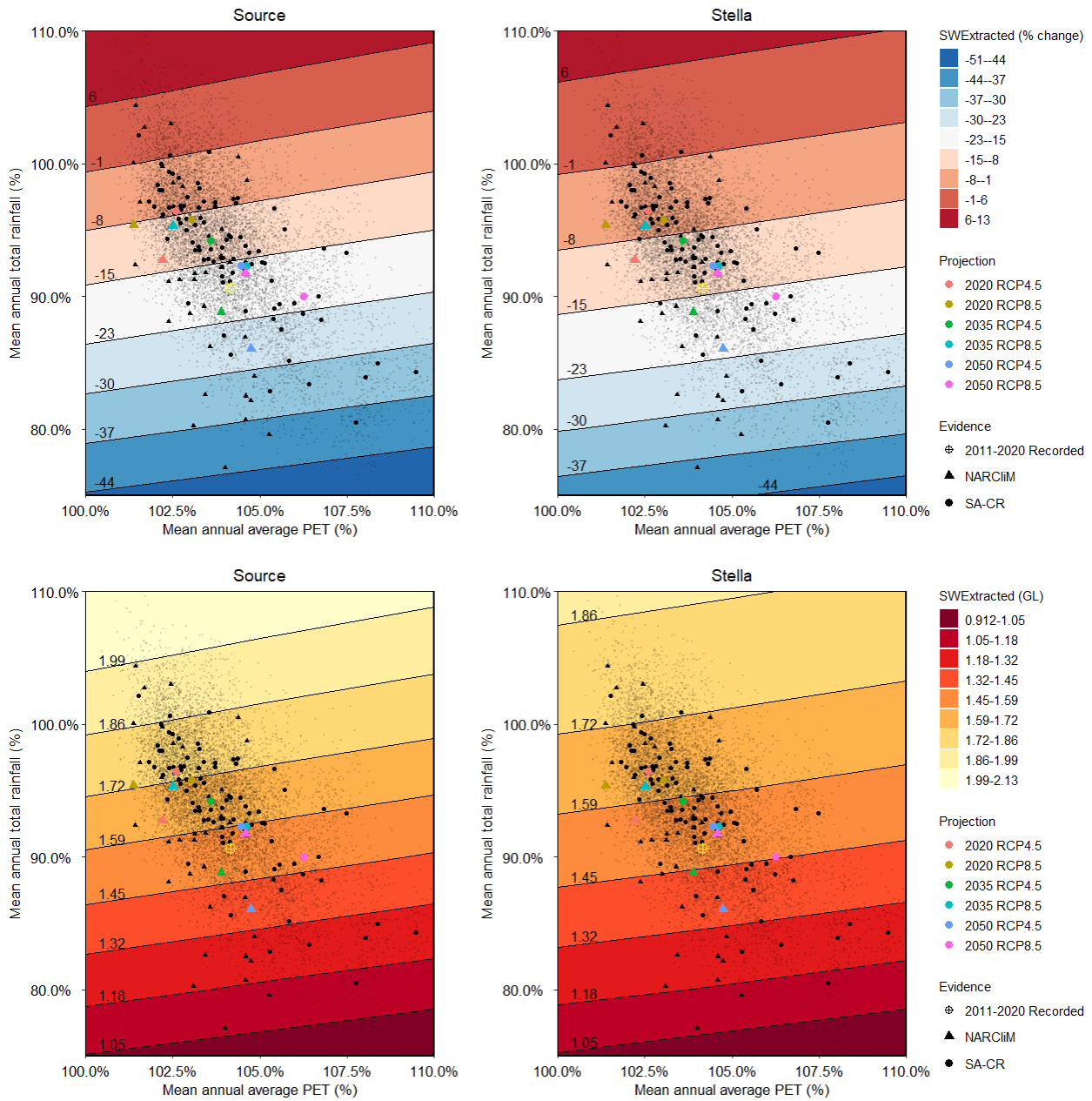
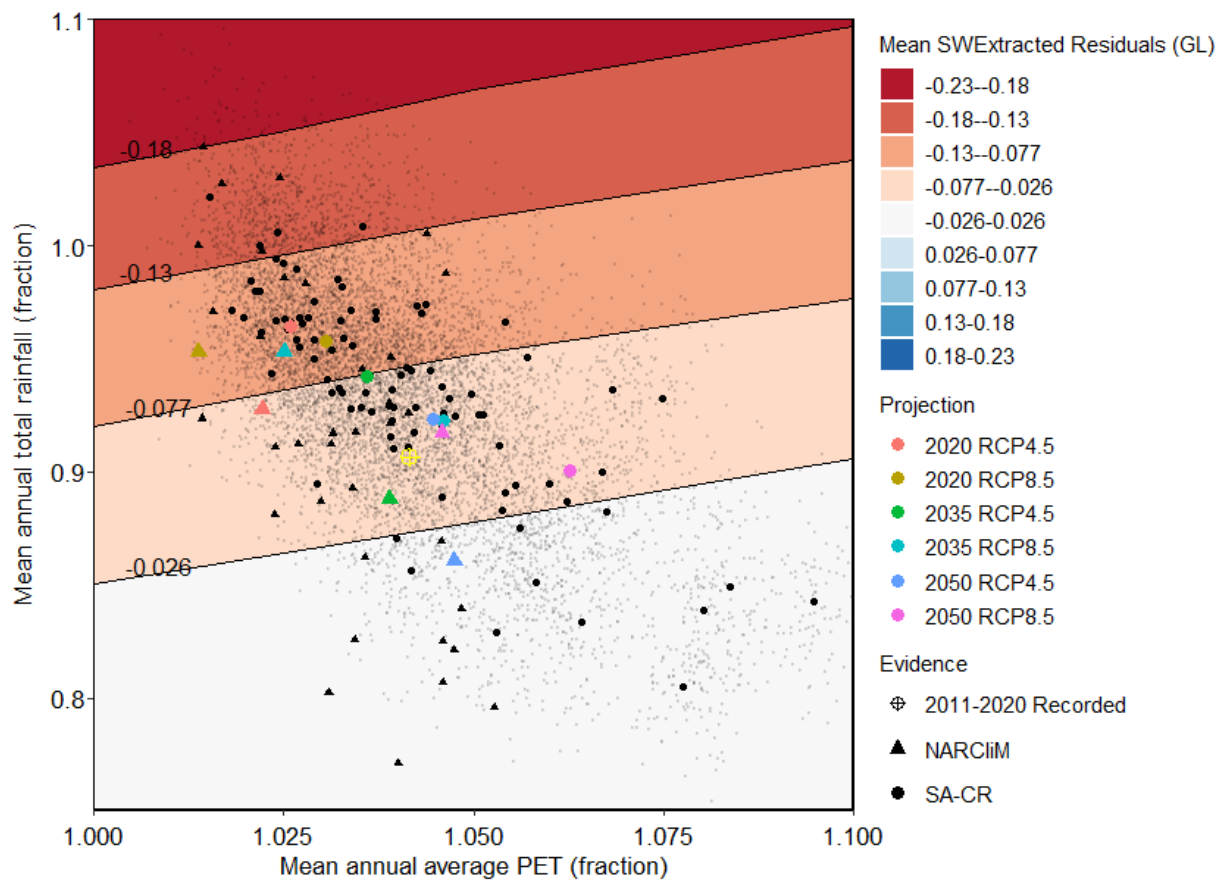
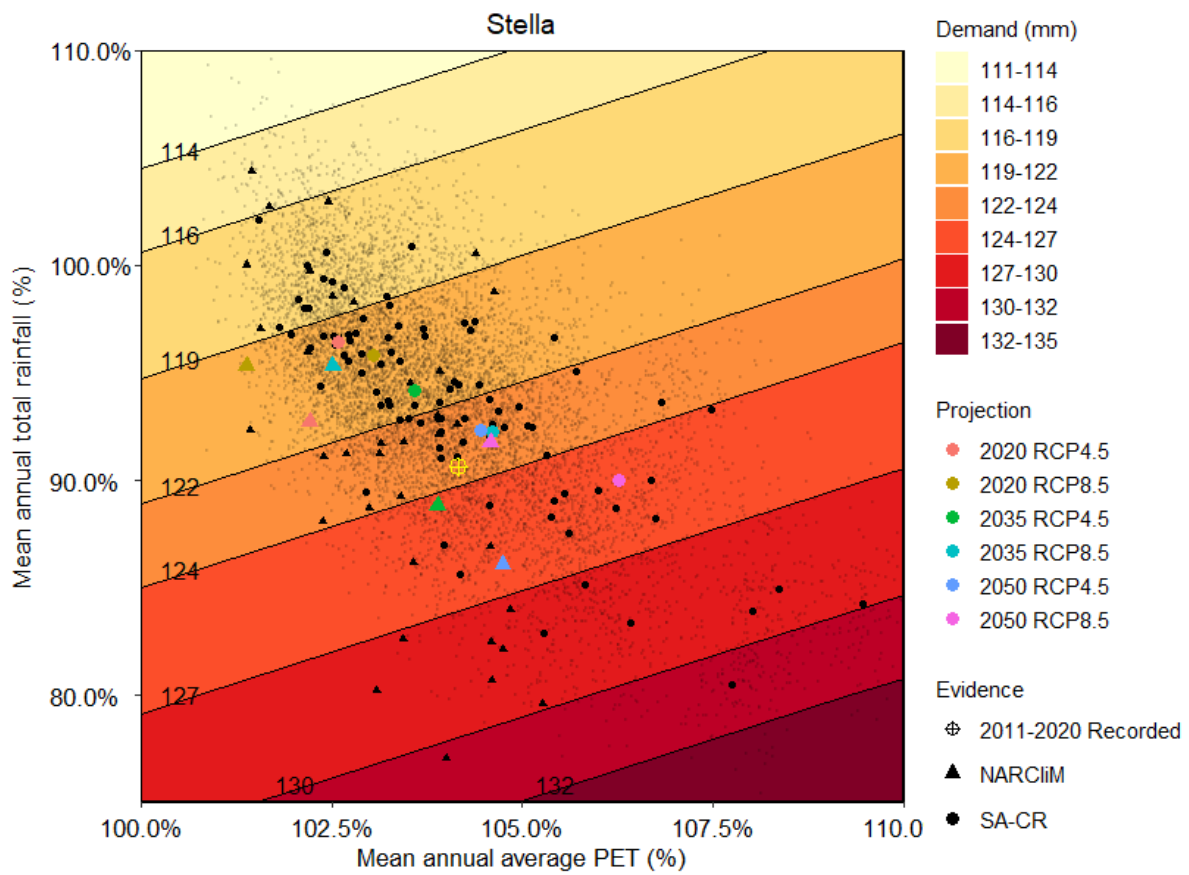
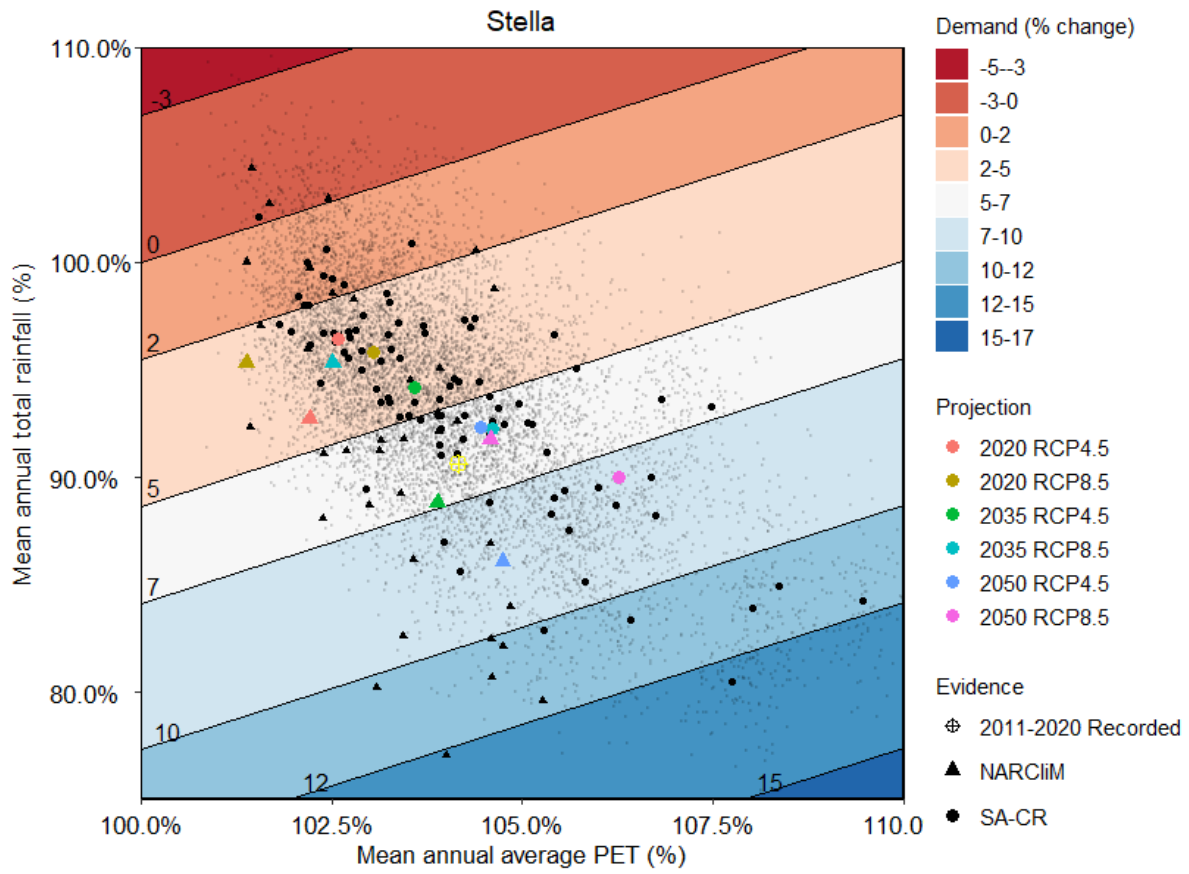


Figure 123. The performance space, both absolute and relative change, of average surface water extraction from simple scaling, both from Source (left) and Stella (right) results.





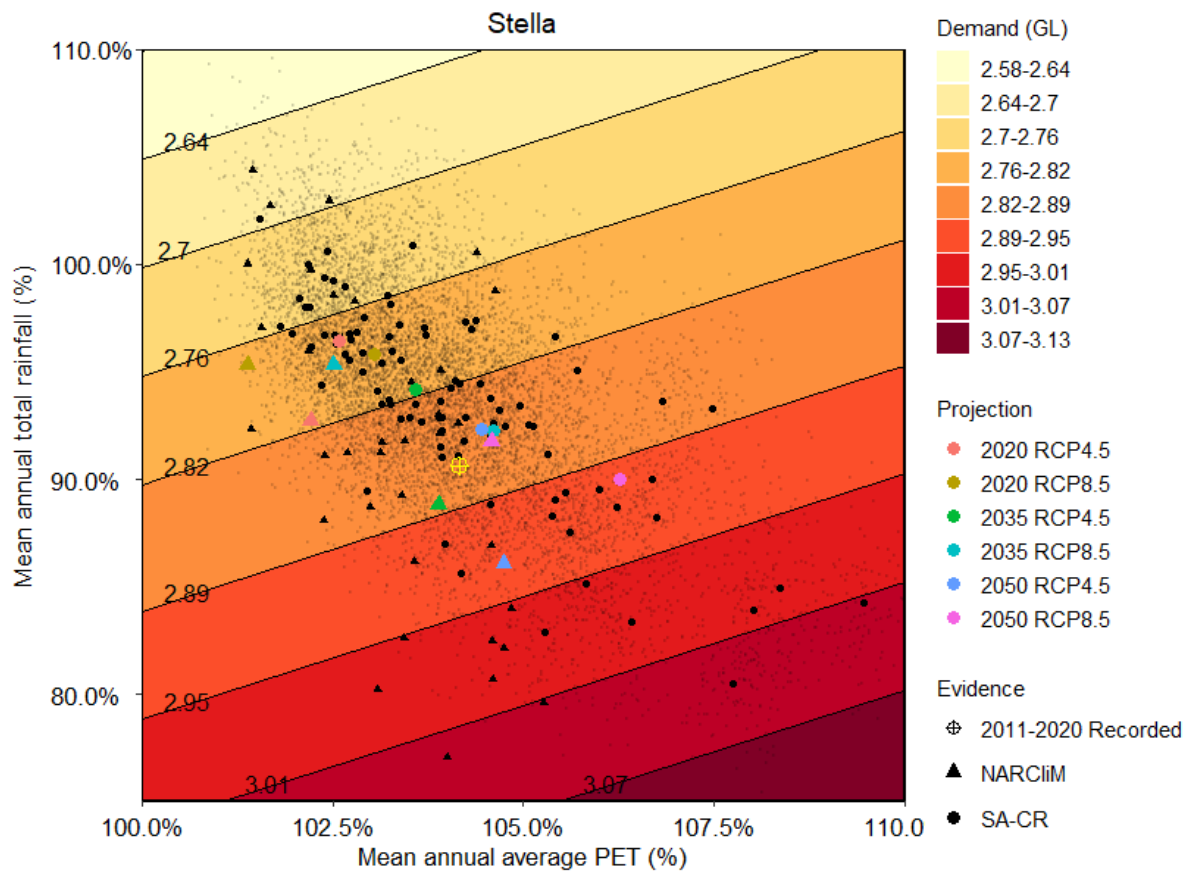


Figure 124. The performance space, both absolute (GL, bottom; mm, middle) and relative change (top), of regression-based demand from simple scaling, from Stella results.

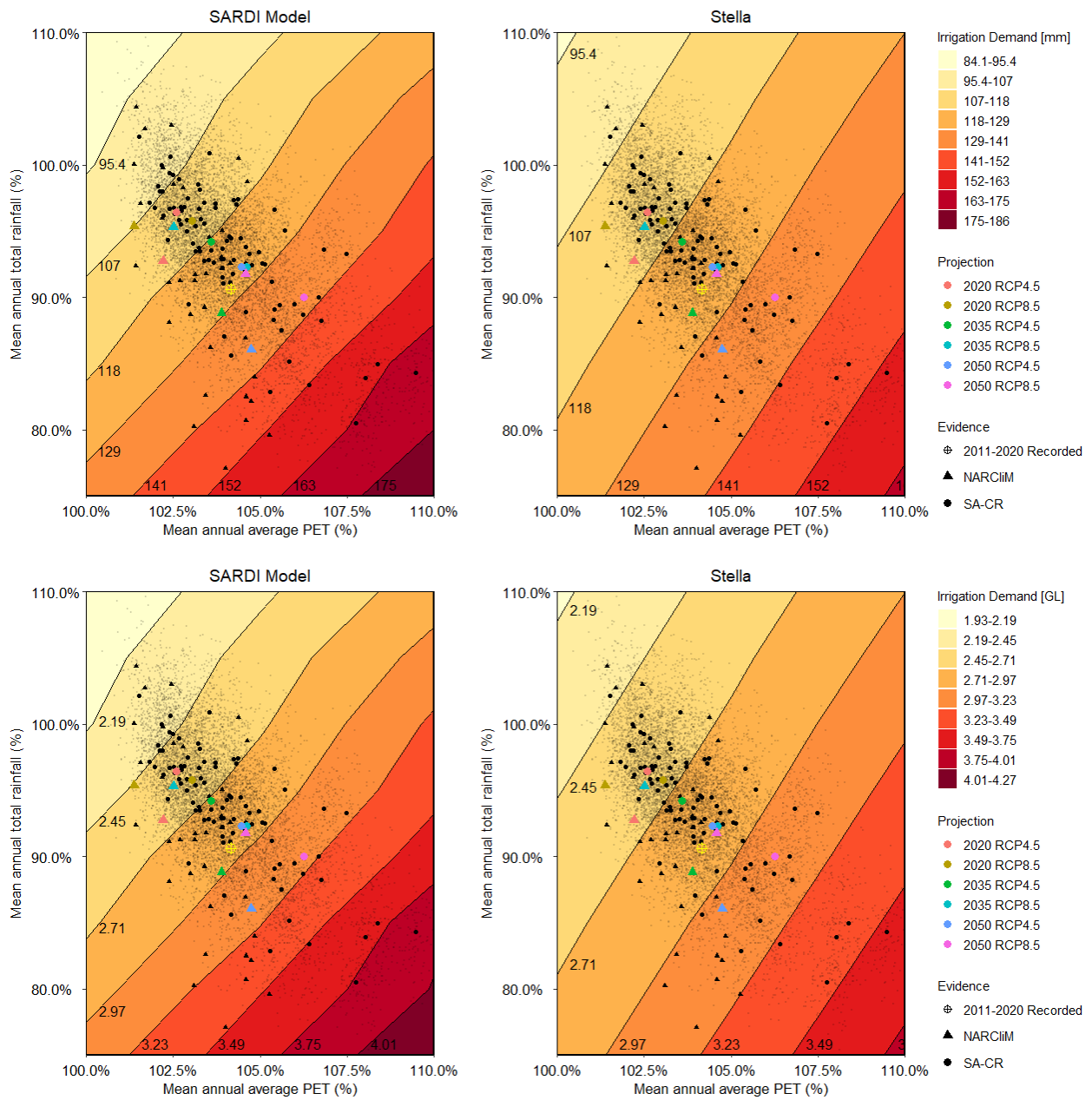


Figure 125. Performance space of absolute irrigation demand (mm top; GL bottom). The performance space of absolute irrigation demand from the regression model is shown for comparative purposes.

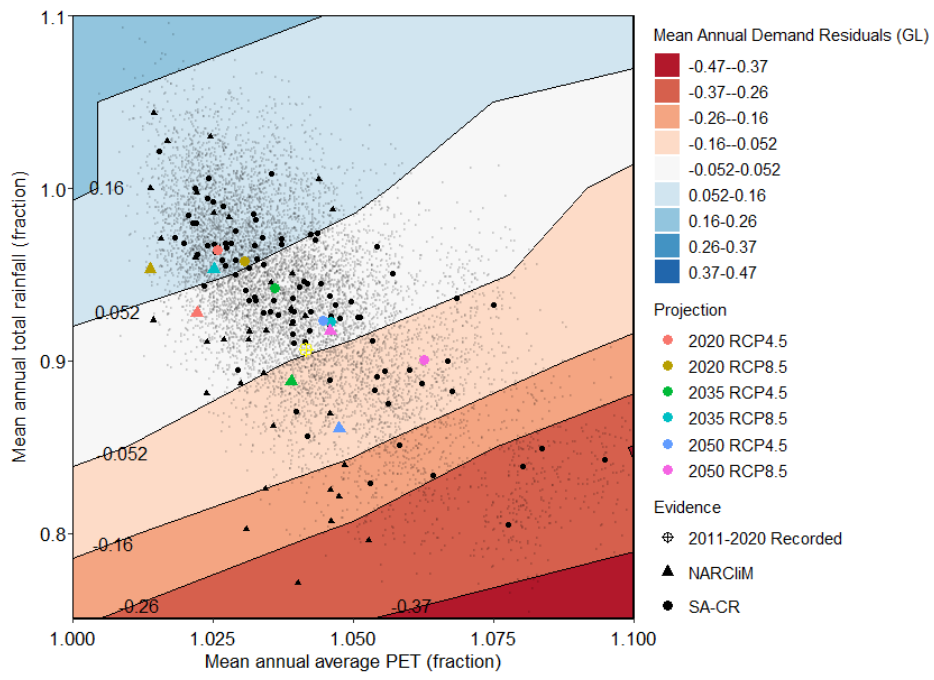


Figure 126. Mean Annual Demand Residuals (GL) between SARDI model and SARDI regression implemented in Stella

Appendix E: Stella diagnostics

Weighted Plots

A key component of Stella model establishment is to develop quantitative relationships between all the key modelling components. In many cases, this is achieved through emulation of component models. This section summarises the performance of this emulation, by representing the Stella regression plotted against the component model data. The following plots show the variable of interest against once forcing variable only (univariate) as this can be represented visually, but many of the components actually have bivariate relationships (see Table 19).

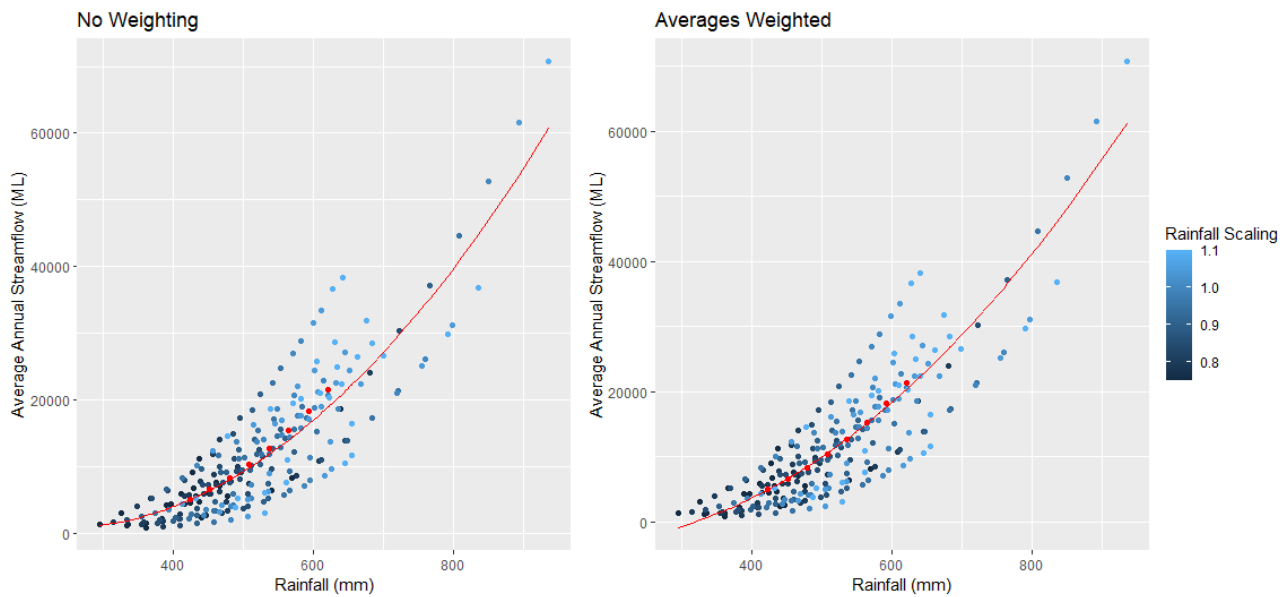


Figure 127. Scatter plots of annual average streamflow for a single PET perturbation (PET=1) and all rainfall perturbations tested (P=0.75-1.1). The scatter represents all of the raw points (from Source), coloured by rainfall perturbation, and the red points are the average of each of these perturbations. The left plot shows a univariate non-linear regression fitted to full scatter of raw data points; the right plots shows a univariate non-linear regression fitted to full scatter, with averages also included and weighted 100, while the other points are weighted 1.

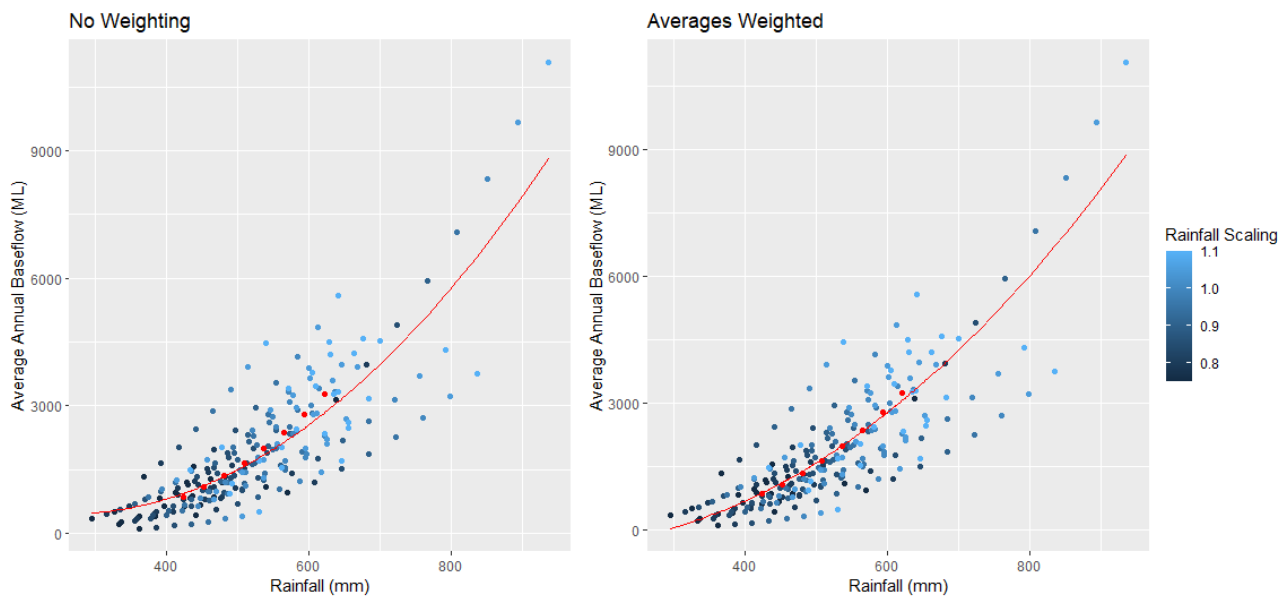


Figure 128. Scatter plots of annual average baseflow for a single PET perturbation (PET=1) and all rainfall perturbations tested (P=0.75-1.1). The scatter represents all of the raw points (from Source and Lyne-Hollick filter), coloured by rainfall perturbation, and the red points are the average of each of these perturbations. The left plot shows a univariate non-linear regression fitted to full

scatter of raw data points; the right plots shows a univariate non-linear regression fitted to full scatter, with averages also included and weighted 100, while the other points are weighted 1.

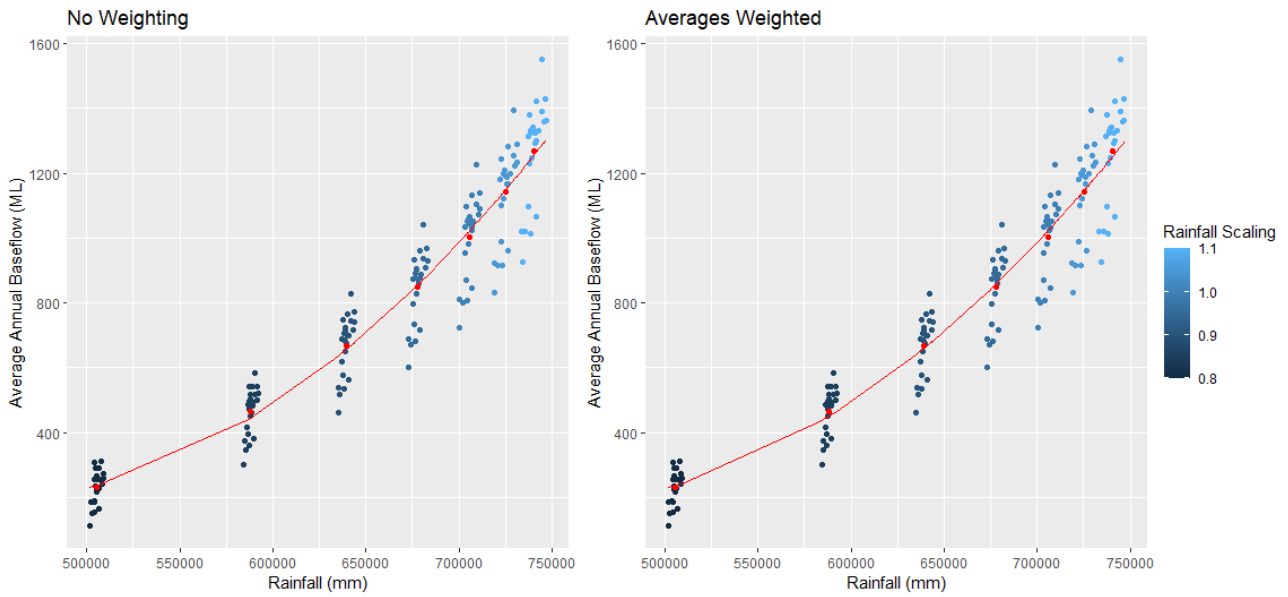


Figure 129. Scatter plots of annual average baseflow for a single PET perturbation (PET=1) and all rainfall perturbations tested (P=0.75-1.1). The scatter represents all of the raw points (from MODFLOW), coloured by rainfall perturbation, and the red points are the average of each of these perturbations. The left plot shows a univariate non-linear regression fitted to full scatter of raw data points; the right plots shows a univariate non-linear regression fitted to full scatter, with averages also included and weighted 100, while the other points are weighted 1.

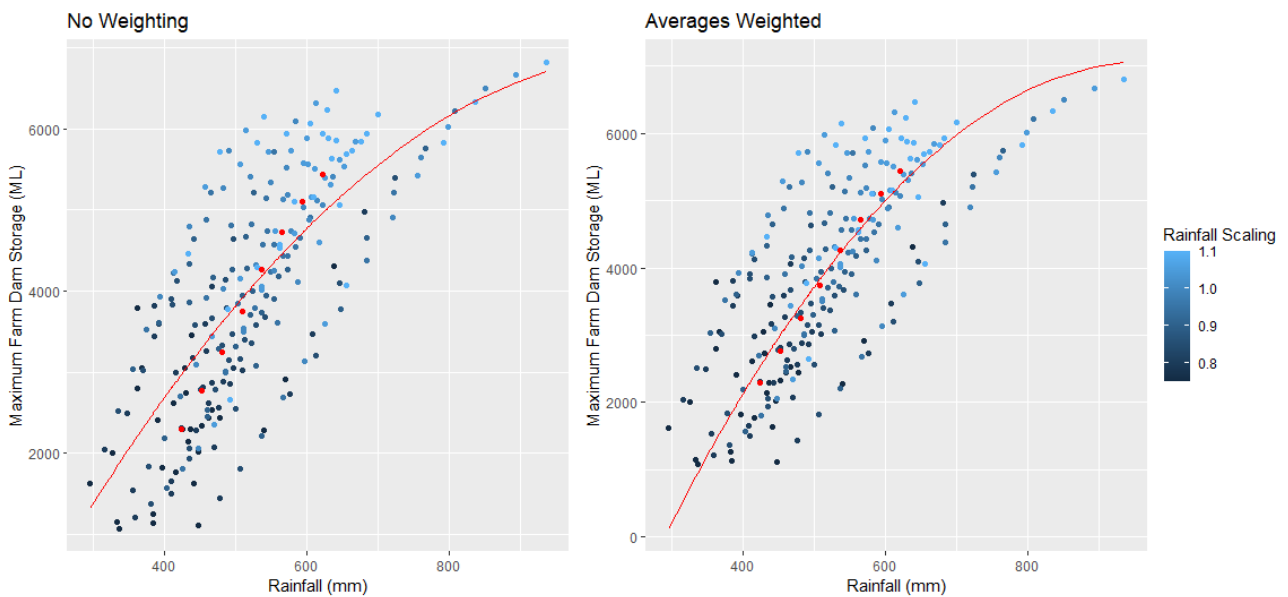


Figure 130. Scatter plots of maximum farm dam storage for a single PET perturbation (PET=1) and all rainfall perturbations tested (P=0.75-1.1). The scatter represents all of the raw points (from Source), coloured by rainfall perturbation, and the red points are the average of each of these perturbations. The left plot shows a univariate non-linear regression fitted to full scatter of raw data points; the right plots shows a univariate non-linear regression fitted to full scatter, with averages also included and weighted 100, while the other points are weighted 1.



Figure 131. Scatter plots of annual average farm dam extraction for a single PET perturbation (PET=1) and all rainfall perturbations tested (P=0.75-1.1). The scatter represents all of the raw points (from Source), coloured by rainfall perturbation, and the red points are the average of each of these perturbations. The left plot shows a univariate non-linear regression fitted to full scatter of raw data points; the right plots shows a univariate non-linear regression fitted to full scatter, with averages also included and weighted 100, while the other points are weighted 1.

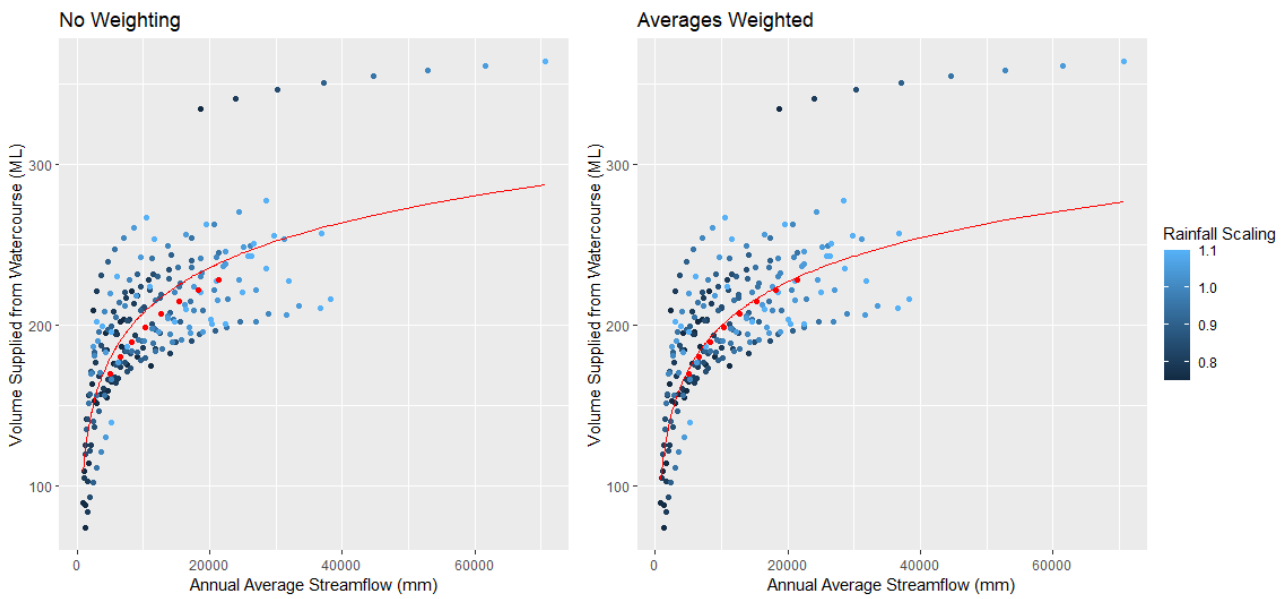


Figure 132. Scatter plots of annual average watercourse extraction for a single PET perturbation (PET=1) and all rainfall perturbations tested (P=0.75-1.1). The scatter represents all of the raw points (from Source), coloured by rainfall perturbation, and the red points are the average of each of these perturbations. The left plot shows a univariate logarithmic regression fitted to full scatter of raw data points; the right plots shows a univariate non-linear regression fitted to full scatter, with averages also included and weighted 100, while the other points are weighted 1.

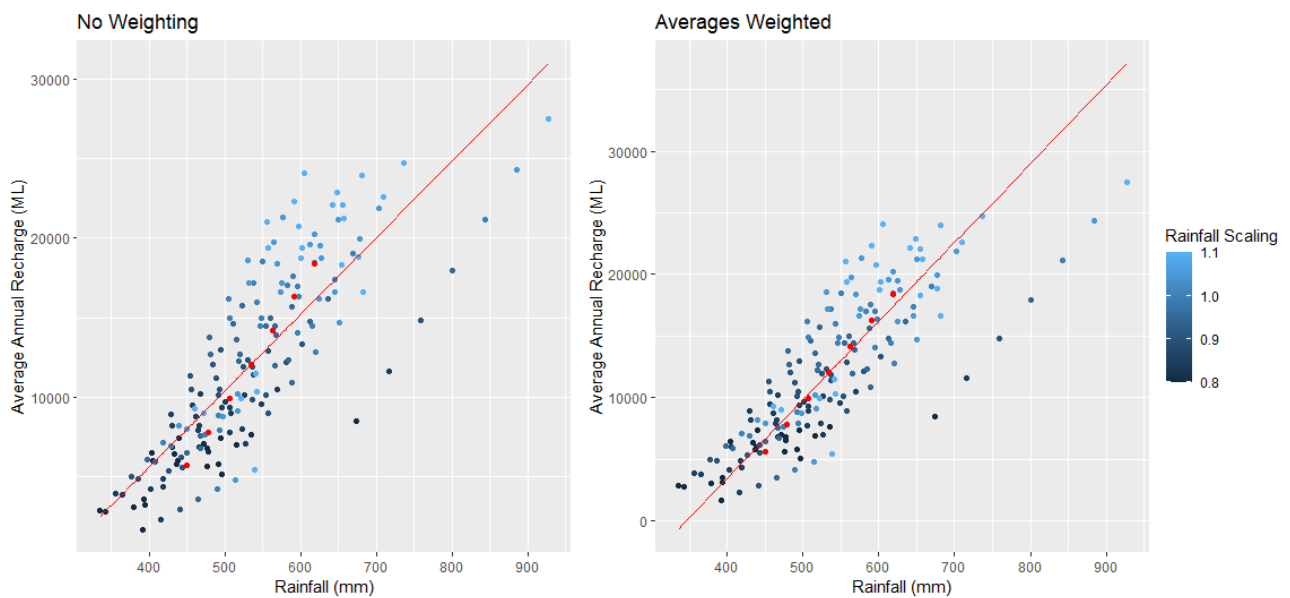


Figure 133. Scatter plots of annual average recharge for a single PET perturbation ($PET=1$) and all rainfall perturbations tested ($P=0.75-1.1$). The scatter represents all of the raw points (from MODFLOW), coloured by rainfall perturbation, and the red points are the average of each of these perturbations. The left plot shows a univariate linear regression fitted to full scatter of raw data points; the right plots shows a univariate non-linear regression fitted to full scatter, with averages also included and weighted 100, while the other points are weighted 1.

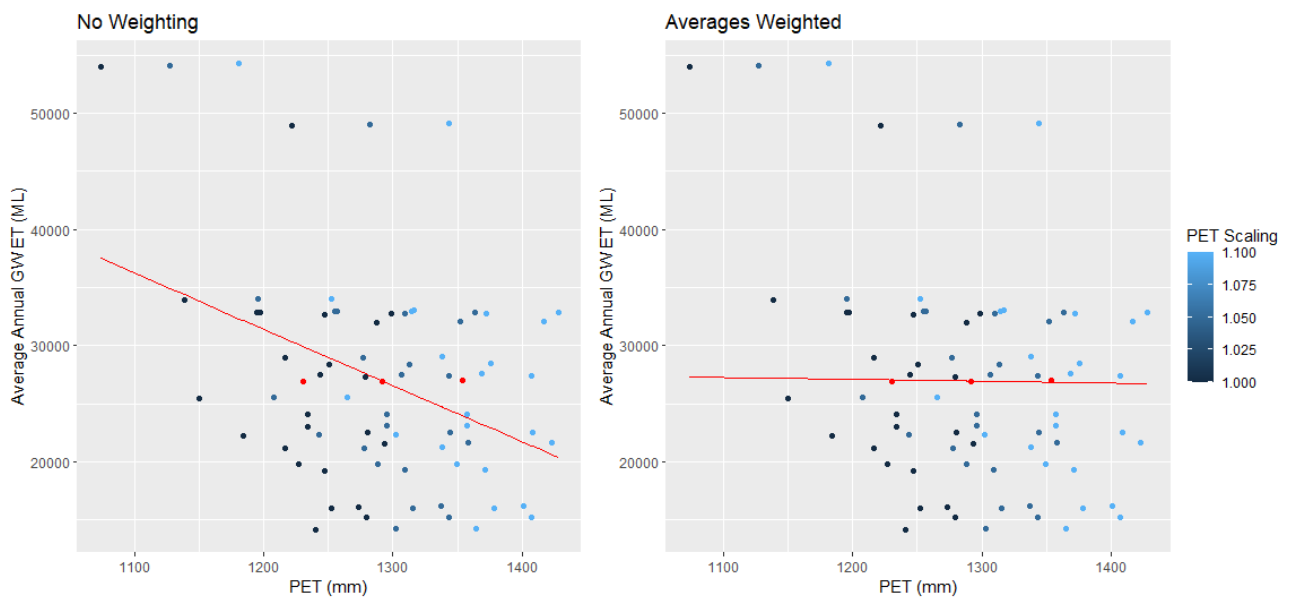


Figure 134. Scatter plots of annual average groundwater ET for a single rainfall perturbation ($P=1$) and all PET perturbations tested ($PET=1-1.1$). The scatter represents all of the raw points (from MODFLOW), coloured by PET perturbation, and the red points are the average of each of these perturbations. The left plot shows a univariate linear regression fitted to full scatter of raw data points; the right plots shows a univariate non-linear regression fitted to full scatter, with averages also included and weighted 1000, while the other points are weighted 1.

Quantile plots

Given the importance of accurately representing demand, an error model is included for the SARDI demand model component of Stella, thereby providing 'stochastic variability' such that overall year-to-year variability of the SARDI model is preserved. To evaluate the quality of this error model, quantile-quantile plots are produced and shown in this section. Specifically, Figure 135 shows the normal quantile-quantile plots of the SARDI and Stella model results individually, as well as the quantile-quantile plot of the two models. This is for a single climate scenario ($P=0.9$, $PET=1.05$).

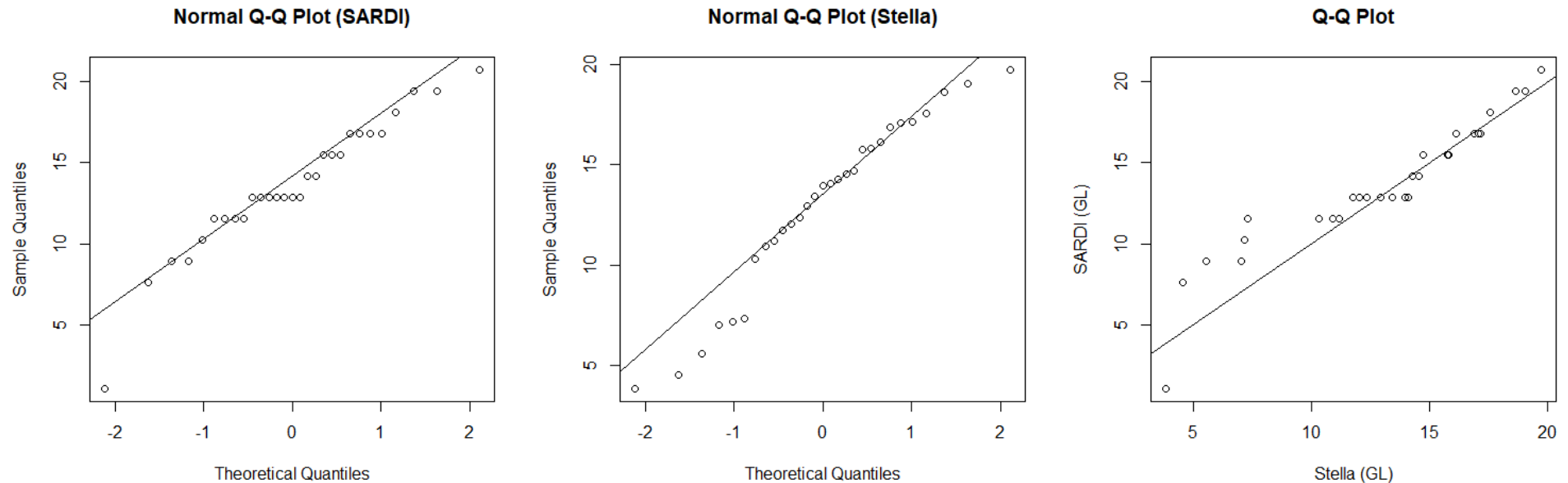


Figure 135. Quantile plots of demand from SARDI model results and SARDI model results implemented in Stella as a regression with normal error term for equivalent recent decade perturbation, $P=0.9$ and $PET=1.05$ for the Barossa PWRA. From left to right: Normal Q-Q plot of SARDI results; Normal Q-Q plot of Stella results; Q-Q plot of Stella and SARDI results.

The quantile-quantile plots show good match between the results from SARDI and Stella for one perturbation (Figure 137). The quantile-quantile plots (Figure 136) show that the models produce similar variability in demand, but are slightly different for high and low demand.

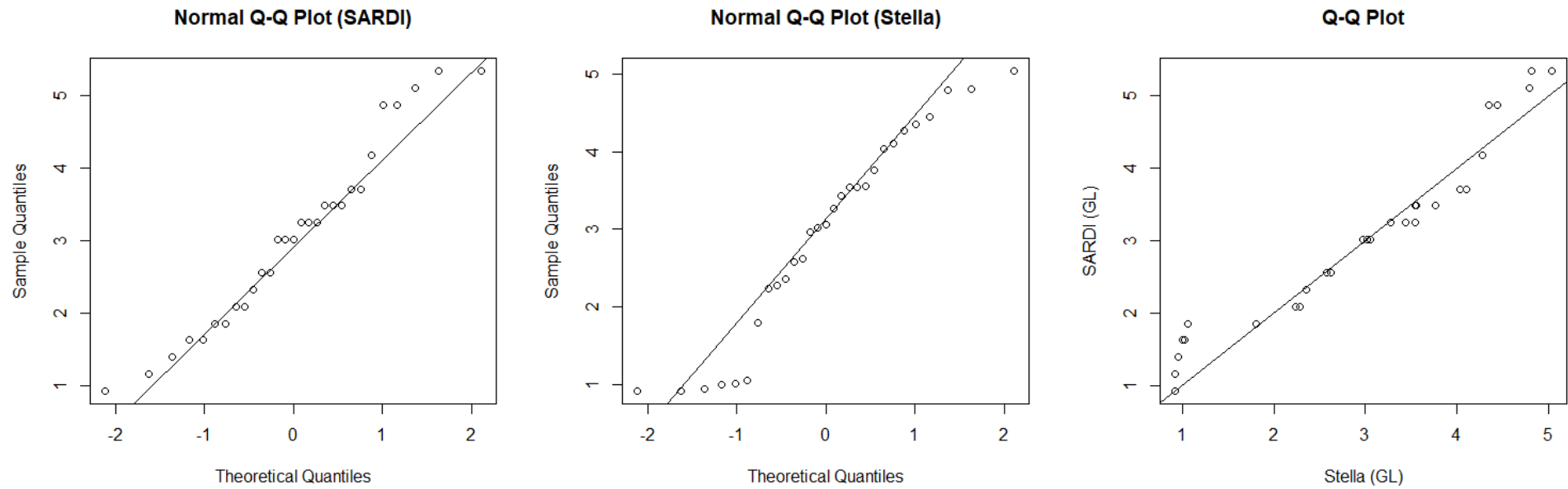


Figure 136. Quantile plots of demand from SARDI model results and SARDI model results implemented in Stella as a regression with normal error term for equivalent recent decade perturbation, $P=0.9$ and $PET = 1.05$ for the Eden Valley. From left to right: Normal Q-Q plot of SARDI results; Normal Q-Q plot of Stella results; Q-Q plot of Stella and SARDI results.

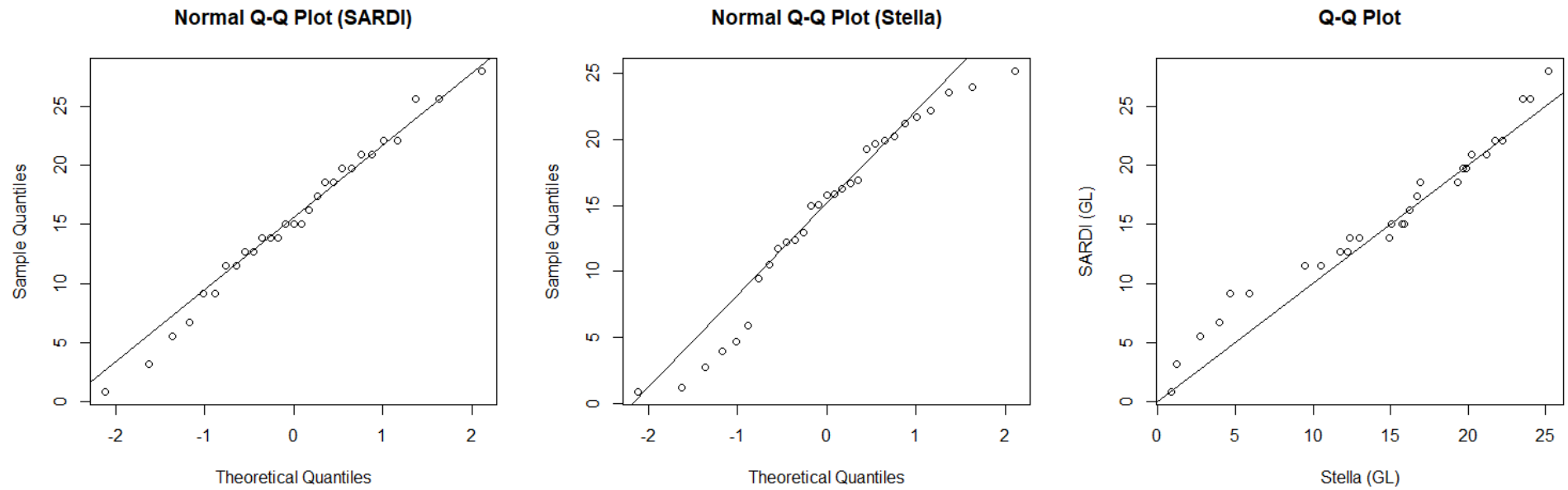


Figure 137. Quantile plots of demand from SARDI model results and SARDI model results implemented in Stella as a regression with normal error term for equivalent recent decade perturbation, $P=0.9$ and $PET = 1.05$ for the Barossa Valley. From left to right: Normal Q-Q plot of SARDI results; Normal Q-Q plot of Stella results; Q-Q plot of Stella and SARDI results.

References

- Allen, R.G., Pereira, L.S., Raes, D. and Smith, M. 1998. Crop evapotranspiration: guidelines for computing crop water requirements. FAO Irrigation and drainage paper No. 56 (Food and Agriculture Organization of the United Nations: Rome, Italy)
- AMLR NRM Board (2009). Water Allocation Plan Barossa Prescribed Water Resources Area, Government of South Australia, Department of Environment, Water and Natural Resources, Adelaide and Mount Lofty Ranges Natural Resources Management Board, Adelaide.
- Anderson, K., 2015, Growth and Cycles in Australia's Wine Industry, A Statistical Compendium, 1843 to 2013, University of Adelaide Press, ISBN: 978-1-925261-08-0.
- Argüeso D, Evans JP and Fita L 2013, Precipitation bias correction of very high resolution regional climate models, *Hydrological and Earth System Sciences*, 17:4379–4388, doi: 10.5194/hess-17-4379-2013.
- Barossa Infrastructure Limited, 2020, BIL Annual Report 2020, 52 pp.
- Bennett, B. S., Zhang, L., Potter, N., & Westra, S. (2018). *Climate Resilience Analysis Framework: Testing the resilience of natural and engineered systems (18/02)*. Goyder Institute for Water Research.
- Bunyip Water Pty Ltd. (n. d.) Bunyip Water, viewed 14 April 2021 <<https://bunyipwater.com.au/>>
- Cranswick, R.H., Pierce, D., Wright, S. & Videka, H., 2015, Barossa Prescribed Water Resources Area Groundwater Resource Capacity—Stage 1: Preliminary Findings, *DEWNR Technical Report 2015/17* (unpublished draft).
- Cranswick, R.H., Pierce, D. & Green, G., 2016, Barossa PWRA Groundwater Resource Capacity: Report 3—Projected Changes to Resource Condition Indicators due to Groundwater Extraction and Climate Change, DEWNR Technical report 2016/06.
- CSIRO and Bureau of Meteorology 2015, Climate Change in Australia Information for Australia's Natural Resource Management Regions: Technical Report, CSIRO and Bureau of Meteorology, Australia
- Devanand, A., Westra, S., Leonard, M., Culley, S. & Bennett, B., 2020, Detailed tutorial: Climate 'Stress-Testing' using *foreSIGHT*, *foreSIGHT* user manual available on CRAN (<https://cran.r-project.org/web/packages/foreSIGHT/index.html>).
- DEW (2021). Construction and calibration of a hydrological model for the Marne River catchment. Technical report 2021, Government of South Australia, Department for Environment and Water, Adelaide.
- DEWNR Technical report 2016/05, Government of South Australia, through Department of Environment, Water and Natural Resources, Adelaide
- Evans JP and Argüeso D 2014, *Guidance on the use of bias corrected data*, NARClIM Technical Note 3, NARClIM Consortium: Sydney, Australia, available at www.crc.unsw.edu.au/sites/default/files/NARClIM/publications/TechNote3.pdf
- Government of South Australia, n. d. South Australia's water information portal, viewed 12 February 2021, <<https://www.waterconnect.sa.gov.au/>>
- Goyder Institute for Water Research, 2015, *SA Climate Ready data for South Australia - A User Guide*, Goyder Institute for Water Research Occasional Paper No. 15/1, Adelaide, South Australia
- Green, D., Maxwell, S., VanLaarhoven, J. & Deane, D., 2014, Barossa Valley Prescribed Water Resources Area hydro-ecological risk assessment, DEWNR Technical Report 2014/08.

- Gross M.H., Alexander L.V., Macadam I., Green D., Evans J.P., 2016, The representation of health-relevant heatwave characteristics in a Regional Climate Model ensemble for New South Wales and the Australian Capital Territory, Australia, *International Journal of Climatology*, 37(3), 1195–1210, doi: 10.1002/joc.4769.
- Hancock, M., Stewart, S. & Green, G., 2014, Interaction between groundwater and surface water systems, Barossa Prescribed Water Resources Area, DEWNR Technical Report 2014/09.
- Hausfather, Z., Peters, G.P., 2020, Emissions – the ‘business as usual’ story is misleading, *Nature*, 577, 618–620.
- Helweg, O.J., 1991. Functions of crop yield from applied water. *Agronomy Journal* 83(4), 769–773. <https://doi.org/10.2134/agronj1991.00021962008300040023x>
- Hope, P. *et al.* 2015, *Southern and South-Western Flatlands Cluster Report*, Climate Change in Australia Projections for Australia’s Natural Resource Management Regions: Cluster Reports, eds. Ekström, M. *et al.*, CSIRO and Bureau of Meteorology, Australia.
- IPCC, 2014: Climate Change 2014: Synthesis Report. Contribution of Working Groups I, II and III to the Fifth Assessment Report of the Intergovernmental Panel on Climate Change [Core Writing Team, R.K. Pachauri and L.A. Meyer (eds.)]. IPCC, Geneva, Switzerland, 151 pp. Ji F, Ekstrom M, Evans JP and Teng J 2014, Evaluating rainfall patterns using physics scheme ensembles from a regional atmospheric model, *Theoretical and Applied Climatology*, 115, 297–304, doi: 10.1007/s00704-013-0904-2.
- Jeffrey, S.J., Carter, J.O., Moodie, K.B. and Beswick, A.R. (2001). *Using spatial interpolation to construct a comprehensive archive of Australian climate data*, *Environmental Modelling and Software*, Vol 16/4, pp 309-330. DOI: 10.1016/S1364-8152(01)00008-1
- Jones-Gill, A. and Savadamuthu, K., 2014, Hydro-ecological investigations to inform the Barossa PWRA WAP review – Hydrology Report, DEWNR Technical Report 2014/14, Government of South Australia, through Department of Environment, Water and Natural Resources, Adelaide
- Knowling, M.J., Bennett, B., Ostendorf, B., Westra, S., Walker, R.R., Pellegrino, A., Edwards, E.J., Collins, C., Pagay, V., Grigg, D., 2021. Bridging the gap between data and decisions: A review of process-based models for viticulture. *Agricultural Systems* 193C. <https://doi.org/10.1016/j.agsy.2021.103209>
- Li, C. and Cranswick, R.H., 2016, Barossa PWRA Groundwater Resource Capacity: Report 2 – Numerical Groundwater Flow Modelling, DEWNR Technical Report 2016/05
- Macadam I, Argüeso D, Evans JP, Liu DL and Pitman AJ 2016, The effect of bias correction and climate model resolution on wheat simulations forced with a Regional Climate Model ensemble, *International Journal of Climatology*, 36, 4577-4591, doi: 10.1002/joc.4653.
- Montazeri, M., Savadamuthu, K., 2020 (updated), Hydrological investigations to inform the Barossa PWRA WAP review – Part 2, DEWNR Technical Note 2018/42
- Payan, I.C., Salançon, E., Genevet, B., Jacquet, O., 2011. Les effets de l’irrigation au vignoble. IFV (Professional French Institute of Vine).
- Phogat, V., Cox, J.W., Mallants, D., Petrie, P.R., Oliver, D.P., Pitt, T.R., 2020. Historical and future trends in evapotranspiration components and irrigation requirements of winegrapes. *Australian Journal of Grape and Wine Research* 26, 312-324. doi: 10.1111/ajgw.12446
- Piani C, Haerter J and Coppola E 2010, Statistical bias correction for daily precipitation in regional climate models over Europe, *Theoretical and Applied Climatology*, 99, 187–192.

Stevens, R., Pech, J., Gibberd, M., Walker, R. and Nicholas, P., 2010. Reduced irrigation and rootstock effects on vegetative growth, yield and its components, and leaf physiological responses of Shiraz. *Australian Journal of Grape and Wine Research*, 16(3), pp.413-425.

Williams, L. and Heymann, H., 2017. Effects of applied water amounts and trellis/training system on grapevine water relations, berry characteristics, productivity and wine composition of 'Cabernet Sauvignon'. *Acta Horticulturae*, (1150), pp.413-426.

Wine Australia, n. d., *Register of Protected GIs and Other Terms*, viewed 12 February 2021 <<https://www.wineaustralia.com/labelling/register-of-protected-gis-and-other-terms>>